

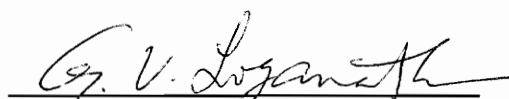
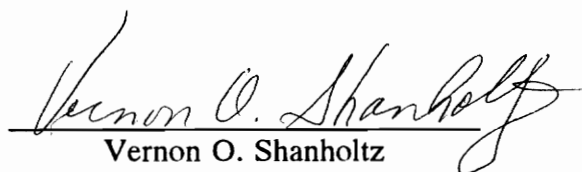
A Comparative Evaluation of Surface Runoff Models and Methods on Small Developing Watersheds in Northern Virginia

by
Aaron Brent Small

Thesis submitted to the Faculty of the
Virginia Polytechnic Institute and State University
in partial fulfillment of the requirements for the degree of

**Master of Science
in
Civil Engineering**

APPROVED:


David F. Kibler, Chairman
G. V. Loganathan
Vernon O. Shanholtz

September 1993
Charles E. Via, Jr. Department of Civil Engineering
Virginia Tech
Blacksburg, Virginia

C.2

LD
5655
V855
1993
5624

C.2

Abstract

Increasing populations in urban regions have prompted the development of areas previously undisturbed. This development has spurred the formation of numerous models and methods to simulate the effects of the urbanization on runoff processes. The engineer who must use these models and methods needs to be aware of their capabilities and performance. Many of the models assume that calibration will take place to improve the final results. Unfortunately, this is not the case for the majority of drainage studies. A qualitative and quantitative evaluation is made to help the engineer decide which model or method is applicable in certain situations.

Simulations are performed on eight watersheds in northern Virginia. Nineteen models are evaluated and compared to gaged events as well as calibrated design storms. The models include EPA SWMM, PSRM-QUAL, TR-20, HEC-1, TR-55, variations of the rational method, three unit hydrograph procedures, the USGS regression equations, and the Anderson method. Coverage is given for all of the models to outline their capabilities. Hydrographs are evaluated with respect to peak flow, time to peak flow, time base, volume, and overall shape. Statistical measures are introduced to quantitatively test the modeled hydrograph to a baseline reference hydrograph.

The statistics yield many errors with the models being evaluated. A selection criteria is given where the models may be chosen based on their performance. The

table is limited to the range of watersheds evaluated. Trends in each model toward basin area, land use condition and general model type are discussed. A cross-calibration technique for improving accuracy of some models is verified.

Acknowledgements

I would first like to thank the Charles E. Via Department of Civil Engineering at Virginia Tech for the continued support through two degrees and a fine education. The fellowship that I received allowed me to continue my education which, otherwise, would not have been possible. I would also like to thank the American Society of Civil Engineers who bestowed the Freeman Fellowship. I am honored to receive both of these awards and it is my sincere hope that I may return the favor to them someday. I especially want to express my gratitude to my advisor and mentor, Dr. David F. Kibler, for the help, encouragement, friendly advice and the overwhelming enthusiasm for the subject of this thesis.

In addition, I would like to thank the other members of my thesis committee, Dr. G. V. Loganathan and Dr. Vernon O. Shanholtz. The support provided by these two saved numerous hours of tedious labors on this thesis. I give much appreciation to the staff at the Information Support Systems Lab, who endured my many annoying phone calls. The staff of the Occoquan Watershed Monitoring Lab deserve much appreciation for their help in data acquisition. Thanks also goes out to all of the graduate students in the trenches for their ideas, suggestions and general comradeship.

Special thanks goes to my family, especially my father. Without his encouragement, I would never have known what Civil Engineering was. Finally I would like to thank my wife, Toni, for her undying support throughout college and especially graduate school. Without her love and friendship (and proofreading), I do not think I would ever have finished this project.

This research has been supported by Prince William County, Virginia under the direction of Fernando Pasquel, Director of the Watershed Management Division, Department of Public Works. I am grateful for this support and it is duly acknowledged.

Table of Contents

Abstract	ii
Acknowledgements	iv
Table of Contents	vi
List of Figures	viii
List of Tables	xiii
Introduction	1
Statement of the Problem	1
Literature Review	4
Description of Models	9
Model Choice	9
Review of Hydrologic Capability of Models and Methods	10
EPA SWMM	11
TR-20	22
HEC-1	26
PSRM-QUAL	30
SCS Unit Hydrograph	34
The Clark Instantaneous Unit Hydrograph	36
The Snyder Unit Hydrograph	38
SCS TR-55	40
The Rational Method	43
The Modified Rational Method	47
The Universal Rational Method	50
The USGS Virginia Regression Equations	51
The Anderson Method	54
Model Capabilities	56
VIPER as a preprocessor	63
Gaged Data and	
Description of Watersheds	67
General Watershed Locations and Regional Descriptions	68
Broad Run Tributary at Buckland	72

South Fork of Broad Run at Arcola	74
Snakeden Branch at Reston	76
Smilax Branch at Reston	79
Stave Run near Reston	80
Holmes Run	82
Watershed Data Acquisition	85
Basis for Comparison	88
Measures of Comparison	88
Example of Statistics	97
Design Rainfall Distributions	98
Method of Analysis	101
Analysis and Results	106
Watershed Dependent Errors	106
Model and Storm Type Error Analysis	116
Generalizations	126
Recommendations	129
Model Performance Indicators	129
Cross-Calibration and Other Implications	134
Recommendations for Further Study	135
References	137
Gaged Storm Events and Design Storm Hyetographs	140
Tables of Evaluation Results	172
Watershed Comparison Graphs	198
Model Comparison Graphs	226
Watershed Maps	259

List of Figures

Figure 2.1 - Horton Infiltration Parameters for Various Soil Types (Aron et al., 1992)	14
Figure 2.2 - Idealized SWMM Subcatchment	18
Figure 2.3 - The Rational Method applied on Subareas	46
Figure 2.4 - The Modified Rational Method Hydrograph.	48
Figure 3.1 - General Watershed Location Map	69
Figure 4.1 - Hydrograph Time Base Estimation	93
Figure 4.2 - Statistical Measures Example Hydrographs	98
Figure 6.1 - Example Calculation of Performance Index	132
Figure A.1 - Snakeden Branch, Gaged Event 1	140
Figure A.2 - Snakeden Branch at Reston, Gaged Event 2	141
Figure A.3 - Snakeden Branch at Reston, Gaged Event 3	141
Figure A.4 - Snakeden Branch at Reston, Gaged Event 4	142
Figure A.5 - Snakeden Branch at Reston, Gaged Event 6	142
Figure A.6 - Stave Run near Reston, Gaged Event 1	143
Figure A.7 - Stave Run near Reston, Gaged Event 2	143
Figure A.8 - Stave Run near Reston, Gaged Event 3	144
Figure A.9 - Stave Run near Reston, Gaged Event 4	144
Figure A.10 - Smilax Branch at Reston, Gaged Event 1	145
Figure A.11 - Smilax Branch at Reston, Gaged Event 2	145
Figure A.12 - Smilax Branch at Reston, Gaged Event 3	146
Figure A.13 - Smilax Branch at Reston, Gaged Event 4	146
Figure A.14 - Smilax Branch at Reston, Gaged Event 5	147
Figure A.15 - Smilax Branch at Reston, Gaged Event 6	147
Figure A.16 - South Fork Broad Run at Arcola, Gaged Event 1	148
Figure A.17 - South Fork Broad Run at Arcola, Gaged Event 2	148
Figure A.18 - South Fork Broad Run at Arcola, Gaged Event 3	149
Figure A.19 - South Fork Broad Run at Arcola, Gaged Event 4	149
Figure A.20 - South Fork Broad Run at Arcola, Gaged Event 5	150
Figure A.21 - South Fork Broad Run at Arcola, Gaged Event 6	150
Figure A.22 - Broad Run Tributary at Buckland, Gaged Event 1	151
Figure A.23 - Broad Run Tributary at Buckland, Gaged Event 2	151
Figure A.24 - Broad Run Tributary at Buckland, Gaged Event 3	152
Figure A.25 - Broad Run Tributary at Buckland, Gaged Event 4	152
Figure A.26 - Broad Run Tributary at Buckland, Gaged Event 5	153
Figure A.27 - Broad Run Tributary at Buckland, Gaged Event 6	153
Figure A.28 - Holmes Run Gage 1 at Falls Church, Gaged Event 1	154

Figure A.29 - Holmes Run Gage 1 at Falls Church, Gaged Event 2	154
Figure A.30 - Holmes Run Gage 1 at Falls Church, Gaged Event 3	155
Figure A.31 - Holmes Run Gage 1 at Falls Church, Gaged Event 4	155
Figure A.32 - Holmes Run Gage 1 at Falls Church, Gaged Event 5	156
Figure A.33 - Holmes Run Gage 1 at Falls Church, Gaged Event 6	156
Figure A.34 - Holmes Run Gage 2 at Falls Church, Gaged Event 1	157
Figure A.35 - Holmes Run Gage 2 at Falls Church, Gaged Event 2	157
Figure A.36 - Holmes Run Gage 2 at Falls Church, Gaged Event 3	158
Figure A.37 - Holmes Run Gage 2 at Falls Church, Gaged Event 4	158
Figure A.38 - Holmes Run Gage 2 at Falls Church, Gaged Event 5	159
Figure A.39 - Holmes Run Gage 2 at Falls Church, Gaged Event 6	159
Figure A.40 - Holmes Run Gage 4 at Falls Church, Gaged Event 1	160
Figure A.41 - Holmes Run Gage 4 at Falls Church, Gaged Event 2	160
Figure A.42 - Holmes Run Gage 4 at Falls Church, Gaged Event 3	161
Figure A.43 - Holmes Run Gage 4 at Falls Church, Gaged Event 4	161
Figure A.44 - Holmes Run Gage 4 at Falls Church, Gaged Event 5	162
Figure A.45 - Holmes Run Gage 4 at Falls Church, Gaged Event 6	162
Figure A.46 - 2 year, 1 hour Yarnell Rainfall	163
Figure A.47 - 5 year, 1 hour Yarnell Rainfall	163
Figure A.48 - 10 year, 1 hour Yarnell Rainfall	164
Figure A.49 - 25 year, 1 hour Yarnell Rainfall	164
Figure A.50 - 50 year, 1 hour Yarnell Rainfall	165
Figure A.51 - 100 year, 1 hour Yarnell Rainfall	165
Figure A.52 - 2 year, 2 hour Yarnell Rainfall	166
Figure A.53 - 5 year, 2 hour Yarnell Rainfall	166
Figure A.54 - 10 year, 2 hour Yarnell Rainfall	167
Figure A.55 - 25 year, 2 hour Yarnell Rainfall	167
Figure A.56 - 50 year, 2 hour Yarnell Rainfall	168
Figure A.57 - 100 year, 2 hour Yarnell Rainfall	168
Figure A.58 - 2 year, 24 hour SCS Type II Rainfall	169
Figure A.59 - 5 year, 24 hour SCS Type II Rainfall	169
Figure A.60 - 10 year, 24 hour SCS Type II Rainfall	170
Figure A.61 - 25 year, 24 hour SCS Type II Rainfall	170
Figure A.62 - 50 year, 24 hour SCS Type II Rainfall	171
Figure A.63 - 100 year, 24 hour SCS Type II Rainfall	171
Figure C.1 - Peak Flow Bias for All Storms, All Models	198
Figure C.2 - Peak Flow Bias for All Storms, Sophisticated Models	199
Figure C.3 - Peak Flow Bias for All Storms, Unit Hydrograph Models	199
Figure C.4 - Peak Flow Bias for All Storms, Design Rainfall Models	200
Figure C.5 - Peak Flow Bias for All Storms, Peak-Only Models	200

Figure C.6 - Peak Flow Standard Error for All Storms, All Models	201
Figure C.7 - Peak Flow Standard Error for All Storms, Sophisticated Models . . .	201
Figure C.8 - Peak Flow Standard Error for All Storms, Unit Hydrograph Models	202
Figure C.9 - Peak Flow Standard Error for All Storms, Design Rainfall Models .	202
Figure C.10 - Peak Flow Standard Error for All Storms, Peak-Only Models	203
Figure C.11 - Volume Bias for All Storms, All Models	203
Figure C.12 - Volume Bias for All Storms, Sophisticated Models	204
Figure C.13 - Volume Bias for All Storms, Unit Hydrograph Models	204
Figure C.14 - Volume Bias for All Storms, Design Rainfall Models	205
Figure C.15 - Volume Standard Error for All Storms, All Models	205
Figure C.16 - Volume Standard Error for All Storms, Sophisticated Models	206
Figure C.17 - Volume Standard Error for All Storms, Unit Hydrograph Models .	206
Figure C.18 - Volume Standard Error for All Storms, Design Rainfall Models . .	207
Figure C.19 - Time to Peak Bias for All Storms, All Models	207
Figure C.20 - Time to Peak Bias for All Storms, Sophisticated Models	208
Figure C.21 - Time to Peak Bias for All Storms, Unit Hydrograph Models	208
Figure C.22 - Time to Peak Bias for All Storms, Design Rainfall Models	209
Figure C.23 - Time to Peak Standard Error for All Storms, All Models	209
Figure C.24 - Time to Peak Standard Error for All Storms, Sophisticated Models	210
Figure C.25 - Time to Peak Standard Error for All Storms, Unit Hydrograph Models	210
Figure C.26 - Time to Peak Standard Error for All Storms, Design Rainfall Models	211
Figure C.27 - Time Base Bias for All Storms, All Models	211
Figure C.28 - Time Base Bias for All Storms, Sophisticated Models	212
Figure C.29 - Time Base Bias for All Storms, Unit Hydrograph Models	212
Figure C.30 - Time Base Bias for All Storms, Design Rainfall Models	213
Figure C.31 - Time Base Standard Error for All Storms, All Models	213
Figure C.32 - Time Base Standard Error for All Storms, Sophisticated Models . .	214
Figure C.33 - Time Base Standard Error for All Storms, Unit Hydrograph Models	214
Figure C.34 - Time Base Standard Error for All Storms, Design Rainfall Models	215
Figure C.35 - Volume-Shape Error for All Storms, All Models	215
Figure C.36 - Volume-Shape Error for All Storms, Sophisticated Models	216
Figure C.37 - Volume-Shape Error for All Storms, Unit Hydrograph Models . . .	216
Figure C.38 - Volume-Shape Error for All Storms, Design Rainfall Models	217
Figure C.39 - Root-Mean-Square Error for All Storms, All Models	217

Figure C.40 - Root-Mean-Square Error for All Storms, Sophisticated Models . . .	218
Figure C.41 - Root-Mean-Square Error for All Storms, Unit Hydrograph Models	218
Figure C.42 - Root-Mean-Square Error for All Storms, Design Rainfall Models .	219
Figure C.43 - Shape Bias for All Storms, All Models	219
Figure C.44 - Shape Bias for All Storms, Sophisticated Models	220
Figure C.45 - Shape Bias for All Storms, Unit Hydrograph Models	220
Figure C.46 - Shape Bias for All Storms, Design Rainfall Models	221
Figure C.47 - Shape Standard Error for All Storms, All Models	221
Figure C.48 - Shape Standard Error for All Storms, Sophisticated Models	222
Figure C.49 - Shape Standard Error for All Storms, Unit Hydrograph Models . . .	222
Figure C.50 - Shape Standard Error for All Storms, Design Rainfall Models	223
Figure C.51 - Weighted Shape Standard Error for All Storms, All Models	223
Figure C.52 - Weighted Shape Standard Error for All Storms, Sophisticated Models	224
Figure C.53 - Weighted Shape Standard Error for All Storms, Unit Hydrograph Models	224
Figure C.54 - Weighted Shape Standard Error for All Storms, Design Rainfall Models	225
Figure D.1 - Peak Flow Bias for all models, all storms	226
Figure D.2 - Peak Flow Bias for All Models, Gaged Storms	227
Figure D.3 - Peak Flow Bias for All Models, 1-hr Yarnell Storms	227
Figure D.4 - Peak Flow Bias for All Models, 2-hr Yarnell Storms	228
Figure D.5 - Peak Flow Bias for All Models, 24-hr SCS Storms	228
Figure D.6 - Peak Flow Standard Error for All Models, All Storms	229
Figure D.7 - Peak Flow Standard Error for All Models, Gaged Storms	229
Figure D.8 - Peak Flow Standard Error for All Models, 1-hr Yarnell Storms . . .	230
Figure D.9 - Peak Flow Standard Error for All Models, 2-hr Yarnell Storms . . .	230
Figure D.10 - Peak Flow Standard Error for All Models, 24-hr SCS Storms	231
Figure D.11 - Volume Bias for All Models, All Storms	231
Figure D.12 - Volume Bias for All Models, Gaged Storms	232
Figure D.13 - Volume Bias for All Models, 1-hr Yarnell Storms	232
Figure D.14 - Volume Bias for All Models, 2-hr Yarnell Storms	233
Figure D.15 - Volume Bias for All Models, 24-hr SCS Storms	233
Figure D.16 - Volume Standard Error for All Models, All Storms	234
Figure D.17 - Volume Standard Error for All Models, Gaged Storms	234
Figure D.18 - Volume Standard Error for All Models, 1-hr Yarnell Storms	235
Figure D.19 - Volume Standard Error for All Models, 2-hr Yarnell Storms	235
Figure D.20 - Volume Standard Error for All Models, 24-hr SCS Storms	236
Figure D.21 - Time to Peak Bias for All Models, All Storms	236

Figure D.22 - Time to Peak Bias for All Models, Gaged Storms	237
Figure D.23 - Time to Peak Bias for All Models, 1-hr Yarnell Storms	237
Figure D.24 - Time to Peak Bias for All Models, 2-hr Yarnell Storms	238
Figure D.25 - Time to Peak Bias for All Models, 24-hr SCS Storms	238
Figure D.26 - Time to Peak Standard Error for All Models, All Storms	239
Figure D.27 - Time to Peak Standard Error for All Models, Gaged Storms	239
Figure D.28 - Time to Peak Standard Error for All Models, 1-hr Yarnell Storms .	240
Figure D.29 - Time to Peak Standard Error for All Models, 2-hr Yarnell Storms .	240
Figure D.30 - Time to Peak Standard Error for All Models, 24-hr SCS Storms . .	241
Figure D.31 - Time Base Bias for All Models, All Storms	241
Figure D.32 - Time Base Bias for All Models, Gaged Storms	242
Figure D.33 - Time Base Bias for All Models, 1-hr Yarnell Storms	242
Figure D.34 - Time Base Bias for All Models, 2-hr Yarnell Storms	243
Figure D.35 - Time Base Bias for All Models, 24-hr SCS Storms	243
Figure D.36 - Time Base Standard Error for All Models, All Storms	244
Figure D.37 - Time Base Standard Error for All Models, Gaged Storms	244
Figure D.38 - Time Base Standard Error for All Models, 1-hr Yarnell Storms . .	245
Figure D.39 - Time Base Standard Error for All Models, 2-hr Yarnell Storms . .	245
Figure D.40 - Time Base Standard Error for All Models, 24-hr SCS Storms . . .	246
Figure D.41 - Volume-Shape Error for All Models, All Storms	246
Figure D.42 - Volume-Shape Error for All Models, Gaged Storms	247
Figure D.43 - Volume-Shape Error for All Models, 1-hr Yarnell Storms	247
Figure D.44 - Volume-Shape Error for All Models, 2-hr Yarnell Storms	248
Figure D.45 - Volume-Shape Error for All Models, 24-hr SCS Storms	248
Figure D.46 - Root-Mean-Square Error for All Models, All Storms	249
Figure D.47 - Root-Mean-Square Error for All Models, Gaged Storms	249
Figure D.48 - Root-Mean-Square Error for All Models, 1-hr Yarnell Storms . . .	250
Figure D.49 - Root-Mean-Square Error for All Models, 2-hr Yarnell Storms . . .	250
Figure D.50 - Root-Mean-Square Error for All Models, 24-hr SCS Storms	251
Figure D.51 - Shape Bias for All Models, All Storms	251
Figure D.52 - Shape Bias for All Models, Gaged Storms	252
Figure D.53 - Shape Bias for All Models, 1-hr Yarnell Storms	252
Figure D.54 - Shape Bias for All Models, 2-hr Yarnell Storms	253
Figure D.55 - Shape Bias for All Models, 24-hr SCS Storms	253
Figure D.56 - Shape Standard Error for All Models, All Storms	254
Figure D.57 - Shape Standard Error for All Models, Gaged Storms	254
Figure D.58 - Shape Standard Error for All Models, 1-hr Yarnell Storms	255
Figure D.59 - Shape Standard Error for All Models, 2-hr Yarnell Storms	255

Figure D.60 - Shape Standard Error for All Models, 24-hr SCS Storms	256
Figure D.61 - Weighted Shape Standard Error for All Models, All Storms	256
Figure D.62 - Weighted Shape Standard Error for All Models, Gaged Storms . . .	257
Figure D.63 - Weighted Shape Standard Error for All Models, 1-hr Yarnell Storms	257
Figure D.64 - Weighted Shape Standard Error for All Models, 2-hr Yarnell Storms	258
Figure D.65 - Weighted Shape Standard Error for All Models, 24-hr SCS Storms	258
Plate A.1 - Sub-Area Delineation of Stave Run near Reston, VA	Folio A
Plate A.2 - Land Use Map of Stave Run near Reston, VA	Folio A
Plate A.3 - SCS Hydrologic Soil Group Map of Stave Run near Reston, VA	Folio A
Plate A.4 - Sub-Area Delineation of Smilax Branch at Reston, VA	Folio A
Plate A.5 - Land Use Map of Smilax Branch at Reston, VA	Folio A
Plate A.6 - SCS Hydrologic Soil Group Map of Smilax Branch at Reston, VA	Folio A
Plate A.7 - Sub-Area Delineation of Snakeden Branch at Reston, VA	Folio A
Plate A.8 - Land Use Map of Snakeden Branch at Reston, VA	Folio A
Plate A.9 - SCS Hydrologic Soil Group Map of Snakeden Branch at Reston, VA	Folio A
Plate A.10 - Sub-Area Delineation of South Fork Broad Run at Arcola, VA	Folio A
Plate A.11 - Land Use Map of South Fork Broad Run at Arcola, VA	Folio A
Plate A.12 - SCS Hydrologic Soil Group Map of South Fork Broad Run at Arcola, VA	Folio A
Plate A.13 - Sub-Area Delineation of Broad Run Tributary at Buckland, VA	Folio A
Plate A.14 - Land Use Map of Broad Run Tributary at Buckland, VA	Folio A
Plate A.15 - SCS Hydrologic Soil Group Map of Broad Run Tributary at Buckland, VA	Folio A
Plate A.16 - Sub-Area Delineation of Holmes Run near Falls Church, VA	Folio A
Plate A.17 - Land Use Map of Holmes Run near Falls Church, VA	Folio A
Plate A.18 - SCS Hydrologic Soil Group Map of Holmes Run near Falls Church, VA	Folio A

List of Tables

Table 1.1 - Models and Methods Tested	4
Table 2.1 - Kinematic Wave Assumptions	17
Table 2.2 - Physical Input Parameters for SWMM	21
Table 2.3 - Physical Input Parameters for TR-20	26
Table 2.4 - Physical Input Parameters for HEC-1 (KW)	29
Table 2.5 - PSRM-QUAL Physical Input Parameters	33
Table 2.6 - Physical input parameters for SCS Unit Hydrograph (Sub-areas within HEC-1)	35
Table 2.7 - Physical Input Parameters for Clark's Instantaneous Unit Hydrograph	37
Table 2.8 - Physical Input Parameters for Snyder's Unit Hydrograph	40
Table 2.9 - Physical Input Parameters for TR-55 (1986 Version)	43
Table 2.10 - Physical Input Parameters for The Rational Method	45
Table 2.11 - Physical Input Parameters for the Modified Rational Method	49
Table 2.12 - Physical Input Parameters for The Universal Rational Method	51
Table 2.13 - Physical Input Parameters for the USGS Virginia/Urban Equations	54
Table 2.14 - Physical Inputs Parameters for The Anderson Method	55
Table 2.15 - Capabilities of Models - Rainfall Options	57
Table 2.16 - Capabilities of Models - Precipitation Loss Options	58
Table 2.17 - Capabilities of Models - Hydrograph/Peak Generation Methods	59
Table 2.18 - Capabilities of Models - Reach/Reservoir Routing Options	60
Table 2.19 - Capabilities of Models - Computer Requirements and Options	61
Table 2.20 - Capabilities of Models - Other Model Options	62
Table 2.21 - Model Files Created by VIPER	63
Table 2.22 - VIPER Input Parameters	65
Table 3.1 - List of Watersheds	67
Table 3.2 - General Watershed Data for Broad Run Tributary at Buckland	73
Table 3.3 - General Watershed Data for South Fork Broad Run at Arcola	75
Table 3.4 - General Watershed Data for Snakeden Branch at Reston	78
Table 3.5 - General Watershed Data for Smilax Branch at Reston	80
Table 3.6 - General Watershed Data for Stave Run near Reston	81
Table 3.7 - General Watershed Data for Holmes Run	83
Table 3.8 - Land Use Classification Categories	86
Table 3.2 - Example Analysis Results	99
Table 3.3 - Results of Calibration Models	102
Table 3.4 - Number of Hydrographs Computed for each Watershed and Model	103
Table 6.1 - Model Performance Indicators	130

Table B.1 - Peak Flow Bias - Average	172
Table B.2 - Peak Flow Bias - Standard Deviation	173
Table B.3 - Peak Flow Standard Error - Average	174
Table B.4 - Peak Flow Standard Error - Standard Deviation	175
Table B.5 - Volume Bias - Average	176
Table B.6 - Volume Bias - Standard Deviation	177
Table B.7 - Volume Standard Error - Average	178
Table B.8 - Volume Standard Error - Standard Deviation	179
Table B.9 - Time to Peak Bias - Average	180
Table B.10 - Time to Peak Bias - Standard Deviation	181
Table B.11 - Time to Peak Standard Error - Average	182
Table B.12 - Time to Peak Standard Error - Standard Deviation	183
Table B.13 - Time Base Bias - Average	184
Table B.14 - Time Base Bias - Standard Deviation	185
Table B.15 - Time Base Standard Error - Average	186
Table B.16 - Time Base Standard Error - Standard Deviation	187
Table B.17 - Volume-Shape Error - Average	188
Table B.18 - Volume-Shape Error - Standard Deviation	189
Table B.19 - Root-Mean-Square Error - Average	190
Table B.20 - Root-Mean-Square Error - Standard Deviation	191
Table B.21 - Shape Bias - Average	192
Table B.22 - Shape Bias - Standard Deviation	193
Table B.23 - Shape Standard Error - Average	194
Table B.24 - Shape Standard Error - Standard Deviation	195
Table B.25 - Weighted Shape Standard Error - Average	196
Table B.26 - Weighted Shape Standard Error - Standard Deviation	197

Chapter 1

Introduction

1.1 Statement of the Problem

The recent movement of the population to urban areas has required the development of lands for housing, commercial and industrial uses from the previously abundant agricultural or undeveloped lands. (UNDIESA, 1989) Unfortunately, this development in small watersheds causes peak runoff increases which creates many problems. (Riordan et. al., 1978) The developer must hire an engineer who determines measures to correct the increase. This could be in the form of detention ponds, or if storm water quality is a problem, a Best Management Practice (BMP). In order to determine runoff quantity, or the extent of water quality deterioration, the engineer must perform calculations appropriate to the given situation. Many government agencies as well as many studies in the private sector have formulated equations and methods for determining runoff quantity and quality. A problem arises when each of the models or methods yield different results for the same watershed situation. The usual reasons for these discrepancies are the assumptions and computation errors imbedded within the calculation method or most likely the inappropriate use of the model/methods on the given design situation. (Woolhiser and Brakensiek, 1982)

The purpose of this research is to evaluate the so called desk-top models and methods and the more numerically complex models. The models are compared with actual rainfall/runoff data for watersheds located in Northern Virginia. A desk-top model incorporates such simplified methods as the United States Soil Conservation Service's Technical Release 55, *Urban Hydrology for Small Watersheds* (SCS TR-55), and the Rational Method. (Kibler, 1982b) The more sophisticated models would include the United States Environmental Protection Agency's *Storm Water Management Model* (EPA SWMM) and the SCS Technical Release 20, *Computer Program for Project Formulation - Hydrology* (SCS TR-20).

There is a trend toward the use of sophisticated models for design instead of simpler models. Regulatory agencies and municipalities play a large role in this growing trend due to the increasing number of requirements concerning the allowable changes in runoff conditions and regionalization of storm water management facilities. (Hann, 1978) One use of simpler methods in municipalities and regulatory agencies is to verify the results from the more sophisticated models submitted for review by the hired consultant. (Keser, 1978) Consulting engineers need to be convinced that they can save their client money, in certain cases, by using the more sophisticated, and supposedly more accurate, models instead of the less expensive and more simplified desk-top models. To convince the engineer, it will be necessary to show that the savings can justify the initial capital investment and that the time to process the data

required for the more complex models is warranted. What is needed is the solid evidence stating which models provide the most accurate prediction of the design parameters while remaining simple to use and still within the consultants budget. The purpose of this thesis is to provide a method for choosing the models based on capabilities as well as performance.

One other problem associated with the use of the desk-top models as well as the sophisticated models is their use in design of storm water drainage and detention facilities on the ungaged watershed. The shortage of data, due to lack of gaging at the site, is the reason calibration of the watershed model is not possible. A solution to this is to apply a "cross-calibration" technique to substitute for the lack of data. By cross-calibrating with different models or methods, the engineer can minimize errors under the assumption that all models will give an approximate value for the actual flood flow. By taking an average of the design flows from each of the methods applied, the engineer can obtain a better estimate of the observed flow. By minimizing possible errors, a more cost effective and safe alternative can be found.

Table 1.1 lists the models and methods tested in this study. These models and methods were chosen because of their applicability to the developing watershed. Another reason is the widespread use by the consulting engineering community for the design or analysis of urban drainage systems.

Table 1.1 - Models and Methods Tested

FULL HYDROGRAPH SIMULATION MODELS :

- EPA Storm Water Management Model, SWMM 4.05 (1991)
- SCS Computer Program for Project Formulation-Hydrology, TR-20 (1983)
- US Army Corps of Engineers Flood Hydrograph Package, HEC-1 (1990)
- Penn State Runoff Quality Model, PSRM-QUAL (1991)

UNIT HYDROGRAPH METHODS:

- SCS Curvilinear Unit Hydrograph (1949)
- Snyder Unit Hydrograph (1938)
- Clark Unit Hydrograph (1945)

DESIGN RAINFALL, HYDROGRAPH METHODS:

- SCS Urban Hydrology for Small Watersheds, TR-55 (1986)
- Rational Method (1850)
- Modified Rational Method (1974)
- Universal Rational Method

DESIGN RAINFALL, PEAK ONLY METHODS:

- United States Geological Survey Virginia Regression Equations (1978)
 - The Anderson Method (1968)
-

1.2 Literature Review

There have been only a few model comparison studies in the past.

Unfortunately none of these include the current capability of many of the more sophisticated models to run on the standard desktop personal computer. Most of these studies also failed to take into account the small developing and urban watersheds with

1. Introduction

extremely short times of concentration. Many drainage engineers are using simple and sometimes outdated procedures as the basis for their design. Economic considerations are one of the single most important reasons for using a different model in the design of drainage and storm water management facilities. For instance, TR-55 tends to provide a conservative estimate of the flood peak due to the assumptions inherent in the method. A structure designed by this method would be sufficient, however it is more than likely oversized. An oversized facility is a waste of the funds that could have been appropriated toward the use of a more sophisticated model which would provide a less conservative design with possible increase in overall project savings. (Linsley, 1978)

Linsley gave a critical review of the available storm water models in 1971, and concluded that most of the models developed at that time were for large river basins or agricultural watersheds and hence not relevant for the small urban or developing watershed. In 1973, Papadakis and Pruehl tested EPA SWMM with another kinematic urban watershed model on the Blood Run watershed near Cincinnati, Ohio. They concluded that the infiltration parameters had a very distinctive effect on the runoff hydrograph and that the small urban watershed is "very flashy." (Overton and Meadows, 1976)

Keser (1978) conducted a comparison of two versions of the Rational Method, two types of synthetic unit hydrographs and six other methods which solve the full

dynamic equations of flow. Kinematic wave approximation models were included in the set of full dynamic models. Each of the models were applied on two small, highly impervious watersheds near Hannover, Germany. Varying results in hydrograph shape were shown, but the chosen rainfall distribution was found to be the greatest factor. When all of the models were calibrated, the full simulation models produced results which coincided almost perfectly. The other models contained more errors in their calibrations.

A major literature search which compared models was completed by the American Society of Agricultural Engineers. (Renard and Fogel, 1982) This study compared 75 different watershed models. The authors listed the processes simulated as well as the geographic area and land uses where the models should be used. Of the models included in this list only a few are in widespread use today. Some models included are SWMM, TR-20, HEC-1 and an early version of PSRM. Unfortunately, this study did not compare each of the models quantitatively for ungaged watershed prediction and most of the models could only be implemented on the mainframe computer.

Kibler et al (1987) completed a study comparing many different models and methods for design flow determination on a 95 acre site in Bellevue, Washington. This study mainly focused on the rainfall distributions used in the models and their use in developing flood frequency curves. The conclusion of the paper was that the

choice of the rainfall distribution is crucial, although no firm conclusion on model choice could be made. Giotom and Woodward (1988) evaluated the predictive capabilities of many of the models compared in this evaluation on the 560 acre Walnut Gulch experimental rangeland watershed near Tombstone, Arizona. However, only peak flows for design recurrence intervals were modeled and compared with the Log Pearson Type III (LP III) flows calculated from the observed flows.

Kibler et al (1989) describes a continuation to a study where some desktop procedures are compared to a calibrated simulation model. The Penn State Runoff Model (PSRM) was calibrated on seven watersheds throughout Pennsylvania. Design storms were run through the calibrated PSRM models and the results are compared to some design rainfall based methods. Kibler et al concluded that both the graphical and tabular procedures in the current 1986 SCS TR-55 had a "... marked improvement ...over the 1975 version..." and that the Rational Method with Rawls C-factor also did very well on small developing watersheds. The SCS Curvilinear Unit Hydrograph and the Espey 10-min Unit Hydrograph also were determined to be valid procedures in Pennsylvania.

A study by Jennings et al (1989) compared SCS TR-55, USGS regression equations and observed flood frequency curves on four urban sites as well as other USGS hydrologic simulators. They found that the regression equations overestimate the computer flood frequency curves. TR-55 was found to not only overestimate the

actual frequency data, but on some watersheds to overestimate the regression equation flood peaks by a factor of two.

Meadows (1989) studied the effects of TR-55 on the coastal areas of South Carolina. He concluded that TR-55 was applicable for areas where surface flow dominated the time of concentration. In areas where base flow contributes largely to the time of concentration calculation, TR-55 is not applicable. Also, the shape of the 484 unit hydrograph on which TR-55 is based was found to be inappropriate for coastal and lowland areas. Overton (1989) indicates that the lack of a scientific basis in TR-55 is a serious liability in peak flow and hydrograph calculations

Chapter 2

Description of Models

The first documented use of a basic hydrologic model was in 1674 in France.

Pierre Perrault was the first person to prove quantitatively in his book *De l'origine des fontaines* that rainfall and snow melt were responsible for river flow . This discovery formed the basis of the concept of the hydrologic cycle, which is the basis of all watershed hydrologic models used today.

2.1 Model Choice

There are many ways in which engineers design drainage and storm water management structures. The choice of hydrologic model often depends on what type of structure and how much damage that could be caused by the destruction of the structure. Some models, such as the USGS regression equations, provide only peak flows for design rainfall events, while others, such as EPA SWMM, provide full hydrographs for any rainfall hyetograph. These differences require some distinction when comparing various models. Table 1.1 classifies the drainage models used in this study by the type of input required and output received. Peak discharge methods do not provide sufficient information for the design of a detention basin. However, the

use of a full simulation model is hardly justified in the design of a simple roadway culvert.

Many of the inputs for the models are similar. All of the models require some representation of the watershed physical characteristics such as the basin slope and the drainage area. Infiltration and other major losses play an important role in all of the models studied. Some representation of precipitation, be it a design rainfall, uniform intensity or a time series hyetograph, is also required in all of the models presented. A computer program was written which requires the minimum number of input parameters. The program uses the minimum parameters to calculate the rest of input parameters for the models used in this evaluation. The Virginia Interactive Program for Efficient Runoff (VIPER) data manager provides an environment for which a minimum amount of data is entered. VIPER provides the input data files in proper format for most of the models in the study. In this way, consistency of watershed parameters between the models is maintained.

2.2 Review of Hydrologic Capability of Models and Methods

A simple review is presented to provide a basis for comparison and physical description of the differences in computational methods for each model. A listing of the input requirements as well as the available sources of the input is also included.

Finally, the level of sophistication and amount of output produced by each model is reviewed.

2.2.1 EPA SWMM

The United States Environmental Protection Agency's Storm Water Management Model (SWMM) was developed in 1969-1970 by a consortium of contractors, Water Resources Engineers, Inc. (now Camp, Dresser and McKee, Inc.), Metcalf and Eddy, Inc. and the University of Florida. Since the first version was introduced in 1971, three major revisions were completed. The latest version, SWMM 4.05, is perhaps the most comprehensive simulation model for the microcomputer today. Huber and Heaney (1981) give a very good summary of the capabilities of the Storm Water Management Model (SWMM) version 3, which is the major version still in use in the hydrologic modeling community. SWMM version 4.05, which is gaining popular use, is the SWMM version used in this study.

SWMM requires about 500 kilobytes of core storage to run on the computer and is able to run on mainframe, minicomputers as well as microcomputers. It is the ability to run on the microcomputer which has enabled SWMM to be useful to the typical consulting engineer. It is unreasonable to expect every consultant to be able to afford the more expensive hardware required by other complex simulators. SWMM

and many complex simulation models were developed at the same time including the Hydrologic Simulator Program-FORTRAN (HSPF) and the Stanford Watershed Model.

Some recent changes to SWMM include free format of the input data cards, input in either English or Metric units, continuous rainfall simulation from National Weather Service data as well as improved input and output entry. SWMM has adapted at a competitive rate with the changing microcomputer technology. Other enhancements and refinements are referred to in the SWMM4 User's Manual. (Huber et al, 1988)

SWMM allows for many different configurations of rainfall data, including actual historical storms as well as design rainfall hyetographs. Varying time increments of precipitation is also handled by SWMM, although it is much more difficult to use than a constant time increment rainfall. Cumulative distributions and incremental distributions of precipitation are handled with the same level of ease. Snowfall events are also allowed, but with an increasing amount of data input requirements.

The infiltration of the rainfall into the groundwater table can be accomplished in SWMM by one of two methods. The Horton equation, developed by Horton in 1939-1940, was the method utilized for infiltration since the first introduction of SWMM. This empirical method employs a first order decay from a maximum infiltration rate to a minimum infiltration rate. The maximum infiltration rate allows

the user to specify the Antecedent Moisture Condition (AMC) of the soils. In continuous simulation, the infiltration rate is allowed to recover as outlined in the SWMM manual. (Huber et. al., 1988) The Horton equation shown in (2.1) is not applied directly in SWMM. The modified Horton method uses the accumulated rainfall volume and the accumulated infiltration volume to locate a time of ponding. This is found by integrating (2.1). The modified method takes into account multi-peaked hyetographs where the rainfall rate drops below the infiltration rate and runoff is not produced. The parameters required by SWMM for modeling are the maximum and minimum infiltration rates, and the decay constant.

$$f = f_o + (f_o - f_c) e^{-kt} \quad (2.1)$$

Where:

t	= time in hours
f	= infiltration rate at time t, in in/hr {cm/hr}
f _o	= maximum infiltration rate in in/hr {cm/hr}
f _c	= minimum infiltration rate in in/hr {cm/hr}
k	= decay constant in hr ⁻¹

The parameters for the Horton equation may be determined from soil surveys of the watershed and area-weighted to obtain average infiltration parameters for a given sub-basin. Figure 2.1 shows a graph of infiltration rates for a given type of soil. (Aron et al., 1992)

The other method utilized in SWMM for infiltration is the Green-Ampt equation. This equation allows for a more physically based method to be employed

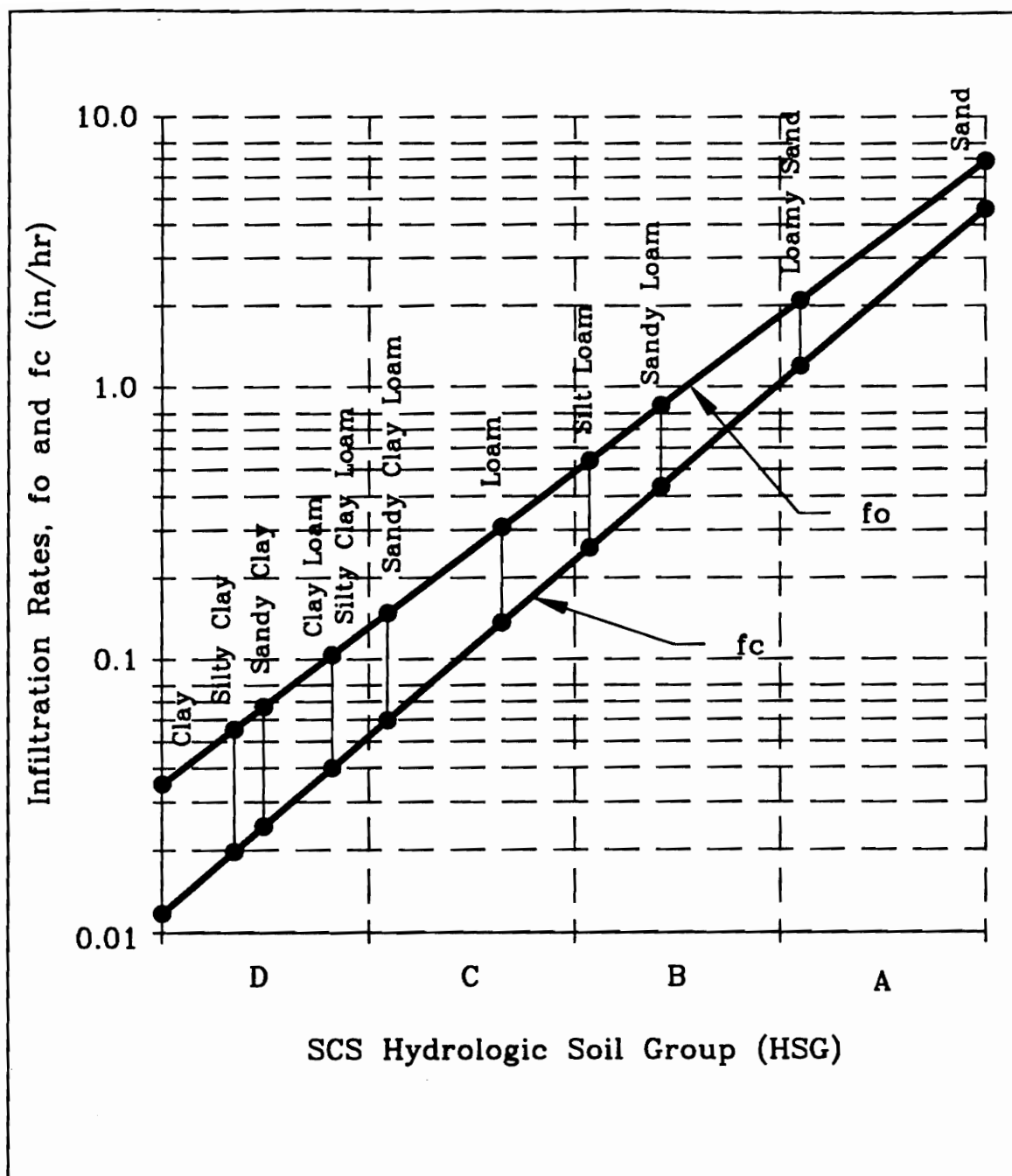


Figure 2.1 - Horton Infiltration Parameters for Various Soil Types (Aron et al., 1992)

while still maintaining some semblance of accuracy. The Green-Ampt equation is not used in this study for the SWMM models. For a full explanation of the equation, refer to the SWMM user's manual.

Evaporation and depression storage are determined separately by SWMM. If evaporation rates are unknown, as assumed in this study, then they are not included in the input file and SWMM assumes a default evaporation rate of 0.1 inches (0.25 cm) per month. For the event-base models typically used in drainage design, evaporation is essentially negligible. Depression storage is separated into the pervious area depression storage and the impervious depression storage. They are supplied to SWMM in convenient units of watershed inches (or cm). If unknown, the default values recommended by SWMM are 0.25 in (0.635 cm) and 0.016 in (.0406 cm) for the pervious and impervious areas respectively. Infiltration processes are not assumed to begin until the depression storage volumes are filled and evaporation of them has not occurred.

Once rainfall excess volumes are determined by subtracting the losses from the precipitation volumes, a hydrograph can be generated. SWMM utilizes the kinematic wave approximation to the full dynamic equations for overland and channel/pipe flow. A Newton-Raphson numerical scheme is used to solve the differential equation shown in (2.2). The basic assumption of the kinematic approximation is that the momentum equation can be reduced. The reduction is found by assuming the bed slope is equal

to the energy slope. By using a uniform flow equation with the mass conservation equation one can derive the kinematic wave equation for overland flow as formulated in (2.2).

$$q = \frac{\partial A}{\partial t} + \alpha m A^{m-1} \frac{\partial A}{\partial x} \quad (2.2)$$

Where:

- q = rainfall excess rate
- A = cross sectional flow area
- t = time
- x = distance in direction of flow
- α = constant depends on uniform flow equation used
= $1.486/n \sqrt{s}$ for Manning's turbulent flow equation
- n = Manning's roughness coefficient
- s = bed slope
- m = exponent depends on uniform flow equation used
= 5/3 for Manning's turbulent flow

The kinematic wave equation is derived by making the assumptions listed in

Table 2.1.

The overland flow from each of the sub-basins is calculated on a flow per unit width of flow area basis. It is then multiplied by the width of the basin. Flows are routed through the main channel to the outlet of the sub-basin where they enter either the downstream drainage network to be combined with the other sub-basin flows or the outlet of the watershed. Figure 2.2 depicts an idealized subcatchment as computed in SWMM.

Table 2.1 - Kinematic Wave Assumptions

-
- Bed slope equals the energy gradient
 - Uniform flow can be defined by a friction loss equation (in the case of the models in this evaluation, Manning's equation is used)
 - Roughness coefficients developed for steady flow are applicable
 - Pressure gradient is hydrostatic
 - Water surface is horizontal across cross section (No lateral accelerations)
-

The width of the sub-basins can be hard to determine, especially when modeling natural, meandering channels or when the main channel is located to one side of the sub-basin. The SWMM user's manual suggests the employment of a skew factor to provide an average overland flow width. (2.3) is used in this study to determine a "best guess" at the overland flow width.

$$W = (2 - S_k)L$$

$$S_k = \frac{|A_1 - A_2|}{A_1 + A_2} \quad (2.3)$$

Where:

- W = width of overland flow
- L = length of main channel
- Sk = area skew coefficient
- A1 = area to one side of the main channel
- A2 = area to the other side of main channel

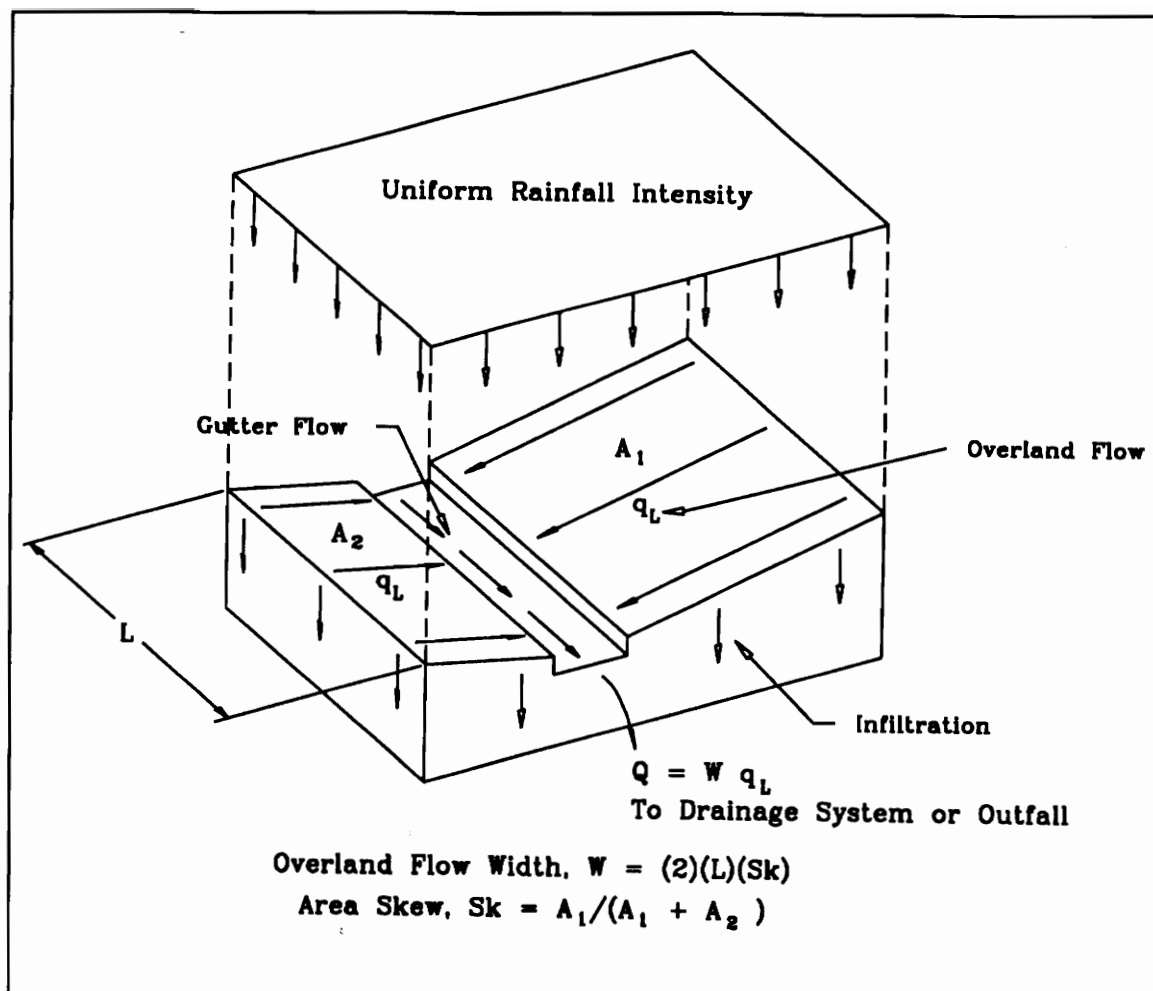


Figure 2.2 - Idealized SWMM Subcatchment

The width of the sub-basins provides a valuable calibration parameter and is probably the single most important variable in determining hydrograph shape. SWMM divides the overland flow into unit width segments of two differing types: impervious areas and pervious areas. This division requires the use of three more parameters:

percent of impervious area and the pervious and impervious roughness coefficients. The impervious area is that area directly connected to the drainage network which provides no infiltration losses.

Once the flows are determined at the outlets of the sub-areas, these flows are routed and combined in a separate block of the overall SWMM program through the drainage system to the outlet of the watershed. This is accomplished by kinematic wave routing within the channel or pipe elements. Detention storage elements utilize the modified Puls technique to route the flows through the reservoir by supplying the rating curve information. Inflows into the drainage network are only allowed at so-called manholes which contain no losses and are the only places where hydrographs can be evaluated or combined. Many different configurations of channel geometry are allowed including channels with irregular shape and compound roughness. The irregular sections require the section station-elevation information while all other sections are described by as many as three dimensions.

The additional features of SWMM make it a worthwhile model to use for the design and analysis of complicated and unusual hydraulic structures design. SWMM is divided into different programming modules called "blocks." SWMM's many other blocks (not described here) enable the user to model combined sewer facilities as well as water treatment facilities, pollutant washoff and removal processes and continual rainfall/runoff simulation. Separate blocks of SWMM also enable the user to model

different sections of the test system using different configurations without recalculating the previous sections over again. This capability could save time on a huge sewer project but hardly seems necessary for the small housing development with only a few drainage pipes. The overwhelming disadvantage of SWMM is the requirement for a large amount of data to accomplish what could be a much simpler task. On a 200 acre watershed one would expect SWMM to model the hydrologic process well, but probably not within the boundaries of economic practicality.

Table 2.2 lists the required input for SWMM to determine runoff quantity, mainly hydrographs, at a specific point. Also listed are the possible source maps and references where this data could be obtained. As can be seen in Table 2.2, the input data for SWMM can be overwhelming. It is this requirement that causes the typical consulting engineer to frown on the use of SWMM for design. If the use of such a functional model can be justified then maybe more common use of SWMM will result.

The output to the SWMM model is quite extensive but can provide very useful information. Echoing of the input data can be accomplished depending on the options in the input file. Graphs of precipitation, infiltration and runoff can be provided as well as other options. A continuity check in each block of operations is provided automatically and a step-by-step listing of each calculation with daily, monthly and yearly summaries for each drainage element can also be requested. Separate ASCII files of the hydrographs can be generated for further analysis by separate post-

Table 2.2 - Physical Input Parameters for SWMM

<u>Input Variable</u>	<u>Likely Source of Data</u>
OVERALL RUNOFF BLOCK:	
Rainfall Hyetograph	Gage Records/Design Storm
Monthly Evaporation Rates	Local Records/Pan Testing/Default
FOR EACH SUBAREA COLLECTOR CHANNEL:	
Collector Downstream Element	Drainage Network Schematic
Type of Collector Channels	Site Plan/Topo Maps/Proposed
X-Section Geometry of Collector Channels	Site Plan/Topo Maps/Proposed
Length of Collector Channels	Site Plan/Topo Maps/Proposed
Slope of Collector Channels	Site Plan/Topo Maps/Proposed
Manning's 'n' of Collector Channels	Topo Maps/Handbooks/Experience
Bankfull Depths of Collector Channels	Topo Maps
Initial Depth of Collector Channels	Site Visit/Experience/Assumption
FOR EACH SUBAREA:	
Downstream Collector ID	Drainage Network Schematic
Overland Flow Width	Topo Map/Calculation
Drainage Area	Topo Map
Percent Impervious	Topo Map/GIS/Population Estimates
Ground Slope	Topo Map
Manning's 'n' on Impervious Areas	Topo Maps/Handbooks/Experience
Manning's 'n' on Pervious Areas	Topo Maps/Handbooks/Experience
Impervious Area Depression Storage	Topo Maps/Handbooks/Experience
Pervious Area Depression Storage	Topo Maps/Handbooks/Experience
Maximum Horton Infiltration Rate	Soil Survey/Handbooks/Experience
Minimum Horton Infiltration Rate	Soil Survey/Handbooks/Experience
Horton Infiltration Decay Rate	Soil Survey/Handbooks/Experience
TRANSPORT BLOCK OVERALL:	
Number of Nodes there is Inflow from RUNOFF	Drainage Network Schematic
FOR EACH ELEMENT IN DRAINAGE NETWORK:	
Three Upstream Element IDs	Drainage Network Schematic
Element Type (Shape)	Site Plan/Topo Map
Element Length	Site Plan/Topo Map/Proposed
Element Slope	Site Plan/Topo Map/Proposed
Three Characteristic Cross Section Dimensions	Site Plan/Topo Map/Proposed
Element Manning's 'n'	Land Use Maps/Handbooks/Experience
Number of Barrels	Site Plan/Topo Map/Proposed
SPECIAL CASE: IRREGULAR (NATURAL) CHANNELS:	
Left and Right Overbank Manning's 'n'	Site Visit/Handbooks/Experience
Station and Elevations of Cross Section	Site Plan/Topo Map/Proposed
FOR EACH RESERVOIR:	
Initial Elevation	Site Visit/Assumption
Depth-Area-Volume-Outflow Data	Topo Maps/Hydraulic analysis

processor programs, too. Table 2.15 through Table 2.20 evaluate the capabilities of SWMM in comparison to the other models presented in this evaluation.

2.2.2 TR-20

The United States Department of Agriculture, Soil Conservation Service (SCS) Technical Release 20, *Computer Program for Project Formulation-Hydrology* (TR-20) computer program was developed in order to automate previously published standard SCS procedures. Although primarily developed for agricultural watersheds, TR-20 has had much use in developing regions and has even been adopted by many municipalities as the model of choice for engineers submitting plans for review. (Prince William County, 1992) This popularity of TR-20 was brought on due to the relative ease of estimating the model parameters, and because the program was readily available for use on personal computers as early as 1982.

TR-20 develops the hydrograph by the SCS curvilinear unit hydrograph procedure. This procedure is based on empirical studies completed by the SCS on experimental agricultural watersheds. The only parameters required for the procedure are the SCS lag time and the drainage area. The lag time has been found to be related empirically to the time of concentration of the basin. (Williams, 1981) The use of the unit hydrograph allows precipitation to be either a design storm or a recorded storm event. Infiltration and other losses are subtracted from precipitation using the

controversial SCS runoff curve number (CN) method. The CN method is based on results from agricultural watershed runoff studies and empirically derived. Lists of curve numbers are published extensively. The curve number is a function of land use and SCS hydrologic soil group (HSG). The hydrologic soil groups can be found in local soil survey reports, which SCS has published for most of the United States. The controversial nature of the curve number stems from the fact that there is no physical basis for the curve number calculations. The only way to actually determine a curve number would be to back-calculate from a homogenous gaged watershed. Unfortunately, homogenous watersheds are not easy to come by and must be artificially created which brings in experimental errors. The sub-areas in TR-20 must be homogenous but soil and land use delineations do not always follow the sub-area boundaries. Therefore, an area-weighted composite of the curve number is used to take all land uses and soil types which may fall within a particular sub-basin.

Once the rainfall abstractions are determined and removed from the precipitation, the unit hydrograph may be applied using the rainfall excess to determine the sub-basin outflow. Channel routing in TR-20 is accomplished using a Modified Attenuation-Kinematic (Mod-AttKin) methodology. This method is an attempt to utilize kinematic wave channel routing, which provides only translation, and a modified Puls (a.k.a.: storage indication) method, which provides the peak reduction seen in natural channels. A typical cross section for the reach of interest is developed

to determine the stage-storage-discharge table for input to the program. TR-20 calculates the routing constants from the relation shown in (2.4).

$$Q = x A^m \quad (2.4)$$

where Q = discharge at current elevation
A = cross-sectional area of flow at current elevation
x = routing constant coefficient
m = routing constant exponent

The routing constants will not remain constant for irregular shaped sections or for compound channels. The routine in TR-20 is believed to be a simple linear regression of log-transformed data (the details of the method are not published). This method would approximate any section while still maintaining constant routing constants. Unfortunately, the Mod-AttKin method is frequently unstable and has a very weak theoretical basis. It is expected (and hoped) that the method will be removed in future releases of the program. Reservoir routing is accomplished by the modified Puls method.

Table 2.3 lists all input required for TR-20 as well as possible sources for this data. TR-20 requires all input in fixed-field format ASCII files typical of many FORTRAN programs at the time. This inconvenience is easily remedied by a pre-processing program which could also be used to generate the cross section table for channel routing or reservoir routing tables. The number of time steps is limited to 300

ordinates and a minimum time step of 0.1 hours. These two limitations severely limit TR-20's abilities as an effective runoff model for developing watersheds. The minimum time step also sets limits on minimum reach length for stable channel routing. The limitation on the number of ordinates sets limits on the resolution of the precipitation input. By increasing the time step to fit the whole storm into the 300 ordinates, small amounts of rainfall and short duration, intense storm bursts are reduced or simply eliminated. One solution is to provide a cumulative rainfall volume curve which defines the storm. This curve would maintain the total volume but unfortunately would still reduce maximum intensities to lower values.

Output from TR-20 is variable depending on the options entered in the input file. Complete cross section routing information can be presented if desired as well as the plot of the section. Complete summary tables are provided which show all results from the hydrologic operations, routing calculations and a listing of peak discharges at each sub-area and channel reach or reservoir. Input files for SCS's economic analysis program as well as their flood frequency analysis program can also be created. Hydrographs can be output to ASCII text files for post processing or for direct entry into the SCS DAMS2 computer program for reservoir analysis. Table 2.15 through Table 2.20 summarize the capabilities of TR-20 as compared with the other models used in this study.

Table 2.3 - Physical Input Parameters for TR-20

<u>Input Variable</u>	<u>Likely Source of Data</u>
OVERALL:	
Hydrological Computation Order	Drainage Network Schematic
Rainfall Hyetograph	Gage Records/Design Storm
FOR EACH SUBAREA:	
Downstream Drainage Element ID	Drainage Network Schematic
Drainage Area	Topo Map
SCS Curve Number	Soil Survey/Land Use Maps/GIS
Time of Concentration:	SCS Segmental Method
• 2-yr, 24-hr Storm Volume	Local IDF Curves
• Sheet Flow Length	Site Plan/Topo Map/Proposed
• Sheet Flow Slope	Site Plan/Topo Map/Proposed
• Sheet Flow Manning's 'n'	Topo Maps/Handbooks/Experience
• Concentrated Flow Types	Site Plan/Topo Map/Proposed
• Concentrated Flow Lengths	Site Plan/Topo Map/Proposed
• Concentrated Flow Slopes	Site Plan/Topo Map/Proposed
• X-Section Area of Channel Flow	Site Plan/Topo Maps/Proposed
• X-Section Wetted Perimeter of Channel Flows	Site Plan/Topo Maps/Proposed
• Length of Channel Flow	Site Plan/Topo Maps/Proposed
• Slope of Channel Flow	Site Plan/Topo Maps/Proposed
• Manning's 'n' for Channel Flow	Topo Maps/Handbooks/Experience
FOR EACH ELEMENT IN DRAINAGE NETWORK:	
Element IDs	Drainage Network Schematic
Elevation-Cross Sectional Area-Outflow Table	Calculation
• Element Type (Shape)	Site Plan/Topo Map
• Element Length	Site Plan/Topo Map/Proposed
• Element Slope	Site Plan/Topo Map/Proposed
• Characteristic Cross Section Dimensions	Site Plan/Topo Map/Proposed
• Element Manning's 'n'	Land Use Maps/Handbooks/Experience
FOR EACH RESERVOIR:	
Initial Elevation	Site Visit/Assumption
Elevation-Surface Area-Outflow Data	Topo Maps/Hydraulic analysis

2.2.3 HEC-1

The United States Army Corps of Engineers has combined many of the programs developed for hydrology and flood control into an integrated set of programs: *HEC-1, Flood Hydrograph Package*. HEC-1 uses commonly used methods

for stream network watershed simulation. These methods include the SCS unit hydrograph, Snyder's unit hydrograph, Clark's instantaneous unit hydrograph and the kinematic wave equations. For stream routing the Muskingum method, Muskingum-Cunge diffusion routing, kinematic wave channel routing and simple time-lag routing. Other features include ogee spillways and on-line pumps for reservoirs. Many configurations of rainfall input are included as well. They range from the actual gaged storm to a design probable maximum precipitation (PMP) storm. Weighting to account for spatial distributions of rainfall is a major advantage of HEC-1 over other models of its type. The many options within the HEC-1 package account for the great variability of hydrologic practice which, along with frequent updates and well written documentation, explain the popularity of the program.

This study will refer to HEC-1 as a set of specific operations within the whole package. Specifically, the kinematic wave overland flow hydrograph coupled with Muskingum-Cunge diffusion routing is used to produce the hydrograph. This convention is to maintain consistency in the study by evaluating the more sophisticated models as well as the unit hydrographs featured in HEC-1. The kinematic wave routine is considered sophisticated because it requires more inputs than other hydrograph procedures and has a more physical basis by looking at the flow process.

Rainfall abstractions are computed by the SCS curve number method because of the availability of information on the curve number and its relative popularity. The

number of routing methods is limited because the kinematic wave hydrograph generation routine in HEC-1 requires either kinematic wave channel routing or diffusion routing within the collector channels. Muskingum-Cunge diffusion routing is the routing method chosen specifically because of the physical basis of the routing technique. The method is also independent of the time step, unlike the kinematic wave routing. The pipe flow routing scheme does not, however, accurately account for surcharge or pressure flow. In fact, the cross sectional area of flow is allowed to exceed the pipe diameter.

The HEC-1 user's manual contains a lengthy derivation of the equations and explains the finite difference solution technique used in the kinematic overland flow equations (HEC, 1990). It is the finite difference solution technique which makes HEC-1 different from all the other models featured in this study which use the kinematic wave equations. The finite difference technique is dependent on time step as well as channel reach length or overland flow length. This would imply that the errors introduced by the method would vary with watershed size. This variation is the focus of the evaluation presented in Chapter 5.

Table 2.4 lists the inputs for the HEC-1 routines used in this study and the possible sources of this information. Table 2.15 through Table 2.20 lists the options and other features included in the HEC-1 package in addition to the capabilities of the routines outlined here and compares these capabilities with the other models.

Table 2.4 - Physical Input Parameters for HEC-1 (KW)

<u>Input Variable</u>	<u>Likely Source of Data</u>
OVERALL:	
Hydrological Computation Order	Drainage Network Schematic
Rainfall Hyetographs w/ Weighting Factor	Gage Records/Design Storm
FOR EACH SUBAREA:	
Drainage Area	Topo Map
SCS Curve Number for Impervious Areas	Soil Survey/Land Use Maps/GIS
SCS Curve Number for Pervious Areas	Soil Survey/Land Use Maps/GIS
Percent Impervious	Topo Map/GIS/Population Estimates
Overland Flow Length for Impervious Areas	Site Plan/Topo Map/Proposed
Overland Flow Length for Pervious Areas	Site Plan/Topo Map/Proposed
Overland Flow Slope for Impervious Areas	Site Plan/Topo Map/Proposed
Overland Flow Slope for Pervious Areas	Site Plan/Topo Map/Proposed
Manning's 'n' on Impervious Areas	Topo Maps/Handbooks/Experience
Manning's 'n' on Pervious Areas	Topo Maps/Handbooks/Experience
FOR EACH SUBAREA COLLECTOR CHANNEL:	
Shape of Collector Channels	Site Plan/Topo Maps/Proposed
X-Section Geometry of Collector Channels	Site Plan/Topo Maps/Proposed
Length of Collector Channels	Site Plan/Topo Maps/Proposed
Slope of Collector Channels	Site Plan/Topo Maps/Proposed
Manning's 'n' of Collector Channels	Topo Maps/Handbooks/Experience
Bankfull Depths of Collector Channels	Topo Maps
Initial Depth of Collector Channels	Site Visit/Experience/Assumption
SPECIAL CASE: IRREGULAR (NATURAL) COLLECTORS:	
Overbank Manning's 'n'	Site Visit/Handbooks/Experience
Station and Elevations of Cross Section	Site Plan/Topo Map/Proposed
FOR EACH ELEMENT IN DRAINAGE NETWORK:	
Element Shape	Site Plan/Topo Maps/Proposed
X-Section Geometry of Element	Site Plan/Topo Maps/Proposed
Element Length	Site Plan/Topo Map/Proposed
Element Slope	Site Plan/Topo Map/Proposed
Element Manning's 'n'	Land Use Maps/Handbooks/Experience
Bankfull Depths of Channels/Diam. of Pipes	Topo Maps
Initial Depth within Elements	Site Visit/Experience/Assumption
SPECIAL CASE: IRREGULAR (NATURAL) CHANNELS:	
Left and Right Overbank Manning's 'n'	Site Visit/Handbooks/Experience
Station and Elevations of Cross Section	Site Plan/Topo Map/Proposed
FOR EACH RESERVOIR:	
Initial Elevation	Site Visit/Assumption
Elevation-Area/Volume-Outflow Data	Topo Maps/Hydraulic analysis

2.2.4 PSRM-QUAL

The Pennsylvania State University in cooperation with the Pennsylvania Department of Environmental Resources and the United States Environmental Protection Agency developed the Penn State Runoff Quality Model (PSRM-QUAL) as an attempt to modify the Penn State Runoff Model (PSRM) to account for storm water quality as well as quantity. The new PSRM-QUAL represents a drastic change from the previous release of PSRM.

PSRM-QUAL computes runoff by solving the kinematic wave equations as in SWMM and HEC-1. However, PSRM-QUAL computes the solution by the method of characteristics. This method is numerically superior to both the Newton-Raphson scheme and the finite difference schemes. The numerical superiority should provide better flood hydrograph estimation. The method uses a cascade of drainage sub-strips with a length which is a fraction of the overall sub-basin length in order to simulate sediment transport on the overland flow plane. Flow is then diverted into the channels which drain immediately below a sub-area where it is routed to the outlet using the Muskingum method.

The Muskingum method is a marked improvement over the previous version of PSRM which used time lagging to route the sub-area hydrographs to the outlet. The Muskingum method uses an explicit equation to route flows to a downstream point which is documented extensively in the literature (Gupta, 1989, Viessman et al, 1977)

and therefore needs no further explanation. If surcharge occurs in the drainage element, it will bypass the element at a different rate than the fraction which flows through the element. This feature is somewhat unique and is a logical element of larger runoff events. Reservoirs are routed using the modified Puls method while allowing for the possibility of temporary flow bypass into a reservoir from a drainage element and later drainage of the reservoir. This option could be highly effective in the sizing of on-line detention basins which are sized based on a fixed outflow rate which may not be exceeded.

The input to PSRM-QUAL is essentially the same as for SWMM and HEC-1. The rainfall input can be for a gaged storm or design storm. The only limitation is in the length of the storm and the time step. These parameters vary depending on the number of sub-basins within the watershed, which of course may vary from run to run. This limitation causes severe problems when dealing with a 24-hour storm as used by SCS. The time step encountered on most watersheds was found to be 20 minutes. This is a gross increment to use for rainfall considering that the time of concentration for a small 50 acre basin could be around 30 minutes. Unfortunately, limiting the time step also limits the duration because, depending on the number of sub-areas, the incremental storm volumes must be consolidated. The consolidation causes short, high intensity rainfall periods to be reduced, which diminishes accuracy and is not representative of reality. The time limitations are solely due the lack of memory

available for PSRM-QUAL because it is written in the BASIC programming language. If the language were changed, making the model memory efficient, then the time limitations would not be a problem.

Rainfall is allowed to vary spatially as well as temporally in PSRM-QUAL. An impressive routine for distributing the rainfall from multiple gages is presented in the users manual where the reader is referred for more information. Multiple rainfall "bursts" are also allowed, but the main reason for this inclusion in PSRM-QUAL is for quality simulations rather than quantity simulation.

Infiltration is computed by the SCS curve number method combined with concepts from the Horton equation. The curve number is used to determine the soil infiltration capacity. The infiltration capacity is then decayed similar to the Horton equation but what is different is the use of a deep percolation equation for recovery of the infiltration rate between storm bursts. This innovative approach to infiltration is augmented by the addition of depression storage losses as well as a coefficient to adjust the initial soil storage capacity. All calculations, including losses and overland flow, are computed separately for pervious areas and added to the impervious area flows before entering the routing computations.

One of the major disadvantages of PSRM-QUAL is the lack of output received from the model. Data is output in a tabular form for all temporal quantities such as infiltration and effective precipitation as well as the runoff. A graphical package is

Table 2.5 - PSRM-QUAL Physical Input Parameters

<u>Input Variable</u>	<u>Likely Source of Data</u>
OVERALL:	
Hydrological Computation Order	Drainage Network Schematic
Rainfall Hyetographs w/ Coordinates	Gage Records/Design Storm
FOR EACH SUBAREA:	
Drainage Area w/ Coordinates	Topo Map
Total Flow Length	Site Plan/Topo Map/Proposed
Ground Slope	Site Plan/Topo Map/Proposed
Impervious Fraction	Topo Map/GIS/Population Estimates
SCS Curve Number for Impervious Areas	Soil Survey/Land Use Maps/GIS
SCS Curve Number for Pervious Areas	Soil Survey/Land Use Maps/GIS
SCS Initial Abstraction Factor	Soil Survey/Default Values
Impervious Area Depression Storage	Topo Maps/Handbooks/Experience
Pervious Area Depression Storage	Topo Maps/Handbooks/Experience
Manning's 'n' on Impervious Areas	Topo Maps/Handbooks/Experience
Manning's 'n' on Pervious Areas	Topo Maps/Handbooks/Experience
FOR EACH ELEMENT IN DRAINAGE NETWORK:	
Ratio of In-bank to Overbank Flow Velocities	Calculation from Section/Defaults
Muskingum Weighting Factor, x	Site Visit/Handbooks/Experience
Full Flow Capacity	Manning's Equation/Chezy etc.
• X-Section Geometry of Element	Site Plan/Topo Maps/Proposed
• Element Slope	Site Plan/Topo Map/Proposed
• Element Manning's 'n'	Land Use Maps/Handbooks/Experience
Full Flow Travel Time	Manning's Equation/Chezy etc.
• Element Length	Site Plan/Topo Map/Proposed
FOR EACH RESERVOIR:	
Reservoir Type (On-Line or Off-Line)	Site Plan/Proposed
Initial Elevation	Site Visit/Assumption
Elevation-Storage-Outflow Data	Topo Maps/Hydraulic analysis

included in PSRM-QUAL which is able to plot all of this data to the screen as well as provide printouts. Unfortunately this is the only data output for the model. Items such as a check in continuity or even an echo print of the input listing are not supplied by the model. This lack of output is very disconcerting because it does not allow the user to check for mistakes in the data or even possible instabilities in the

computations. One solution to this would be to provide another file with this information in addition to the present file. All of the options and capabilities of PSRM-QUAL are listed with the other models in Table 2.15 through Table 2.20 . Table 2.5 contains the relevant input for the model to obtain the outflow hydrograph for a watershed.

2.2.5 SCS Unit Hydrograph

The SCS unit hydrograph method (SCS UH) is the same that is used in the TR-20 computer program and the HEC-1 flood hydrograph package. Unit hydrographs can be applied in many different ways. For this study the SCS unit hydrograph is applied on the test watersheds as a whole as well as on a multitude of sub-basins. It is obvious that the SCS unit hydrograph is easier to apply to the whole watershed because there are fewer parameters for the designer to estimate. However, discretization of the watershed should give a more realistic solution by taking into account the spatial heterogeneity of the watershed. The Muskingum routing method is used to route the sub-area unit hydrograph flows to the outlet. The HEC-1 package is used in this study for the sub-area SCS unit hydrograph simulations while a modified version of a program found in the Penn State Urban Hydrology Model (PSUHM) was used to determine the direct runoff hydrographs on the whole basin. HEC-1 may be used for the whole basin simulation but the BASIC program is faster and

Table 2.6 - Physical input parameters for SCS Unit Hydrograph (Sub-areas within HEC-1)

<u>Input Variable</u>	<u>Likely Source of Data</u>
OVERALL:	
Hydrological Computation Order	Drainage Network Schematic
Rainfall Hyetographs w/ Weighting Factor	Gage Records/Design Storm
FOR EACH SUBAREA:	
Drainage Area	Topo Map
SCS Curve Number	Soil Survey/Land Use Maps/GIS
Percent Impervious	Topo Map/GIS/Population Estimates
Time Lag:	From Time of Conc. (SCS Seg. Meth./Others)
• 2-yr, 24-hr Storm Volume	Local IDF Curves
• Sheet Flow Length	Site Plan/Topo Map/Proposed
• Sheet Flow Slope	Site Plan/Topo Map/Proposed
• Sheet Flow Manning's 'n'	Topo Maps/Handbooks/Experience
• Concentrated Flow Types	Site Plan/Topo Map/Proposed
• Concentrated Flow Lengths	Site Plan/Topo Map/Proposed
• Concentrated Flow Slopes	Site Plan/Topo Map/Proposed
• X-Section Area of Channel Flow	Site Plan/Topo Maps/Proposed
• X-Section Wetted Perimeter of Channel Flows	Site Plan/Topo Maps/Proposed
• Length of Channel Flow	Site Plan/Topo Maps/Proposed
• Slope of Channel Flow	Site Plan/Topo Maps/Proposed
• Manning's 'n' for Channel Flow	Topo Maps/Handbooks/Experience
FOR EACH ELEMENT IN DRAINAGE NETWORK (SUBAREA MODELS ONLY):	
Muskingum Weighting Factor, x	Site Visit/Handbooks/Experience
Full Flow Travel Time:	From Manning's Equation
• X-Section Geometry of Element	Site Plan/Topo Maps/Proposed
• Element Slope	Site Plan/Topo Map/Proposed
• Element Manning's 'n'	Land Use Maps/Handbooks/Experience
• Element Length	Site Plan/Topo Map/Proposed
FOR EACH RESERVOIR:	
Initial Elevation	Site Visit/Assumption
Elevation-Area/Volume-Outflow Data	Topo Maps/Hydraulic analysis

used for the whole basin simulation but the BASIC program is faster and computationally equivalent to the HEC-1 hydrographs using the same method.

2.2.6 The Clark Instantaneous Unit Hydrograph

The Clark Instantaneous Unit Hydrograph (Clark IUH) is a variation of basic unit hydrograph theory (Clark, 1945). The basis of the instantaneous unit hydrograph lies in the time-area curve developed for a particular basin. This curve will be unique to all basins, but synthetic approximations to these curves are possible. The curve is constructed by determining iso-temporal lines where the time to reach the outlet is the same for all points on the line. Equal increments of time are used and the area between these incremental lines is determined. Cumulative area contributing to runoff is plotted as a function of time to complete the curve. The curve is typically S-shaped and serves as one of three parameters used to determine the synthetic unit hydrograph. A sub-area hydrograph is computed by converting the ordinates of the time-area curve to volumes assuming one inch of runoff.

The inflow hydrograph is then routed through a linear reservoir. This operation accounts for the storage effects of the watershed based on two parameters. The parameters are the time of concentration (t_c) of the basin and the Clark Storage coefficient (R). The time of concentration is simply determined in any of the traditional manners while the storage coefficient is determined from experience and/or other references. One simple method of determining R is to calculate it as a fraction of the time of concentration, typically 0.5. Once the unit hydrograph is determined

then the direct runoff hydrograph is computed by the traditional unit hydrograph technique.

Table 2.7 - Physical Input Parameters for Clark's Instantaneous Unit Hydrograph

<u>Input Variable</u>	<u>Likely Source of Data</u>
OVERALL:	
Hydrological Computation Order	Drainage Network Schematic
Rainfall Hyetographs w/ Weighting Factor	Gage Records/Design Storm
FOR EACH SUBAREA:	
Drainage Area	Topo Map
SCS Curve Number	Soil Survey/Land Use Maps/GIS
Percent Impervious	Topo Map/GIS/Population Estimates
Clark Storage Coefficient, R	Handbooks/Experience/Estimating Calcs.
Time of Concentration:	SCS Segmental Method/Others
• 2-yr, 24-hr Storm Volume	Local IDF Curves
• Sheet Flow Length	Site Plan/Topo Map/Proposed
• Sheet Flow Slope	Site Plan/Topo Map/Proposed
• Sheet Flow Manning's 'n'	Topo Maps/Handbooks/Experience
• Concentrated Flow Types	Site Plan/Topo Map/Proposed
• Concentrated Flow Lengths	Site Plan/Topo Map/Proposed
• Concentrated Flow Slopes	Site Plan/Topo Map/Proposed
• X-Section Area of Channel Flow	Site Plan/Topo Maps/Proposed
• X-Section Wetted Perimeter of Channel Flows	Site Plan/Topo Maps/Proposed
• Length of Channel Flow	Site Plan/Topo Maps/Proposed
• Slope of Channel Flow	Site Plan/Topo Maps/Proposed
• Manning's 'n' for Channel Flow	Topo Maps/Handbooks/Experience
FOR EACH ELEMENT IN DRAINAGE NETWORK (SUBAREA MODELS ONLY):	
Muskingum Weighting Factor, x	Site Visit/Handbooks/Experience
Full Flow Travel Time:	Manning's Equation/Chezy etc.
• X-Section Geometry of Element	Site Plan/Topo Maps/Proposed
• Element Slope	Site Plan/Topo Map/Proposed
• Element Manning's 'n'	Land Use Maps/Handbooks/Experience
• Element Length	Site Plan/Topo Map/Proposed
FOR EACH RESERVOIR:	
Initial Elevation	Site Visit/Assumption
Elevation-Area/Volume-Outflow Data	Topo Maps/Hydraulic analysis

This study will utilize the Clark instantaneous unit hydrograph found in the HEC-1 flood hydrograph package. As in the SCS unit hydrograph method, two

separate situations using the Clark instantaneous unit hydrograph are used. The whole basin hydrograph as well as the sub-area hydrograph are simulated in HEC-1.

Muskingum channel routing and modified Puls routing for the reservoirs are used in the sub-area simulations. Since a time-area curve can be tedious to produce, HEC-1 has a built-in synthetic time-area curve which is used throughout the evaluation.

Therefore the only parameters required for the method in this study are the time of concentration of the basin and the Clark storage coefficient, R . The Muskingum routing parameters are also required for the sub-area models as well.

2.2.7 The Snyder Unit Hydrograph

The Snyder Unit Hydrograph (Snyder UH) was developed from large, typically undeveloped watersheds in the early stages of synthetic unit hydrograph developments (Snyder, 1945). The Snyder unit hydrograph method only calculates seven points on the unit hydrograph. The first three points are the initial time and flow, the peak time and flow and the final hydrograph time given as the time base with flow equal to the initial value. The remaining four points are derived from the hydrograph widths at 50 percent of the peak flow and at 75 percent of peak flow. These points are used to locate the intermediate points on the hydrograph. The method calculates these points and expects the engineer to interpolate a smooth curve through these points where the volume under the curve equals one inch of runoff on the basin. This proves to be a

tedious process, but HEC-1 provides an adequate solution. A synthetic time-area curve is generated and routed through a linear reservoir. The time of concentration and the storage coefficient are adjusted until the unit hydrograph produced is coincident with the calculated Snyder values. In this way a full unit hydrograph is determined while still maintaining the one inch volume constraint. This method is also applied separately on the basin as a whole and on individual sub-areas with Muskingum routing in the sub-area simulation.

The parameters needed to calculate the Snyder unit hydrograph points are the Snyder lag time and the Snyder C_p coefficient. The lag time is essentially equivalent to the SCS lag time and can be computed as a function of the time of concentration or by the traditional Snyder method. The traditional method of calculating the Snyder lag time is to relate the hydrologically longest flow path length, the distance along this path to the centroid and a coefficient representative of the slope of the basin. The exact equations in the method are well documented in the literature and need not be repeated here. The C_p coefficient is a measure of the storage capacity of the basin. Values are found in many hydrology textbooks. Table 2.8 summarizes the input variables necessary for development of the Snyder unit hydrograph within the HEC-1 package. Table 2.15 through Table 2.20 list the capabilities of the unit hydrograph procedures as used in this evaluation.

Table 2.8 - Physical Input Parameters for Snyder's Unit Hydrograph

<u>Input Variable</u>	<u>Likely Source of Data</u>
OVERALL:	
Hydrological Computation Order	Drainage Network Schematic
Rainfall Hyetographs w/ Weighting Factor	Gage Records/Design Storm
FOR EACH SUBAREA:	
Drainage Area	Topo Map
SCS Curve Number	Soil Survey/Land Use Maps/GIS
Percent Impervious	Topo Map/GIS/Population Estimates
Snyder's Peaking Coefficient, C_p	Handbooks/Experience/Estimating Calcs.
Snyder's Standard Lag:	
• Total Flow Length	Site Plan/Topo Map/Proposed
• Snyder's Slope/Storage Coefficient, C_t	Handbooks/Experience/Estimating Calcs.
• Length from Centroid to Outlet	Site Plan/Topo Map/Proposed
FOR EACH ELEMENT IN DRAINAGE NETWORK (SUBAREA MODELS ONLY):	
Muskingum Weighting Factor, x	Site Visit/Handbooks/Experience
Full Flow Travel Time:	Manning's Equation/Chezy etc.
• X-Section Geometry of Element	Site Plan/Topo Maps/Proposed
• Element Slope	Site Plan/Topo Map/Proposed
• Element Manning's 'n'	Land Use Maps/Handbooks/Experience
• Element Length	Site Plan/Topo Map/Proposed
FOR EACH RESERVOIR:	
Initial Elevation	Site Visit/Assumption
Elevation-Area/Volume-Outflow Data	Topo Maps/Hydraulic analysis

2.2.8 SCS TR-55

The Soil Conservation Service, in an attempt to make TR-20 easier to use on the small developing basin, compiled *Technical Release 55, Urban hydrology for Small Watersheds* (TR-55). The method is based on the results of hundreds of runs using TR-20 on many different basins and configurations. The results are then generalized into tabular form based on few parameters. The first disadvantage noticed is the use of the 24 hour SCS design storm. The long storm duration is not always

necessary for the size of basin recommended for use by TR-55. The longer storms tend to produce large flood peaks and correspondingly large detention basins. TR-55 is limited to basins with sub-areas having a time of concentration of less than two hours and routing travel times up to three hours. Only the most intense 8.5 hours contributes to the peak flow on a basin with a limiting time of concentration using the SCS rainfall distribution. (SCS, 1986) The use of the 24 hour storm is required because daily rainfall records were used in the development of the storm distribution.

The disadvantages of TR-55 are outweighed by its ease of use for many engineers. This would explain its popularity for the design of hydraulic structures. Only six parameters need to be calculated to determine the hydrograph used for the design. The SCS rainfall distribution type and the 24 hour design rainfall for the specific frequency of occurrence are easily determined. The United States Weather Bureau's Technical Paper 40 (TP-40) lists 24 hour rainfall amounts for areas east of the 105 meridian unless local rainfall frequency data is unavailable. For areas west of the 105 meridian the National Weather Service's NOAA Atlas 2 is used. Alaska and Hawaii use the Weather Bureau's TP-47 and TP-43, respectively (USDA SCS, 1986). The distribution type relies strictly on where the site lies within the United States. The other four parameters are the time of concentration of each of the sub-areas, the travel time to the outlet for each sub-area, the drainage area and the SCS curve number. The curve number is used to transform the rainfall volume into runoff

volume. This is accomplished according to the standard SCS procedure described in the National Engineering Handbook, Chapter 4 (NEH-4) published by SCS. Tables of the many hydrographs produced from the TR-20 runs are consulted to establish the portion of the outfall hydrograph contributed by a sub-area. All of these ordinates of the sub-area hydrographs are superposed to determine the outfall hydrograph. The method provides a very useful means to determine which sub-area contributes the most to the peak runoff. This is especially important if placement of a peak reduction device is desired.

Although based on TR-20, the TR-55 method will produce a hydrograph with some deviation from TR-20. The deviation is mainly due to simplification and interpolation error in the tables. The Penn State Urban Hydrology Model (PSUHM) contains a very convenient working environment in which to generate the TR-55 hydrographs and is used throughout this study. There are many versions of TR-55 on the market under different names. These packages are made only to provide easier input and better output for the TR-55 method. The output for these other programs ranges from simple tabular charts of the hydrograph to extensive graphics compatible with popular CAD packages. Table 2.15 through Table 2.20 are based on the maximum output that could be obtained using the TR-55 method as presented in PSUHM.

Table 2.9 - Physical Input Parameters for TR-55 (1986 Version)

<u>Input Variable</u>	<u>Likely Source of Data</u>
OVERALL:	
SCS Storm Distribution Type	User's Manual/SCS NEH-4
Design Return Period 24-hr Storm Volume	Local IDF Charts/TP-40
FOR EACH SUBAREA:	
Drainage Area	Topo Map
SCS Curve Number	Soil Survey/Land Use Maps/GIS
Time of Concentration:	SCS Segmental Method
• 2-yr, 24-hr Storm Volume	Local IDF Curves
• Sheet Flow Length	Site Plan/Topo Map/Proposed
• Sheet Flow Slope	Site Plan/Topo Map/Proposed
• Sheet Flow Manning's 'n'	Topo Maps/Handbooks/Experience
• Concentrated Flow Types	Site Plan/Topo Map/Proposed
• Concentrated Flow Lengths	Site Plan/Topo Map/Proposed
• Concentrated Flow Slopes	Site Plan/Topo Map/Proposed
• X-Section Area of Channel Flow	Site Plan/Topo Maps/Proposed
• X-Section Wetted Perimeter of Channel Flows	Site Plan/Topo Maps/Proposed
• Length of Channel Flow	Site Plan/Topo Maps/Proposed
• Slope of Channel Flow	Site Plan/Topo Maps/Proposed
• Manning's 'n' for Channel Flow	Topo Maps/Handbooks/Experience
Full Flow Travel Time to Outlet:	Manning's Equation/Chezy etc.
• X-Section Geometry of Element	Site Plan/Topo Maps/Proposed
• Element Slope	Site Plan/Topo Map/Proposed
• Element Manning's 'n'	Land Use Maps/Handbooks/Experience
• Element Length	Site Plan/Topo Map/Proposed

2.2.9 The Rational Method

The rational method is perhaps the oldest method for hydrologic design still in use today and perhaps the simplest to use. The rational method has origins in England circa. 1850. This method has been used extensively in the United States since the turn of the century for all aspects of urban drainage design.

The basic idea of the method is a uniform rainfall intensity falling on an area with a uniform loss coefficient. This uniform rainfall intensity will cause the peak flow of the hydrograph at the time of concentration. The intensity is found, therefore,

using an intensity-duration-frequency curve at a duration equal to the time of concentration. This assumption implies that the frequency of the runoff event is equivalent to the frequency of the rainfall intensity. This implication is assumed in almost all of the models in this evaluation, even though it is not necessarily true.

Perhaps the most important parameter to assess in the rational method is the estimation of the C-factor which represents the transformation from rainfall to runoff. This factor has been found not to be constant, but to be related to many factors including rainfall intensity, soil type, land use, slope, impervious percent and the recurrence interval (Rossmiller, 1980). Rossmiller has developed a formulation based on these factors to gain an idea of the C-factor but for many engineers, experience is much faster and sometimes more accurate. Tables of the C-factor for various land

$$C = \left[0.72 \frac{CN}{100} RI^{0.05} \right] \cdot \left[\left(\frac{CN}{100} \right)^{(0.6S^{0.2})} \right] \cdot \left[\left(0.001 CN^{1.48} \right)^{(0.15 - 0.1I)} \right] \cdot \left[\left(\frac{IMP + 1}{2} \right)^{0.7} \right] \quad (2.5)$$

Where:

C	=	rational method runoff coefficient (C-factor)
CN	=	SCS curve number
RI	=	recurrence interval in years
S	=	watershed slope in percent (e.g. for 2.1% slope, S=2.1)
I	=	rainfall intensity in inches per hour
IMP	=	impervious fraction (e.g. for 6% impervious area, IMP=0.06)

uses, soil types and recurrence intervals have been formulated and presented in many textbooks also. The Rossmiller formulation is used in this study and has been found to be an applicable method by others for urban drainage design (Kibler et al, 1982). This formula is presented in (2.5).

Table 2.10 - Physical Input Parameters for The Rational Method

Input Variable	Likely Source of Data
FOR EACH SUBAREA:	
Drainage Area	Topo Map
Rainfall Intensity at Time of Concentration	Local IDF Curves
- Time of Concentration:	SCS Segmental Method/Others
• 2-yr, 24-hr Storm Volume	Local IDF Curves
• Sheet Flow Length	Site Plan/Topo Map/Proposed
• Sheet Flow Slope	Site Plan/Topo Map/Proposed
• Sheet Flow Manning's 'n'	Topo Maps/Handbooks/Experience
• Concentrated Flow Types	Site Plan/Topo Map/Proposed
• Concentrated Flow Lengths	Site Plan/Topo Map/Proposed
• Concentrated Flow Slopes	Site Plan/Topo Map/Proposed
• X-Section Area of Channel Flow	Site Plan/Topo Maps/Proposed
• X-Section Perimeter of Channel Flows	Site Plan/Topo Maps/Proposed
• Length of Channel Flow	Site Plan/Topo Maps/Proposed
• Slope of Channel Flow	Site Plan/Topo Maps/Proposed
• Manning's 'n' for Channel Flow	Topo Maps/Handbooks/Experience
C-Factor	Experience/Handbooks/Formulas
• SCS Curve Number	Soil Survey/Land Use Maps/GIS
• Return Period	Design Conditions
• Ground Slope	Site Plan/Topo Map/Proposed
• Impervious Fraction	Topo Map/GIS/Population Estimates
• Rainfall Intensity	See Above Calculation
(FOR SUBAREA TIME LAG ROUTING ONLY)	
Full Flow Travel Time to Outlet:	Manning's Equation/Chezy etc.
• X-Section Geometry of Element	Site Plan/Topo Maps/Proposed
• Element Slope	Site Plan/Topo Map/Proposed
• Element Manning's 'n'	Land Use Maps/Handbooks/Experience
• Element Length	Site Plan/Topo Map/Proposed

One procedure for applying the rational method involves application to the sub-areas followed by routing downstream. A triangular hydrograph is used where the

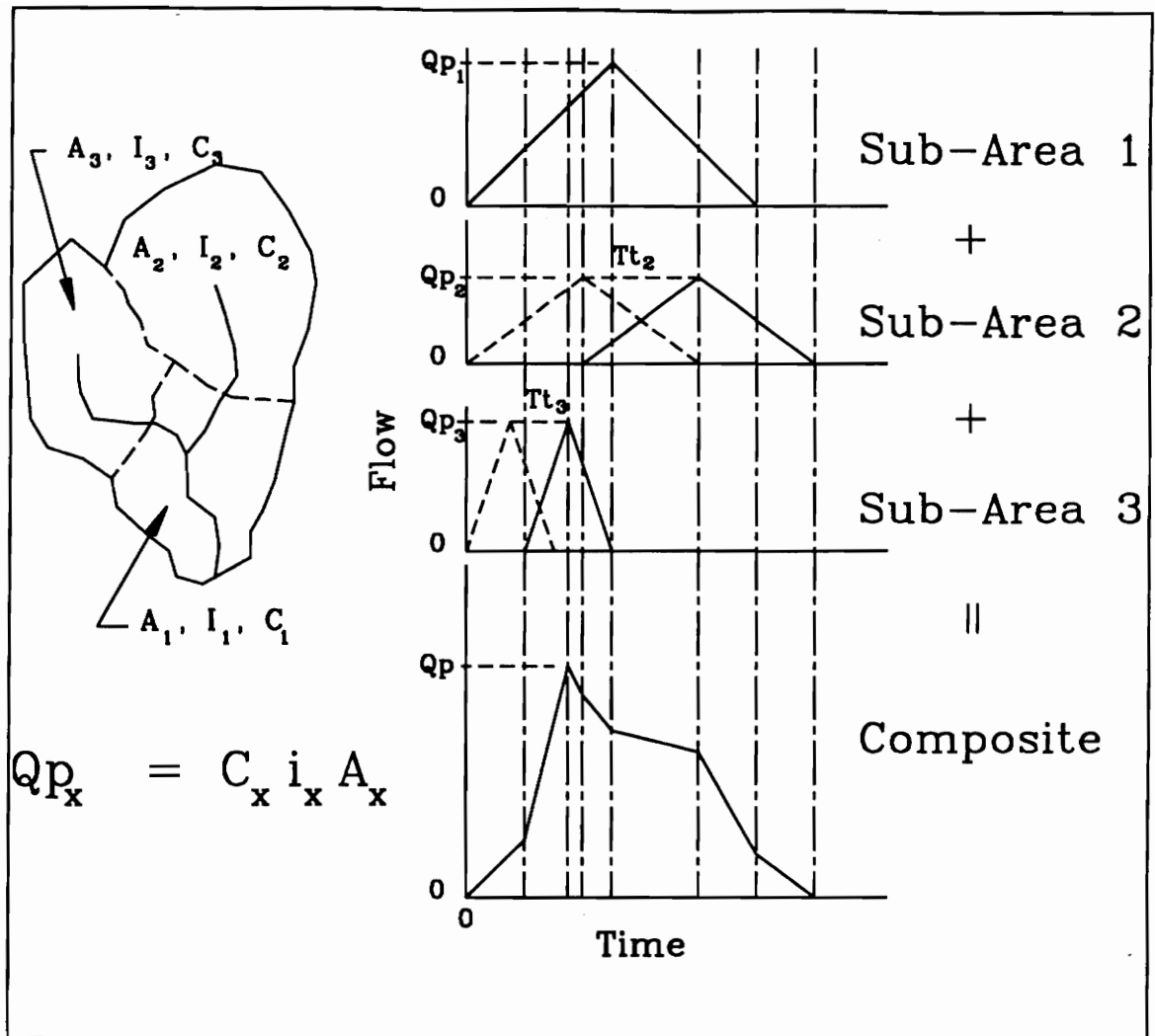


Figure 2.3 - The Rational Method applied on Subareas

peak happens at the time of concentration. The base of the hydrograph lies at twice the time of concentration, assuming the uniform rainfall intensity stops at the time of the peak occurrence. The sub-area triangular hydrographs are lagged by the amount of travel time to the outlet where all are then summed to form the outfall hydrograph.

The rational method applied on the sub-areas is illustrated in Figure 2.3 . An extremely conservative design is established because of the implication that the rainfall intensity is not uniform over the whole watershed but only over the sub-areas. An assumption is made where the worst case of rainfall intensity occurs simultaneously on all the sub-areas. This assumption gives the most conservative estimate possible. Although not hydrologically correct, this technique of applying the rational method to the sub-areas is used in this evaluation to determine its usefulness in urban drainage design. The input requirements for the rational method are listed in Table 2.10. This list is probably the maximum data required for the method especially when only three parameters are required.

2.2.10 The Modified Rational Method

Another variation of the rational method has been developed mainly for the design of detention facilities in urban areas for peak reduction and/or pollutant trapping. The modified rational method, as it is called in this study, is simply application of the rational method while using a fixed rainfall duration. This recognizes the effect of rainfall duration changing which in turn changes the volume of rainfall moving through the detention facilities. The modified rational method is simply a trapezoidal hydrograph with the first point being the start of rainfall occurrence, the second is the peak flow at the time of concentration of the basin, the

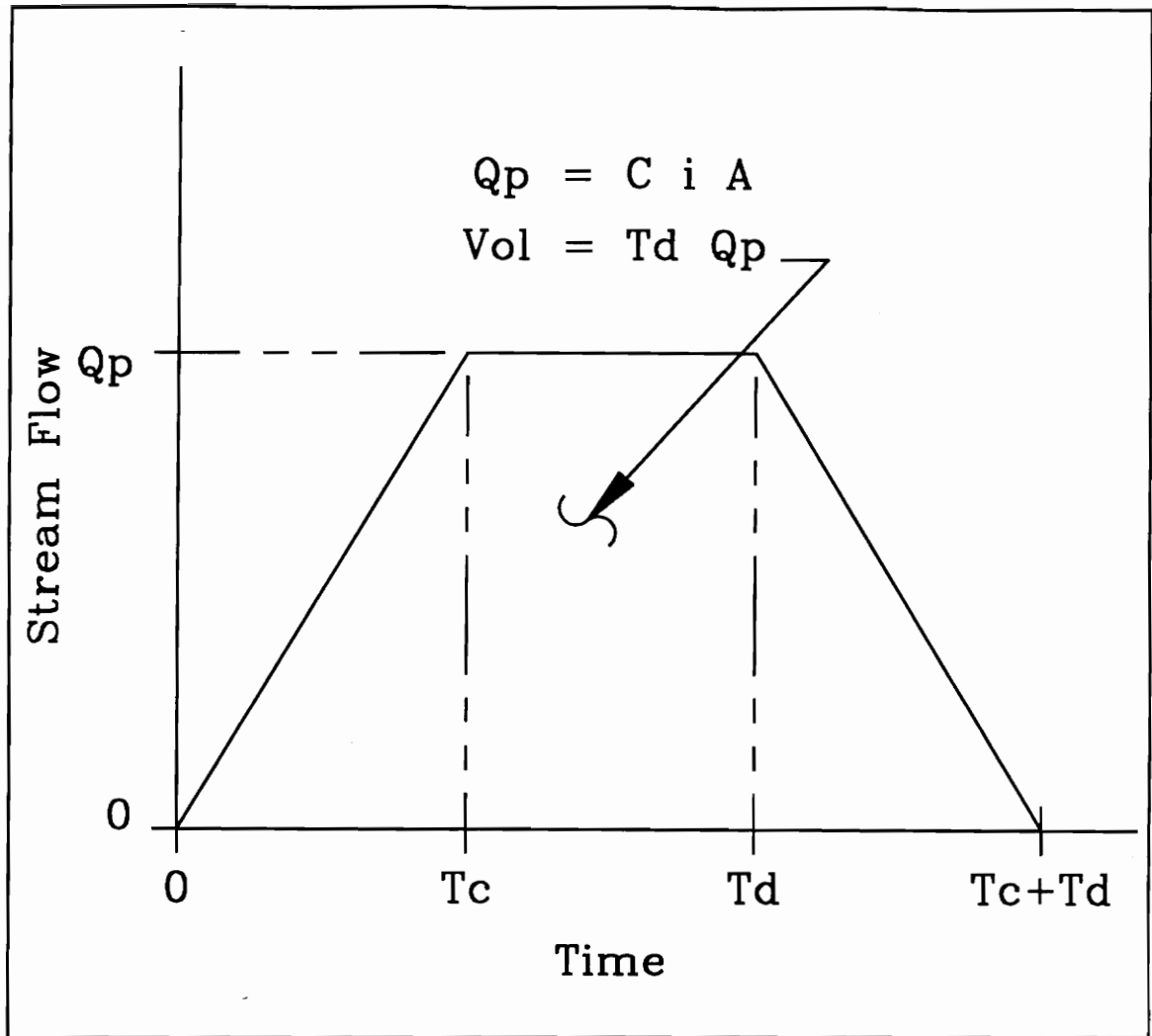


Figure 2.4 - The Modified Rational Method Hydrograph.

third being the peak flow at the maximum rainfall duration and the forth being zero flow at the time of concentration plus the rainfall duration. See Figure 2.4 . This method is applied in the same way as the rational method and requires the same amount of input with the addition of the rainfall duration which depends on the

Table 2.11 - Physical Input Parameters for the Modified Rational Method

<u>Input Variable</u>	<u>Likely Source of Data</u>
FOR EACH SUBAREA:	
Drainage Area	Topo Map
Rainfall Duration	Design Conditions
Rainfall Intensity at Time of Concentration	Local IDF Curves
- Time of Concentration:	SCS Segmental Method/Others
• 2-yr, 24-hr Storm Volume	Local IDF Curves
• Sheet Flow Length	Site Plan/Topo Map/Proposed
• Sheet Flow Slope	Site Plan/Topo Map/Proposed
• Sheet Flow Manning's 'n'	Topo Maps/Handbooks/Experience
• Concentrated Flow Types	Site Plan/Topo Map/Proposed
• Concentrated Flow Lengths	Site Plan/Topo Map/Proposed
• Concentrated Flow Slopes	Site Plan/Topo Map/Proposed
• X-Section Area of Channel Flow	Site Plan/Topo Maps/Proposed
• X-Section Perimeter of Channel Flows	Site Plan/Topo Maps/Proposed
• Length of Channel Flow	Site Plan/Topo Maps/Proposed
• Slope of Channel Flow	Site Plan/Topo Maps/Proposed
• Manning's 'n' for Channel Flow	Topo Maps/Handbooks/Experience
C-Factor	Experience/Handbooks/Formulas
• SCS Curve Number	Soil Survey/Land Use Maps/GIS
• Return Period	Design Conditions
• Ground Slope	Site Plan/Topo Map/Proposed
• Impervious Fraction	Topo Map/GIS/Population Estimates
• Rainfall Intensity	See Above Calculation
(FOR SUBAREA TIME LAG ROUTING ONLY)	
Full Flow Travel Time to Outlet:	Manning's Equation/Chezy etc.
• X-Section Geometry of Element	Site Plan/Topo Maps/Proposed
• Element Slope	Site Plan/Topo Map/Proposed
• Element Manning's 'n'	Land Use Maps/Handbooks/Experience
• Element Length	Site Plan/Topo Map/Proposed

requirements of the user. One example would be the iterative calculation of the rainfall duration which produces the maximum storage requirement for detention basin sizing. The modified rational method is also applied to the sub-areas in much the same way as the rational method as shown in Figure 2.3 . This use carries the same implications and assumptions as applying the rational method on the sub-areas and should be viewed accordingly.

2.2.11 The Universal Rational Method

Yet another modification of the original rational method is the universal rational method. This method takes advantage of the implications found in the intensity-duration-frequency (IDF) curve. The IDF curve implies that for a given recurrence interval an average intensity of rainfall will fall within the duration found. A design rainfall hyetograph can be constructed with increments equivalent to the time of concentration of the basin. This is accomplished by determining the cumulative rainfall volume at each time interval from the IDF curve. The cumulative rainfall volumes are then transformed into incremental volumes which are then transformed to intensities. These are then ranked in a specific order and the rational method is applied for each increment. The ranking is to accommodate the typical shape of a hydrograph. The peak flow will occur at a time equal to three times the time of concentration. The universal rational method was developed as an alternative method to the modified rational method for detention basin sizing. Therefore the volume of the hydrograph will be important in the model evaluation.

Since most local IDF curves do not provide an adequate duration for the universal rational method, a synthetic Yarnell IDF curve is developed. The SCS rainfall distributions can also be modified to determine IDF relations for use in the universal rational method. The Penn State Urban Hydrology Model (PSUHM) contains both the Yarnell and the SCS relations for use in the universal rational

Table 2.12 - Physical Input Parameters for The Universal Rational Method

<u>Input Variable</u>	<u>Likely Source of Data</u>
FOR EACH SUBAREA:	
Drainage Area	Topo Map
Rainfall Duration	Design Conditions
Rainfall Intensities at Increments of Tc	Local IDF Curves/Yarnell Curves/SCS Dist.
- Time of Concentration:	SCS Segmental Method/Others
• 2-yr, 24-hr Storm Volume	Local IDF Curves
• Sheet Flow Length	Site Plan/Topo Map/Proposed
• Sheet Flow Slope	Site Plan/Topo Map/Proposed
• Sheet Flow Manning's 'n'	Topo Maps/Handbooks/Experience
• Concentrated Flow Types	Site Plan/Topo Map/Proposed
• Concentrated Flow Lengths	Site Plan/Topo Map/Proposed
• Concentrated Flow Slopes	Site Plan/Topo Map/Proposed
• X-Section Area of Channel Flow	Site Plan/Topo Maps/Proposed
• X-Section Perimeter of Channel Flows	Site Plan/Topo Maps/Proposed
• Length of Channel Flow	Site Plan/Topo Maps/Proposed
• Slope of Channel Flow	Site Plan/Topo Maps/Proposed
• Manning's 'n' for Channel Flow	Topo Maps/Handbooks/Experience
C-Factors	Experience/Handbooks/Formulas
• SCS Curve Number	Soil Survey/Land Use Maps/GIS
• Return Period	Design Conditions
• Ground Slope	Site Plan/Topo Map/Proposed
• Impervious Fraction	Topo Map/GIS/Population Estimates
• Rainfall Intensity	See Above Calculation

method although under the name of the modified rational method. A modified form of the program contained in PSUHM was created for this study to run in a batch file mode to eliminate waiting on the computer. The computations in the altered program are equivalent to those found in PSUHM and the inputs are listed in Table 2.12.

2.2.12 The USGS Virginia Regression Equations

The United States Geological Survey has developed regression equations for determination of peak flood levels for various recurrence intervals. These equations

were developed in 1978 for the Commonwealth of Virginia based on flow records from 299 sites for recurrence intervals of 2, 5, 10, 25, 50 and 100 years. The equations show flow as a function of drainage area, watershed slope, and a regional factor to account for the differences in regional climates. These equations were developed for streams with drainage areas from 0.1 to 8,000 square miles and slopes from 1.6 to 1,320 feet per mile. The equations are not applicable to watersheds with impoundments, channelization or urbanization. This last limitation is adjusted to add the effects of the developing watersheds.

The effects of urbanization are introduced by using the equations found in the USGS Water Supply Paper 2207, *Flood Characteristics of Urban Watersheds in the United States*. (Sauer et al., 1983) These equations, developed for use nationwide, add the effects of drainage area, imperviousness, the 2-yr, 2-hr rainfall volume, basin storage, slope and a "Basin Development Factor" (BDF). These factors are regressed with the rural flow, obtained from the Virginia equations, to obtain the urban regression equations. Two separate sets of equations were developed to make their use easier. One set of equations contained all seven parameters, while the other only contained the most significant three. The three parameter equations use only the basin area, the BDF and the rural flow as parameters. These equations require much less data yet have about the same standard error as the seven parameter equations.

Perhaps the most difficult parameter to estimate is the basin development factor (BDF). The procedure involves splitting the basin into thirds, the upper, the middle and the lower, with the lower being the furthest downstream and the upper being the furthest upstream. Four factors are then checked on each third to determine the level of channelization and development. Each factor increases the BDF by one, therefore the rural condition would contain a BDF of zero while a fully urban basin would have a BDF of 12. USGS Water Supply Paper 2207 should be consulted for the exact content of the BDF conditions.

The main disadvantage of using the equations is the lack of a hydrograph for use in detention basin design or flood routing analysis. They are very useful in the design of small structures, such as roadway culverts, where only the peak flow is required. The regression equations also only estimate the frequency of occurrence for design stream flows and not the results of actual rainfall or runoff events. The equations do, however, estimate the flood frequency without assuming that the frequency of the rainfall is equivalent to the stream flow frequency. This assumption is used in most hydrologic models.

Plans to computerize the rural and urban regression equations for all of the United States is now in progress by the USGS. The National Flood Frequency (NFF) program should prove to be a valuable resource for engineering designers and planners as well as the portable computer equipped field engineer (Jennings and Cookmeyer,

Table 2.13 - Physical Input Parameters for the USGS Virginia/Urban Equations

<u>Input Variable</u>	<u>Likely Source of Data</u>
FOR WHOLE WATERSHED:	
FOR RURAL FLOW (VIRGINIA EQUATIONS):	
Drainage Area	Topo Map
Ground Slope	Site Plan/Topo Map/Proposed
Regional Factor	State Map of Factors
FOR 3-PARAMETER URBAN EQUATIONS:	
Basin Development Factor (BDF)	Prescribed BDF Procedure
Drainage Area	See Virginia Equations Above
Rural Flow	From Virginia Equations Above
FOR 7-PARAMETER URBAN EQUATIONS	
Basin Development Factor (BDF)	Prescribed BDF Procedure
Drainage Area	See Virginia Equations Above
Rural Flow	From Virginia Equations Above
Impervious Area	Topo Map/GIS/Population Estimates
2-yr, 2-hr Storm Volume	Local IDF Curves/TP-40
Percent Permanent Storage Area	Site Plan/Topo Map/Proposed/Estimate

1989). For this comparison the Virginia and the national urban equations were computerized to allow for easier analysis and to maintain consistency with the watershed physical parameters.

2.2.13 The Anderson Method

The Anderson method is a set of regression equations derived from stream flow data recorded at sites in the northern Virginia area. The method was developed in 1968 by Daniel G. Anderson of the United States Geological Survey. The equation is simple to use and is based on four parameters: the drainage area, the time lag, a coefficient of imperviousness and a flood frequency ratio. The time lag is a function

Table 2.14 - Physical Inputs Parameters for The Anderson Method

<u>Input Variable</u>	<u>Likely Source of Data</u>
FOR WHOLE WATERSHED:	
Drainage Area	Topo Map
Anderson Time to Peak:	Prescribed Equations
• Land Use Condition	Site Plan/Proposed
• Total Flow Length	Site Plan/Topo Map/Proposed
• Ground Slope	Site Plan/Topo Map/Proposed
Flood Frequency Ratio:	Prescribed Chart
• Return Period	Design Conditions
• Percent Impervious Area	Topo Map/GIS/Population Estimates
Anderson's Coefficient of Imperviousness	Prescribed Equation
• Percent Impervious Area	From Flood Frequency Ratio Calculation

of the length and slope of a basin as well as the development condition. Three separate calculations of lag time are given for three different conditions: rural (undeveloped), developed with partial channelization, and completely developed basins. The coefficient of imperviousness is simply a function of the percent impervious area. The flood frequency ratio is a function of return period and percent impervious area. The Anderson method is based on basins up to 570 square miles in drainage area and all ranges of development. This method, like the USGS equations, estimates the flood frequency without the assumption of equivalent rainfall frequency. Also like the USGS equations, the Anderson method only provides the peak flow for a given recurrence interval without a hydrograph.

2.3 Model Capabilities

The following tables list the capabilities of all of the models listed according to their limitations. The listing covers all qualitative aspects of the models without considering performance. Each table covers a separate topic of rainfall-runoff modeling such as rainfall, infiltration and hydrograph development.

Table 2.15 - Capabilities of Models - Rainfall Options

	Gaged Rainfall	SCS 24-hr Design Storm	IDF Based Rainfall	Design Storm Hyetograph (Yarnell)	PMP Design Storm	Rainfall Freq. ≠ Runoff Freq.	Multiple Gages
<p><u>Legend</u></p> <p>○ = Full Capability</p> <p>◐ = Limited Capability</p> <p>◑ = Severly Limited Capability</p> <p>● = Not Available</p>							
SWMM	○	○	●	○	◐	●	◐
PSRM-QUAL	◐	◐	●	○	◐	●	○
TR-20	◐	○	●	○	◐	●	●
HEC-1 (KW)	◐	◐	●	○	○	●	○
SCS UH - Whole Basin	○	○	●	○	○	●	●
SCS UH - Sub-areas	○	○	●	○	○	●	●
Snyder's UH - Whole Basin	○	○	●	○	○	●	●
Snyder UH - Sub-areas	○	○	●	○	○	●	●
Clark IUH - Whole Basin	○	○	●	○	○	●	●
Clark IUH - Sub-areas	○	○	●	○	○	●	●
TR-55	●	○	●	●	●	●	●
Rational - Whole Basin	●	●	○	●	●	●	●
Rational - Sub-areas	●	●	○	●	●	●	●
Modified Rational - Whole Basin	●	●	○	●	●	●	●
Modified Rational - Sub-areas	●	●	○	●	●	●	●
Universal Rational	●	○	●	○	●	●	●
USGS Regression - 3 parameter	●	●	●	●	●	○	●
USGS Regression - 7 parameter	●	●	●	●	●	○	●
Anderson Method	●	●	●	●	●	○	●

Table 2.16 - Capabilities of Models - Precipitation Loss Options

	SCS Curve Number	Green-Ampt Infiltration	Horton Infiltration	Initial & Constant Loss Rate	Exponential Decay Infiltration	Depression Storage Losses	Evaporation/Transpiration Loss	Rainfall to Runoff Constant	Specification of AMC	Recovery of Infiltration Rate
<p><u>Legend</u></p> <p>○ = Full Capability</p> <p>◐ = Limited Capability</p> <p>◑ = Severely Limited Capability</p> <p>● = Not Available</p>										
SWMM	●	○	○	●	●	○	○	●	○	○
PSRM-QUAL	◐	●	◐	●	●	○	○	●	○	○
TR-20	○	●	●	●	●	●	●	●	○	●
HEC-1 (KW)	○	○	◐	○	○	●	○	●	○	○
SCS UH - Whole Basin	○	●	●	●	●	●	●	●	○	●
SCS UH - Sub-areas	○	●	●	●	●	●	●	●	○	●
Snyder's UH - Whole Basin	○	●	●	●	●	●	●	●	○	●
Snyder UH - Sub-areas	○	●	●	●	●	●	●	●	○	●
Clark IUH - Whole Basin	○	●	●	●	●	●	●	●	○	●
Clark IUH - Sub-areas	○	●	●	●	●	●	●	●	○	●
TR-55	○	●	●	●	●	●	●	●	○	●
Rational - Whole Basin	●	●	●	●	●	●	●	○	●	●
Rational - Sub-areas	●	●	●	●	●	●	●	○	●	●
Modified Rational - Whole Basin	●	●	●	●	●	●	●	○	●	●
Modified Rational - Sub-areas	●	●	●	●	●	●	●	○	●	●
Universal Rational	●	●	●	●	●	●	●	○	●	●
USGS Regression - 3 parameter	●	●	●	●	●	●	●	◐	●	●
USGS Regression - 7 parameter	●	●	●	●	●	●	●	◐	●	●
Anderson Method	●	●	●	●	●	●	●	◐	●	●

Table 2.17 - Capabilities of Models - Hydrograph/Peak Generation Methods

	<u>Legend</u>								
	○	◐	◑	◒					
	= Full Capability	= Limited Capability	= Severly Limited Capability	= Not Available					
					Kinematic Wave - Newton-Raphson	Kinematic Wave - Characteristics	Kinematic Wave - Finite Difference	SCS Unit Hydrograph	Snyder's Unit Hydrograph
									Clark's Inst. Unit Hydrograph
									User Developed Unit Hydrograph
									Empirical Relation (Regression)
									Rational Method Based
SWMM	○	◐	◑	◒					
PSRM-QUAL	◐	○	◑	◒					
TR-20	◐	◑	◒	○					
HEC-1 (KW)	◐	◑	○	◒					
SCS UH - Whole Basin	◐	◑	◒	○					
SCS UH - Sub-areas	◐	◑	◒	○					
Snyder's UH - Whole Basin	◐	◑	◒	○					
Snyder UH - Sub-areas	◐	◑	◒	○					
Clark IUH - Whole Basin	◐	◑	◒	○					
Clark IUH - Sub-areas	◐	◑	◒	○					
TR-55	◐	◑	◒	○					
Rational - Whole Basin	◐	◑	◒	○					
Rational - Sub-areas	◐	◑	◒	○					
Modified Rational - Whole Basin	◐	◑	◒	○					
Modified Rational - Sub-areas	◐	◑	◒	○					
Universal Rational	◐	◑	◒	○					
USGS Regression - 3 parameter	◐	◑	◒	○					
USGS Regression - 7 parameter	◐	◑	◒	○					
Anderson Method	◐	◑	◒	○					

Table 2.18 - Capabilities of Models - Reach/Reservoir Routing Options

	Muskingum Reach	Muskingum-Cunge (Diffusion)	Kinematic Wave	Time Lag	Modified Attenuation-Kinematic	Modified Puls (Storage Indication)	Pipe (Sewer) Flow	Pressurized Flow	Backwater Effects	Full Dynamic Flow Routing
<p>Legend</p> <p>○ = Full Capability</p> <p>◐ = Limited Capability</p> <p>◑ = Severly Limited Capability</p> <p>● = Not Available</p>										
SWMM	●	●	○	●	●	○	○	○	○	○
PSRM-QUAL	○	●	●	●	●	○	○	●	●	●
TR-20	●	●	●	●	○	○	○	●	●	●
HEC-1 (KW)	○	○	○	○	●	○	○	●	●	●
SCS UH - Whole Basin	●	●	●	●	●	●	●	●	●	●
SCS UH - Sub-areas	○	●	●	●	●	○	●	●	●	●
Snyder's UH - Whole Basin	●	●	●	●	●	●	●	●	●	●
Snyder UH - Sub-areas	○	●	●	●	●	○	●	●	●	●
Clark IUH - Whole Basin	●	●	●	●	●	●	●	●	●	●
Clark IUH - Sub-areas	○	●	●	●	●	○	●	●	●	●
TR-55	●	●	●	●	○	●	●	●	●	●
Rational - Whole Basin	●	●	●	●	●	●	●	●	●	●
Rational - Sub-areas	●	●	○	○	●	●	●	●	●	●
Modified Rational - Whole Basin	●	●	●	●	●	●	●	●	●	●
Modified Rational - Sub-areas	●	●	○	○	●	●	●	●	●	●
Universal Rational	●	●	●	●	●	●	●	●	●	●
USGS Regression - 3 parameter	●	●	●	●	●	●	○	●	●	●
USGS Regression - 7 parameter	●	●	●	●	●	●	○	●	●	●
Anderson Method	●	●	●	●	●	●	○	●	●	●

Table 2.19 - Capabilities of Models - Computer Requirements and Options

	Computer Required	Free-Format Input	Fixed-Format Input	Echo Listing of Input	Graphics Plotting of Results	ASCII File Output	Compatible with User Programs
<p><u>Legend</u></p> <p>○ = Full Capability</p> <p>◐ = Limited Capability</p> <p>◑ = Severly Limited Capability</p> <p>● = Not Available</p>							
SWMM	○	○	●	○	◐	○	○
PSRM-QUAL	○	○	●	●	○	◑	○
TR-20	○	●	○	○	◐	○	○
HEC-1 (KW)	○	◑	○	○	◐	○	◐
SCS UH - Whole Basin	●	●	◐	○	●	○	○
SCS UH - Sub-areas	◐	●	◐	○	●	○	◐
Snyder's UH - Whole Basin	●	●	◐	○	●	○	◐
Snyder UH - Sub-areas	◐	●	◐	○	●	○	◐
Clark IUH - Whole Basin	●	●	◐	○	●	○	◐
Clark IUH - Sub-areas	◐	●	◐	○	●	○	◐
TR-55	◐	●	◐	○	○	○	○
Rational - Whole Basin	●	●	◐	○	●	○	◑
Rational - Sub-areas	◐	●	◐	○	●	○	○
Modified Rational - Whole Basin	●	●	◐	○	●	○	◑
Modified Rational - Sub-areas	◐	●	◐	○	●	○	○
Universal Rational	●	●	◐	○	●	○	○
USGS Regression - 3 parameter	●	●	◐	○	●	○	◑
USGS Regression - 7 parameter	●	●	◐	○	●	○	◑
Anderson Method	●	●	◐	○	●	○	◑

Table 2.20 - Capabilities of Models - Other Model Options

	Baseflow	Groundwater Flow	Snowfall/Melt Processes	Erosion/Yield	Pollutant Buildup/Washoff	Pollutant Routing	Combined Sewer Overflow	On-Line Pumps/Diversion	Optimization for Calibration	Multi-Configuration Runs
Legend										
○ = Full Capability										
◐ = Limited Capability										
◑ = Severly Limited Capability										
● = Not Available										
SWMM	◐	○	○	○	○	○	○	○	●	◐
PSRM-QUAL	●	●	●	○	○	○	●	◐	●	●
TR-20	○	●	●	●	●	●	●	◐	●	○
HEC-1 (KW)	○	●	○	●	●	●	●	○	○	○
SCS UH - Whole Basin	●	●	●	●	●	●	●	●	●	●
SCS UH - Sub-areas	●	●	●	●	●	●	●	●	●	●
Snyder's UH - Whole Basin	●	●	●	●	●	●	●	●	●	●
Snyder UH - Sub-areas	●	●	●	●	●	●	●	●	●	●
Clark IUH - Whole Basin	●	●	●	●	●	●	●	●	●	●
Clark IUH - Sub-areas	●	●	●	●	●	●	●	●	●	●
TR-55	●	●	●	●	●	●	●	●	●	●
Rational - Whole Basin	●	●	●	●	●	●	●	●	●	●
Rational - Sub-areas	●	●	●	●	●	●	●	●	●	●
Modified Rational - Whole Basin	●	●	●	●	●	●	●	●	●	●
Modified Rational - Sub-areas	●	●	●	●	●	●	●	●	●	●
Universal Rational	●	●	●	●	●	●	●	●	●	●
USGS Regression - 3 parameter	●	●	●	●	●	●	●	●	●	●
USGS Regression - 7 parameter	●	●	●	●	●	●	●	●	●	●
Anderson Method	●	●	●	●	●	●	●	●	●	●

2.4 VIPER as a preprocessor

The similarity of the input parameters required for each of the models is obvious from the data shown in the preceding tables. To facilitate the input of the models and to maintain consistency of parameters across the watershed, the author developed a computer program which creates the input files for each of the models. The Virginia Tech Interactive Program for Efficient Runoff data management (VIPER) was written to accommodate this need. Written in a compiled BASIC programming language, VIPER is able to minimize the number of inputs required for all of the models by calculating some required model parameters. For the fixed-format models,

Table 2.21 - Model Files Created by VIPER

WITHIN VIPER PROGRAM:

SWMM 4.05
TR-20
HEC-1 (KW)
TR-55 (PSUHM File)
Rational Method (with Modified Rational)
1978 Virginia Regression Equations w/ Urban Equations

SUPPLEMENTAL VIPER PROGRAMS:

PSRMVIPER - Creates PSRM-QUAL 1991 Input File
URATVIPER - Universal Rational Method Calculations
UHVIPER - Creates all SCS, Snyder and Clark UH files for HEC-1

all inputs are placed in their proper fields in approximate record order with a minimum of user editing. Table 2.21 lists the models that VIPER is able to process.

Other separate utility programs compatible with VIPER were created to add the lesser used models to VIPER's capabilities while still using the same data files.

The supplemental VIPER programs require a completed VIPER data file and some form of precipitation file. Some of the files created by VIPER require editing. TR-20 and HEC-1 require rearranging of the data file records so that they are in the proper hydrologic computation order. Other manipulation, such as the addition of rainfall records, is also required. Even with all of the required file manipulation, VIPER proves to be invaluable. Table 2.22 list the required input for VIPER to create the runoff model input files. All of the values are not listed, but are required for input in some of the models. The missing values are calculated from the listed inputs based on proven hydrologic concepts.

As can be seen in Table 2.22 input for VIPER is very extensive depending on the amount of detail required in the models. All of this data, however, is used to create the data files. For example, to determine the time of concentration for the entire watershed, VIPER calculates the sub-area time of concentrations and the travel time to the outlet by the SCS segmental method. The maximum sub-area time of concentration plus the travel time to the outlet is the basin time of concentration, which is used in any number of models. VIPER thus provides a very efficient means of calculating all model parameters.

Table 2.22 - VIPER Input Parameters

Watershed Variables:

Watershed Name
 Number of Subareas
 2-yr, 24-hour Storm Volume
 Design Return Period
 Design Storm Volume

Subarea Variables:

Hyetograph Number
 Total Drainage Area
 Drainage Area to One Side of Main Channel
 Directly Connected Impervious Area
 SCS Curve Number (CN)
 Impervious Depression Storage
 Pervious Depression Storage
 Horton Maximum Infiltration Rate
 Horton Minimum Infiltration Rate
 Horton Infiltration Decay Rate
 Overland Sheet Flow Length
 Overland Sheet Flow Slope
 Overland Sheet Flow Manning's Roughness
 Number of Concentrated Flow Sections Within Subarea
 Number of Channel Sections Within Subarea

Concentrated Flow Variables:

Concentrated Flow Section Type (Paved or Unpaved)
 Concentrated Flow Length
 Concentrated Flow Slope
 Downstream Channel/Pipe Element Number

All Channel Flow Variables:

Channel/Pipe Element Number
 Downstream Channel/Pipe Element Number
 Length of Flow
 Channel/Pipe Slope
 Manning's Roughness
 Initial Depth of Flow

Trapezoidal Channel Flow Variables:

Bottom Width
 Right Side Slope (looking downstream)
 Left Side Slope (looking downstream)
 Bankfull Depth

Semicircular Channel/Pipe Flow Variables:

Bankfull Depth (Radius)

Parabolic Channel/Pipe Flow Variables:

Maximum Top Width
 Bankfull Depth

Natural Channel Flow Variables:

Overbank Manning's Roughness
 Left Overbank Station
 Right Overbank Station
 Number of Points on X-section

VIPER also provides full printing of the data as well as plotting of the cross sections for the natural channels and rating curve plots for the detention storage elements. Other parameters that are not generalized, and therefore model specific are input manually by the user when required. Intensity-duration-frequency curve data files are used by some of the methods for determination of the model parameters. These files contain points along the curve on which VIPER linearly interpolates when calculating parameters. The calculation of the Anderson method is completed on a single sheet of paper for each watershed. All of the required data is obtained from values calculated by VIPER and therefore consistent with the other models. A description of how the data is obtained for entry into VIPER is given in Chapter 3.

Chapter 3

Gaged Data and Description of Watersheds

Because this project is sponsored by Prince William County, the watersheds chosen for the model evaluation are located in northern Virginia. They are centered around Prince William County. The northern Virginia area consists of many land uses ranging from the urban streets immediately surrounding Washington, D.C. to the farmland of rural Loudoun County. Development during the 1970s and 1980s was

Table 3.1 - List of Watersheds

<u>Watershed Name</u>	<u>Land Use Condition</u>
Broad Run Tributary at Buckland (USGS 01656600)	Rural Undeveloped Woodlands
South Fork Broad Run at Arcola (USGS 01644250)	Rural Undeveloped Farmlands
Snakeden Branch at Reston (USGS 01645784)	Partially Developed Suburbs
Smilax Branch at Reston (USGS 0164295)	Partially Developed Commercial/Industrial Area
Stave Run near Reston (USGS 01644291)	Partially Developed Commercial/Industrial Area
Holmes Run 1 (OWML Gage)	Fully Developed Suburban/Commercial areas
Holmes Run 2 (OWML Gage)	Fully Developed Suburban/Commercial areas
Holmes Run 4 (OWML Gage)	Fully Developed Suburban/Commercial areas

overwhelming in certain sections of the region. It is during this development period that most of the data was obtained for this study. Being close to the nation’s capitol

and many of the government agencies which monitor stream flow, the northern Virginia area contains an abundance of stream gages. Unfortunately, only a few stream flow gages are located on watersheds that are considered comparable to a "typical" housing development or subdivision. Even fewer contain sufficient precipitation data to reconstruct the hydrograph with the models. The stream flow data must also be detailed enough to distinguish a hydrograph which eliminates even more stream flow data for analysis. The watersheds described in this chapter and the data presented represent the culmination of an intensive search for hydrologic data on small developing watersheds in northern Virginia. Figure 3.1 depicts the location of the watersheds on a regional map.

3.1 General Watershed Locations and Regional Descriptions

Six of the watersheds in the study are located in Fairfax County, the other two are located in Prince William County and Loudoun County. The general climate of these counties is a humid continental and tempered by the Chesapeake Bay in the eastern regions. Temperatures average about 75 degrees fahrenheit in the summer to around 35 degrees fahrenheit in the winter. Average annual temperature is a comfortable 57 degrees fahrenheit. Precipitation takes place all year long but tends to increase in the spring and summer months. Some snowfall occurs during the winters but usually doesn't accumulate in significant quantities. mean Annual snowfall for the

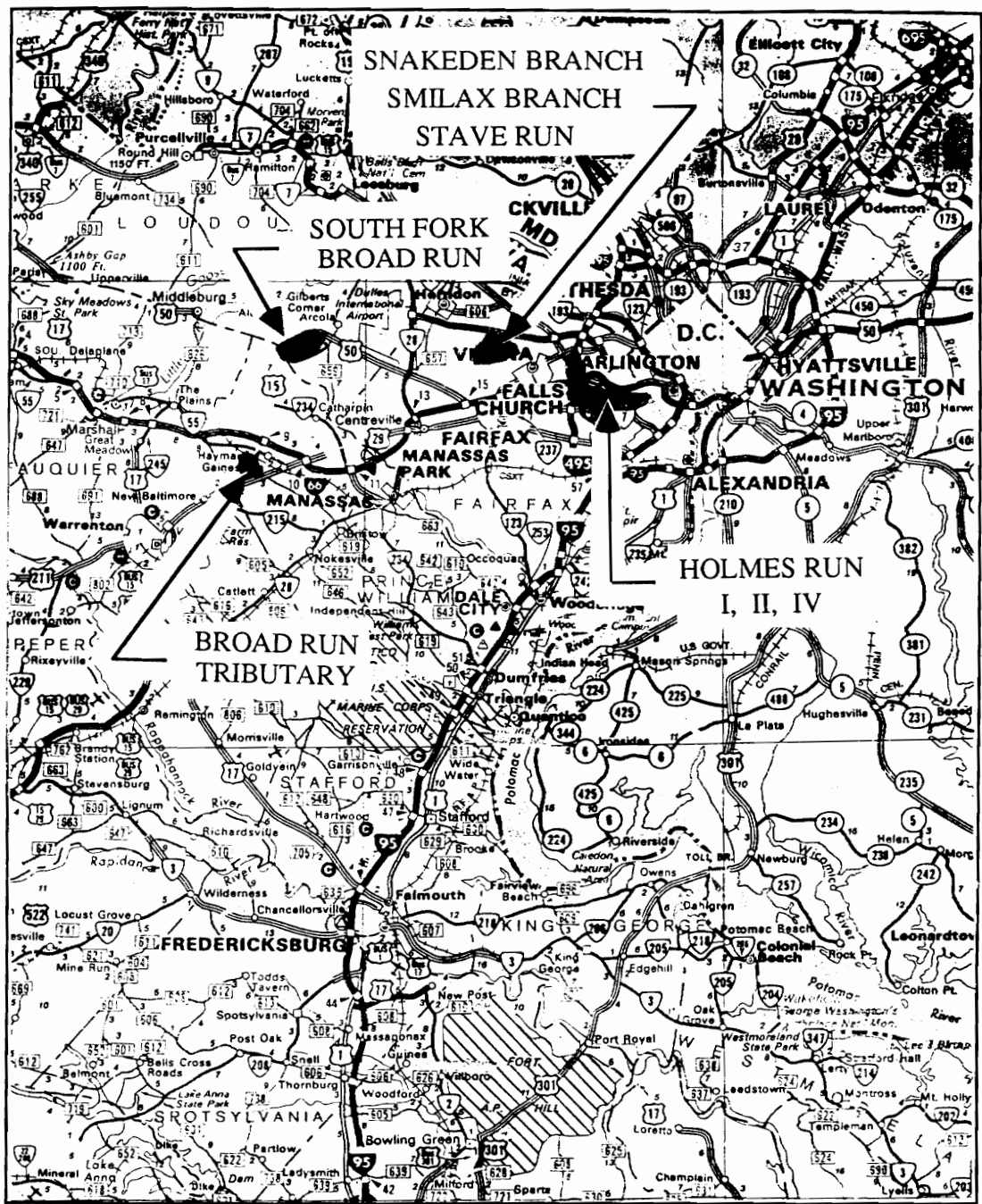


Figure 3.1 - General Watershed Location Map

3. Gaged Data and description of Watersheds

region is around 15 inches. Mean annual rainfall in the region is around 40 inches, with about 9 inches falling in July and August.

Fairfax County is perhaps the most developed county in Virginia. This is because the county is located in the Washington, D.C metropolitan area and contains many suburban towns for commuters to and from the city. The county is divided into five general physiographic regions, the Piedmont Lowland, the Piedmont Upland, the Mixed Piedmont Upland and High Coastal Plain Terraces, the High Coastal Plains, and the Low Coastal Plain Terraces. The watersheds which are located in Fairfax County are found principally on the High Coastal Plain and the Piedmont Lowland.

Three watersheds are located in series on Holmes Run while the other three lie adjacent to one another in the Reston, Virginia vicinity. The Reston watersheds are situated in the Piedmont Lowland physiographic province. This province covers about 18 percent of the whole county. The soils in this province were deposited in the Triassic period over sedimentary rocks consisting of sandstone, shale and conglomerate. The general relief in the Reston area is between 250 to 300 feet above sea level and consists of small rolling hills with steep sections near the larger streams.

The Holmes Run watersheds are located just east of Falls Church, Virginia in the High Coastal Plain physiographic province. The High Coastal Plain comprises about 22 percent of the county and, because of the proximity to Washington, D.C., is the most developed of all the physiographic provinces. Soils are mostly coastal plain

sand, silt and clay of marine or fluvial origin overlying mostly granite gneiss and sericite schist. Relief is generally from 60 to 330 feet above sea level within this province. Wetlands are sparse due to the many undulating and rolling hills found in the province. The drainage pattern is dendritic and well developed in the High Coastal Plain. Interstates 66 and 495 (the Capital Beltway) cross the province and contribute to the relatively high impervious areas in the suburban region.

The South Fork Broad Run at Arcola basin is located in eastern Loudoun County near the Fairfax and Prince William County lines. The watershed is also located in the Piedmont Lowland and has similar physiographic properties as the Reston watersheds. The general relief for this province ranges from 180 to 400 feet above sea level. Hardwood forest covered all of the county originally but have since been cleared for farmlands on over 85 percent of the county. Loudoun County is renowned for its thoroughbred horse farms which are scattered throughout the county. Recent development in the vicinity of Dulles international airport and near the Fairfax County line has converted much of the farmland into developed industrial areas and suburbs.

Prince William County lies south of both Fairfax County and Loudoun County. Broad Run Tributary lies in the extreme western end of Prince William near the Fauquier County line. The watershed lies within the boundaries of the Piedmont Upland physiographic region. This region is similar to the Piedmont Lowland region

except that the drainage pattern is more organized. The relief is wide between streams and undulating and rolling except near the lower tributaries of lower streams. The soil is underlain by sedimentary rocks composed of siltstone, sandstone and conglomerate. The western end of Prince William is dominated by hardwood forest. Some of the land is also used for grazing of farm animals. A high clay content and slow drainage limits much of the development of the land for housing or commercial ventures.

3.2 Broad Run Tributary at Buckland

Broad Run Tributary is one of two watersheds in the analysis considered to be in the rural or undeveloped condition. The gage was placed on the upstream side of US Route 29/15 near the intersection where US 29 and US 15 split in western Prince William County. The USGS maintains the gage and has used the watershed for hydrologic modeling studies in the past. Six events were extracted from the data used for a USGS study instead of trying to extract the data from the whole period of record. Old computer printouts of the data was found in the basement of the USGS Virginia office and dusted off for reentry into the computer for use in this investigation. The small time increment and the accompanying rainfall allowed this data to be the best available for this watershed. The hydrographs are presented in Appendix A along with the rainfall causing the event. This watershed is unusual because the volume in the hydrograph exceeds the volume of rainfall recorded. This is physically impossible and

poses immediate problems with the calibration of the model to these events. The possible problem with the data is that the rainfall gage may have been located at or near one end of the watershed and did not record the spatial variability of the rainfall. By raining harder on the opposite end of the watershed than where the gage is located, the volume in the hydrograph would be higher than recorded by the rain gage. The storm events used are shown graphically in Appendix A.

The land use conditions on the Broad Run Tributary are obtained from aerial photographs of Prince William County for the time period of the rainfall/runoff data. The land use and soils maps presented in Folio A and topographic maps are used to determine the general watershed parameters listed in Table 3.2. The soils data are obtained from the county soil survey and the topographic maps are provided by Prince

Table 3.2 - General Watershed Data for Broad Run Tributary at Buckland

Drainage Area:	504,709 Acres
Percent Impervious:	4.61 Percent
Average SCS Curve Number:	75
Average Slope	0.0168 ft/ft
USGS Basin Development Factor:	3
Maximum Elevation:	433 feet MSL
Minimum Elevation:	295 feet MSL
Number of Sub-Basins:	5
Number of Drainage Elements:	10

William County. Most of the watershed consists of farmland and woods. The impervious fraction is from roads and rooftops. A farm pond located on-line with the stream also serves as the point where the main channel comes together from two separate tributary channels. Meandering is not present on any of the channels on the watershed and provides a unique property among the watersheds in this study. A roadside ditch serves as the main channel on one side while a straight channel flows through the woods on the other. Five approximately equal sized sub-areas are delineated for modeling based on homogeneous channel shapes. Soils on the watershed are somewhat random and seemed to have only a small correlation to the stream bed locations. Hydrologic soil group D soils are abundant closer to the stream beds while hydrologic soil group B soils tend to lie near the ridges, although not always. The hydrologic soil group C soils are scattered in large patches throughout the rest of the watershed. Hydrologic soil group A Soils were not found on the watershed.

3.3 South Fork of Broad Run at Arcola

The South Fork of Broad Run at Arcola lies in southeastern Loudoun County within a rural region with very active farming operations. The USGS maintained a stream flow gage on this stream in the period of 1974 to 1975 when continuous data was recorded for use in a regional modeling study. Rainfall and runoff data is

extracted from the USGS model study for use here, as in the Broad Run Tributary. Despite the similar name and relative closeness, the two Broad Runs are not the same and should not be confused with one another. Six events are chosen from the USGS model study and are presented in Folio A.

The South Fork of Broad Run gage is located at the upstream side of a culvert which crosses US Route 50 near the town of Arcola, Virginia. Data describing the watershed characteristics is presented in Table 3.3. The watershed contains numerous

Table 3.3 - General Watershed Data for South Fork Broad Run at Arcola

Drainage Area:	2591.937 Acres
Percent Impervious:	6.55 Percent
Average SCS Curve Number:	78
Average Slope	0.0210 ft/ft
USGS Basin Development Factor:	2
Maximum Elevation:	497 feet MSL
Minimum Elevation:	285 feet MSL
Number of Sub-Basins:	13
Number of Drainage Elements:	30

farms, which according to the aerial photography, are mainly used for pastures and hay production. Much of the watershed, not used for agricultural fields, is forested. Wetland areas are present on much of the fields on the many tributaries to the main channel. One area maintains a developed condition, but this consists of a small industry and does not contribute greatly to the overall imperviousness. Most of the

impervious area is created by the paved highways and rooftops of houses and barns which are scattered throughout the watershed. Soils are distributed in the pattern typical of northern Virginia soils. The pattern has hydrologic soil group D soils distributed along the streams, followed by hydrologic soil group C near the streams, blending to hydrologic soil group B along the ridges. The soils and land uses are mapped and presented in Folio A. The many distinguishable tributaries to the main stream necessitated a division of the watershed into a minimum of thirteen different sub-areas.

3.4 Snakeden Branch at Reston

Snakeden Branch is one of three watersheds used in this study located in Reston, Virginia in the vicinity of the United States Geological Survey's (USGS) national headquarters. A stream flow gage was placed on Snakeden Branch by the USGS and designated as gage number 01645784, Snakeden Branch at Reston. The drainage area delineated from the Fairfax County topographic maps, at a scale of 1 inch = 500 ft with 5 foot contour intervals, is 525.7 acres or 0.82 square miles. This differs from the published USGS drainage area found for the gage, 0.79 square miles. This difference in drainage area is acceptable because the exact location of the gage on the maps may be in error. The scale and contour interval of the maps also contribute to the difference. Human error in digitizing to area are also to blame for

the discrepancy. The period of record for this gage is from January 1973 to October 1978 as well as from October 1984 to August 1990 intermittently. Precipitation data for the watershed is also provided by the USGS for the period March 1975 to March 1976. The rainfall gage was located near the stream flow gage. The lack of rainfall data severely limits the amount of useful stream flow data that can be used. The rainfall data is available on five minute intervals while the stream flow data is only available on hourly increments. The hourly intervals will be sufficient for satisfactory simulation. Storms are chosen which provide enough detail in the hydrograph to be evaluated successfully. A large amount of error is expected on this watershed solely due to the hourly flow data. It is obvious that the peak flows will not always occur exactly on the hour. The limitation of the amount of rainfall data allows only five events to be useful from the data obtained. Appendix A contains the hydrographs and the hyetographs chosen for simulation on Snakeden Branch.

Table 3.4 lists general watershed parameters for Snakeden Branch model development. Land use maps are developed from 1976 aerial photographs, obtained from Fairfax County, for the region. Soils maps and topography are also obtained from Fairfax County. Six sub-areas are delineated based on the drainage pattern. Eight drainage elements are delineated based on consistency in their cross sections. The general topography gradually slopes toward the main stem of the stream which approximately bisects the watershed. The land use is mostly multi-family residences

Table 3.4 - General Watershed Data for Snakeden Branch at Reston

Drainage Area:	525.71 Acres
Percent Impervious:	42.88 Percent
Average SCS Curve Number:	80
Average Slope	0.0252 ft/ft
USGS Basin Development Factor:	9
Maximum Elevation:	469 feet MSL
Minimum Elevation:	322 feet MSL
Number of Sub-Basins:	6
Number of Drainage Elements:	8

with some single family home lots and a small amount of commercial areas except in the immediate area of the stream bed. This area is mostly wooded, but most likely with light brush and wetlands surrounding the stream itself. The watershed is considered partially developed in this study because of the additional presence of construction within the watershed on areas that were previously undeveloped. Most of the development on the watershed takes place in the span of less than 4 years but the level of development stays fairly constant for the period being modeled. The storms occur from late 1975 to early 1976. Aerial photographs from 1976 are obtained to determine the land use at the time of the events being analyzed. The hydrologic soil groups (HSG) on the watershed are consistent with other watersheds in the Northern Virginia region. Soils of group D are situated in the proximity of the stream bed followed by hydrologic soil group C on areas further upstream. Hydrologic soil group B soils cover the watershed in areas not in the immediate area of the stream bed.

Hydrologic soil group A soils are located in only one isolated spot within the whole basin. The maps of watershed delineation, land use, and hydrologic soil group are digitized for analysis and are presented in Folio A.

3.5 Smilax Branch at Reston

Smilax Branch is also a gaged watershed which drains the area occupied by the USGS national center. The gage, which drains the northeastern part of the USGS center and is designated as gage 01644295 - Smilax Branch at Reston, is located upstream of a culvert under the Dulles airport access road. Most of the wooded portion of the watershed is located on the USGS property. The developed portion of the land consists of multi-family homes in the upper portion of the watershed and a wide USGS center access road running down the middle. Two branches of the main stream flow from the upper regions of the watershed where the USGS road forces them together to form the main stem of Smilax Branch in the ditch adjacent to the road. The main stem flows roughly in the center of the watershed to the gage site. Two other smaller tributaries join the main stem along the way which sets the stage for the sub-area delineation. Five sub-areas are delineated from the topographic maps of Fairfax County. Facts describing the overall watershed are outlined in Table 3.5.

The record of stream flows for Smilax Branch begins on March 1967 and ends in October 1978. Daily discharge values are available for the whole period, but hourly

Table 3.5 - General Watershed Data for Smilax Branch at Reston

Drainage Area:	200.757 Acres
Percent Impervious:	22.58 Percent
Average SCS Curve Number:	73
Average Slope	0.0325 ft/ft
USGS Basin Development Factor:	7
Maximum Elevation:	478 feet MSL
Minimum Elevation:	360 feet MSL
Number of Sub-Basins:	5
Number of Drainage Elements:	9

flows are only available for the period of October 1972 to September 1975. These dates luckily coincide with the period of the rainfall record for the nearby Snakeden Branch. The rainfall data recorded at Snakeden Branch is the only precipitation data available for the Reston watersheds and the stream flow data is limited to the period of record of the precipitation data. The proximity of the precipitation gage is justified for use on Smilax Branch. Six individual hydrographs on hourly increments are extracted from the record and are presented in Appendix A. The hydrologic soil groups on Smilax Branch have the same patterns as found on Snakeden Branch. The soils, land use and watershed delineation maps are displayed in Folio A.

3.6 Stave Run near Reston

Stave Run is the smallest watershed in the investigation and also contains the highest percent impervious area. The 50.38 acre watershed drains the southeastern

Table 3.6 - General Watershed Data for Stave Run near Reston

Drainage Area:	50.375 Acres
Percent Impervious:	56.40 Percent
Average SCS Curve Number:	84
Average Slope	0.0333 ft/ft
USGS Basin Development Factor:	8
Maximum Elevation:	463 feet MSL
Minimum Elevation:	359 feet MSL
Number of Sub-Basins:	1
Number of Drainage Elements:	1

portion of the USGS National Center at Reston. The main building housing the USGS offices is located on the watershed and, along with the parking lot, covers half of the basin. Table 3.6 lists the overall watershed parameters for Stave Run. Stave Run is not split into sub-areas due to the relative homogeneity of the watershed parameters and only one discernable drainage channel. The watershed is still considered partially developed because of the undeveloped nature of the lower half of the watershed.

Precipitation data from Snakeden Branch is again employed for use on Stave Run and correlated with the stream flow data. Daily discharges are recorded for Stave Run for the period of October 1971 to April 1982. Unit values for the stream flow data must be on small increments because of the size of the basin. Hourly stream flow values are available for most of the period of record from October 1971 to September 1974 and from September 1978 to the end of the record. This coincides with the precipitation data from Snakeden Branch nicely. Unfortunately only three events have

enough detail to obtain a hydrograph. One other hydrograph is available on an analog strip chart and is added to obtain a total of four storm events. The time period of the events coincides with the construction of the USGS building. The construction contributes to the classification of partial development. The maps characterizing the watershed are furnished in Folio A, while the storm events extracted from the stream flow record and the precipitation data are located in Appendix A.

3.7 Holmes Run

The three fully developed basins are the only basins where the data is not provided by the USGS. The Virginia Tech Occoquan Watershed Monitoring Laboratory (OWML) provides the data for three gages located on the Holmes Run basin near Falls Church, Virginia. Gages 1 and 2 have been in operation since 1985 and are providing stream flow data on small increments, 15 minutes during events and hourly between events. Table 3.7 lists the watershed characteristics of the land contributing to each of the three gages. Obviously Gage 1 contains the sub-areas from Gage 2 which, in turn, contains sub-areas from Gage 4. The remainder of this description of the Holmes Run watershed will describe the watershed contributing to Gage 1 since this also describes portions of Gages 2 and 4. The watersheds are treated separately for analysis but contain the same data for the common sub-areas and will be termed based on their gage number. The obvious correlation between the

Table 3.7 - General Watershed Data for Holmes Run

Upper Gage (#4):

Drainage Area:	1669.281 Acres
Percent Impervious:	33.20 Percent
Average SCS Curve Number:	77
Average Slope	0.0270 ft/ft
USGS Basin Development Factor:	10
Maximum Elevation:	399 feet MSL
Minimum Elevation:	295 feet MSL
Number of Sub-Basins:	5
Number of Drainage Elements:	15

Middle Gage (#2):

Drainage Area:	3163.250 Acres
Percent Impervious:	33.20 Percent
Average SCS Curve Number:	77
Average Slope	0.0270 ft/ft
USGS Basin Development Factor:	10
Maximum Elevation:	399 feet MSL
Minimum Elevation:	248 feet MSL
Number of Sub-Basins:	14
Number of Drainage Elements:	38

Lower Gage (#1):

Drainage Area:	4114.813 Acres
Percent Impervious:	32.78 Percent
Average SCS Curve Number:	77
Average Slope	0.0270 ft/ft
USGS Basin Development Factor:	11
Maximum Elevation:	499 feet MSL
Minimum Elevation:	228 feet MSL
Number of Sub-Basins:	22
Number of Drainage Elements:	52

watersheds will not cause much of a problem with the model comparison analysis.

Errors within each watershed across all models will be addressed separately and

"filtered" out of the comparison between the models. The natural correlation between the Holmes Run watersheds will thus be eliminated.

Development has occurred on the Holmes Run watershed extensively and is fairly constant throughout. The land use consists of single-family homes, apartment buildings, golf courses, commercial strip malls, large industrial complexes and interstate highways. Only in the direct vicinity of the main stream bed is development halted. A park was created to allow a buffer zone between the development and the stream bed. Folio A includes the land use map of the Holmes Run watershed. The sub-areas are delineated based on the drainage pattern found on the watershed. Soils for the Holmes Run watershed present a unique problem. Due to the extent of development, most of the soils have been altered such that the initial characteristics of the soils are not retained. Most of the soils on the watershed are classified as "blank" on the Fairfax County soil maps because of the modified soil profiles. This modification requires an assumption on the part of the modeler. It has been shown previously on the other watersheds in this study that most of the soils in northern Virginia contain a similar pattern. Assuming the pattern holds true for the Holmes Run watershed, a hydrologic soil classification which lies between hydrologic soil group B and hydrologic soil group C is used where the soil is classified as "blank". The rest of the soils which are classified do follow the pattern of the other basins and help validate the assumption.

3.8 Watershed Data Acquisition

The VIPER program described in Chapter 2 is used as the media for storing and manipulating the watershed data for input into the various models. Topographic maps, aerial photographs and soils survey maps form the basic elements where the data is obtained. Aerial photographs are used to determine land use maps and manning's roughness values. Topography is used to delineate the watersheds into sub-catchments as well as determining flow lengths and slopes. Channel shapes are determined from the topographic maps as are the detention storage elements within the drainage network. Detention storage values are held constant at 0.016 for impervious areas and 0.25 inches for pervious areas. These values are based on defaults as specified in the SWMM user's manual. Overland flow Manning's roughness values are found based on values suggested in the PSUHM program. Channel Manning's roughness values are calculated based on the charts and method described by Chow (1959).

The Horton infiltration parameters, the impervious fraction and the SCS curve numbers are calculated based on weighted averages of land use and hydrologic soil groups for each sub-area to obtain an average parameter for the sub-area. A Geographic Information System (GIS) developed at the Information Support Systems Laboratory at Virginia Tech is employed to discretize each land use/HSG element. Fourteen categories are used in the land use examination. These categories, listed in

Table 3.8 - Land Use Classification Categories

<u>Category</u>		<u>Code</u>
<u>Main</u>	<u>Sub-Category</u>	<u>Code</u>
1. Urban	< 1/2 Acre Single Family Residential	111
	> 1/2 Acre Single Family Residential	112
	Multi-Family Residences (Apartments, etc.)	113
	Commercial	12
	Industrial	13
	Transportation (Highways, Railroads, etc.)	14
	Industrial Commercial Complexes	15
	Mixed Urban	16
	Other (Schools, etc.)	17
2. Agricultural	Cropland/Pasture (incl. Golf Courses)	21
	Orchards/Groves/Vineyards	22
	Other	23
3. Rangeland		3
4. Forest		4
5. Water	Streams/Canals	51
	Lakes/Reservoirs	52
6. Wetlands		6
7. Barren Lands	Sandy, Other Than Beach	73
	Exposed Rock	74
	Transitional Lands (Construction Sites)	76
	Mixed Barren Lands	77

Table 3.8, are based on the USGS system described by Anderson (1976). The land use maps are digitized onto the computer along with the soils and sub-area delineation maps. Each of these images are then rasterized onto a common grid where each raster contains information about its land use, hydrologic soil group, and sub-area number. A cross-tabulation is calculated whereby all of the land use/HSG areas can be determined for each sub-area within a watershed. Each of the land use/HSG groups is

assigned a curve number as found in the TR-55 manual. Horton parameters are determined for each based on Figure 2.1 . The Horton decay rate is kept constant at 0.0115 per hour as recommended in the SWMM manual. Since Figure 2.1 gives a range of Horton parameters for a given hydrologic soil group, then a linear interpolation of the parameter based on the curve number variation within each land use/HSG is used. This allows the Horton parameters to vary with the land use. Impervious fractions for each land use category are found based on values listed in the TR-55 manual and other references. Area-weighted composite parameters are obtained for the impervious fraction, Horton parameters and curve numbers. Without the capabilities of the GIS, the break down of the land use/HSG categories is less complex and would probably be done by hand with more error introduced. A more accurate estimate of these parameters is found using the system with much less effort than required by traditional methods like the planimetering of areas.

Chapter 4

Basis for Comparison

4.1 Measures of Comparison

In order to quantify differences between a models output and a stream gage record or another calibrated model, certain points along the respective hydrographs need to be determined. There are many ways to compare hydrographs. Measures of the shape of the hydrographs, as well as differences at specific hydrograph points must be computed. To maintain a common reference for all of the measures, one must define a set of normalized quantities. Yen (1981) gives various measures of peak flow, time to peak, volume and overall fit of the hydrograph. Systematic errors as well as overall errors need to be identified and quantified.

Throughout this chapter the terms "reference hydrograph" and "comparison hydrograph" are used. The comparison hydrograph is simply the hydrograph calculated by the models using only the raw physical data from the watershed. The reference hydrograph is a flood hydrograph measured by the gages on the watersheds or computed by a calibrated model. The calibrated model is required for comparison of models which are based solely on a design storm. The calibrated models are also used to determine the effects of a design storm on models which can handle a gaged rainfall as the precipitation input. The calibrated model uses the gaged rainfall and

runoff for calibration and verification and is then extended to the design rainfall events. It must be assumed that the design rainfalls are within the calibrated model's range of sensitivity, since there is insufficient runoff data to compute a frequency curve to determine the frequency of the gaged runoff peaks.

The average error (or bias) of a parameter estimate is the systematic overprediction or underprediction of a particular model when tested on a variety of watersheds and storm events. The bias measured for a particular watershed across many models will measure the systematic errors in determining the watershed parameters. These, in effect, are errors made by the modeler. The systematic errors are evaluated along with the errors found in the models. The normalized error is defined in (3.2).

$$\epsilon_i = \frac{X_{C,i} - X_{R,i}}{X_{R,i}} \quad (3.2)$$

Where:

ϵ_i	= normalized error for event i
$X_{C,i}$	= comparison hydrograph parameter for event i
$X_{R,i}$	= reference hydrograph parameter for event i

The parameters, $X_{C,i}$ and $X_{R,i}$, should define the shape of the hydrograph as well as have significance to engineers for design. The peak flow is the most obvious of the points on a hydrograph to evaluate. The time to peak and the volume are also significant values which need to be compared. The time base of the hydrograph could

be a significant factor when looking at studies where the inter-event time is important. All of these are easily determined from the hydrographs generated in the models.

A measure of the overall accuracy of a model at a point is given by the standard error as shown in (3.3).

$$SE_X = \sqrt{\frac{1}{N} \sum_{i=1}^N \left[\frac{X_{C,i} - X_{R,i}}{X_{R,i}} \right]^2} \quad (3.3)$$

Where:

SE_X	= normalized standard error of parameter X
N	= number of hydrograph pairs compared
$X_{C,i}$	= computed parameter for event i
$X_{R,i}$	= reference parameter for event i

The standard error is also normalized by the reference quantity which is either the gaged value of the parameter or the value computed from the calibrated model based on the compared design rainfall event. Averaging the errors across different watersheds yields the accuracy for the model, while averaging the error across the models would yield the accuracy of the modeling efforts on a particular watershed. Taking these facts into account, it will be easy to determine if basin size or number of sub-catchments inhibits the modeling process by introducing unwanted errors.

The overall fit, or shape, of the hydrograph is also an important quantity to consider when comparing models. Deviations from the reference hydrograph can be found by comparing individual points on the hydrograph. The difference in time step is treated by using a time step common to both hydrographs. Linear interpolation

between hydrograph points is necessary to determine the flow at points where the comparison time step is between the hydrograph's known points. A time step of 1 minute will account for every possible model time step. The linear connection between known points is necessary and would explain some of the differences observed in the models.

A good measure of fit of the hydrographs is found in the volume-shape error. This is simply the ratio of the difference in volume to the reference volume. The volume-shape error also measures the shape of the hydrograph incrementally over time. An exact match will yield a result of zero. An absolute value is used in order to measure the total error in volume. Therefore even though the volumes of two hydrographs are the same, the volume-shape error will be non-zero. This measure is calculated using (3.4).

$$\epsilon_{VS} = \frac{1}{V_R} \sum_{i=1}^N |Q_{C,i} - Q_{R,i}| \Delta t \quad (3.4)$$

Where:

ϵ_{VS}	= volume-shape error
N	= number of time increments = $T_b/\Delta t$
$Q_{C,i}$	= flow for comparison hydrograph at time increment i
$Q_{R,i}$	= flow for reference hydrograph at time increment i
V_R	= total reference hydrograph volume
T_b	= largest time base of two hydrographs
Δt	= time increment (1 minute for all calculations)

In order to provide a number of time increments between hydrographs with different time bases, the shape parameters are computed to the largest time base. The values for the hydrograph with the shorter time base are assumed to remain constant at a final flow rate for times exceeding it's time base. The final flow rate is the lesser of 1% of the peak flow or the last value in the model's computations. If neither of these values are achieved (possibly by the models time constraints) then a straight line is extrapolated between the last two points on the hydrograph to 1% of the peak flow. The estimate of the base flow will determine a satisfactory estimate of the volume and the time base. Overestimation and underestimation of both the volume and the time base is possible depending on where the hydrograph estimate is required. See Figure 4.1 .

A better measure of the error in hydrograph shape is the root-mean-square error (RMS). For simulations where the shape of the hydrograph is paramount, this measure would provide the most use. The root-mean-square of the comparison

$$\epsilon_{RMS} = \frac{\sqrt{t_b}}{V_R} \sqrt{\sum_{i=1}^N (Q_{C,i} - Q_{R,i})^2 \Delta t} \quad (3.5)$$

Where:

ϵ_{RMS}	= root-mean-square error
N	= number of time increments = $T_b/\Delta t$
$Q_{C,i}$	= flow for comparison hydrograph at time increment i
$Q_{R,i}$	= flow for reference hydrograph at time increment i
V_R	= total reference hydrograph volume
T_b	= largest time base of two hydrographs
Δt	= time increment (1 minute for all calculations)

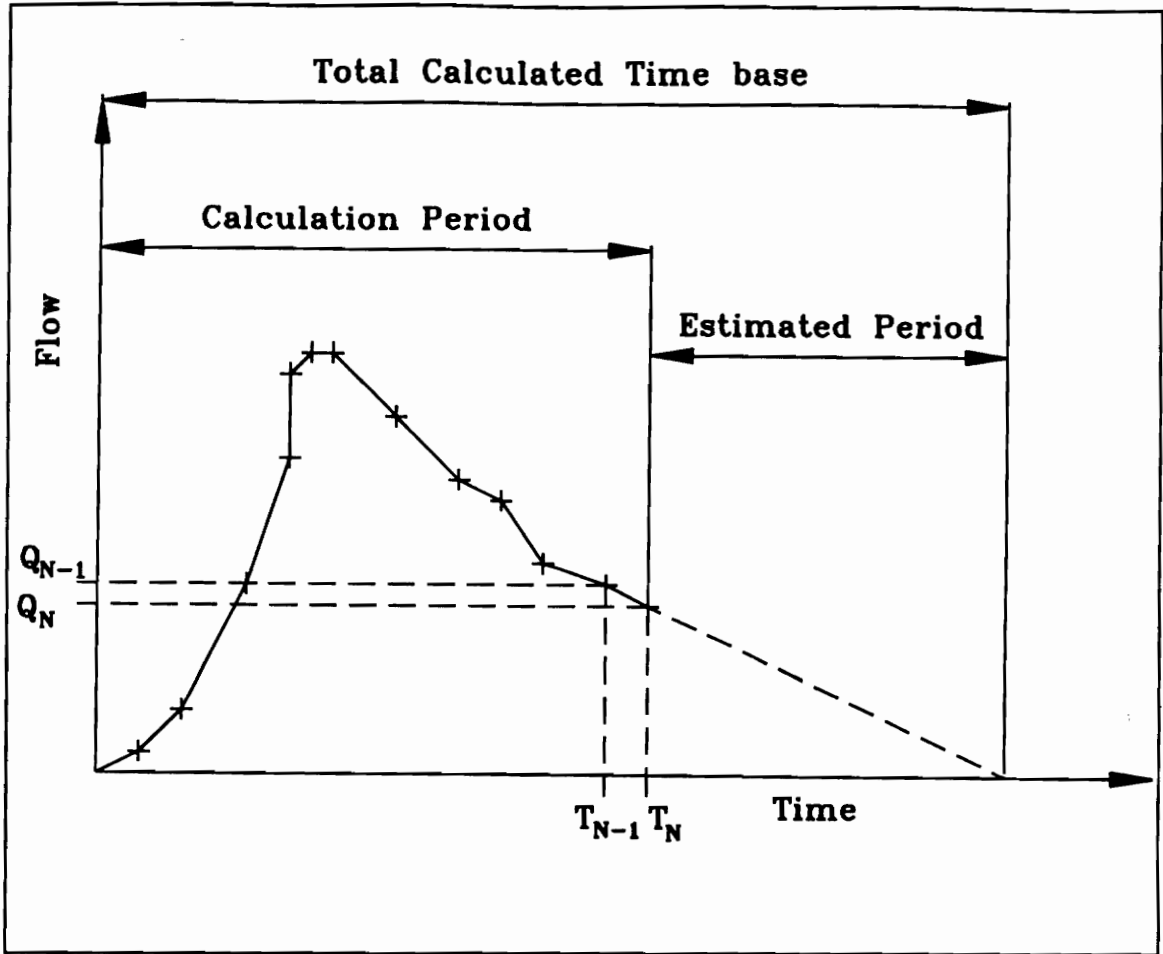


Figure 4.1 - Hydrograph Time Base Estimation

hydrograph is calculated and divided by the mean flow from the reference hydrograph to normalize the quantity. The root-mean-square error is given in (3.5).

HEC-1 uses a measure of the shape of a hydrograph in its optimization routine. The optimization routine is used to compare a computed hydrograph to an

observed event for calibration. (HEC-1, 1990) The weighted shape standard error, as it will be called here, is simply the squared difference between each point multiplied by a weight to bias the result toward the peak. The weight is given by (3.6).

$$Wt_i = \frac{(Q_{R,i} + Q_{C,i})}{\left(\frac{2}{N} \sum_{i=1}^N Q_{R,i} \right)} \quad (3.6)$$

Wt_i	= weight at time interval i
$Q_{C,i}$	= flow for comparison hydrograph at time increment i
$Q_{R,i}$	= flow for reference hydrograph at time increment i
N	= number of time increments = $T_{bR}/\Delta t$
T_{bR}	= reference hydrograph's time base
Δt	= time increment

The term in the denominator of (3.6) is simply the average flow in the reference hydrograph. This weighting procedure biases the standard error toward peak flows and away from the low flows by assigning a larger weight to the larger flows. This is supposed to result in a hydrograph with more predictability of the peak while maintaining shape with much less attention emphasized on the trailing end of the hydrograph. The weighted shape standard error is normalized to provide a standard means of comparing the hydrographs.

The normalizing measure used in this study is the average flow for the reference hydrograph. The average flow was chosen over the reference incremental flow because of the possibility of the reference incremental flow being zero. The average flow also weights each increment equally while the incremental peak flow

would contain smaller errors in the larger flows and larger errors in the smaller flows.

This would essentially negate the effect of the HEC-1 weighting procedure. The equation for the weighted shape standard error is given by (3.7).

$$SE_{wts} = \sqrt{\sum_{i=1}^N \left[\left(\frac{Q_{C,i} - Q_{R,i}}{Q_{R,avg}} \right)^2 \frac{WT_i}{N} \right]} \quad (3.7)$$

Where:

SE_{wts}	= weighted shape standard error
$Q_{C,i}$	= flow for comparison hydrograph at time increment i
$Q_{R,i}$	= flow for reference hydrograph at time increment i
$Q_{R,avg}$	= average flow for reference hydrograph
WT_i	= weight from (3.6) at time increment i
N	= number of time increments = $T_{b \max}/\Delta t$
$T_{b \max}$	= maximum time base of two hydrographs
Δt	= time increment (1 minute for all calculations)

An unweighted standard shape error will show the difference in the hydrograph shapes without being biased toward the peak. This standard error measures the overall accuracy of the fit of the hydrograph with equal weight. The shape standard error is given in (3.8).

$$SE_s = \sqrt{\sum_{i=1}^N \left(\frac{Q_{C,i} - Q_{R,i}}{Q_{R,avg}} \right)^2 \cdot \frac{1}{N}} \quad (3.8)$$

Where:

SE_s	= shape standard error
$Q_{C,i}$	= flow for comparison hydrograph at time increment i
$Q_{R,i}$	= flow for reference hydrograph at time increment i
$Q_{R,avg}$	= average flow for reference hydrograph
N	= number of time increments = $T_{b \max}/\Delta t$
$T_{b \max}$	= maximum time base of two hydrographs
Δt	= time increment (1 minute for all calculations)

The shape bias (or error) shown in (3.8) measures the accumulated systematic differences in the shape normalized by the average reference flow. This also serves as a measure of the fit of the hydrographs while showing if the comparison hydrograph flows are generally larger or smaller than the reference hydrograph.

$$\epsilon_s = \sum_{i=1}^N \frac{Q_{C,i} - Q_{R,i}}{Q_{R,avg}} \quad (3.9)$$

Where:

ϵ_s	= shape bias (or error)
$Q_{C,i}$	= flow for comparison hydrograph at time increment i
$Q_{R,i}$	= flow for reference hydrograph at time increment i
$Q_{R,avg}$	= average flow for reference hydrograph
N	= number of time increments = $T_{b \max}/\Delta t$
$T_{b \max}$	= maximum time base of two hydrographs
Δt	= time increment (1 minute for all calculations)

The average of each of the preceding measures is employed to determine an effective means of measuring tendencies across watershed type or model. These averages also imply a measure of the spread or standard deviation of the measures. It is the average and the standard deviation of the measures which provide the means of comparing models and quantifying the tendencies of each model. A large average with a small standard deviation for a certain model would imply that the model has a tendency away from the objective of the measure being analyzed. Small averages would seem to imply exactly what the measure is suggesting. However, a large standard deviation would imply that other factors are causing the tendency implied by

the average. The average error and standard deviation calculation are shown in (3.10) and (3.11), respectively.

$$\overline{M}_X = \frac{\sum_{i=1}^N M_{Xi}}{N} \quad (3.10)$$

$$S_X = \sqrt{\frac{\sum_{i=1}^N (M_{Xi} - \overline{M}_X)^2}{N - 1}} \quad (3.11)$$

Where:

M_{Xi}	= the i^{th} measure being analyzed (e.g., volume bias)
N	= the number of measures being analyzed
\overline{M}_X	= the average of the measures being analyzed
S_X	= the standard deviation of the measures being analyzed

4.2 Example of Statistics

Figure 4.2 shows two hydrographs superimposed for evaluation. These hydrographs provide an example of the analysis measures. In order to effectively evaluate the measures described in this chapter, the results of the example analysis are shown in Table 3.2. Numerous evaluations, like that shown in the example, are used to compute the summary statistics in Appendix B.

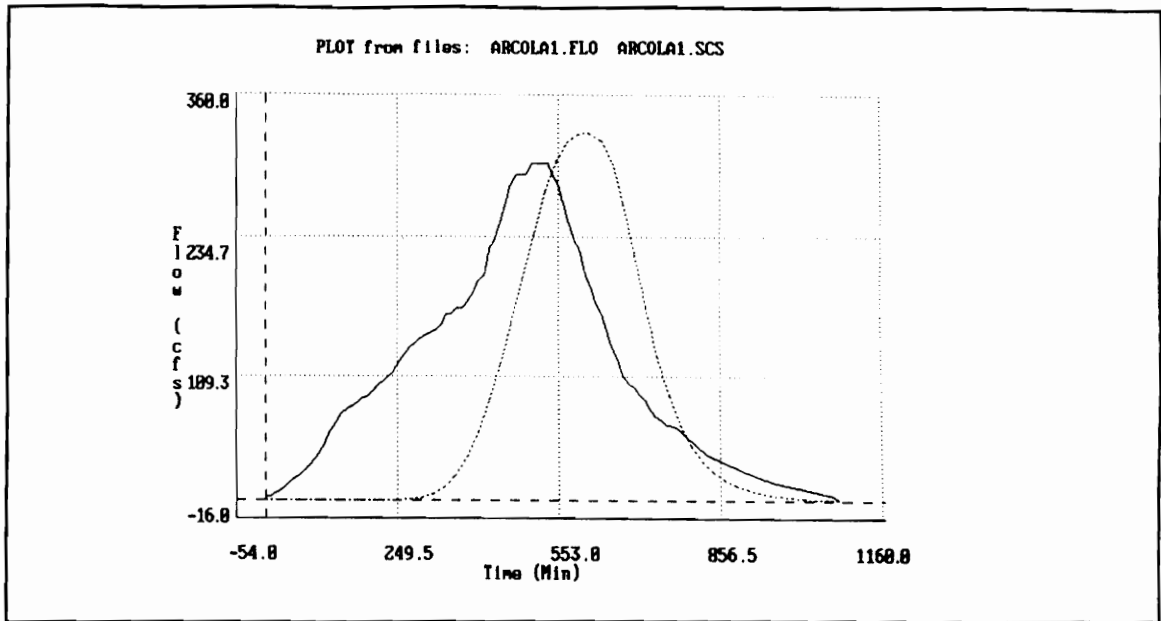


Figure 4.2 - Statistical Measures Example Hydrographs

4.3 Design Rainfall Distributions

The methods chosen for this study rely on many types of parameters, but an important input not yet discussed is the rainfall distribution. While the sophisticated models and the unit hydrographs are able to use a gaged storm, the other methods are not. A gaged storm is not always available at each and every site where hydrologic analysis is to take place. A design storm approach is taken in many engineering designs due to the lack of gaged data and the relative ease at which to construct the

Table 3.2 - Example Analysis Results

HYDANALZ.BAS
 Hydrograph file Analyzer
 Version 1.0
 April 1993
 Written in QuickBASIC 4.5 (c) Microsoft Corp.
 Written and compiled by Aaron B. Small, copyright(c) 1993

Watershed: South Fork Broad Run at Arcola
 Storm: Gaged Storm 1
 Model: SCS Unit Hydrograph (Whole Basin)

		Reference Hydrograph	Comparison Hydrograph
Qp (cfs)	=	298.000	326.400
Tp (min)	=	500.000	609.000
Tb (min)	=	1070.000	987.000
Vol (Ac-ft)	=	158.691	122.018

Peak Flow Bias	=	0.0953
Volume Bias	=	-0.2311
Time to Peak Bias	=	0.2180
Time Base Bias	=	-0.0776

Peak Flow Standard Error	=	0.0953
Volume Standard Error	=	0.2311
Time to Peak Standard Error	=	0.2180
Time Base Standard Error	=	0.0776

Volume-Shape Error	=	0.6352
Root-Mean-Square Error	=	0.8187
Shape Bias	=	-0.2339
Shape Standard Error	=	0.8259
Weighted Shape Standard Error	=	0.8614

design rainfall. Two basic types of design rainfall generation methods are employed in order to compare all of the models equally.

The SCS has developed a 24 hour duration rainfall event for locations throughout the United States. The four rainfall distributions are created to provide a

maximum amount of runoff potential by placing an intense peak centrally located within the storm. The SCS rainfall distributions for the Prince William County vicinity are listed in Appendix A. The northern Virginia region uses the Type II distribution as specified by SCS. The rainfall volumes for the SCS distribution is from the National Weather Service's Technical Paper 40 (TP-40) (Hershfield, 1961). The volumes in TP-40 are calculated from daily rainfall frequency analysis for the entire United States. Six design frequencies are used in the models to simulate runoff events. The frequencies most common to engineering design are the 2, 5, 10, 25, 50, and 100 year recurrence intervals. These return periods cover a wide range of design situations.

Yarnell developed a method of constructing a synthetic rainfall distribution. Found in the Penn State Urban Hydrology Model (PSUHM), this method is limited to a maximum 2 hour duration and minimum 5 minute increment. Because of the association between the rainfall duration and the time of concentration of the basin, both 1 hour and 2 hour duration storms are generated using this method. Appendix A contains the hyetographs produced by the Yarnell method. The same six return periods are used for both the 1 hour and 2 hour storms for a total of 12 Yarnell design events for input into the watershed models. These storms compare with the models using similar durations and with the runoff peak methods. All of the design rainfall hyetographs are displayed in Appendix A.

4.4 Method of Analysis

Direct comparison between a hydrograph produced by a design rainfall method and that recorded by the stream flow gage is not possible. In order to accomplish a comparison between all of the models and in order to contrast the results produced by a stream flow gage the author has developed a calibrated model for each of the watersheds. The calibrated model is based on the rainfall and runoff recorded at the site and then used to simulate a design rainfall. The assumption is made that the design storms simulated are within the range of the calibration events. The gaged storms are chosen to cover a wide range. Unfortunately, without a frequency analysis to determine the recurrence interval of the storm, a best guess at the valid range is attempted. None of the watersheds available for this study have the required data for an adequate frequency analysis.

Table 3.3 gives the results of the calibrations for each of the watersheds. Time was a major factor in the calibration and is reflected in the results. Had more time been permitted, a better calibration might have resulted. The calibrated models are minimized mostly with respect to shape and volume. Different calibrations will result if the peak flow is the calibration target.

Most of the watersheds contain 6 gaged events. With the addition of 18 design storm events (6-1 hour Yarnell, 6-2 hour Yarnell, 6-24 hour SCS), a total of 24 events is modeled with the sophisticated models and the unit hydrograph models. For the

Table 3.3 - Results of Calibration Models

Stat Measure	S.F. Broad Run		Broad Run Trib.		Snakeden Br.		Smilax Branch		Stave Run		Holmes Run 1		Holmes Run 2		Holmes Run 4	
	Avg Err	Std Dev	Avg Err	Std Dev	Avg Err	Std Dev	Avg Err	Std Dev	Avg Err	Std Dev	Avg Err	Std Dev	Avg Err	Std Dev	Avg Err	Std Dev
Ev	-0.002	0.387	-0.066	1.098	0.253	0.179	0.161	0.384	1.374	2.836	0.271	0.549	0.331	0.429	0.572	1.506
Eqp	0.051	0.384	-0.432	0.541	-0.104	0.117	0.179	0.877	-0.289	0.596	0.067	0.554	0.644	0.556	0.603	1.674
Etp	0.023	0.343	-0.148	0.310	-0.009	0.045	0.201	0.490	1.325	2.857	0.329	0.658	-0.020	0.052	-0.054	0.309
Etib	0.002	0.204	1.195	2.178	0.366	0.514	-0.146	0.268	1.313	3.071	0.039	0.520	-0.234	0.057	-0.024	0.151
SEv	0.328	0.144	0.909	0.469	0.253	0.179	0.340	0.201	1.626	2.652	0.414	0.428	0.365	0.394	0.903	1.297
SEqp	0.233	0.292	0.590	0.314	0.113	0.106	0.624	0.583	0.573	0.171	0.453	0.259	0.644	0.556	0.913	1.496
SEtp	0.241	0.220	0.251	0.216	0.033	0.028	0.211	0.485	1.517	2.727	0.365	0.635	0.049	0.018	0.223	0.199
SEtib	0.133	0.142	1.231	2.153	0.491	0.360	0.217	0.202	1.692	2.813	0.310	0.396	0.234	0.057	0.101	0.106
Evs	0.810	0.841	1.023	0.519	0.444	0.059	0.618	0.188	2.321	3.426	0.686	0.466	0.565	0.359	1.002	1.218
Erms	1.223	1.260	1.355	0.197	0.634	0.126	1.007	0.286	2.402	1.548	1.153	0.815	1.085	0.861	1.665	1.981
Es	0.003	0.384	-0.248	0.572	0.259	0.183	0.124	0.346	0.427	0.947	0.115	0.313	0.209	0.280	0.386	1.020
SEs	1.229	1.275	1.086	0.300	0.692	0.249	0.970	0.230	2.308	1.408	0.619	0.361	0.646	0.579	1.129	1.410
SEwts	1.824	2.234	1.232	0.720	1.072	0.526	1.632	0.546	3.903	2.723	0.834	0.629	1.145	1.378	2.267	3.814
No. Storm	6		6		5		6		4		6		6		6	
Type	SCS UH (sub)		Clark IUH (sub)		Clark IUH (sub)		Clark IUH (sub)		Clark IUH (sub)		Clark IUH (sub)		Clark IUH (sub)		Clark IUH (sub)	

Table 3.4 - Number of Hydrographs Computed for each Watershed and Model

Number of Runs		Snakeden Branch	Stave Run	Smilax Branch	SF Broad Run-ARC	Broad Run	Holmes Run 1	Holmes Run 2	Holmes Run 4
1	SWMM	23	22	24	24	24	24	24	24
2	PSRM-QUAL	23	22	24	24	24	24	24	24
3	TR-20	23	22	24	24	24	24	24	24
4	HEC-1	23	22	24	24	24	24	24	24
5	SCS UH Whole	23	22	24	24	24	24	24	24
6	SCS UH Subareas	23	22	24	24	24	24	24	24
7	Snyder UH Whole	23	22	24	24	24	24	24	24
8	Snyder UH Subareas	23	22	24	24	24	24	24	24
9	Clark UH Whole	23	22	24	24	24	24	24	24
10	Clark UH Subareas	23	22	24	24	24	24	24	24
11	TR-55	6	6	6	6	6	6	6	6
12	Rational Whole	6	6	6	6	6	6	6	6
13	Rational Subareas	6	6	6	6	6	6	6	6
14	Mod. Rational Whole	12	12	12	12	12	12	12	12
15	Mod. Rational Subareas	12	12	12	12	12	12	12	12
16	Universal Rational	12	12	12	12	12	12	12	12
17	USGS-3 Regression	6	6	6	6	6	6	6	6
18	USGS-7 Regression	6	6	6	6	6	6	6	6
19	Anderson	6	6	6	6	6	6	6	6

design rainfall methods, between 6 and 12 events are modeled depending on the models capabilities. Only 6 runoff peaks are calculated for the peak only methods based on the constraints of the equations. For those methods where only six events

are possible, comparisons are made with the calibrated model having a storm duration approximately equal to the time of concentration of the basin being modeled.

The unit hydrograph methods used to develop the calibration model were arbitrarily chosen. The choice was made by choosing the model which performed the best without calibration to the gaged flows. One may argue that the full simulation models would have been a better choice instead of the unit hydrographs. The full simulation models were tried by the time required to adequately calibrate them was substantially longer than the unit hydrograph models. The time requirement was the sole reason for not using the simulation models. If more time was allowed for the completion of this project, the full simulation models would have been the choice.

Another alternative reviewed for calibration model development was a linear programming optimization scheme. This method stems directly from unit hydrograph theory. Assuming each watershed contains a single unit hydrograph describing its drainage characteristics, a linear program is formulated relating the gaged rainfall to the resulting gaged hydrographs for all of the storms recorded. This method was not chosen because the size of the linear program would exceed the memory capacity of all available computers. This method was abandoned in favor of the synthetic unit hydrograph methods before other memory-conservative numerical routines were attempted. For single hydrograph that did not exceed the memory capacity, this method performed almost flawlessly.

A bias may be introduced through the choice of the unit hydrograph methods instead of the sophisticated models or the linear programming approach. This possibility can only be addressed by using a better calibration model. The inherent assumptions of the unit hydrograph methods will be introduced in the calibrated design storm hydrographs. Linear reservoirs and superposition of routed hydrographs are among these assumptions. The errors shown in Table 3.3 include the errors produced by the unit hydrograph assumptions. These errors are offset by similar errors in the unit hydrograph comparison storms. This will produce a bias, but this is not measurable without further evaluation using a different model or method for calibration.

Chapter 5

Analysis and Results

The design and gaged hyetographs are simulated with the models where appropriate. The simulations produced 2,458 different hydrographs for the evaluation. An additional 144 hydrographs were generated from the design rainfalls on the calibrated watershed models. The calibrations will serve as the baseline indicator for the design storm simulations. The model hydrographs are compared to the reference hydrographs using the statistics described in Chapter 4. The statistics are presented in Appendix B for all storms simulated with a model for a particular watershed. Averages of these statistics along with the standard deviations of the averages are also tabulated in Appendix B. These values form the basis of the graphs presented in Appendix C and Appendix D.

5.1 Watershed Dependent Errors

Under ideal conditions, a model yields results consistently across a wide range of watersheds. Unfortunately, each watershed is different and the modeling requires some skill on the part of the user. Errors introduced by the modeler into the process need to be identified. These errors are designated as watershed dependent errors here. By averaging all of the models together for each watershed these errors may be isolated.

Errors within the models themselves are examined by comparing the watersheds. Each of the models contain limitations and interdependency on the physical watershed parameters. Variation of results with respect to basin size is one obvious inconsistency observed. Other prevalent errors are those introduced by the level of urban development. It is these trends embedded within the models that are the focus of this study. Generalizations concerning model type are also identified for further evaluation.

Appendix C contains 54 graphs which depict each statistic averaged for each watershed. The graphs are further broken down by model category. Another 247 graphs are omitted. The omitted graphs would contain illustrations of each statistic versus the watersheds for every model. The graphs are substituted by the data contained in the tables in Appendix B. Another 1204 graphs could also have been plotted if the storm type was singled out. The results where the storm type is identified do not take into account the watershed errors. These values are presented in the next section and are graphed in Appendix D. Graphing all of the results independently of each other would be overwhelming and unnecessary.

The graph showing all of the models averaged together could be slightly deceiving. The upper and lower lines on the graph represent one standard deviation and should contain approximately 68 percent of the models results. The middle line is the average result for each watershed. The graphs contain slight deviations from what

is implied. The deviations are found in all of the statistics except those describing the peak flow. The peak only, rational and modified rational methods on the whole basin models used in the project do not form a full flood hydrograph like the other methods. The analysis program must compute all of the statistics from a full hydrograph. This limitation allows for a quick and easy way of analyzing the data in a systematic manner. In order to achieve a full hydrograph for some of the methods a simple triangular form was used. The time of the peak flow for these models occurs at 1 minute and the base time is always 2 minutes. The times are arbitrary. Using the time of concentration as the time to peak would have been a better choice. This choice was not realized until after the analysis was run. Further analysis should address this and provide a proper solution. To avoid biasing the results because of the inclusion of these imitation hydrographs, an evaluation is made by viewing the tables in Appendix B. Recognizing the existence of the imitation statistics removes any possible misinterpretation. These errors could be singled out, but would require a more tedious analysis.

The peak flow is perhaps the most important quantity to isolate in drainage modeling. It is also, however, the hardest for the models to estimate. The modeling of the peak flow is evaluated using the peak flow bias and the peak flow standard error. Figure C.1 and Figure C.6 show the peak flow bias and peak flow standard error, respectively. A definite disagreement is found between the results for each

watershed. Holmes Run 2 is the hardest to model as the peak is grossly overestimated. The large variability of the peak flow bias and standard error is mainly due to the HEC-1 model of Holmes Run 2. This model may be flawed because of an off-line reservoir near the gage site. Releases from this pond may cause changes in the gage that is not due to direct runoff from the watershed. However, this does not seem to affect the other models and must be attributed solely to HEC-1. In general HEC-1 did very poorly on all of the Holmes Run watersheds. This poor performance is unsettling because of the popularity of HEC-1 and its use on urban watersheds. The models of Smilax Branch also did poorly overall in peak flow estimation. This is brought on by possible changes in the land use condition for the period of modeling. The hourly gaged data may also play a part in the deviations of Smilax Branch.

Figure C.2, Figure C.3, Figure C.4, and Figure C.5 depict the peak flow bias for each model category. The Rational method performed very well on the small watersheds while the regression equations performed well on the large rural basin. The results of the peak only methods are unpredictable on the small developing watersheds. In general, the peak flow is the hardest quantity to estimate with any accuracy using the models on an ungaged watershed. All of the models presented here gave results with large standard deviations of at least 30 percent. This is especially disturbing considering the fundamental use of the peak flow in the design of drainage structures. The lack of good calibration models with respect to the peak flow also

contributes to the discrepancy. In order to maintain overall hydrograph shape, volume, and timing, the analyst usually tolerates some error in peak flow. Unfortunately, the loss in peak flow accuracy is usually necessary to select a single calibrated model for the watersheds. The alternative would be to have different sets of the model parameters representing storm type and size. This is not feasible in view of the limited number of rainfall events observed.

An analysis of the volume bias gives an indication of errors produced in the infiltration and loss calculations within a model. Averaging the volume bias from all of the models for a given watershed shows a general underestimation for all of the watersheds. This tells us that losses are overestimated on each of the watersheds. Further analysis of each model is required to determine which calculation methods produce the trend. Figure C.11 depicts the volume bias averaged from all of the models on each watershed. Figure C.12, Figure C.13 and Figure C.14 illustrate the volume bias graphed according to model category. The effects caused by the whole basin models using the rational and modified rational methods yield a discrepancy in the design rainfall model calculation. This is caused by the imitation hydrograph used for these models. These two results contribute to the underestimation and are noted. The sophisticated models did not underestimate as much as the design rainfall models, but the scatter within the models was much greater. The curve number method is used in the unit hydrograph methods calculation. The curve number methodology is the

primary reason for the underestimation of the volume for the unit hydrograph methods. The curve number method seems to overestimate the infiltration volume. The overestimate occurs because the curve numbers are derived from a defined antecedent moisture condition. The condition allows more initial abstraction and less volume for runoff. Examination of the timing of the hydrograph verifies this hypothesis. The results from the South Fork Broad Run models contain a smaller deviation than the other watersheds. The curve numbers are estimated better for this watershed because of the type of watershed from which the curve number is derived. In general, the systematic volume errors were nearly equal on each watershed. The errors were also found not to be dependent on watershed type or overall model type. Figure C.15 illustrates the accuracy of the volume estimation on each of the watersheds. A roughly constant accuracy is recorded which is independent of watershed type, or model type. However, PSRM-QUAL causes a strange pattern of variability in the accuracy of the sophisticated model category. This is probably due to the unique way in which infiltration is calculated within this model. The pattern does not seem to contain a trend with respect to basin size or development condition. A combination of these factors, or even other variables, must be the cause of PSRM-QUAL's variability. Storm magnitude is one possible variable which is not tested here. The tables in Appendix B show that the variability seen in the overall sophisticated model category is not seen individually in SWMM, TR-20 or HEC-1.

The timing of the hydrograph is dependent on the size and development condition of the basin. Hydrographs for the Stave Run and South Fork Broad Run models exhibit deviations from the other models. Figure C.19 and Figure C.23 illustrate the peak time bias and standard error. The graphs show a slight underestimation of the peak time. However, the graphs do display an overall constant accuracy except for Stave Run and the South Fork Broad Run watersheds. These basins represent the extremes of size and development condition. Once again HEC-1 is the main cause of the timing inaccuracy with the SCS unit hydrograph methods also contributing. Figure C.24, Figure C.25, Figure C.26, Figure C.20, Figure C.21, and Figure C.22 illustrate the peak time statistics differentiated by model category. The underestimation found in the peak time bias on the design rainfall methods is mainly due to the inclusion of the whole basin rational methods. The unit hydrograph models reveal a dependence of the peak time on the use of discretized models over whole basin models. This is most likely the reason for the Stave Run dissimilarity. The design rainfall models did not contain many systematic errors and did very well in estimating the peak flow time on all of the watersheds consistently. The time base of the hydrograph contains similar trends. Figure C.27 through Figure C.34 in Appendix C contain the graphs of the time base statistics.

Overall, all of the models underestimated the time base. The accuracy of the large rural basin was poor with respect to the design rainfall models. The large basin

did, however, do very well with the unit hydrograph models. The scatter of the bias results is large for Stave Run and the South Fork Broad Run models. The two basins contain characteristics which cause deviations within the models. For Stave Run, this deviation is possibly caused by an inaccurate estimation of the impervious fraction or the fact that only one sub-area is used. The rural nature of the South Fork Broad Run basin may contribute to the large standard deviations recorded. More than likely, the overestimation of the rainfall losses discussed previously is the major cause of the decrease in the time base. Loss of the volume of runoff will decrease the time base significantly. Peak flow and peak flow timing will also be affected positively.

The shape of the hydrograph is of value to an engineer for the design of detention facilities as well as quality management controls. The exact time distribution of the runoff is required and may be a major design consideration for these structures. The accuracy of the volume-shape error given in Figure C.35 to Figure C.38 correlates with the reasoning expressed about the overall volume accuracy. The measure explains that the underestimated volume is located in a correlating distribution with the reference hydrographs. As shown in the individual model tables in Appendix B, each of the sophisticated models contributes differently depending on the watershed. While the overall category of sophisticated models is relatively constant across the watersheds, the individual models are not. No set pattern can be discerned from this statistic as to the cause of these inconsistencies. The root-

mean-square error exaggerates the shape errors to produce seemingly immense differences on each watershed. By examining the plots in Figure C.39 to Figure C.42, the differences in the watersheds are obvious. These graphs give disturbing results but help define the differences in the model type. The Holmes Run watershed models all did poorly and exhibit the complexities involved in urban watershed modeling. The rural watershed models fared much better than the others, probably due to their relatively simple configurations. Smilax Branch also did poorly but this is probably due to a change in the land use conditions as mentioned previously. The sophisticated models had a particularly hard time with the urban Holmes Run basins. The category is plagued by having HEC-1 within its grouping. This model had severe problems with the urban basins and the South Fork Broad Run basin. Overall the South Fork Broad Run basin did the best. A reliable measure to determine how good the shape values are is obtained by viewing the results from the peak only imitation hydrographs. These results have no correlation and represent a wild guess at the shape. As can be seen in the tables in Appendix B, these values did fairly well as compared to the other models. Unfortunately, this evaluation does not say much for the full hydrograph models' ability to simulate the shape of the hydrograph on the ungaged watershed.

The shape bias results disclose a general trend for the models to underestimate the shape. An underestimate means that the ungaged flows are generally less than the

baseline hydrographs. Figure C.44 shows that the sophisticated models contain less average systematic errors on the urban watersheds but still maintain a high spread. A high spread is also found on the large rural watershed. This high spread is exhibited on the unit hydrograph methods as well as the design rainfall methods. Antecedent moisture condition is probably the major factor contributing to the errors on the South Fork Broad Run watershed. The underestimation seen in Figure C.46 on Stave Run is due to the trapezoidal hydrograph on the modified rational method and the triangular hydrograph on the rational method. These are used here only because Stave Run contains only one sub-area. However, the rational method applied to the sub-areas was very consistent, although largely underestimated. The effects of the imitation hydrographs from the whole watershed rational methods is also realized. Surprisingly, TR-55 did much better than most of the other models, regardless of category. The overall accuracy (standard error) of the shape statistic is seen in ? through Figure C.50. These show a relatively constant accuracy for all of the models across the watersheds. The scale of the graph was changed to reflect the increase in variability with this statistic. Once again the Holmes Run 2 watershed proved to be the most difficult to model. The small rural basin, Broad Run Tributary, maintained a small variability for every category of model along with the best overall average.

The weighted shape standard error is an extremely good indicator of shape as well as peak flow estimating performance. As mentioned previously, the peak flow is

perhaps the hardest hydrograph parameter to model. The weighted shape statistic also reflects and indicates the overall hydrograph shape error. A major increase in scale for the graphs presented in Appendix C is warranted. Unfortunately, the statistic simply exaggerates the results from the peak flow and shape analysis without yielding anything new. Holmes Run 2 is again shown as being inaccurate with high variability. Only the unit hydrograph models displayed an approximately constant statistic with respect to the watersheds. For the other model categories, the small developing watershed (Stave Run) is easy to model, while the Holmes Run basins all proved to be quite a challenge. The size of the basin and development condition both contribute to the deviations from the baseline hydrographs.

5.2 Model and Storm Type Error Analysis

In order to provide a proper comparison, the models are evaluated according to individual storm type. The storm type refers to the one of four rainfall distributions: gaged rainfall, 1-hour Yarnell design storms, 2-hour Yarnell design storms, and the 24-hour SCS rainfall. The statistics are calculated and averaged holding the storm type as a constant. These averages are then plotted, along with their standard deviations, against each of the models. The plots are presented in Appendix D. A true comparison of the models to one another is possible only when using a common rainfall. This common rainfall should last over a common time period and maintain

similar distribution properties. An overall average across all storms is also presented but cannot be used without due thought to the number of events at which the average is founded.

Figure D.1 through Figure D.5 illustrate the peak flow bias for each of the models on various storms. For the overall average of all storms, HEC-1 is the model that stands out. HEC-1 overestimates the peak flow by approximately 200 percent. The standard deviation is also beyond any reasonable limit. The Anderson method and the modified rational method applied to the sub-areas also give high bias values with high standard deviations. Only the unit hydrograph models applied to the whole basin give values remotely close to the baseline values. However, for the gaged storms, the unit hydrograph models applied to the sub-areas were much closer to the baseline values. The whole basin unit hydrograph models underestimate the peak flow for these storms. TR-20 came closest to simulating the gaged storms with only slight systematic underestimation. Not surprisingly, TR-20 correlates very well to the SCS unit hydrograph models for the whole basin and the sub-areas. The SCS unit hydrograph models give approximately the same bias independent of whether applied to the sub-areas or the whole basin. Figure D.3 illustrates the effect of the 1 hour design storm on the peak flow. Many of the design rainfall methods and the peak flow methods are represented as well as the sophisticated and unit hydrograph models. The universal rational method performed as well as SWMM and PSRM-QUAL. The

unit hydrograph models performed even better on the 1 hour storm than on the gaged storms. Again, HEC-1 systematically overestimated the peak flows on the 1 hour storm. While the peak only methods overestimated the peak flows, they did as well as the sophisticated models for the most part. The USGS equations performed better than the Anderson Method. On the 24 hour SCS storm, TR-55 achieved the same level of precision as TR-20 and the unit hydrograph methods. The universal rational method performed surprisingly well for the 24 hour event, surpassing all of the other models. Only on the 24 hour event did the sophisticated models reverse their relative rankings. In the other events TR-20 performed better than PSRM-QUAL, which, in turn, did better than SWMM. In the 24 hour event this is reversed with SWMM performing as well as the unit hydrograph events. The overall trend of the sub-area unit hydrograph models to perform worse than the whole basin models is held independent of the design storm type. HEC-1 operated with much less systematic variation on the 24 hour event, although still maintaining the status of the worst estimator.

The same patterns are seen in the overall accuracy of the peak estimation of the models as is seen in the peak flow bias plots. Figure D.6 through Figure D.10 depict the overall accuracy of each of the models for estimating peak flows. Once again the unit hydrograph methods performed better than most of the sophisticated models. Only TR-20 achieved similar results. Also the whole basin unit hydrograph models were slightly more accurate than the sub-area unit hydrographs. HEC-1 again

performed unexpectedly poor. Only the modified rational method applied on the sub-areas and the Anderson method performed as poor as HEC-1. The other design rainfall models and the peak only methods functioned at about the same level of accuracy. SWMM also acted at this level. PSRM-QUAL falls somewhere between SWMM and the unit hydrograph models. For the 24 hour events, again the universal rational method performed surprisingly better than expected. HEC-1 also improved for the longer events. TR-55 did not prove as accurate for peak flow estimation as the unit hydrograph models or the sophisticated models with the exception of HEC-1.

The models selected for this investigation all perform better than anticipated on the volume estimation. The plots of the volume bias and standard error are listed in Appendix D, Figure D.11 to Figure D.20. SWMM, HEC-1, TR-55, the modified rational and the universal rational method provide the least systematic deviation from the baseline hydrographs. SWMM and HEC-1, however, also contained the largest standard deviations of all of the models. HEC-1 appears to contain this deviation independent of storm type, while SWMM only exhibited this behavior on the gaged storms. The modified rational method applied to the sub-areas had a spread only a bit smaller than SWMM and HEC-1, and this appears to be due to varying results from the 1 and 2 hour storm periods. The unit hydrograph models, PSRM-QUAL, and TR-20 all performed similarly. This is expected because all of these methods rely on the curve number for rainfall losses. These models have been shown previously to

underestimate the flows by overestimating the initial abstraction. With the 24-hr storms the curve number based models all did very well with almost no systematic errors. Again the universal rational method did surprisingly well with only a little systematic underestimation of the volume on the 24-hr events. The overall accuracy of the models are depicted with patterns similar to the volume bias results. SWMM provided the most accurate results but again contained a high standard deviation due to the gaged storms. PSRM-QUAL, TR-20 and the unit hydrograph methods produced approximately the same accuracy. The rational method applied on the sub-areas correlated well with the two sophisticated models and the unit hydrograph models for the 1 hour storm and even contained a tiny standard deviation for the 2 hour event simulations. The modified rational method proved to contain good answers for both the 1 and 2 hour simulations but were very different. The effect of the time of concentration of the basins is evident for this model. HEC-1 continued to give poor results except on the 24 hour SCS events. For the SCS unit hydrographs applied on the whole basin, the 24 hour event proved to be a challenge. The 24 hour storm universal rational method provided predictable results but only as accurate as the HEC-1 simulations. The 1 hour universal rational method simulation performed very well as compared with the SWMM simulation, and has approximately the same accuracy as the estimation of the 24 hour event. PSRM-QUAL, HEC-1 and the unit hydrographs all improved their accuracy with increasing storm durations. The

exceptions to this rule are the unit hydrograph methods applied on the whole basin for the 24 hour rainfall.

The timing of the hydrograph peak was estimated very well by all of the methods with the omission of the rational based methods. TR-55 surpassed all of the models in overall performance with only a 2.9 percent systematic underestimation and a 3.1 percent accuracy. The standard deviations of these statistics are practically negligible. SWMM, TR-20, HEC-1 and the sub-area applied unit hydrographs did as well as TR-55, but only on the 24 hour events. The overall performance of TR-55 is reduced by this comparison since TR-55 is only based on the 24 hour event. It is expected that TR-55 would correlate with TR-20 if TR-55 were able to simulate shorter storms. The increase in storm duration increased the predictability of the hydrograph timing results. Only the SCS whole basin unit hydrograph method failed to exhibit this trend. HEC-1 did not provide the extravagant deviant results for this parameter, but deviated slightly from the other models accuracy on the Yarnell design storms. SWMM and TR-20 proved to be the most predictable models for estimating the peak flow time on the gaged storms. All of the models used on the gaged storms overestimated the time to the peak, but underestimated the peak flow time on the design storms. The sub-area unit hydrographs proved to be better than the whole unit hydrograph models with the systematic errors but contained less accuracy at estimating the peak flow time. The rational method, modified rational method, and the universal

rational method all did poorly when compared to the other models' peak flow prediction.

The time base statistics plotted in Table B.0 to Table B.0, are a general indicator of the storage and transport capabilities of the models. In general, SWMM was the only model that did not systematically overestimate or underestimate the time base. All of the other models underestimated the time base for all of the storms except the universal rational method. This method only overestimated the time base on the 1 hour storm event. The 24 hour storm time base is underestimated by the universal rational method. The differences cause the large standard deviation observed on the overall storm plot of the time base statistic, Table B.0. The accuracy of this method is also poor, as can be seen in Table B.0. The rational method and modified rational method, both applied to the sub-areas, give predictable results but are less accurate than those observed in the other models. HEC-1, TR-20, PSRM-QUAL, and the unit hydrograph methods maintain a relatively constant ability to estimate the time base of the hydrograph. All of those models underestimate the time base with approximately equal standard deviations. HEC-1 did not maintain this similarity due to the high standard deviation observed in the gaged storms. The whole basin unit hydrograph only performed slightly better than the sub-area unit hydrographs in estimating the time base. The accuracy of the whole basin unit hydrograph models is better than the sub-area unit hydrographs and is also more predictable. The Snyder

and Clark unit hydrographs performed slightly better than the SCS unit hydrograph models. This is especially pronounced in the whole basin models. The trend where the models improve accuracy as the storm duration increases is observed on the time base statistics as well.

The volume-shape error correlates with the other volume statistics. Some exaggeration is shown, which would be attributed to the shape. Figure D.41 to Figure D.45 are plotted to show the volume-shape errors distribution across the models. The root-mean-square error verifies the exaggeration shown in the volume-shape error plots. In general the whole basin unit hydrographs performed better than the sub-area unit hydrographs. The SCS unit hydrograph method yielded slightly worse results than the other unit hydrograph methods. The sophisticated models varied greatly when simulating the gaged storms but improved significantly on the design storms. HEC-1, unfortunately only showed significant improvement on the 24 hour duration storm. Of the design rainfall methods compared, only TR-55 performed as well as the sophisticated and the unit hydrograph models. Large differences from the baseline hydrograph shapes are observed for the modified rational method applied on the sub-areas. The universal rational method fared the best among the rational based methodologies. TR-20 correlated well with the unit hydrograph models and also provided the best results among the sophisticated models. SWMM performed consistently across all storm types. PSRM-QUAL yields a better hydrograph fit than

SWMM for all storms except for the 1 hour events. All of the models improved the hydrograph shape indicators as the storm duration increased. The root-mean-square errors are plotted in Figure D.46 through Figure D.50.

The shape bias, pictured in Figure D.51 to Figure D.55, illustrates the systematic overestimation or underestimation of the overall shape of the hydrograph as compared to the baseline hydrographs. SWMM, HEC-1, TR-55, the sub-area modified rational method, and the universal rational method all preserve a small systematic error in the shape. The other models tend to underestimate the shape. Again this may be associated with the volume and the time base relations already observed. Systematic underestimation of these statistics would, in turn, imply a general underestimation of the shape. The rational method applied on the sub-areas provided the worst estimate of the shape. The relatively large standard deviation of PSRM-QUAL shown on the overall shape bias plot, Figure D.51, is due to the large error on the shorter duration design storm. The effects of the Horton-SCS infiltration method used in this model are the probable cause of this anomaly. Again the SCS unit hydrograph performed slightly worse than the Snyder and Clark unit hydrograph models. The sub-area unit hydrographs performed slightly worse than the whole basin models. SWMM proved to contain the least systematic error for shape over all storm durations. Improvement is gained, however, on all of the models as the storm duration increases.

The standard errors of the shape follow the exact same pattern as the root-mean-square error plots. The shape standard error plots are shown in Appendix D, Figure D.56 to Figure D.60. However, the weighted shape standard error tells a slightly different story. A prejudice is introduced into this statistic by emphasizing the peak flow. A change in the plot scale for the weighted shape standard error was required for Figure D.61 through Figure D.65. The statistic describes how each model simulates the hydrograph in the region of the peak flow. For the average of all of the storms, HEC-1 and the sub-area rational methods did extremely poor. SWMM maintained an average accuracy similar to most of the other models but did not prove to be very predictable. Only the unit hydrograph models and TR-20 sustained a consistent standard deviation across all storm types. The whole basin models fared slightly better than the sub-area models. The SCS unit hydrograph only exhibited this trend on the longer duration storms. For the 24 hour duration, the universal rational method performed as well as the unit hydrograph methods and maintained a smaller standard deviation than the sophisticated models. The longer the duration of the storm, the more reliable the models became in predicting the shape of the hydrograph in the vicinity of the peak flow.

5.3 Generalizations

The overall analysis of the watersheds yields some interesting results. The sophisticated models provide good estimates of the hydrograph measures but do so with large variations within each watershed. The unit hydrographs were very consistent and should prove to be very useful for drainage design. The curve number method must be used cautiously because of the trend to overestimate the rainfall losses. The design rainfall models performed as expected. These models work better on the smaller basins with errors increasing with larger basin size. The peak-only methods are quite inaccurate on developed basins. However, their use on the large rural basin is satisfactory and within the range of error expected when using these methods. The Holmes Run 2 watershed was the absolutely hardest to model. This is especially true for the HEC-1 model. The models of Holmes Run 1 and 4 also performed poorly. The Smilax Branch basin was also hard to model because of insufficient watershed data. Changes in the watershed during the simulation time may have occurred. Sensitivity analysis on the watersheds may be needed to determine the nature of the errors observed. Isolation of the exact nature of the discrepancies found in each model category is difficult. Further study of each model is required to isolate the source of the errors.

Overall, all of the models performed well. A few generalizations can be made about the models based on the plots in Appendix D. HEC-1 did not perform well on

the urban watersheds. This may be due to flaws in the Holmes Run watersheds.

Because of this possibility, HEC-1 should not be dismissed as a possible alternative in hydrologic modeling. Definite care should be used when applying this model and verification of the models results is required. Another possibility which may have caused all of the models to deviate for the urban basins is the simplifications made in the modeling process. The many complex drainage systems in urban regions require much more effort than could be applied here. SWMM and the kinematic wave hydrograph in HEC-1 were designed for the complex urban basin. These models were applied with a limited knowledge about the sub-surface drainage network on the Holmes Run basins. Based on previous performance with these models, SWMM and HEC-1 should perform better on the more complex basin than shown here.

Dismissing these models based solely on this study would be a mistake.

Longer storms improve accuracy for many of the models. This is likely related to the infiltration and loss calculations imbedded in the models. For the longer storms, antecedent moisture in the soil would not play as large a role. The ratio of runoff volume to infiltration volume is much higher for the longer storms because the soil is not able to absorb the rainfall as fast later in the storm. Most of the models use the curve number method to estimate rainfall loss. This method has been observed to overestimate the loss quantity. On the longer storms, the initial abstraction is filled up early in relation to the storm duration. The curve number method works well on the

longer storms because the effect of the initial abstraction term is reduced. A better handle on the initial abstraction term is required for the curve number method to function better.

The fact that the whole basin unit hydrograph methods performed better than the sub-area unit hydrograph methods for most of the indicators is easily explained. The two statistics where the sub-area models performed better are the volume and time base indicators. These two statistics are closely related to the infiltration and loss functions within the models. Both types of unit hydrograph models use the curve number method for loss estimation. Apparently the discretization of the watershed improves the accuracy of the curve number method. The improvement of the other statistics on the whole basin models can be traced to the assumptions of unit hydrograph theory. Unit hydrograph theory is based on the assumption of superposition of linear reservoir systems. The sub-area unit hydrographs are superposed and routed to form the outfall hydrograph. The whole basin unit hydrograph model does not rely on this assumption as heavily as the sub-area models. The linear reservoir assumption introduces more errors into the sub-area models. It is the combination of the linear reservoir assumption and the weighting of the curve number method which differentiate the sub-area models from the whole basin unit hydrograph models.

Chapter 6

Recommendations

A quantitative evaluation of the 19 hydrologic model configurations has been completed. The previous sections along with the plots in Appendix C and Appendix D illustrate many different tendencies of the models. The peak flow, runoff volume, timing and the overall shape of the hydrograph are all important parameters in the design of drainage structures. It is up to the engineer to decide which model to use. This decision is based on the capabilities of the models as well as performance. The best performance within the capabilities of the model is desired, if economically feasible. The performance of a model should also be weighed against the cost of obtaining the required data for each model and simulating the watersheds.

6.1 Model Performance Indicators

Table 6.1 is formulated based on the results from the simulations performed in this study. This table contains each of the models ranked by overall performance. Additional information is provided concerning the trends toward basin size and development condition. Because the duration of the storm proved to be significant, it is also included in the table. The performance indicator is a number calculated from the various statistics. This number is a weighted average of the average statistic and

Table 6.1 - Model Performance Indicators

	Scale														
	Worst							Best							
	1													100	
	Peak Flow Estimation	Volume Estimation	Time to Peak Estimation	Time Base Estimation	Hydrograph Shape Prediction	Urban Area Simulation	Partially Developed Area Simulation	Rural Area Simulation	Small Basins (< 2 sq.miles)	Large Basin (> 2 sq.miles)	Gaged Storm Simulation	Short (1-2 hr) Design Storms	Long (24 hr) Design Storms	Overall Performance *	
SWMM	72	87	92	84	40	1	83	86	83	12	63	76	85	65	
PSRM-QUAL	76	87	89	83	43	78	86	87	86	81	74	73	82	79	
TR-20	79	87	93	86	53	85	87	86	86	86	80	79	80	82	
HEC-1 (KW)	1	82	87	84	1	48	84	79	83	55	52	1	72	44	
SCS UH - Whole Basin	84	84	86	81	57	83	83	86	83	84	77	80	76	80	
SCS UH - Sub-areas	80	87	89	84	55	83	85	87	85	85	77	80	81	81	
Snyder's UH - Whole Basin	86	86	88	85	63	88	84	87	84	88	76	82	86	83	
Snyder UH - Sub-areas	82	87	88	84	57	83	84	88	84	85	76	80	83	82	
Clark IUH - Whole Basin	86	86	88	85	62	88	83	87	84	88	76	82	84	83	
Clark IUH - Sub-areas	80	87	88	84	55	83	83	87	83	85	75	80	81	81	
TR-55	89	99	100	98	88	83	91	89	89	86	0	0	79	76	
Rational - Whole Basin	88	0	0	0	0	95	98	96	97	96	0	95	0	51	
Rational - Sub-areas	83	93	93	90	56	77	82	84	81	80	0	66	0	68	
Modified Rational - Whole Basin	89	0	0	0	0	96	98	96	97	96	0	96	0	51	
Modified Rational - Sub-areas	65	94	94	90	1	63	79	83	78	70	0	36	0	58	
Universal Rational	91	96	87	89	71	83	85	76	84	80	0	84	80	77	
USGS Regression - 3 parameter	87	0	0	0	0	93	97	97	96	94	0	95	0	51	
USGS Regression - 7 parameter	86	0	0	0	0	92	96	97	96	94	0	94	0	50	
Anderson Method	70	0	0	0	0	84	90	96	91	88	0	88	0	47	

*Overall Performance = Arithmetic Average of Other Performance Indicators

the standard deviations. The standard deviation is included to give an indication of the predictability of the average. The calculation is a simple average of the weighted statistics over the performance class for each model. For the shape category, all of the shape statistics are weighted with their respective standard deviations. The weighted quantities are then averaged, with equal weight, for all of the shape statistics. This value is then normalized by an error of 3 to obtain a ratio. The error of 3 is chosen because it is the maximum quantity for most of the plots. The normalizing error represents a deviation of 300 percent. Most of the models performed within this range. The normalized ratio is then reset on a scale from 1 to 100 for convenience. The performance indicator increases with improved performance. Some of the performance indicators become less than zero after the final calculation. To maintain consistency, these values are truncated to a value of 1, being the worst on the scale. Performance indicators with a value of zero are not applicable within the given category. See the example calculation in Figure 6.1 .

Table 6.1 is based solely on the results of this study. The lack of universal data limit use of this table within the range of watersheds and models modeled. More research is required to expand this table and confirm or contradict the results. The use of this table for model selection should not be done blindly, but with much scrutiny because of the limited data used to generate table. Some of the results are clearly inappropriate. One instance is the use of SWMM for the urban watershed simulation.

Performance Indicator Calculation for:

- **Peak Flow Estimation**
- **EPA SWMM model**

$$PI_{x, Q_p} = 100 - \left[\frac{\sum_{k_x \in Q_p} \left[\left(\left| \overline{M_{Q_p}} \right| \cdot \frac{2}{3} \right) + \left(S_{Q_p} \cdot \frac{1}{3} \right) \right]}{3} \right] \cdot 99 \right]$$

Where:

PI_{x, Q_p}	=	Performance indicator for model x and peak flow
$\overline{M_{Q_p}}$	=	Average of statistic measuring peak flow performance
S_{Q_p}	=	Standard deviation of statistic measuring peak flow performance
k_x	=	Set of all statistics for model x

Using all statistics measuring peak flow performance, we get:

$$PI_{x, Q_p} = 100 - \left[\left(\left| \epsilon_{Q_p} \right| + \left| SE_{Q_p} \right| \right) \cdot 2 + \left(S_{\epsilon_{Q_p}} + S_{SE_{Q_p}} \right) \cdot 11 \right]$$

Where:

ϵ_{Q_p}	=	Average peak flow bias
$S_{\epsilon_{Q_p}}$	=	Standard deviation of peak flow bias
SE_{Q_p}	=	Average peak flow standard error
$S_{SE_{Q_p}}$	=	Standard deviation of peak flow standard error

Substituting from Table B.1, B.2, B.3, B.4:

$$PI_{x, Q_p} = 100 - \left[\left((0.310 + 0.408) \cdot 2 + (0.299 + 0.126) \right) \cdot 11 \right]$$

$$PI = 79$$

Figure 6.1 - Example Calculation of Performance Index

This model was designed specifically for the case of the urban basin. The inability of SWMM to perform well in the urban setting is mainly due to the lack of detail about the drainage network within the particular watersheds used in this study. One must not discount the fact that the data is based on only 2 rural basins, 3 developed basins and 3 urban basins. Expansion of the data set is necessary to explain the errors found in this study. All 8 of the watersheds are located within 30 miles of each other. The effects of regionalization cannot be determined from the data available. Adding watersheds outside of the area should help explain these effects.

To utilize Table 6.1 efficiently, the engineer should review the capabilities of the models as well as the required input before model selection is made. The tables in Chapter 2 should provide an adequate reference for this review. Depending on the modeling requirements of the project, some of the models may be eliminated. For example, if a small urban watershed is being modeled and pollutant simulation is required, only two models are available (SWMM and PSRM-QUAL are the only options for pollutant simulation). In cases, like the example, where more than one model is available, Figure 5.31 is used to select the model based on the performance for a small urban watershed. In the example, PSRM-QUAL is the optimal choice based on performance. While the table is adequate for effective model selection, the plots in Appendix C and Appendix D and the tables in Appendix B should be used for

more complex situations. Also, experience with each model should not be omitted in the selection process.

6.2 Cross-Calibration and Other Implications

The cross-calibration of models to obtain a more accurate estimate of the peak flow is verified by this study. The use of the USGS Virginia regression equations for verification of the results of a more advanced model is justified. Table 6.1 indicates that the regression equations can be used to estimate the flood peak for the short duration design events adequately. Cross-calibration is recommended to improve the accuracy of the more sophisticated models. The simple calculation procedure of the regression equations from actual watershed data can be accomplished in just a few minutes. The potential cost savings introduced in the design of hydraulic structures by cross-calibration could be significant.

Other implications of this study result from isolated modeling techniques. The only difference in TR-20 and the SCS sub-area unit hydrograph models is the channel routing scheme. The slightly larger errors found for the TR-20 method imply that the routing scheme is the cause for this difference. The close correlation of TR-20 with TR-55 indicate that TR-55 is a valid simplification of the more sophisticated model. This is, however, limited to 24-hour SCS design event and the limits imposed by the

method. The rational and modified rational whole basin models also exhibit good performance on all of the basins for peak flow estimation.

The USGS is ready to release new equations for use in Virginia. These equations are more regionalized and have improved statistical performance. We should expect the new equations to perform better than the 1978 equations. An evaluation of the new equations with the other models will need to be conducted for further verification of the cross-calibration technique.

6.3 Recommendations for Further Study

Further evaluation of the models is required in order to obtain an accurate estimate of model performance. This study attempted to evaluate many different models for many different situations. This attempt limits the results of the study which provides a starting point for model selection based on performance. Further study is required in specific areas pointed out in this evaluation. Separating out the individual components of the models needs to be done to truly evaluate each of the models. By looking at each model in detail, the differences will become apparent.

The most obvious limitation of this study is the limited number of gaged events for each watershed. The lack of data is due to the geographical limitations imposed. By increasing the boundaries of the study area to outside of the northern Virginia region, more data would become available. What is required is continuous (minimum

5 minute increments) rainfall/runoff data for small (less than 2 square miles) watersheds. The Virginia Agricultural Extension Service operates many small rural basins with records of sufficient duration to facilitate flood frequency analysis. There are a few urban watersheds located in Maryland which also contain adequate data. Using larger, less developed watersheds will also improve the data set.

Improvement of the calibration models would also enhance the model results significantly. The linear programming procedure described in Chapter 4 would provide a unit hydrograph with a minimum of error. Using a more sophisticated model for the calibration model would provide numerous variables to simulate many different physical processes. Either of these methods should yield a better calibration model but with a much greater time or computer requirement.

References

Anderson, Daniel G., Effects of Urban Development on Floods in Northern Virginia, United States Geological Survey, Water Resources Division, 1968.

Aron, Gert, B. A. Dempsey and T. A. Smith III, Penn State Runoff Quality Model (PSRM-Q) User Manual, Department of Civil and Environmental Engineering and the Environmental Resource Research Institute, The Pennsylvania State University, University Park, PA, April 1992.

Espey, W. H. and D. G. Altman, "Nomographs for Ten Minute Unit Hydrographs for Small Urban Watersheds", in EPA Report EPA-600/9-78-035, Washington D.C., 1978.

Gupta, Ram S., Hydrology and Hydraulic Systems, Prentice Hall Inc., Englewood Cliffs, NJ, 1989.

Hershfield, D. M., Rainfall Frequency Atlas of the United States for Durations from 30-Minutes to 24-Hours and Return Periods from 1 to 100 Years, United States Department of Commerce, Weather Bureau, Technical Paper No. 40, Washington D.C., 1961.

Huber, Wayne C., R. E. Dickenson and T. O. Barnwell, Jr., Storm Water Management Model, Version 4: User's Manual, Department of Environmental Engineering Sciences, University of Florida, Gainesville, FL, Draft of August 1988.

Keser, J., "Comparative Investigation of Computer Methods", Urban Storm Drainage: Proceedings from International Conference held at the University of Southampton, University of Southampton, Southampton, Great Britain, 1978.

Kibler, David F., T. A. Seybert and E. L. White, Penn State Urban Hydrology Model User's Manual, Water Resources Program, Department of Civil Engineering, The Pennsylvania State University, University Park, PA, July 1990.

Kibler, David F., G. A. Krallis, and M. E. Jennings, "Model Choice and Scale in Urban Drainage Design", Proceedings from American Society of Civil Engineers Meeting of the Hydraulics Division, Williamsburg, VA, August 1987.

Kibler, David F., G. Aron, K. A. Riley, E. L. White and G. Osei-Kwando, Recommended Hydrologic Procedures for Computing Urban Runoff from Small Developing Watersheds in Pennsylvania, Technical Completion Report, Department of Civil Engineering, The Pennsylvania State University, 1982a.

Kibler, David F., "Desk-Top Methods for Urban Storm Water Calculation", Urban Storm Water Hydrology, American Geophysical Union Water Resources Monograph no. 7, Kibler, D.F., Ed., AGU, Washington, D.C., 1982b.

Miller, Earley M., Technique for Estimating Magnitude and Frequency of Floods in Virginia, U.S. Geological Survey, Water Resources Investigations 78-5, January 1978.

Nace, R., "General Evolution of the Concept of the Hydrologic Cycle", Three Centuries of Scientific Hydrology, United Nations Educational, Scientific and Cultural Organizations (UNESCO), World Meteorological Organization (WMO), and the International Association of Hydrological Sciences (IAHS), Paris, France, 1974

Overton, D. E. and M. E. Meadows, Storm Water Modeling, Academic Press Inc., New York, NY, 1976

Prince William County, Prince William County Design and Construction Standards Manual, Prince William County Department of Public Works, Prince William County, Virginia, Reprinted July 1992.

Riordan, E. J., N. S. Grigg and R. L. Hiller, "Measuring the Effects of Urbanization on the Hydrologic Regime", Urban Storm Drainage: Proceedings from International Conference held at the University of Southampton, University of Southampton, Southampton, Great Britain, 1978.

Rossmiller, Ronald L., "The Rational Method Revisited", Proceedings from International Symposium on Urban Storm Runoff, University of Kentucky, Lexington, KY, July 1980.

Sauer, V. B., W. O. Thomas, Jr., V. A. Stricker and K. V. Wilson, Flood Characteristics of Urban Watersheds in the United States, United States Geological Survey, Water Supply Paper 2207, United States Government Printing Office, Washington D. C., 1983

United Nations Department of International Economic and Social Affairs, World Population Prospects, UN Building, New York, NY, 1989.

United States Army Corps of Engineers, HEC-1 Flood Hydrograph Package, User's Manual, Hydrologic Engineering Center, Davis, CA, September 1990.

United States Department of Agriculture, Soil Conservation Service, Technical Release 55, Urban Hydrology for Small Watersheds, SCS Engineering Division, Washington D.C., June 1986.

United States Department of Agriculture, Soil Conservation Service, National Engineering Handbook, Section 4 - Hydrology, SCS Engineering Division, Washington D.C., 1985.

United States Department of Agriculture, Soil Conservation Service, Technical Release 20, TR-20 Computer Program for Project Formulation - Hydrology, SCS Northeast NTC and Hydrology Unit, Washington D.C., Draft of 2nd Edition, May 1983.

Viessman, W., J. W. Knapp and G. L. Lewis, Introduction to Hydrology, 2nd Edition, IEP, A Dun-Donelley Publisher, New York, 1977.

Virginia Department of Transportation, "Drainage Manual", Location and design division, Hydraulics Section, VDOT, Commonwealth of Virginia, reprinted March 1990.

Williams, Keith K., "Equivalent Synthetic Unit Hydrographs", Proceedings from Second International Conference on Urban Storm Drainage, University of Illinois at Urbana-Champaign, Urbana, IL, June 1981.

Woolhiser, D. A. and D. L. Brakensiek, "Hydrologic System Synthesis", Hydrologic modeling of Small Watersheds, American Society of Agricultural Engineers Monograph no. 5, Haan, C.T., Johnson, H.P. and Brakensiek, D.L., Ed., ASAE, St. Joseph, MI, 1982.

Yen, Ben C., "Some Measures for Evaluation and Comparison of Simulation Models", Proceedings from Second International Conference on Urban Storm Drainage, University of Illinois at Urbana-Champaign, Urbana, IL, June 1981.

Appendix A

Gaged Storm Events and Design Storm Hyetographs

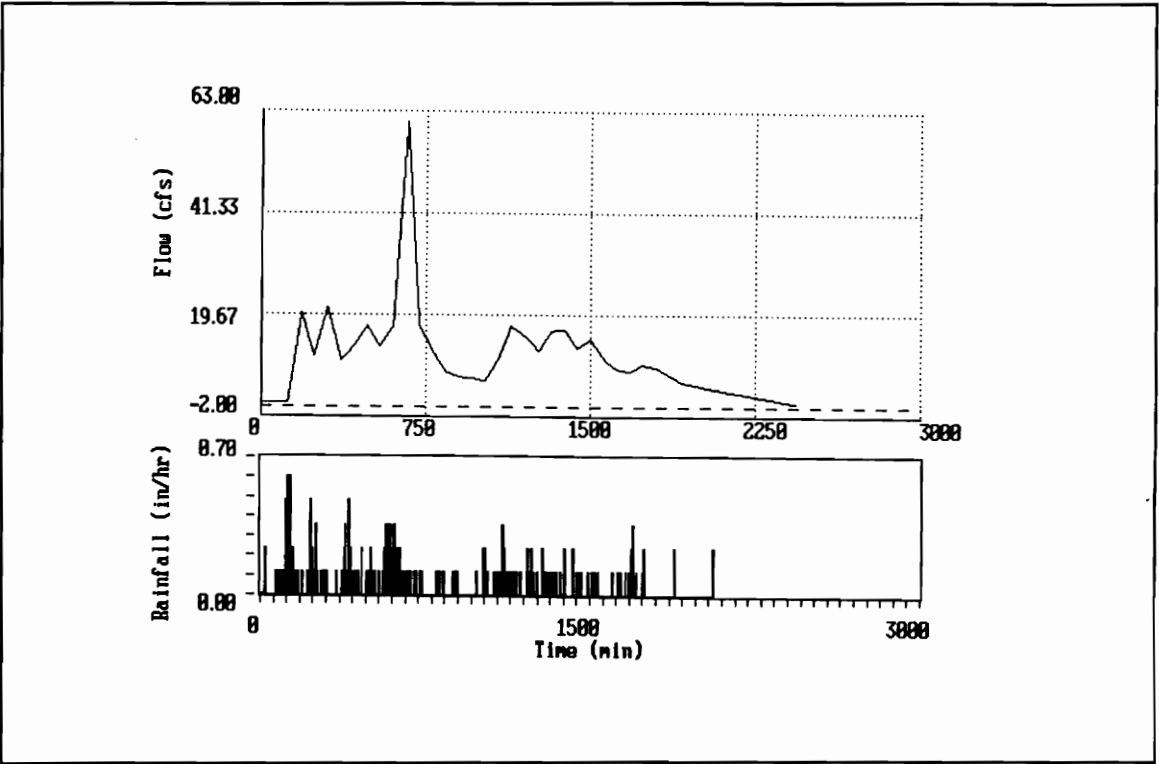


Figure A.1 - Snakeden Branch, Gaged Event 1

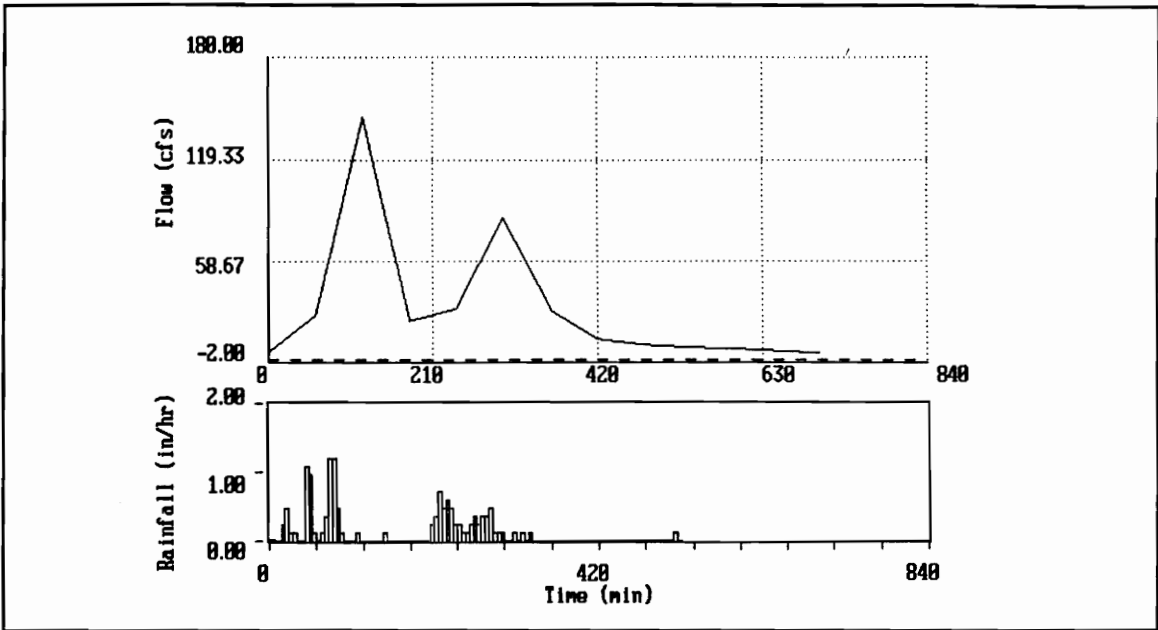


Figure A.2 - Snakeden Branch at Reston, Gaged Event 2

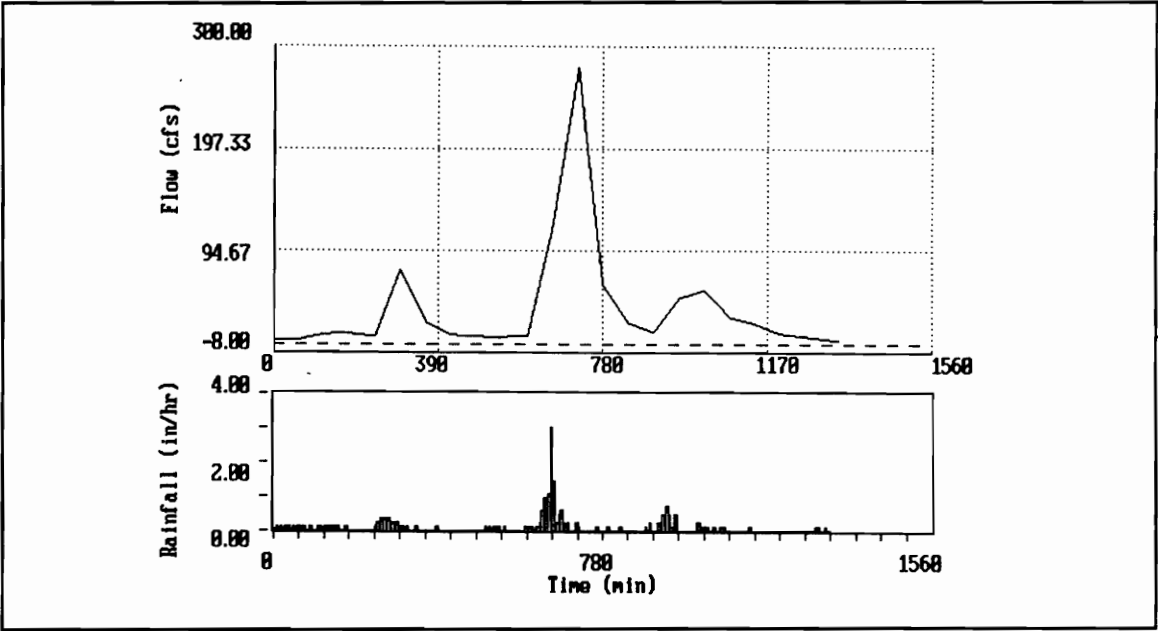


Figure A.3 - Snakeden Branch at Reston, Gaged Event 3

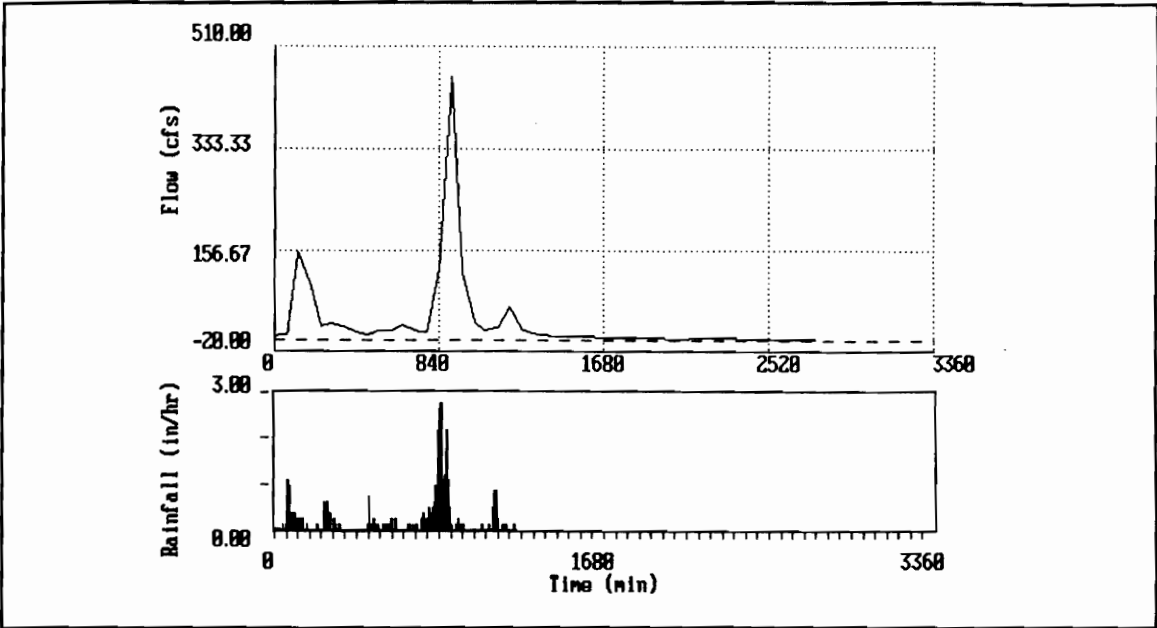


Figure A.4 - Snakeden Branch at Reston, Gaged Event 4

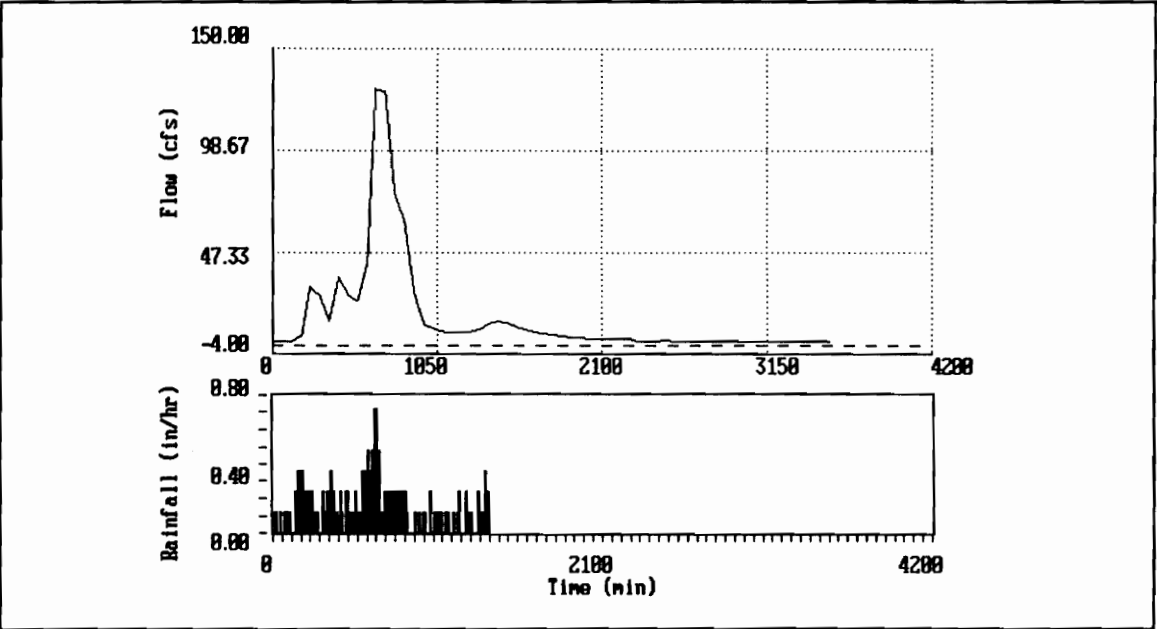


Figure A.5 - Snakeden Branch at Reston, Gaged Event 6

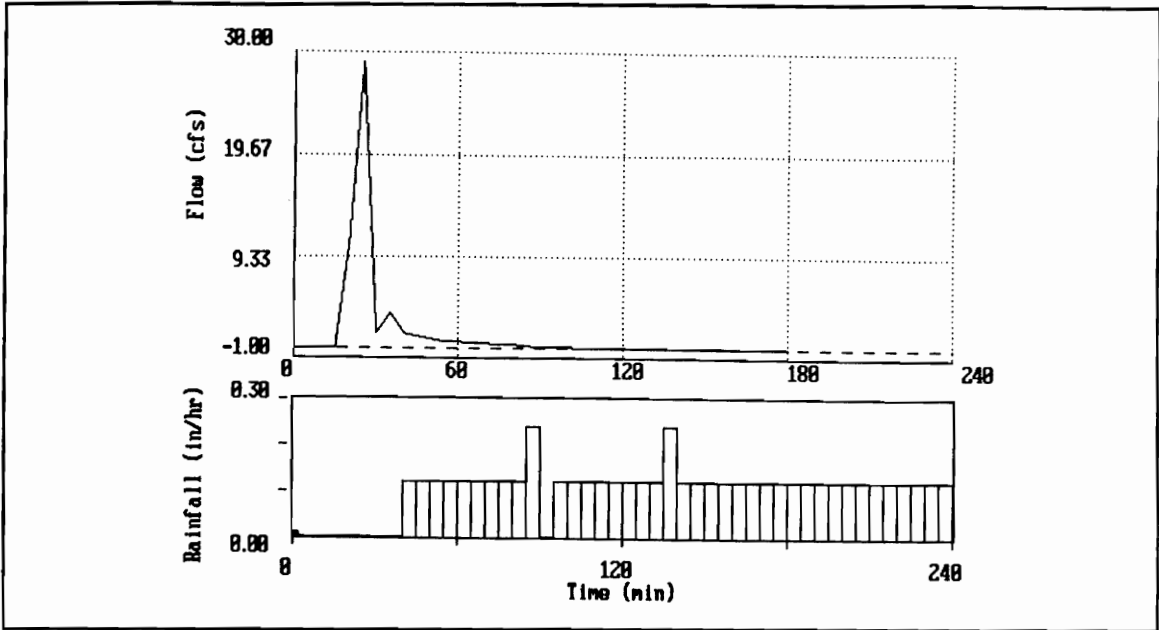


Figure A.6 - Stave Run near Reston, Gaged Event 1

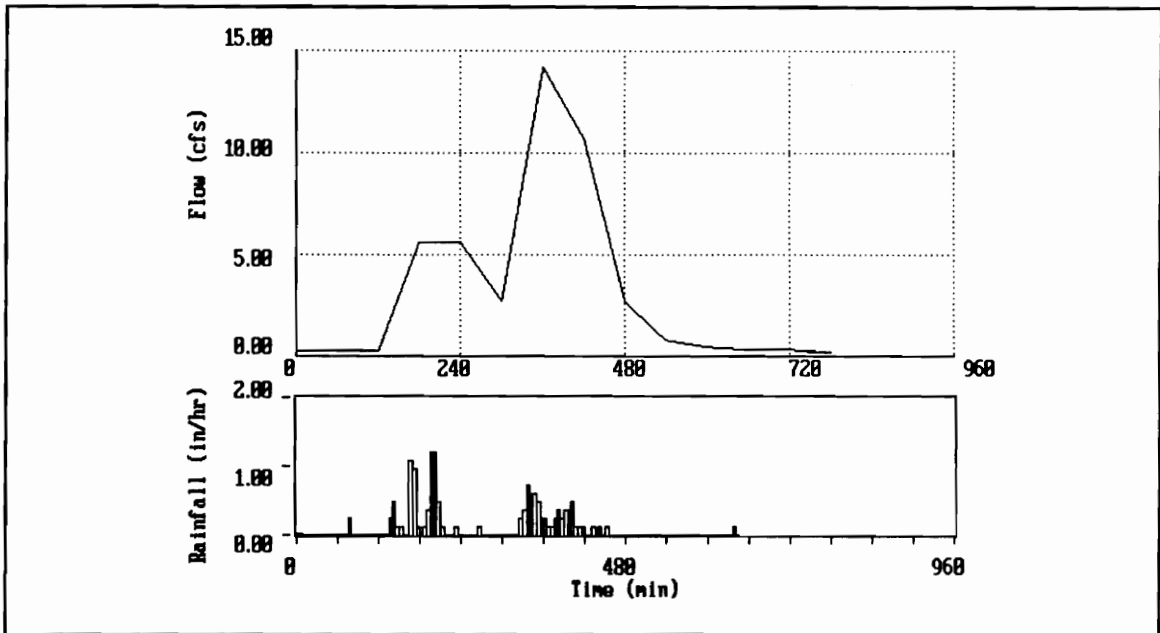


Figure A.7 - Stave Run near Reston, Gaged Event 2

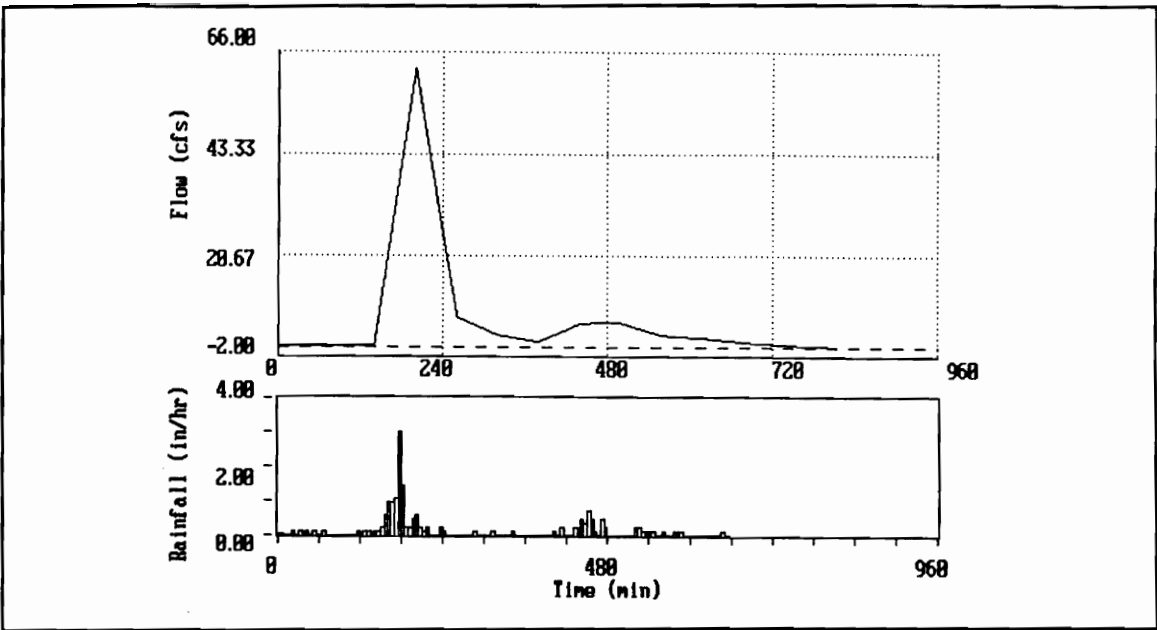


Figure A.8 - Stave Run near Reston, Gaged Event 3

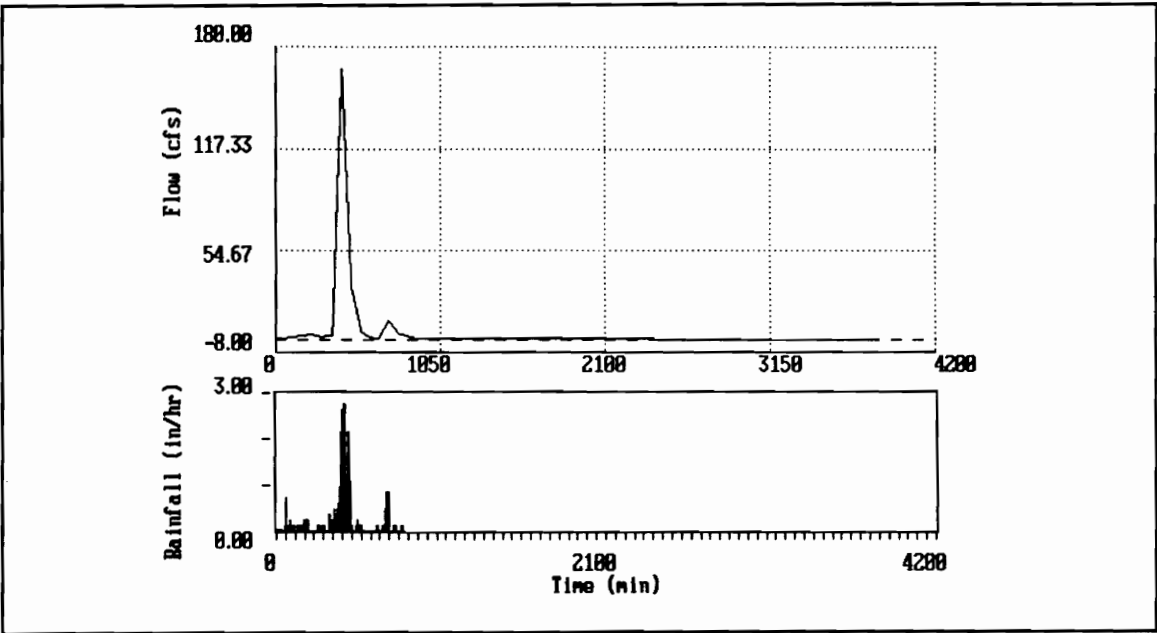


Figure A.9 - Stave Run near Reston, Gaged Event 4

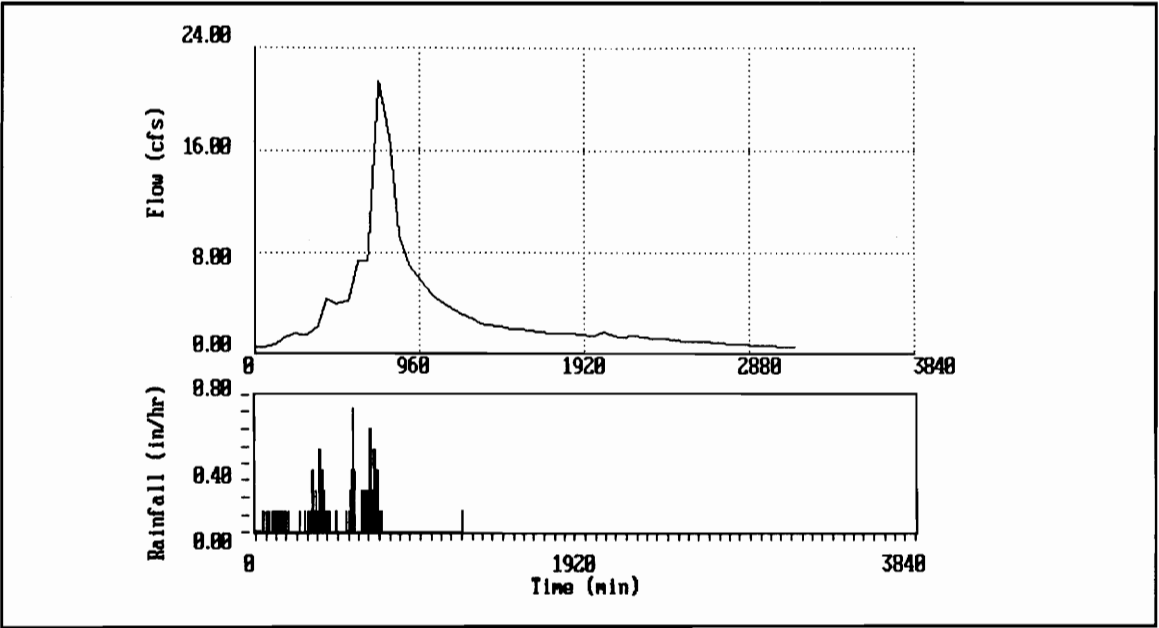


Figure A.10 - Smilax Branch at Reston, Gaged Event 1

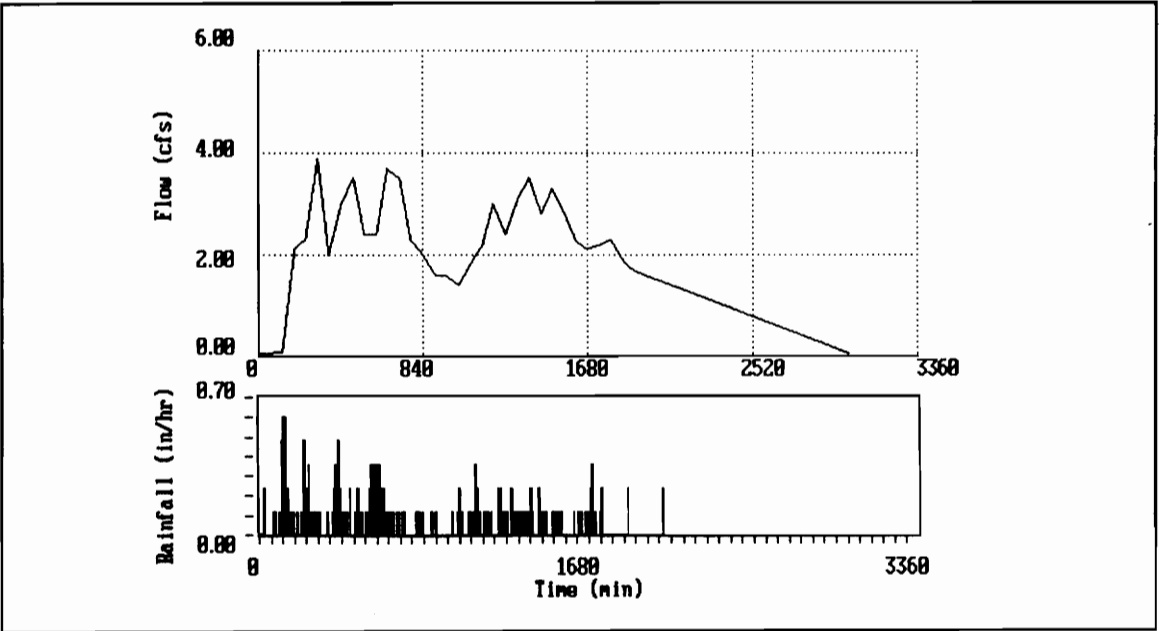


Figure A.11 - Smilax Branch at Reston, Gaged Event 2

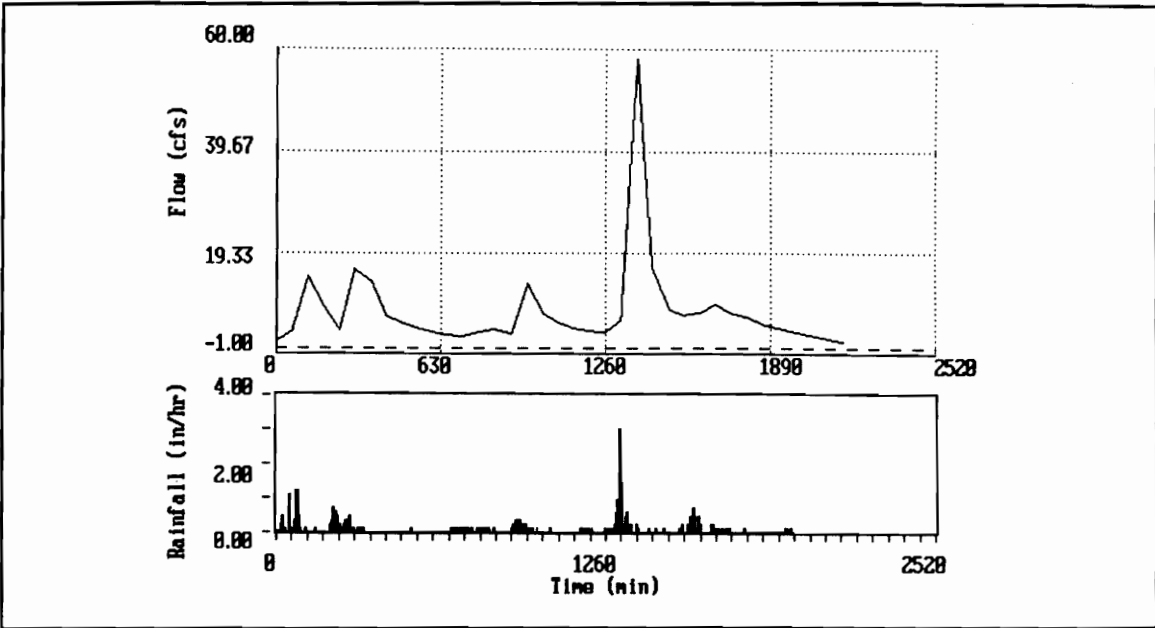


Figure A.12 - Smilax Branch at Reston, Gaged Event 3

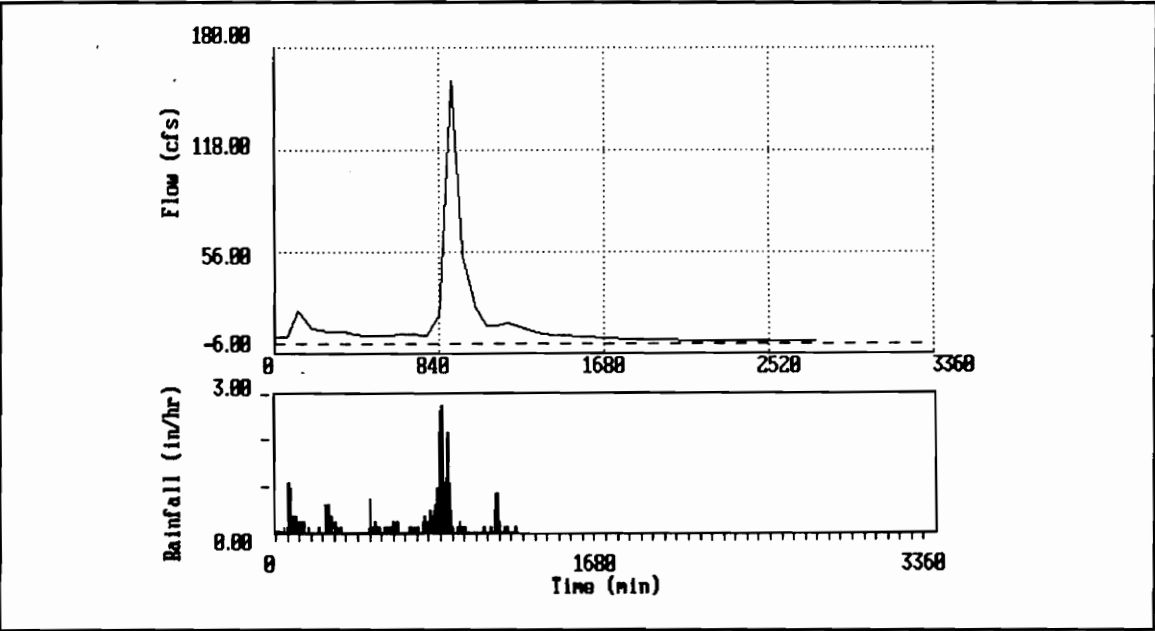


Figure A.13 - Smilax Branch at Reston, Gaged Event 4

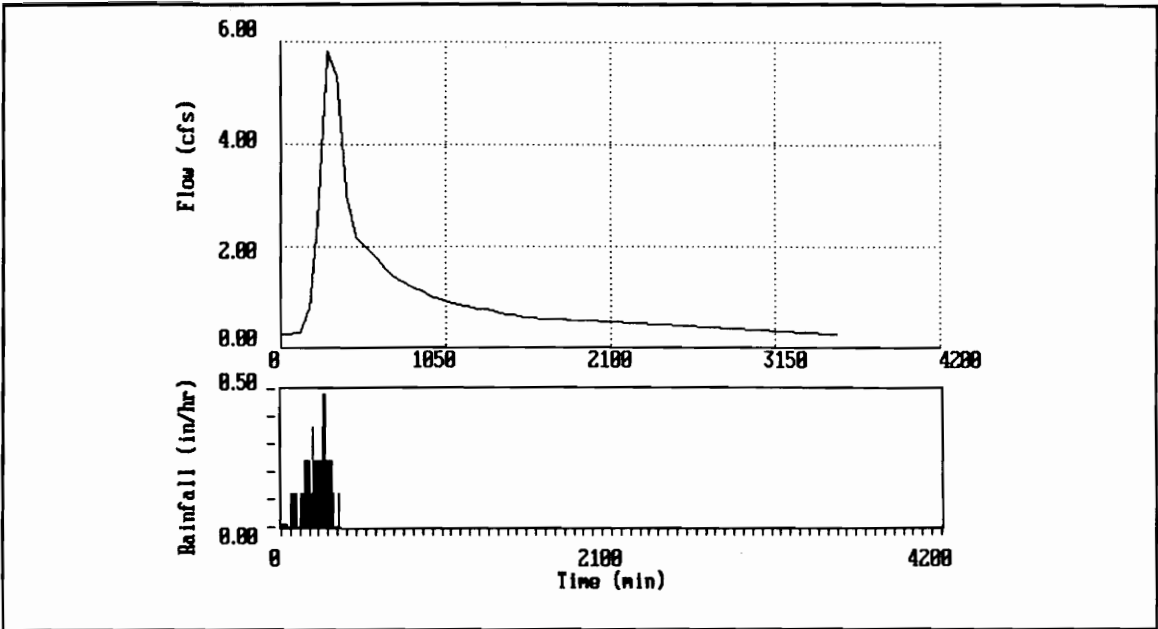


Figure A.14 - Smilax Branch at Reston, Gaged Event 5

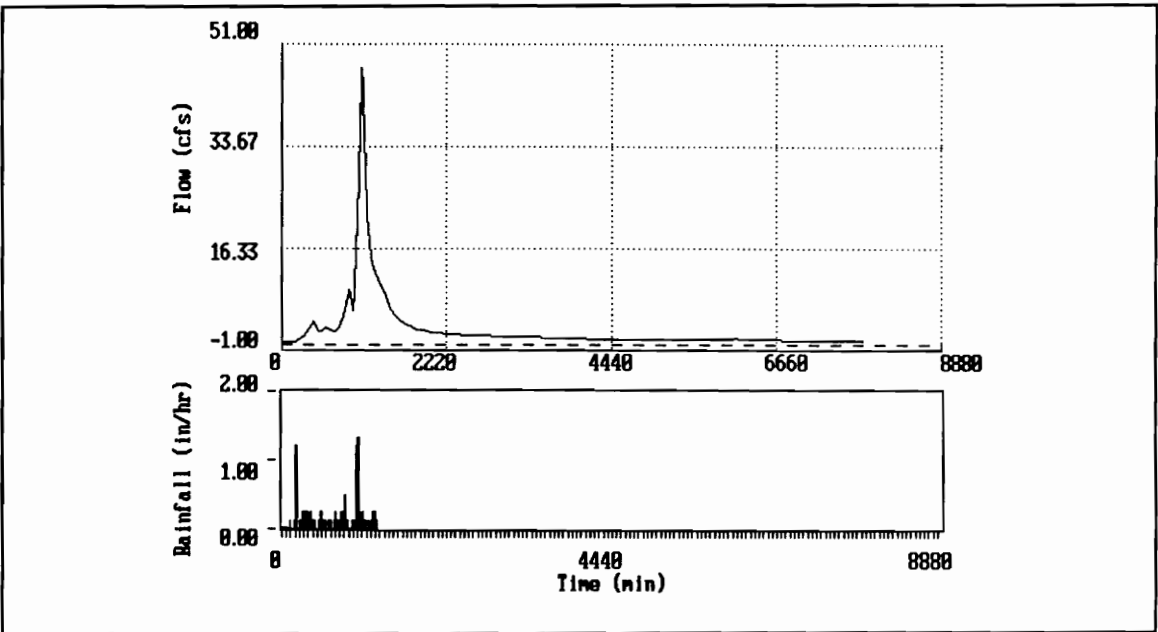


Figure A.15 - Smilax Branch at Reston, Gaged Event 6

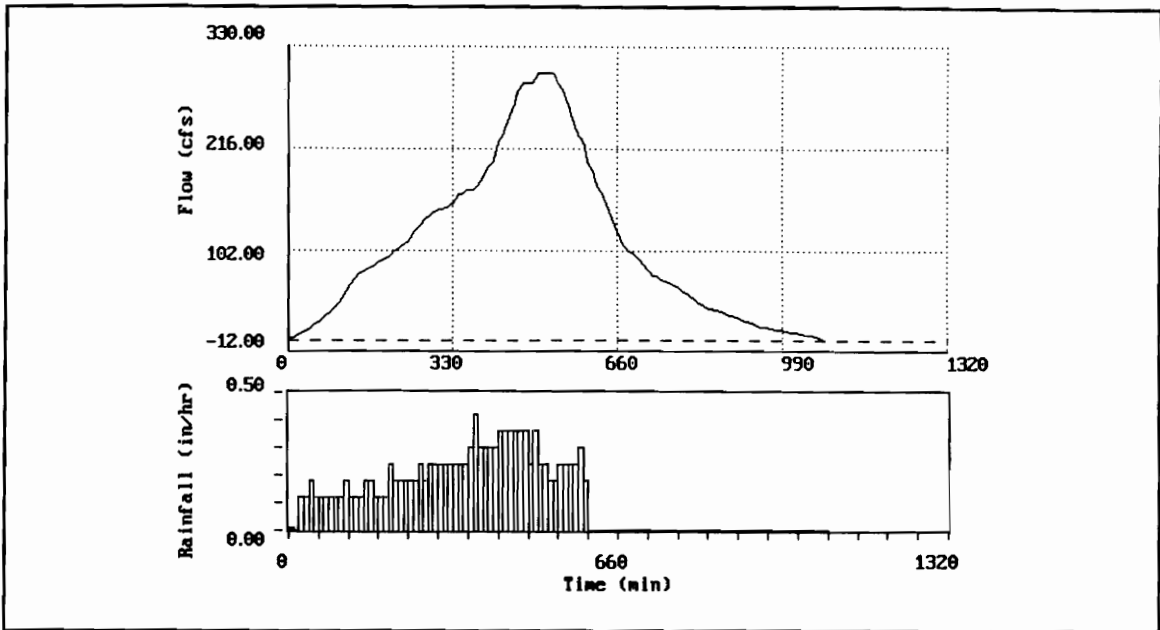


Figure A.16 - South Fork Broad Run at Arcola, Gaged Event 1

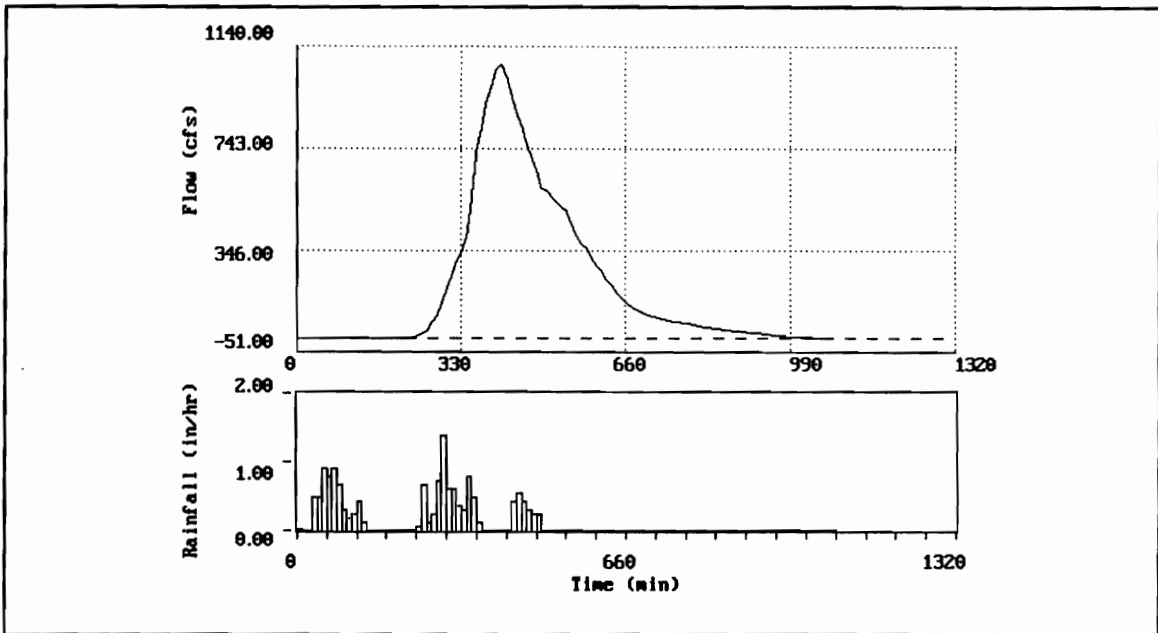


Figure A.17 - South Fork Broad Run at Arcola, Gaged Event 2

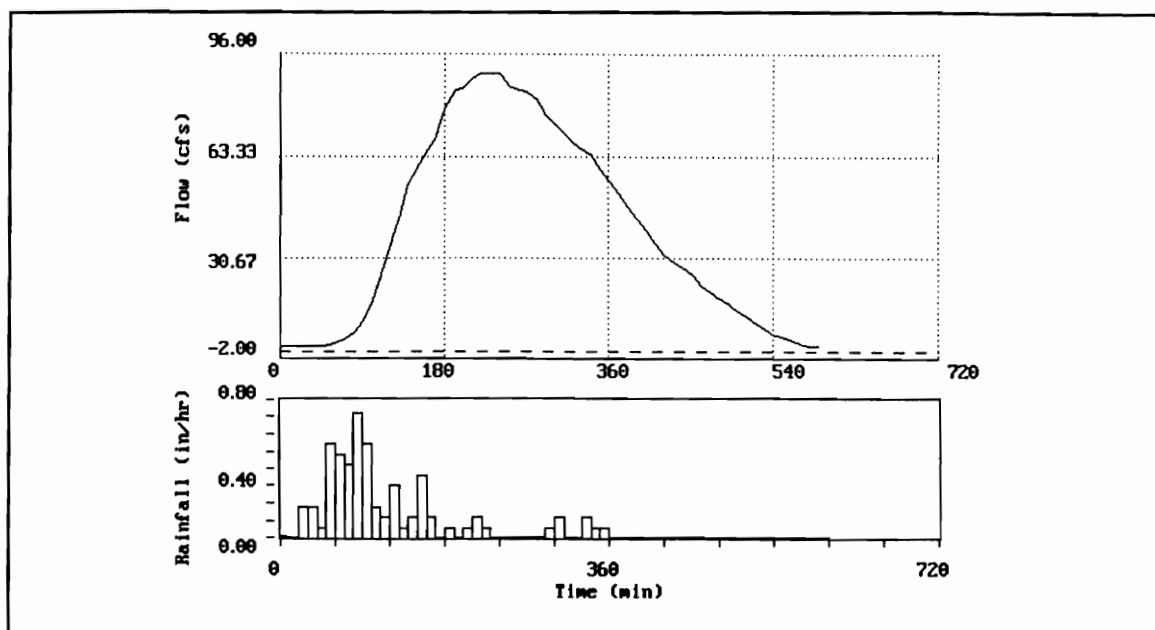


Figure A.18 - South Fork Broad Run at Arcola, Gaged Event 3

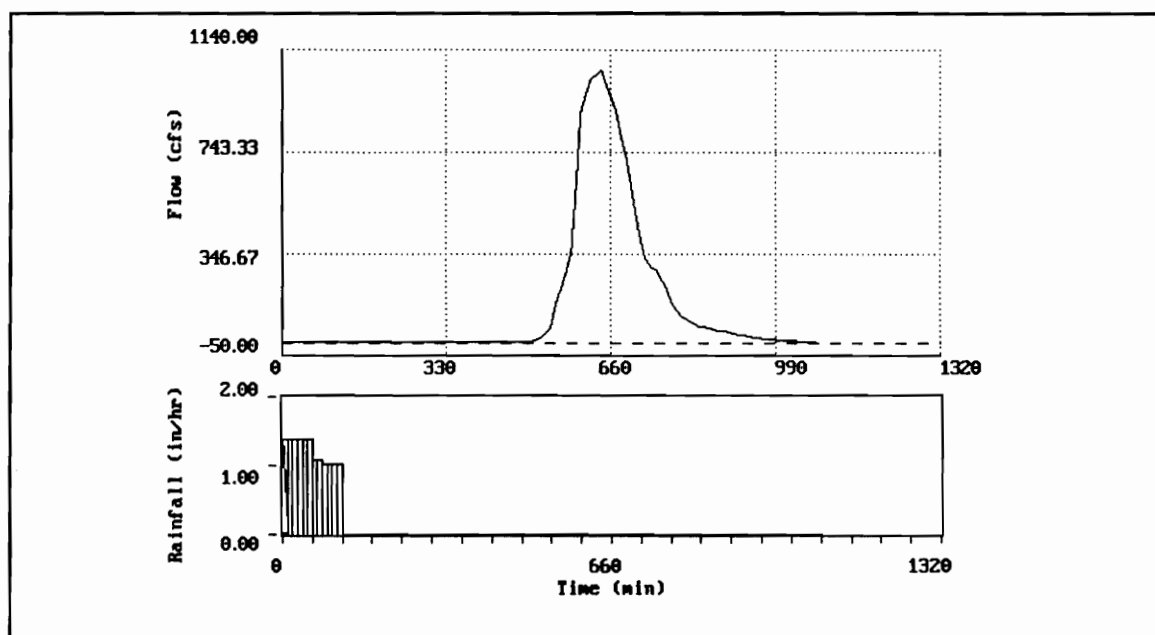


Figure A.19 - South Fork Broad Run at Arcola, Gaged Event 4

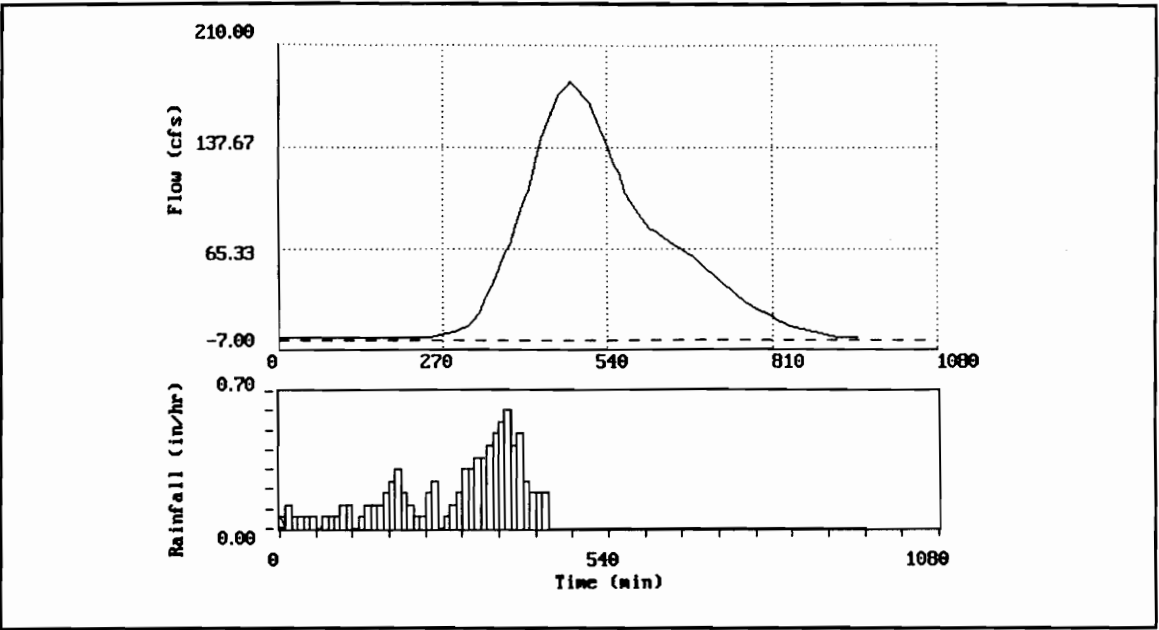


Figure A.20 - South Fork Broad Run at Arcola, Gaged Event 5

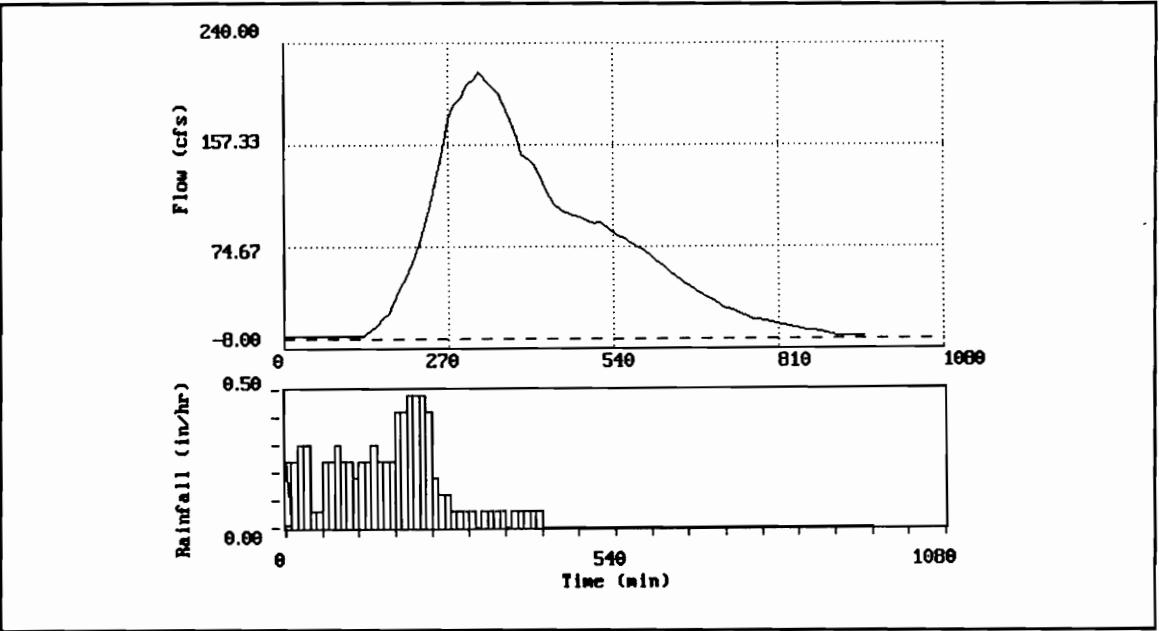


Figure A.21 - South Fork Broad Run at Arcola, Gaged Event 6

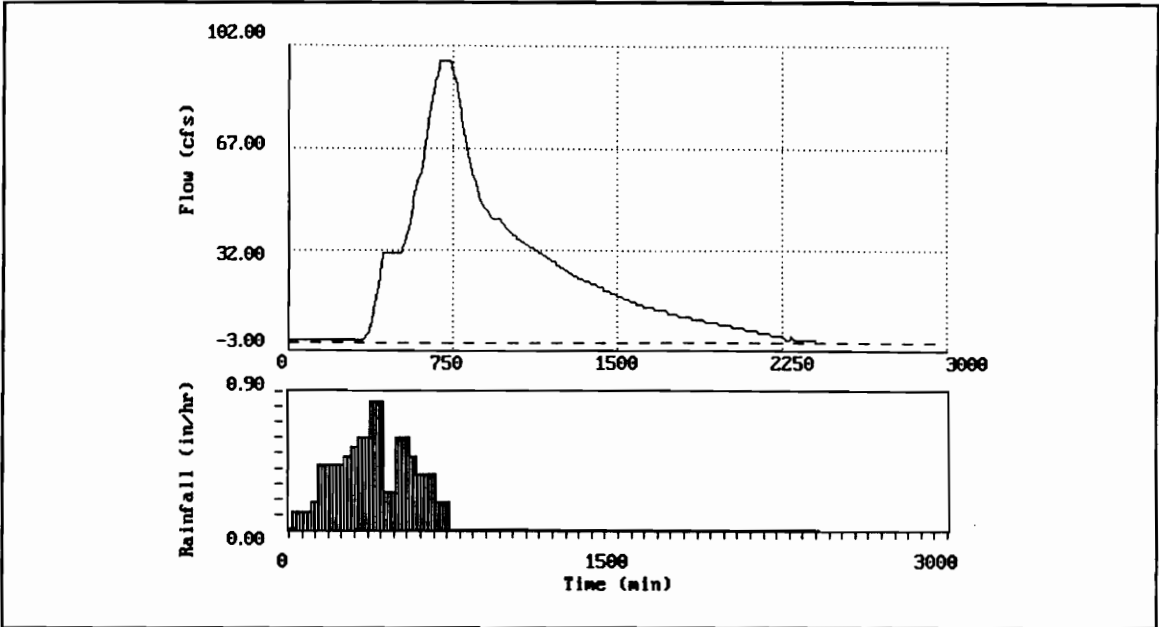


Figure A.22 - Broad Run Tributary at Buckland, Gaged Event 1

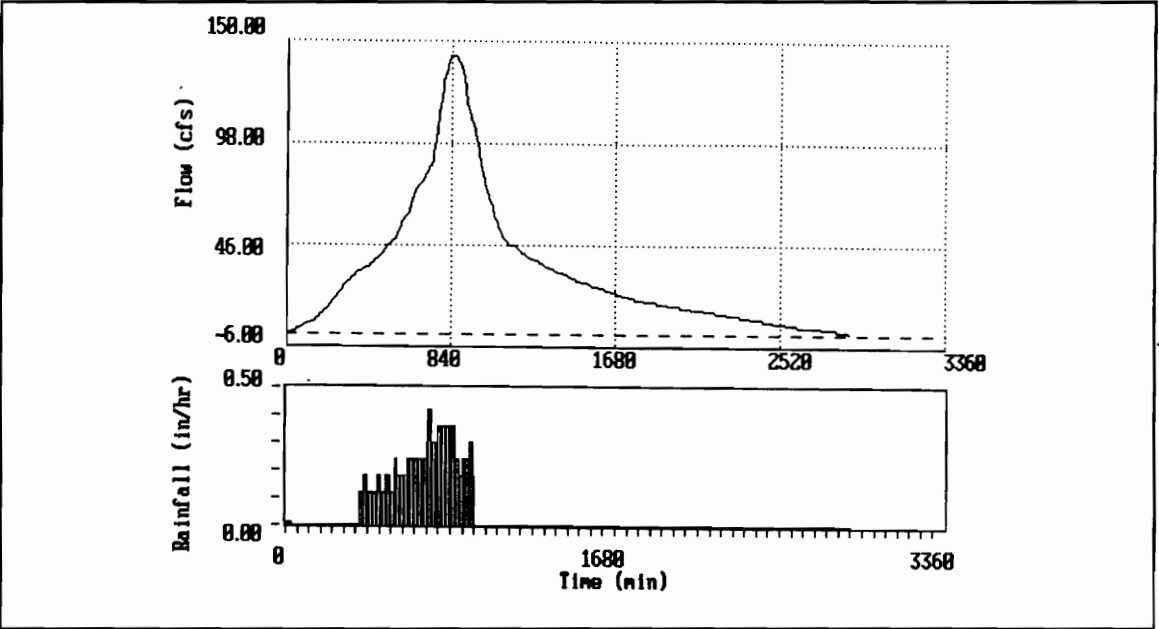


Figure A.23 - Broad Run Tributary at Buckland, Gaged Event 2

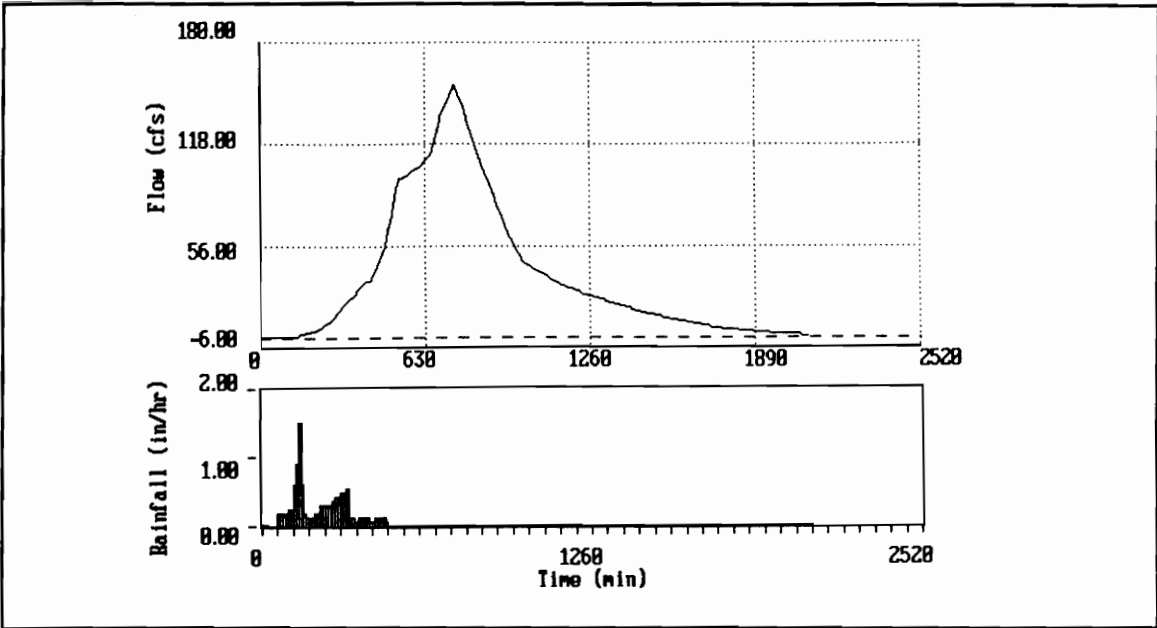


Figure A.24 - Broad Run Tributary at Buckland, Gaged Event 3

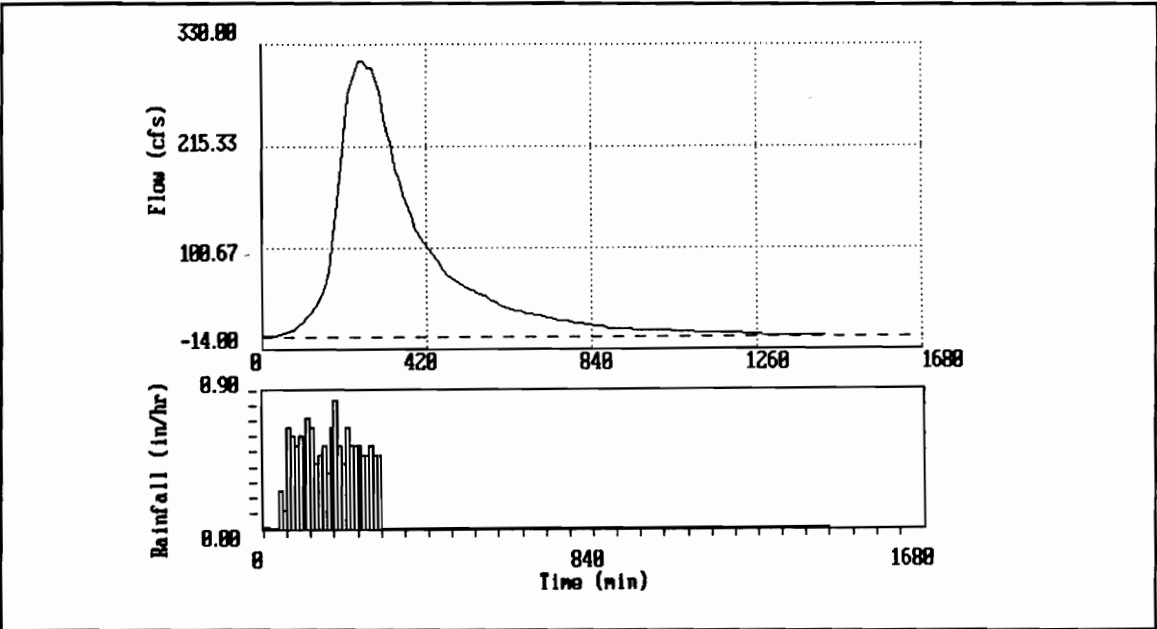


Figure A.25 - Broad Run Tributary at Buckland, Gaged Event 4

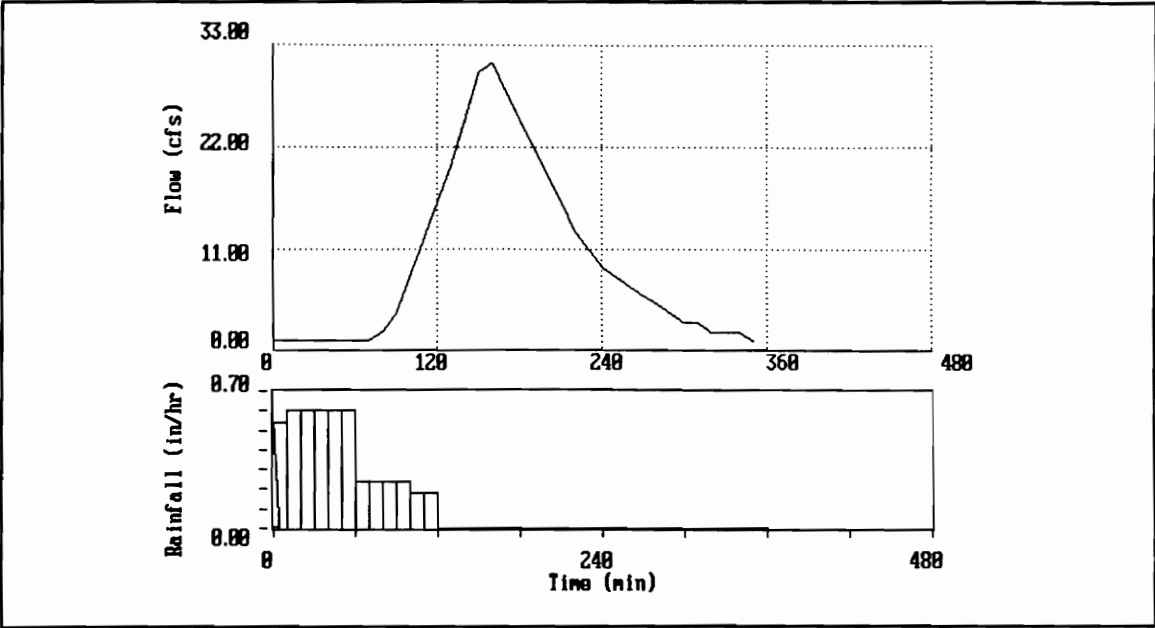


Figure A.26 - Broad Run Tributary at Buckland, Gaged Event 5

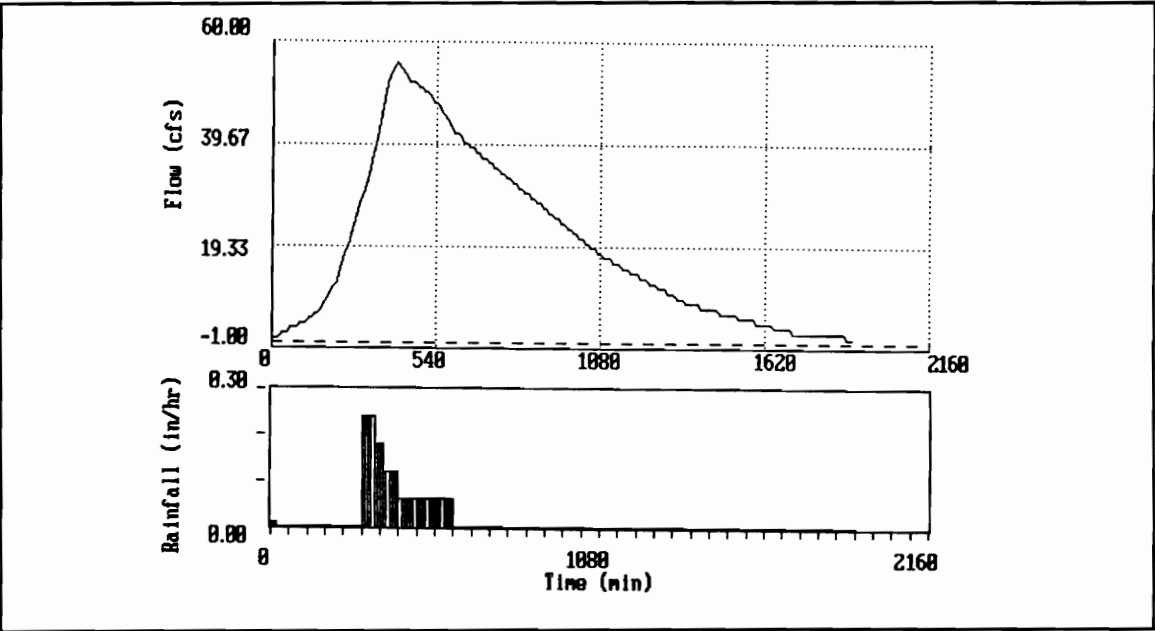


Figure A.27 - Broad Run Tributary at Buckland, Gaged Event 6

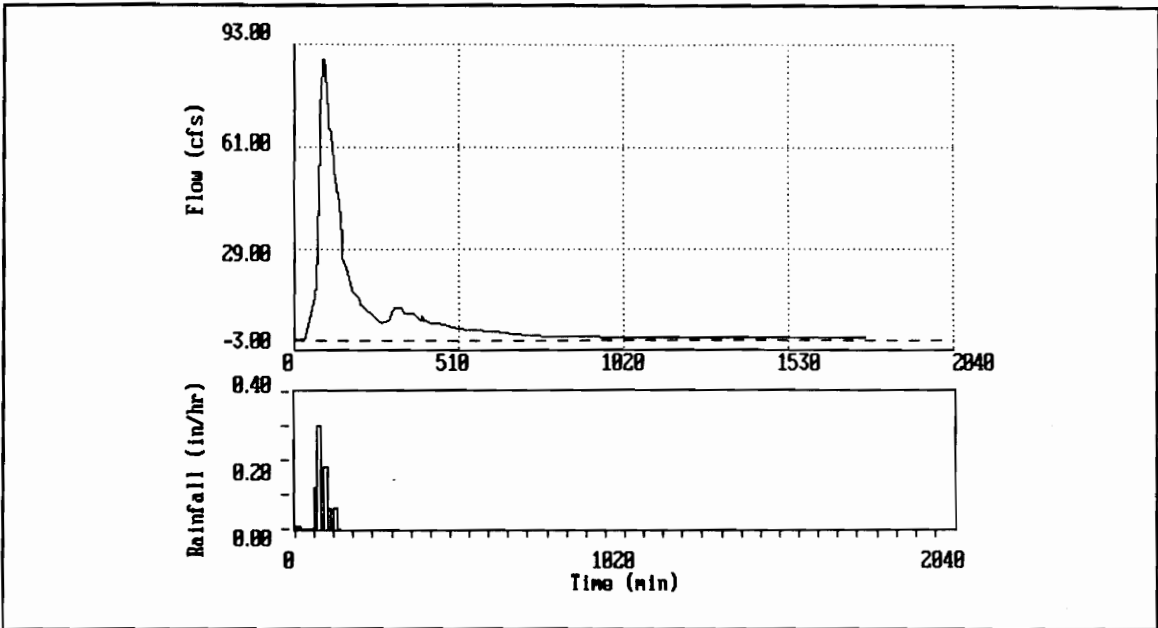


Figure A.28 - Holmes Run Gage 1 at Falls Church, Gaged Event 1

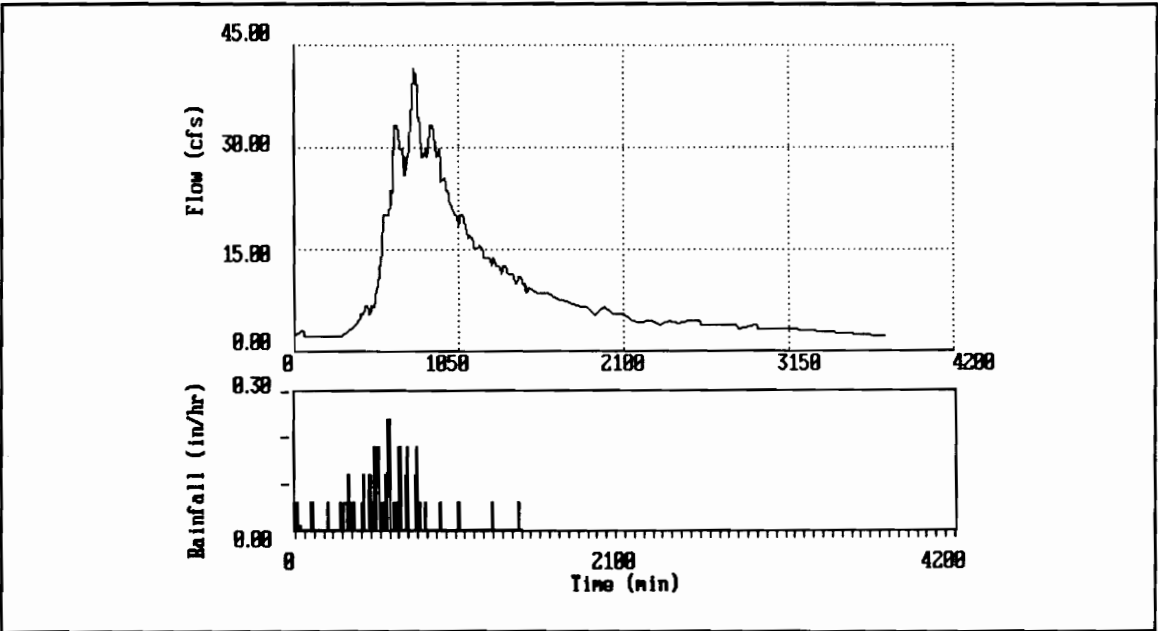


Figure A.29 - Holmes Run Gage 1 at Falls Church, Gaged Event 2

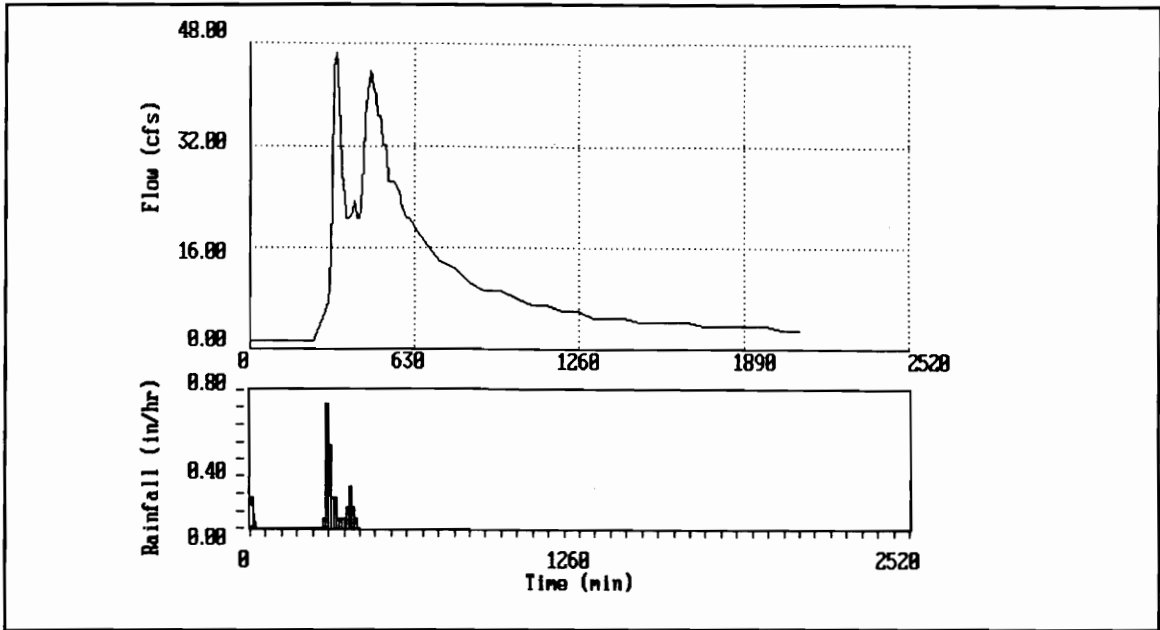


Figure A.30 - Holmes Run Gage 1 at Falls Church, Gaged Event 3

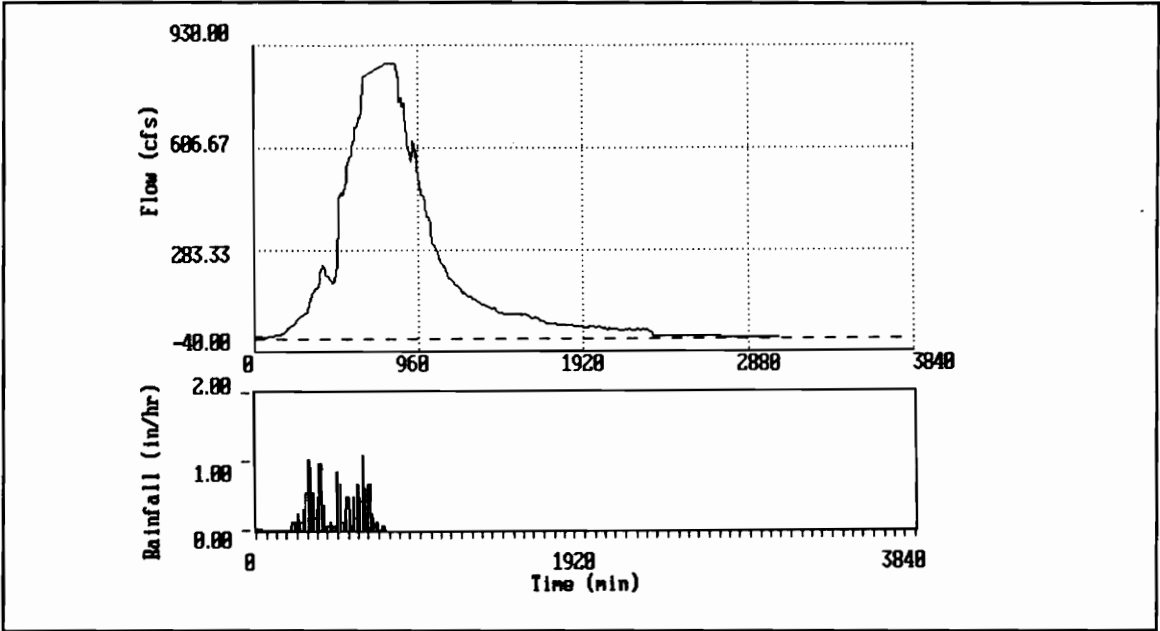


Figure A.31 - Holmes Run Gage 1 at Falls Church, Gaged Event 4

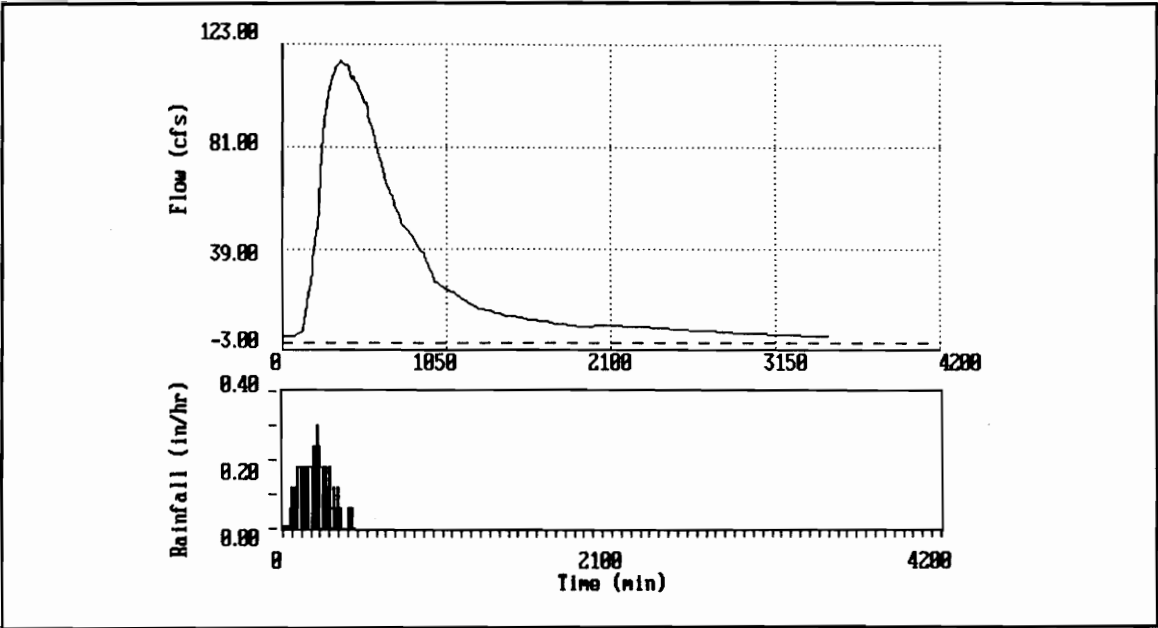


Figure A.32 - Holmes Run Gage 1 at Falls Church, Gaged Event 5

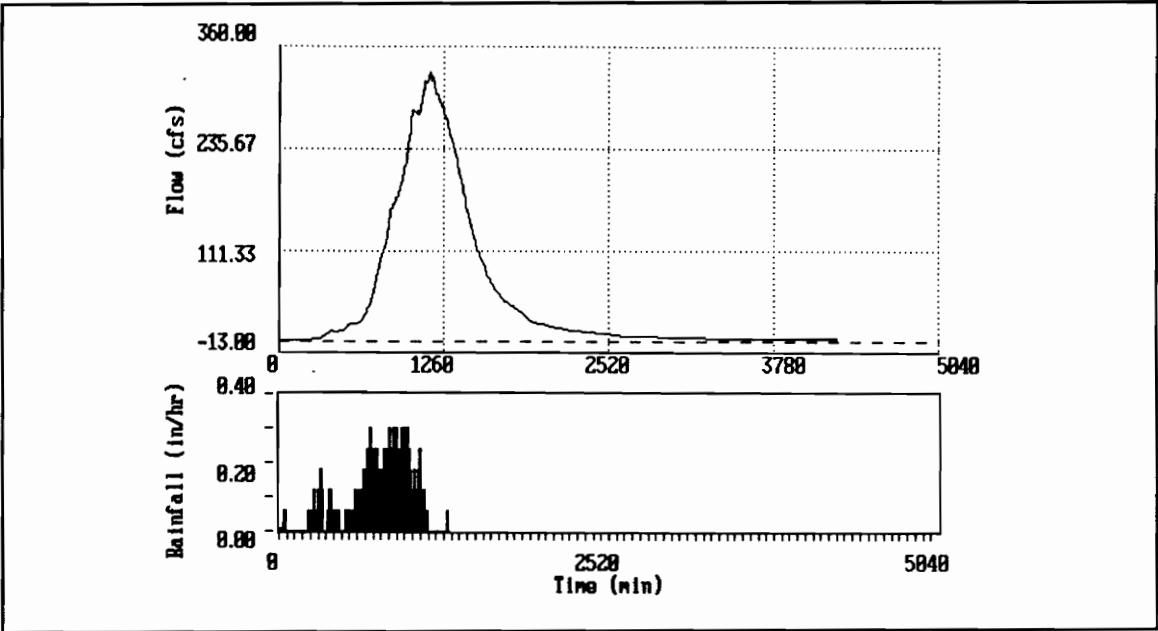


Figure A.33 - Holmes Run Gage 1 at Falls Church, Gaged Event 6

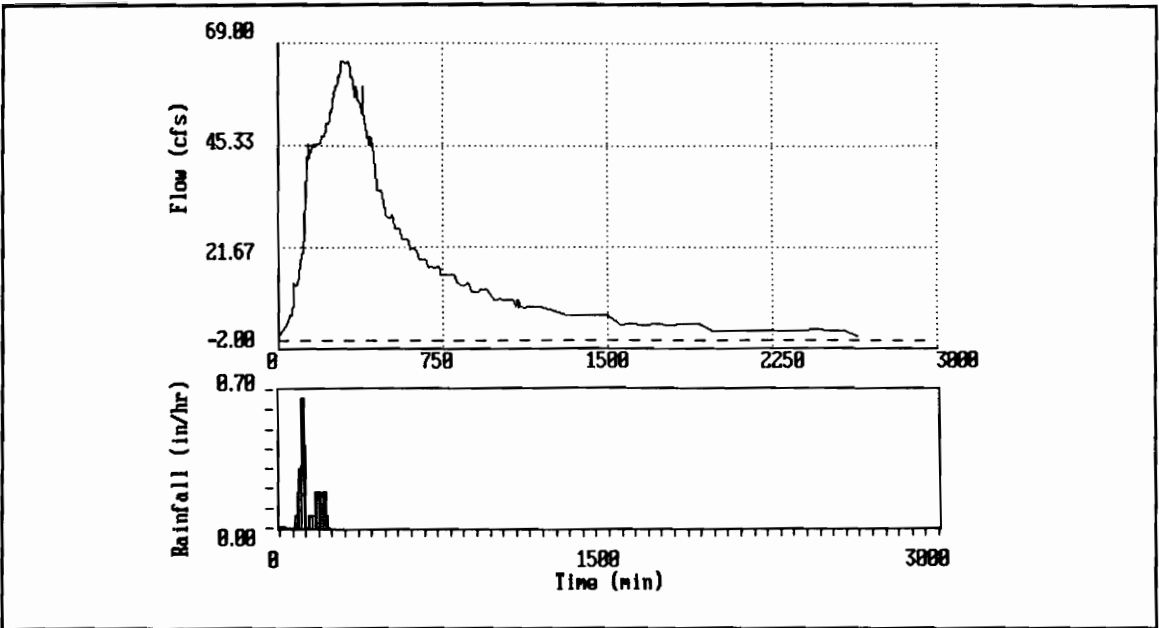


Figure A.34 - Holmes Run Gage 2 at Falls Church, Gaged Event 1

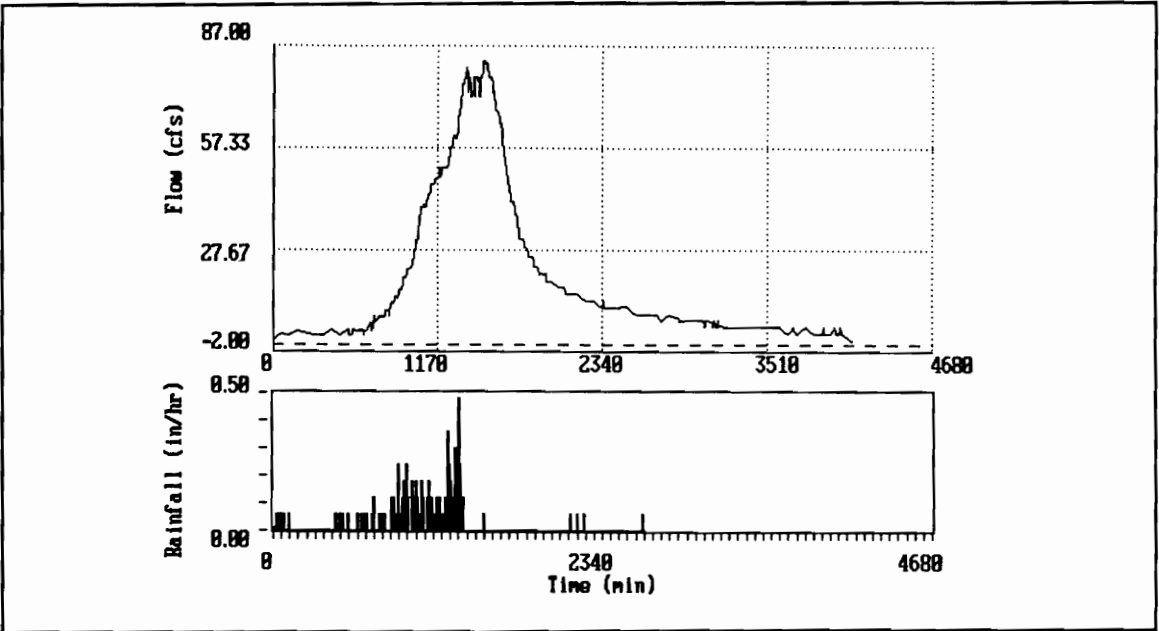


Figure A.35 - Holmes Run Gage 2 at Falls Church, Gaged Event 2

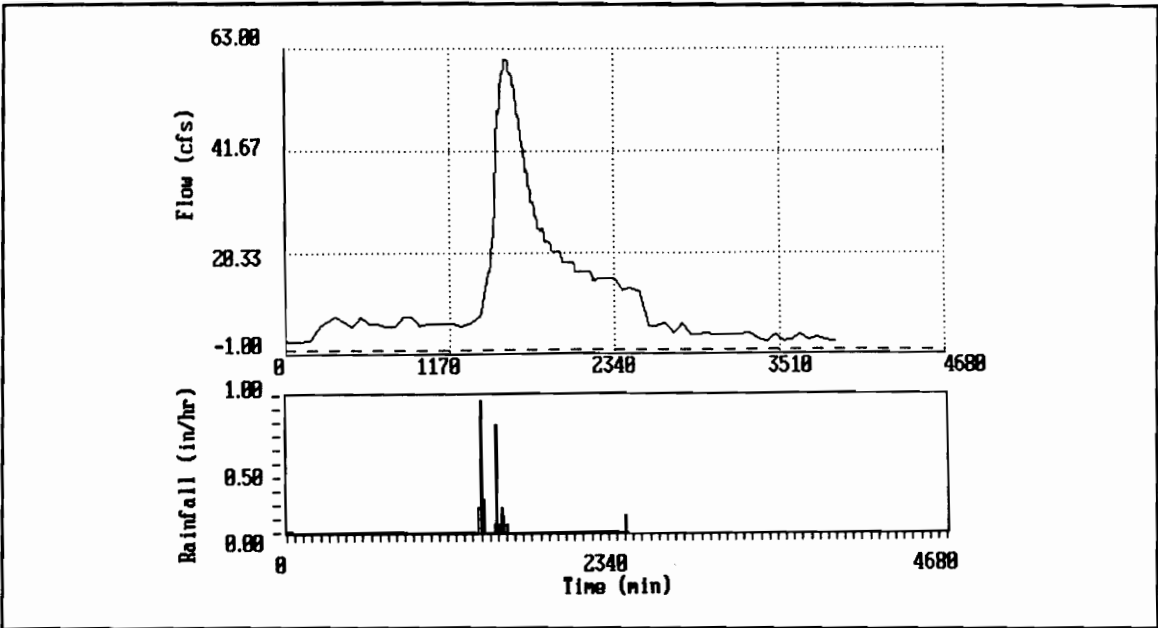


Figure A.36 - Holmes Run Gage 2 at Falls Church, Gaged Event 3

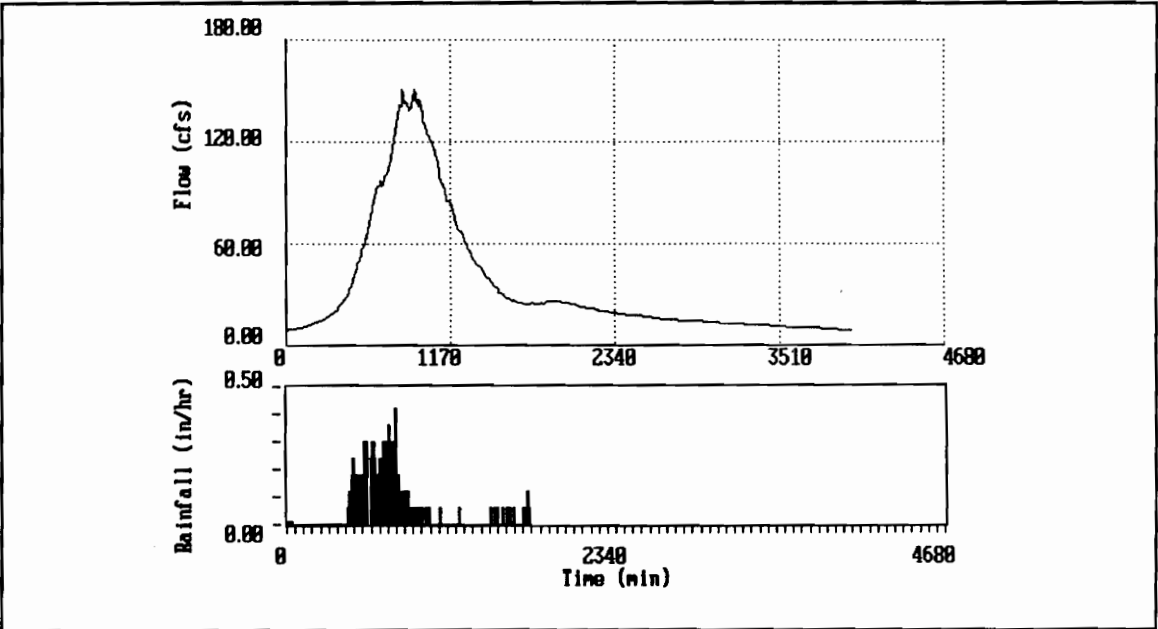


Figure A.37 - Holmes Run Gage 2 at Falls Church, Gaged Event 4

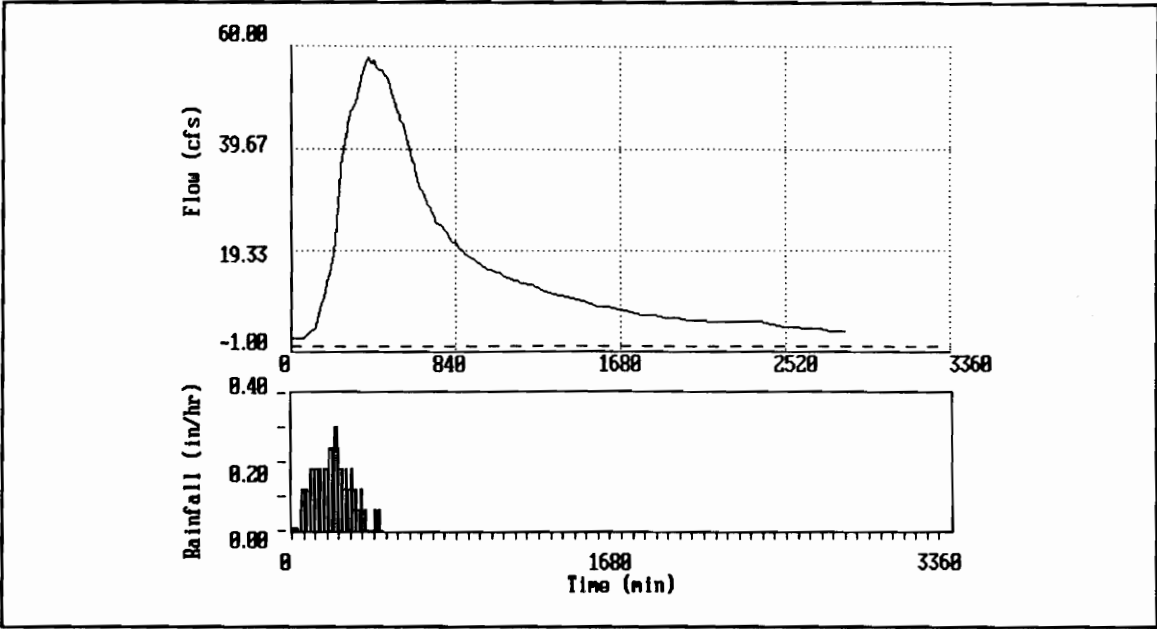


Figure A.38 - Holmes Run Gage 2 at Falls Church, Gaged Event 5

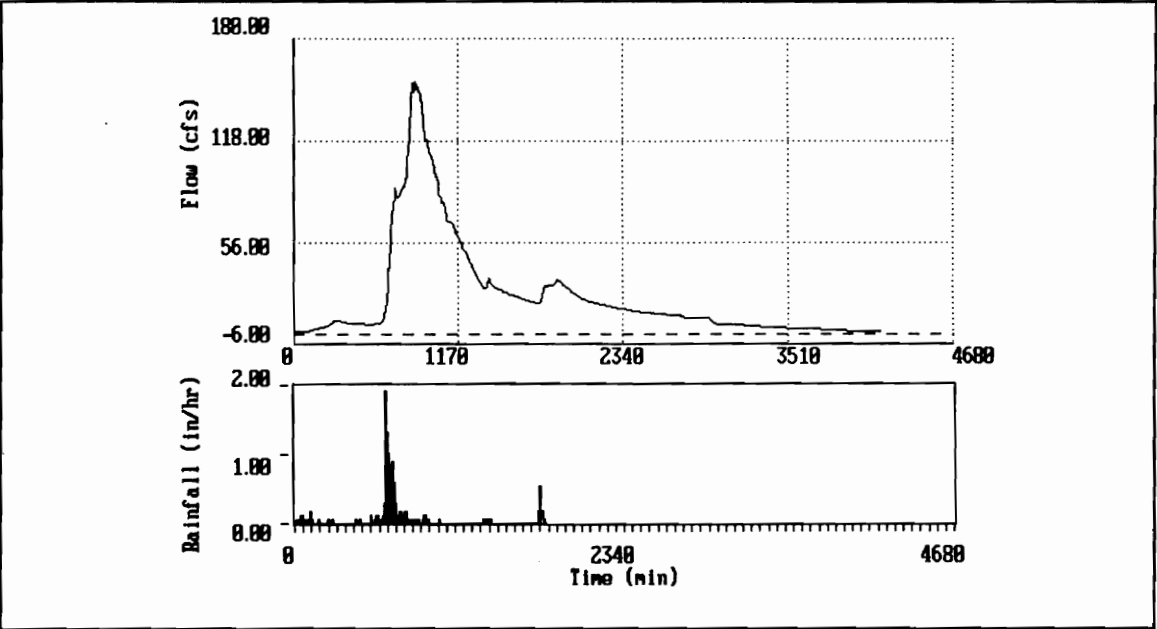


Figure A.39 - Holmes Run Gage 2 at Falls Church, Gaged Event 6

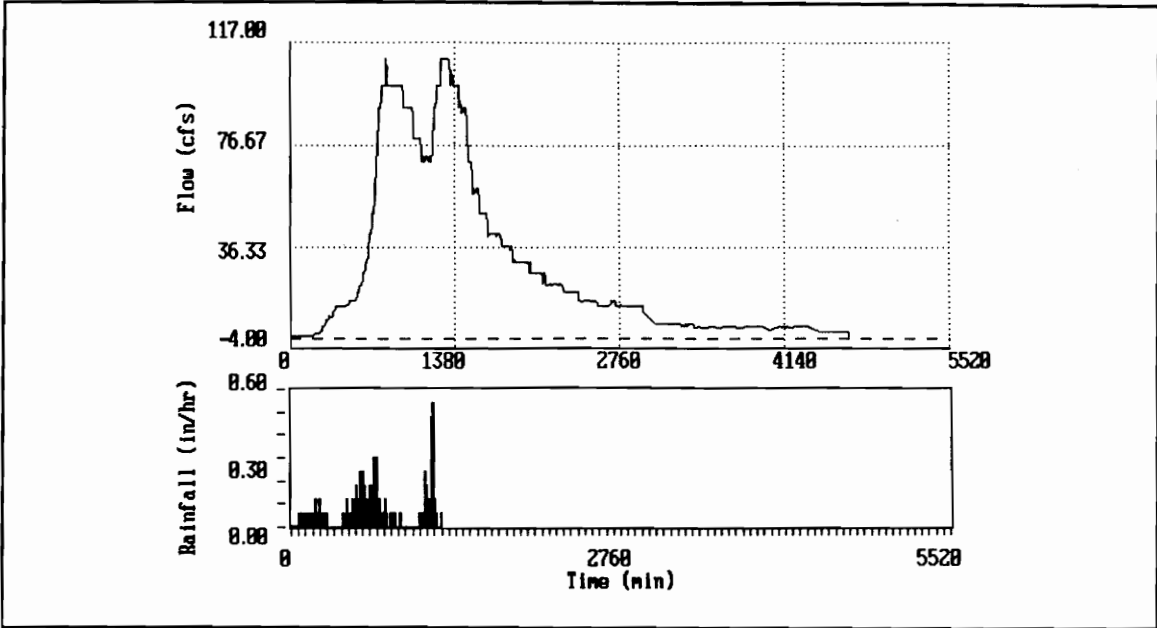


Figure A.40 - Holmes Run Gage 4 at Falls Church, Gaged Event 1

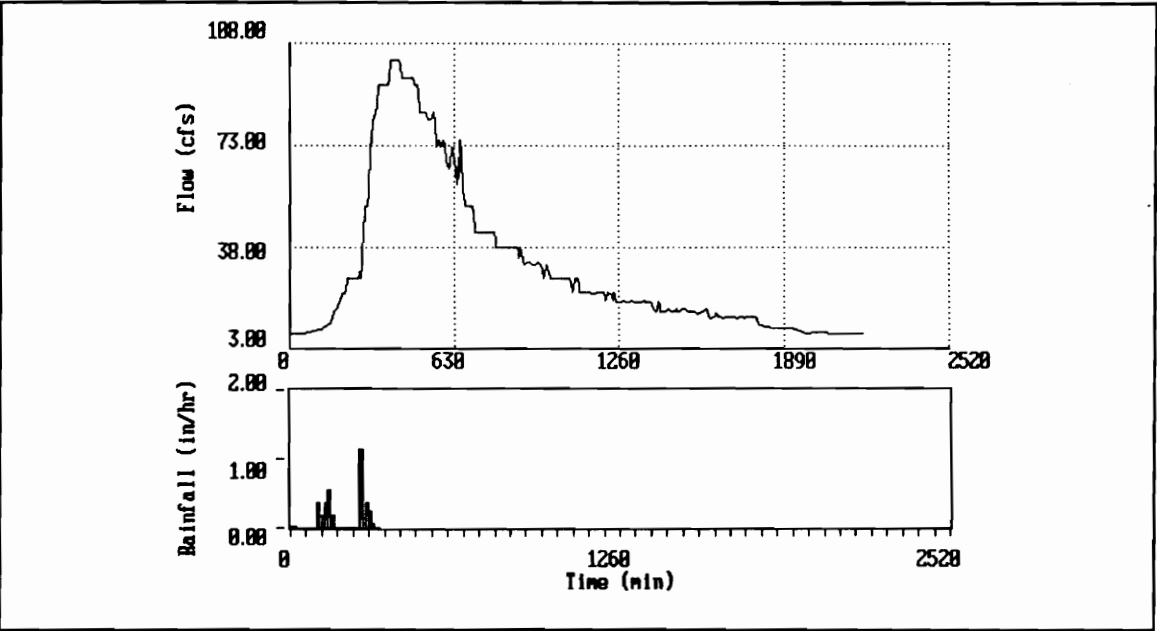


Figure A.41 - Holmes Run Gage 4 at Falls Church, Gaged Event 2

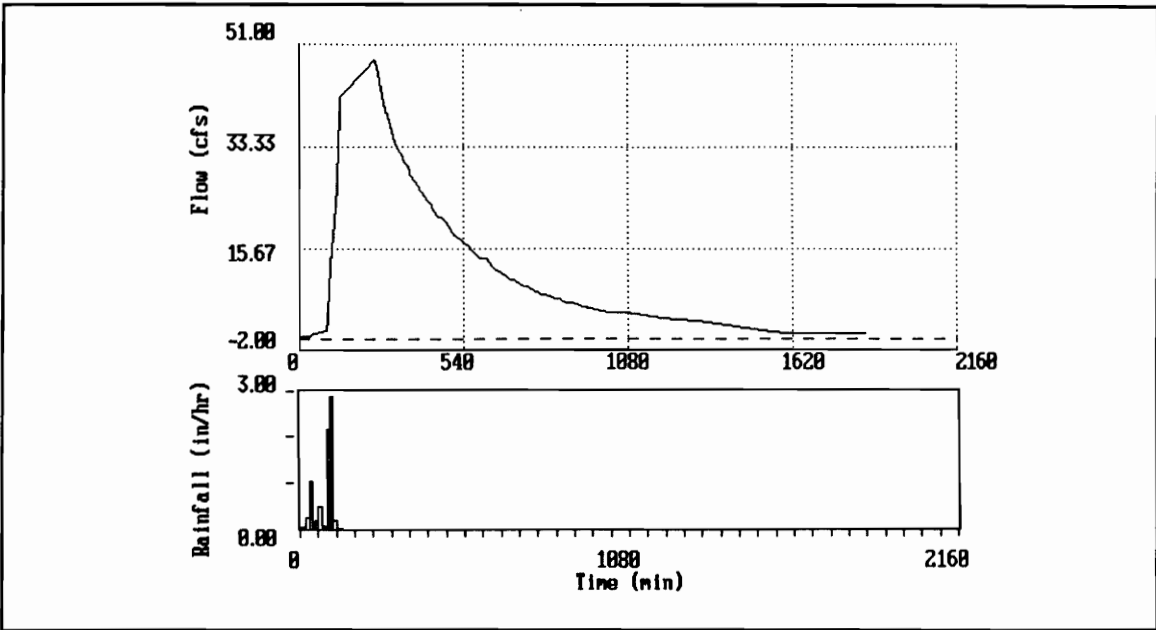


Figure A.42 - Holmes Run Gage 4 at Falls Church, Gaged Event 3

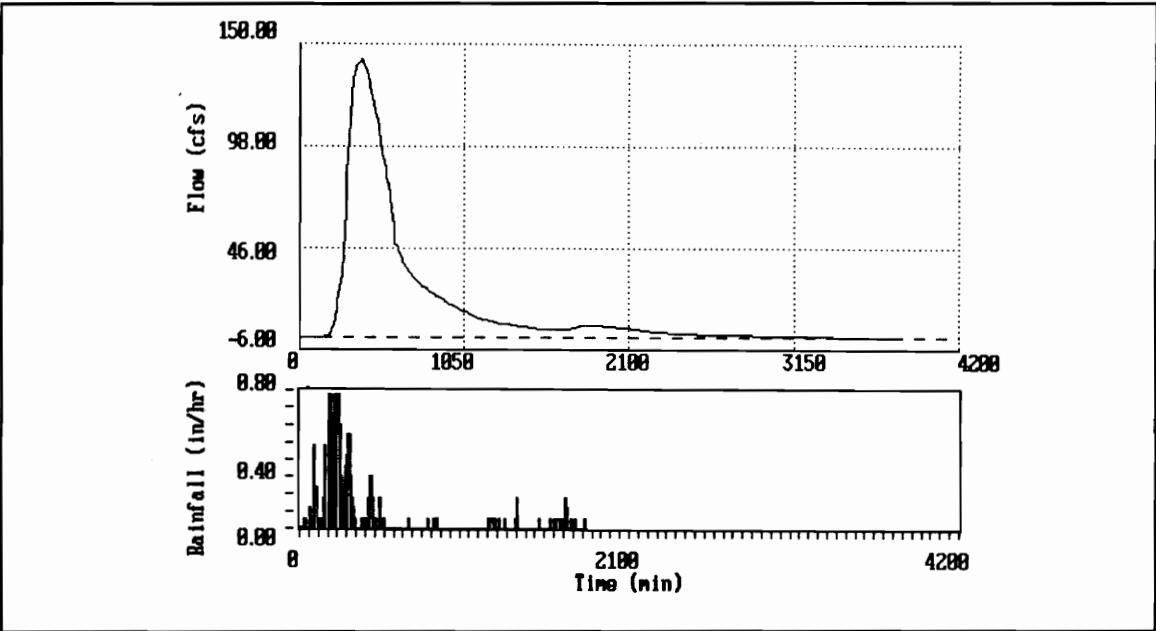


Figure A.43 - Holmes Run Gage 4 at Falls Church, Gaged Event 4

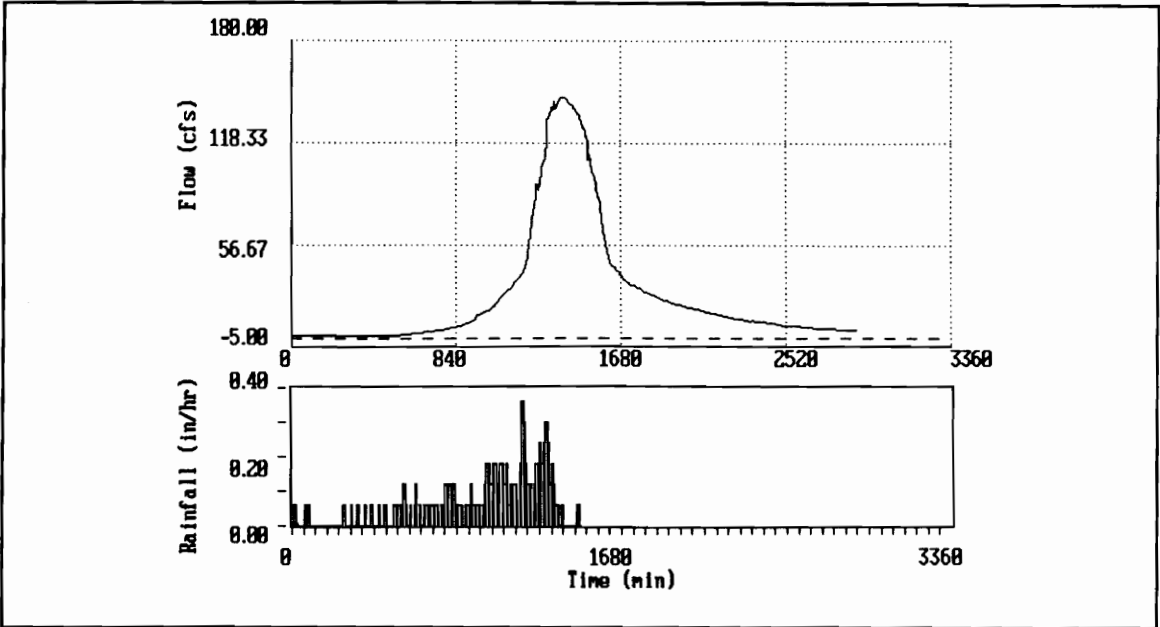


Figure A.44 - Holmes Run Gage 4 at Falls Church, Gaged Event 5

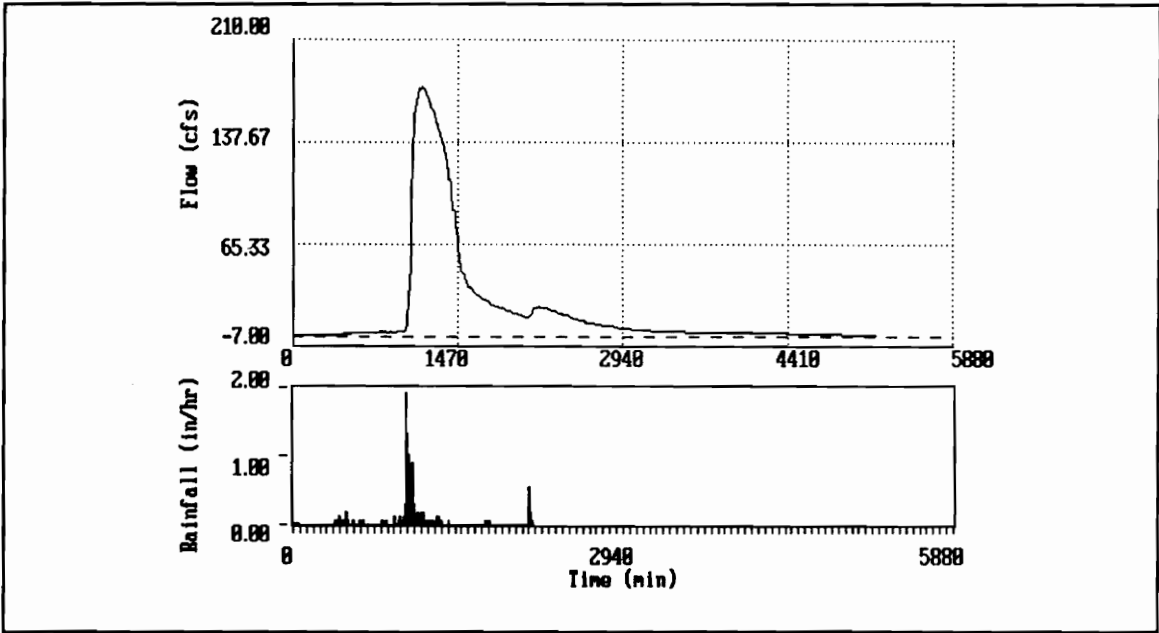


Figure A.45 - Holmes Run Gage 4 at Falls Church, Gaged Event 6

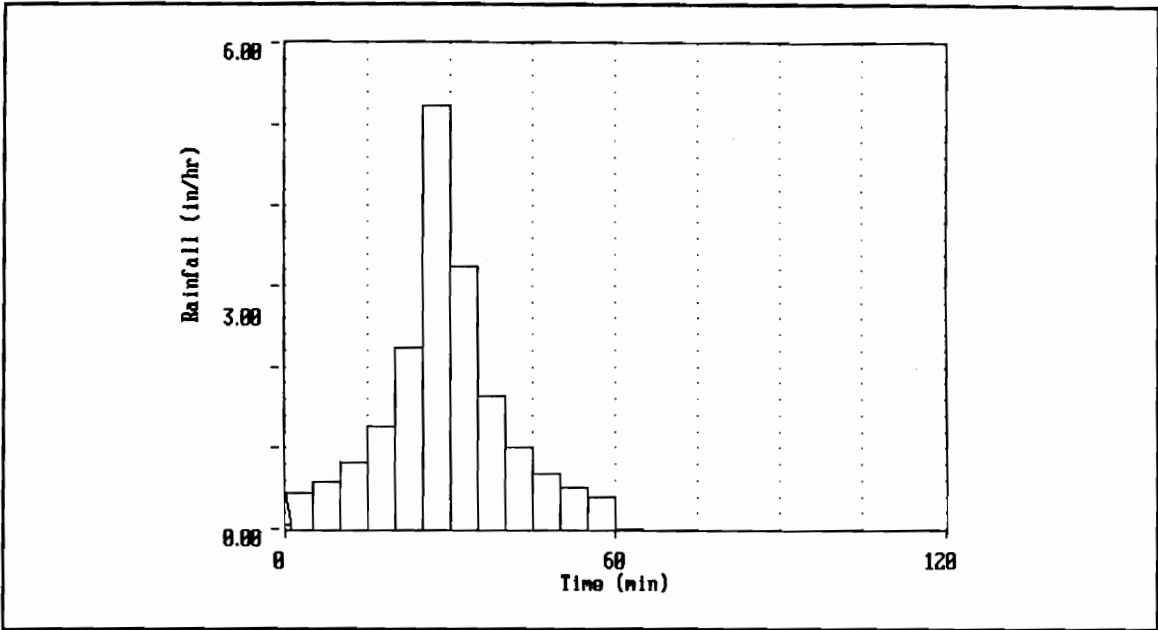


Figure A.46 - 2 year, 1 hour Yarnell Rainfall

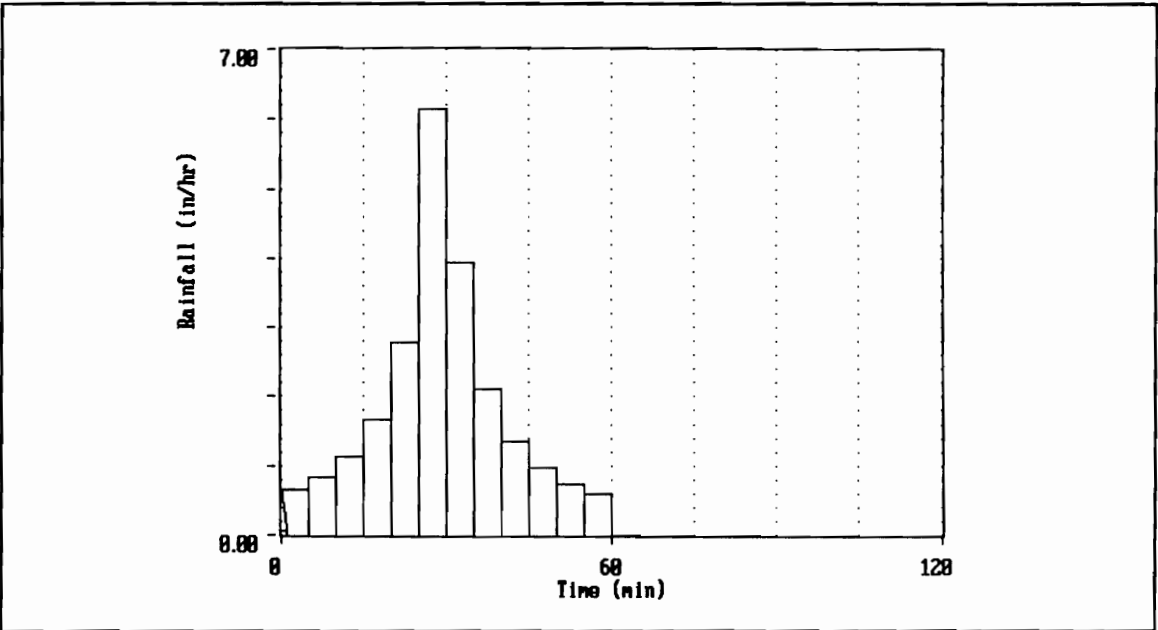


Figure A.47 - 5 year, 1 hour Yarnell Rainfall

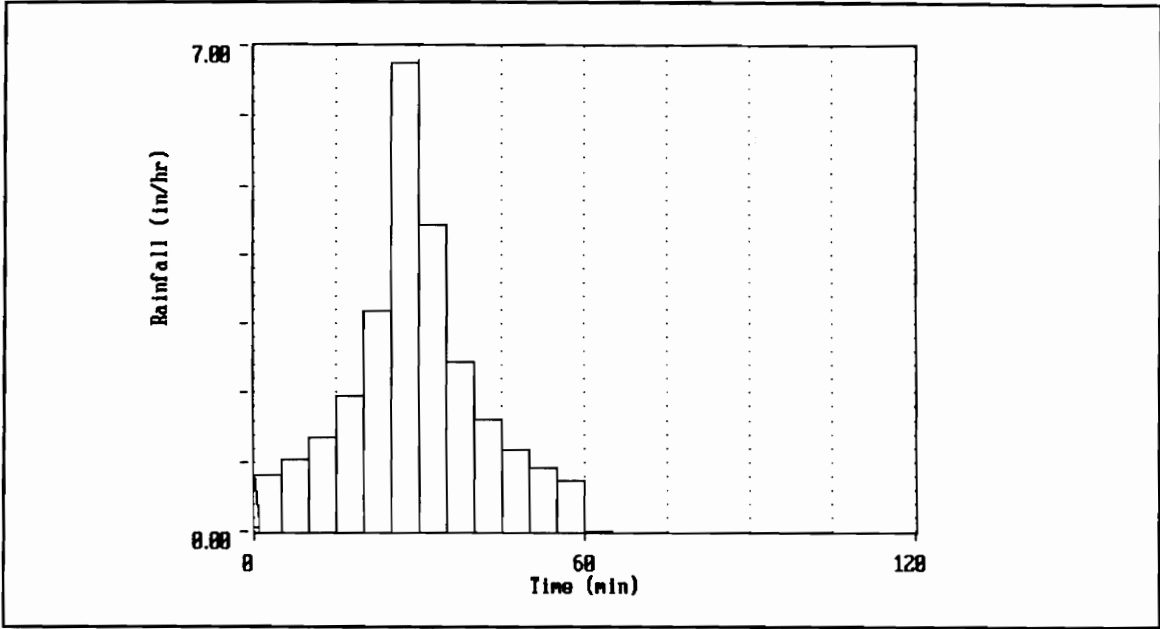


Figure A.48 - 10 year, 1 hour Yarnell Rainfall

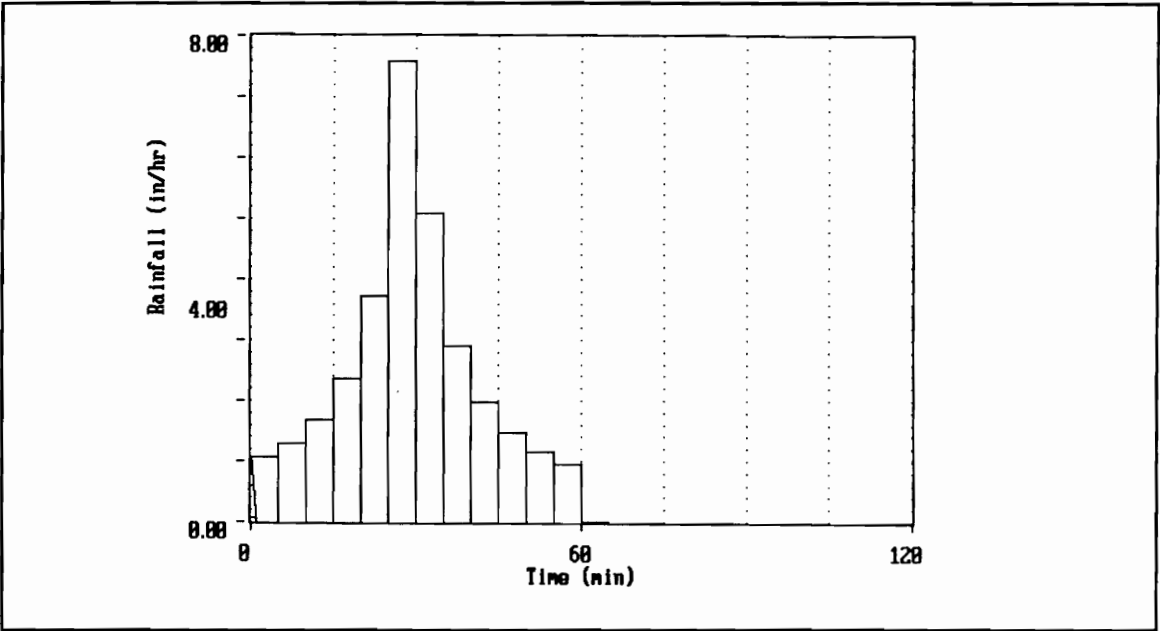


Figure A.49 - 25 year, 1 hour Yarnell Rainfall

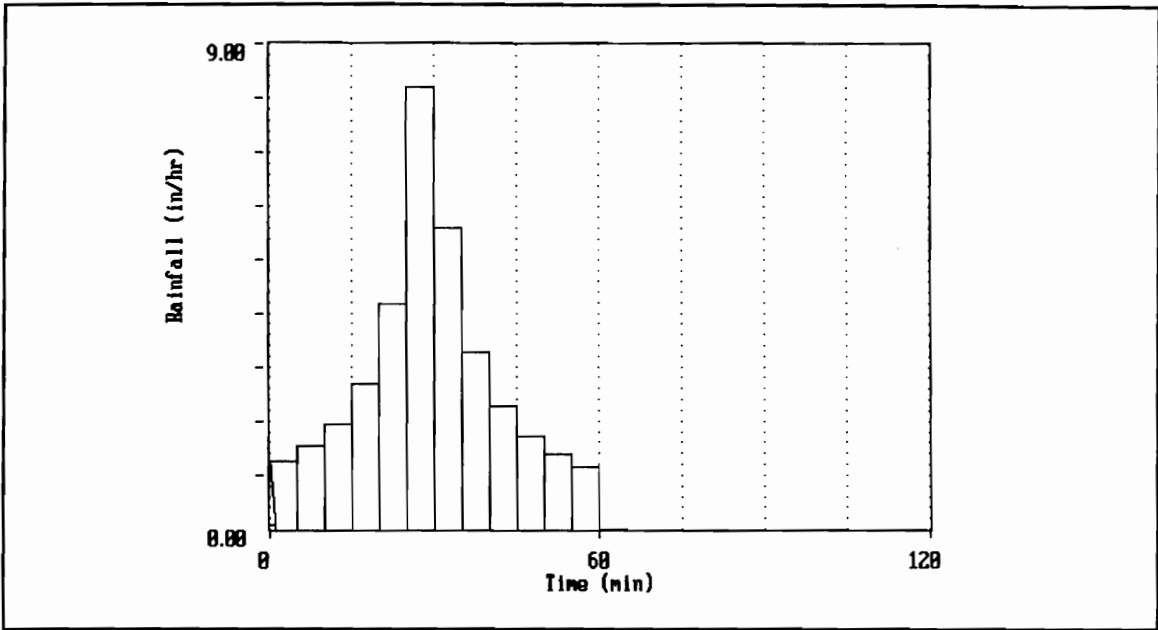


Figure A.50 - 50 year, 1 hour Yarnell Rainfall

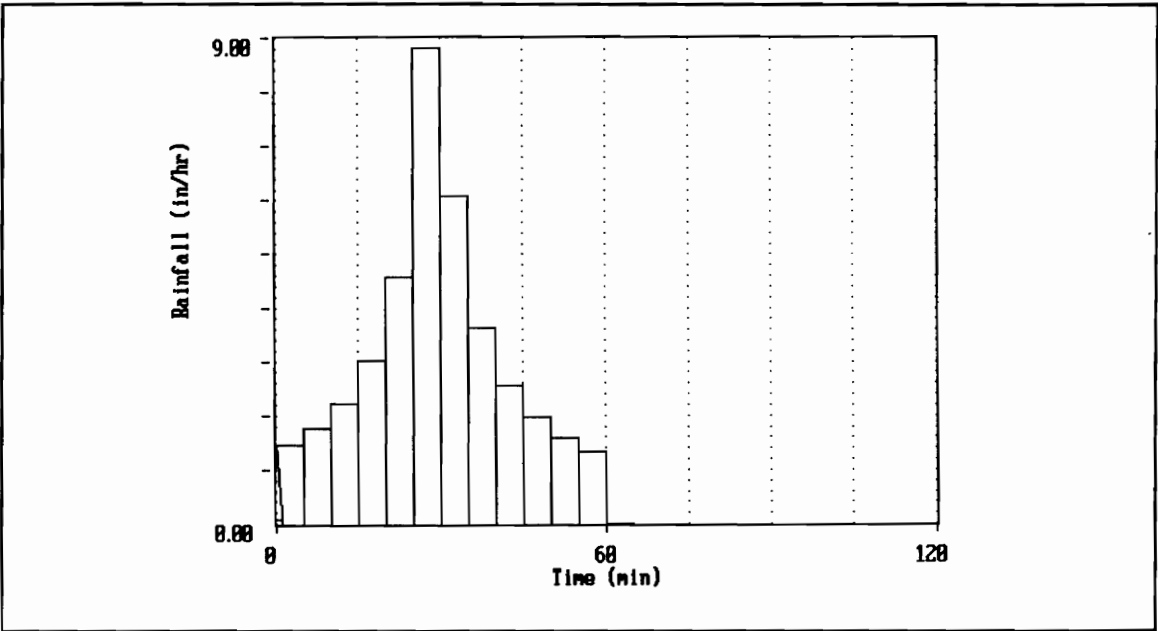


Figure A.51 - 100 year, 1 hour Yarnell Rainfall

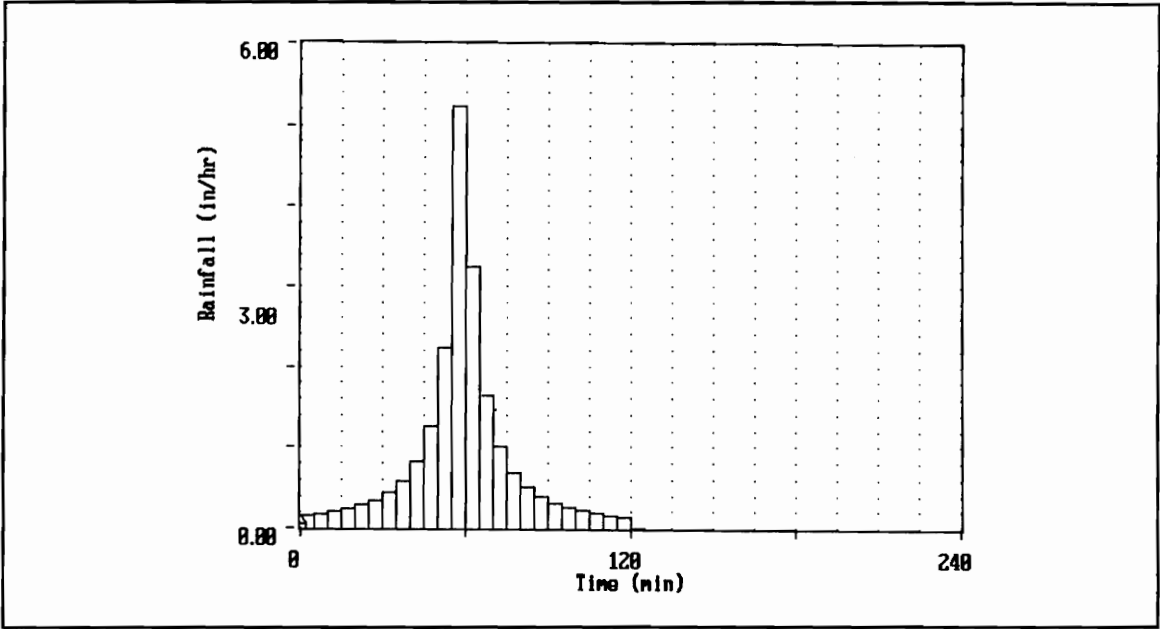


Figure A.52 - 2 year, 2 hour Yarnell Rainfall

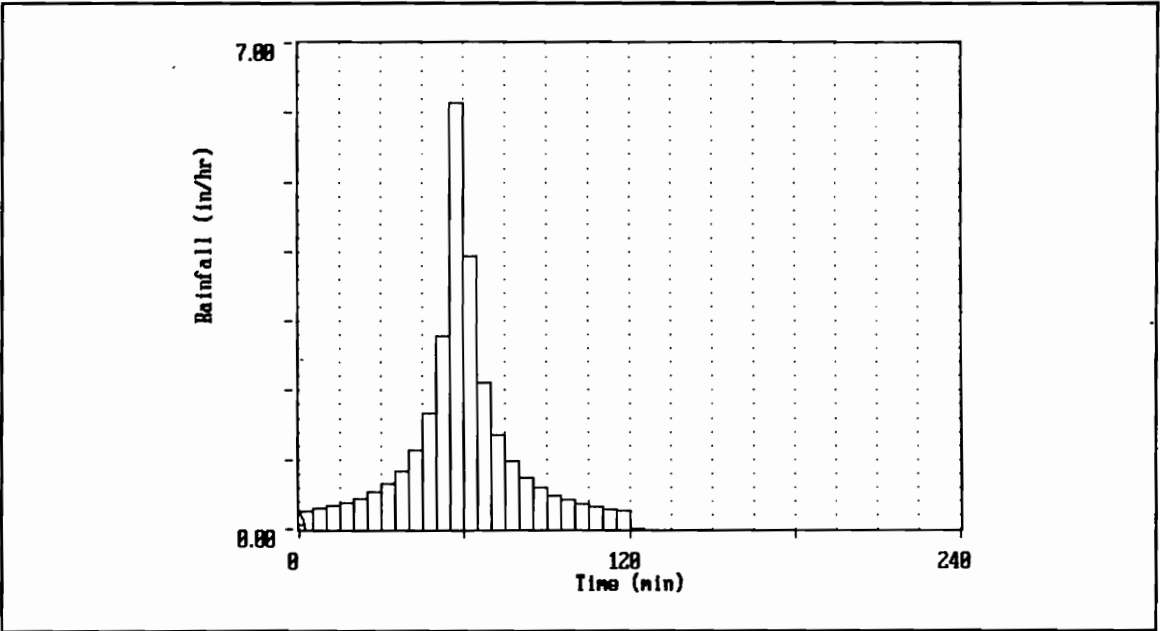


Figure A.53 - 5 year, 2 hour Yarnell Rainfall

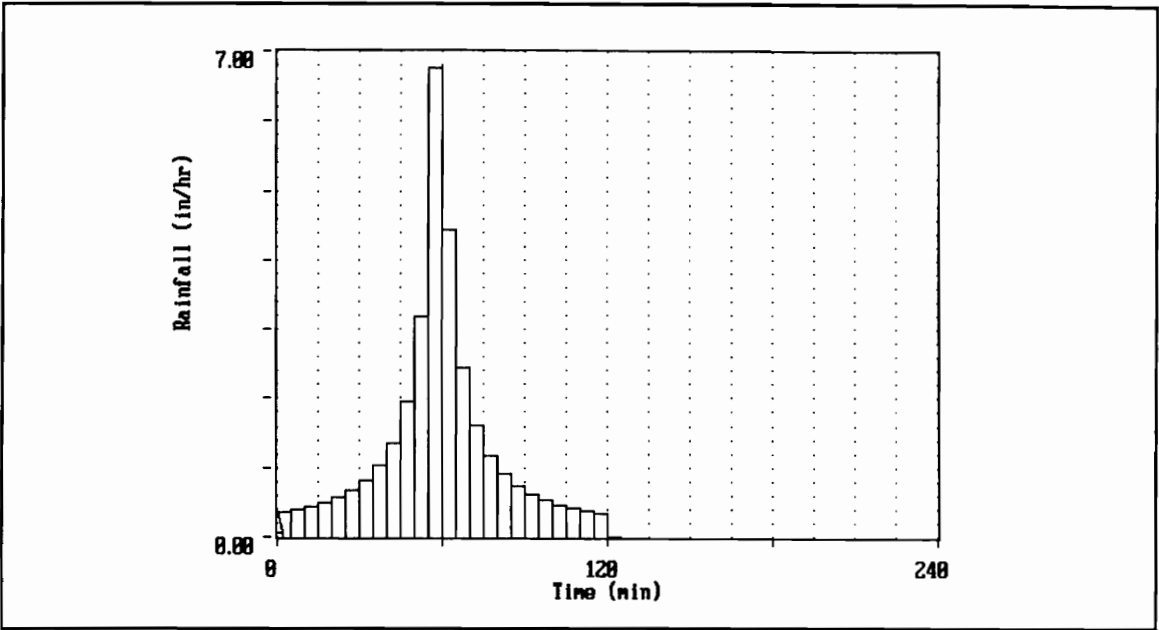


Figure A.54 - 10 year, 2 hour Yarnell Rainfall

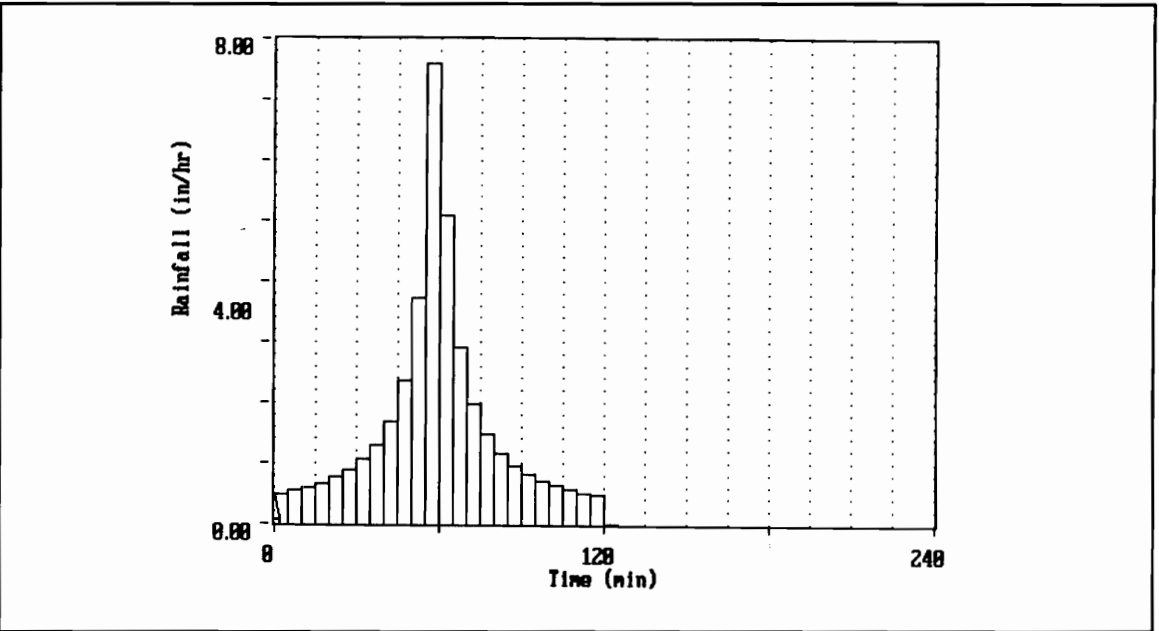


Figure A.55 - 25 year, 2 hour Yarnell Rainfall

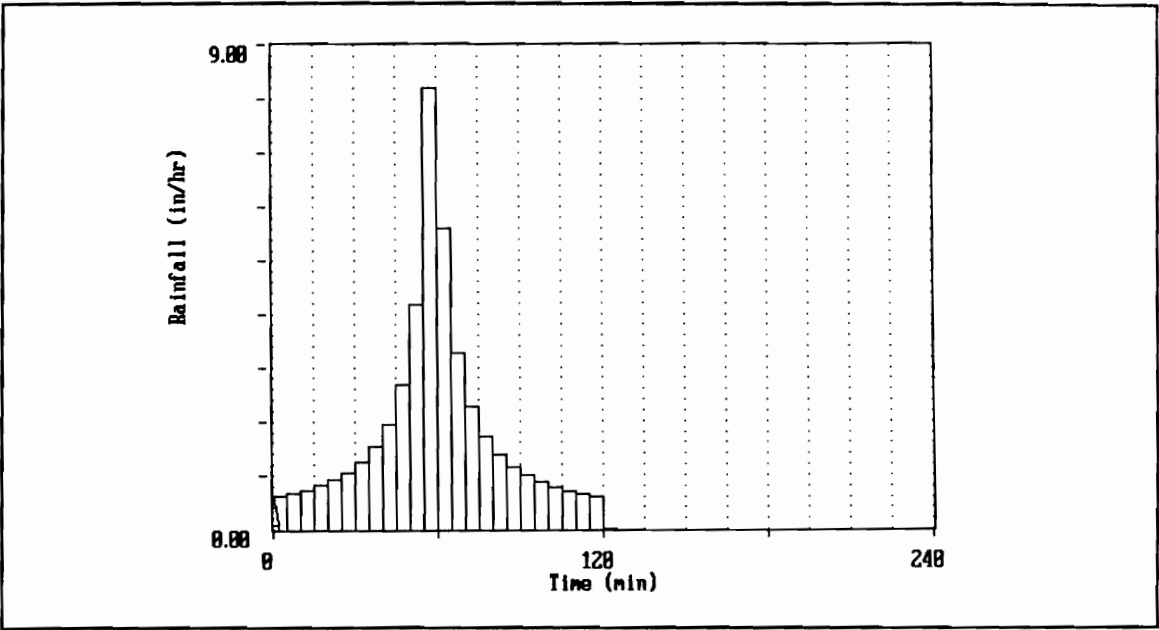


Figure A.56 - 50 year, 2 hour Yarnell Rainfall

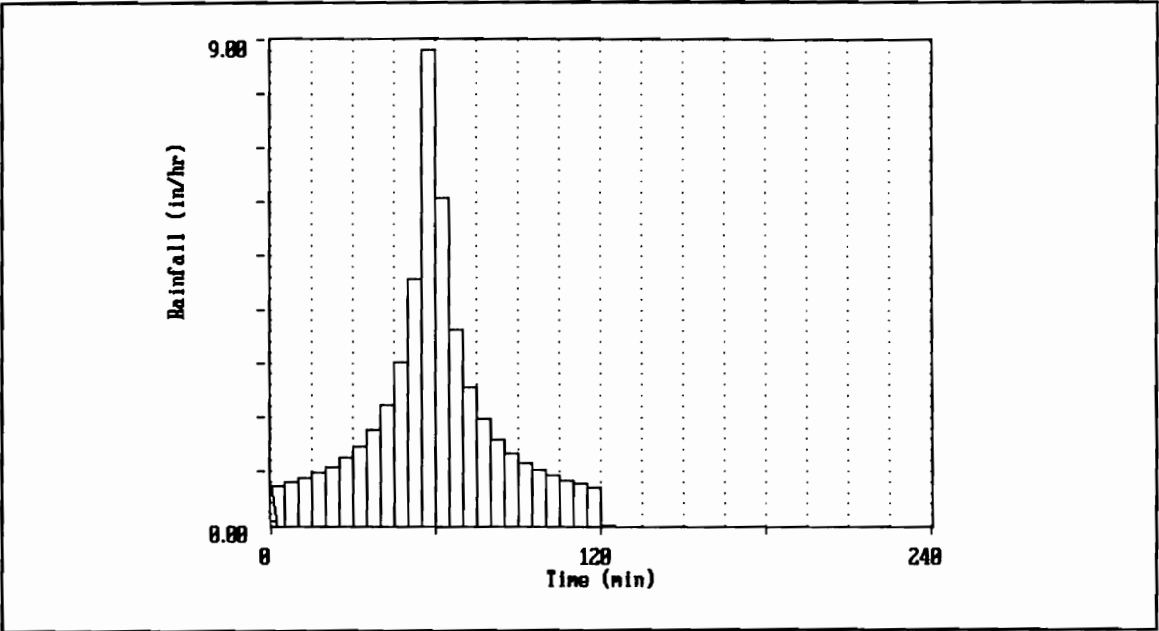


Figure A.57 - 100 year, 2 hour Yarnell Rainfall

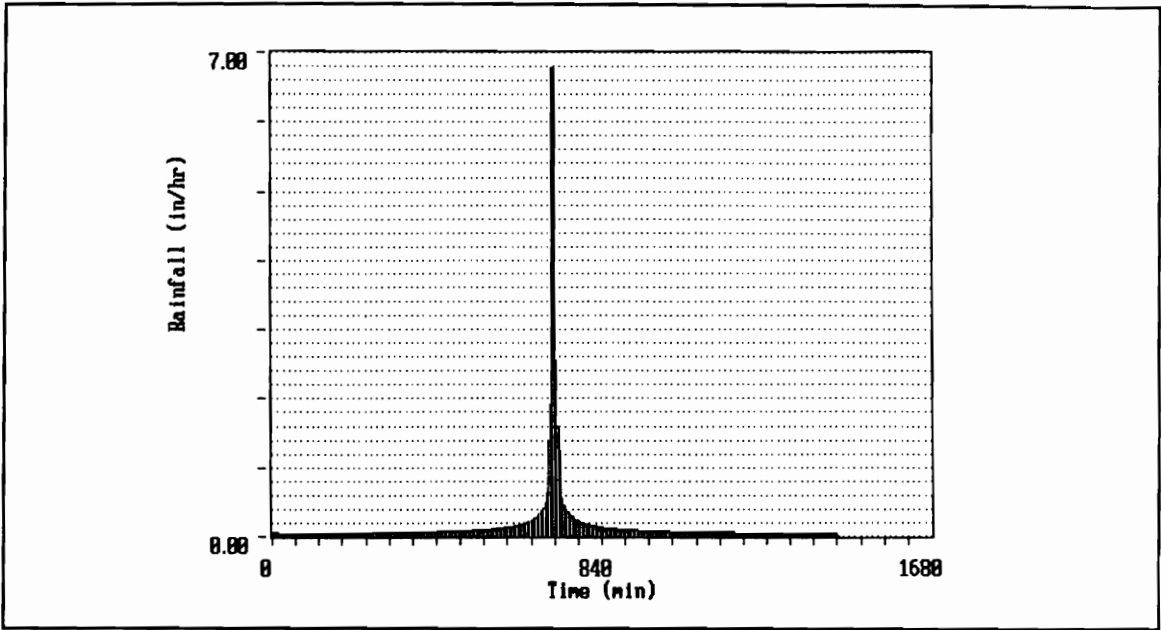


Figure A.58 - 2 year, 24 hour SCS Type II Rainfall

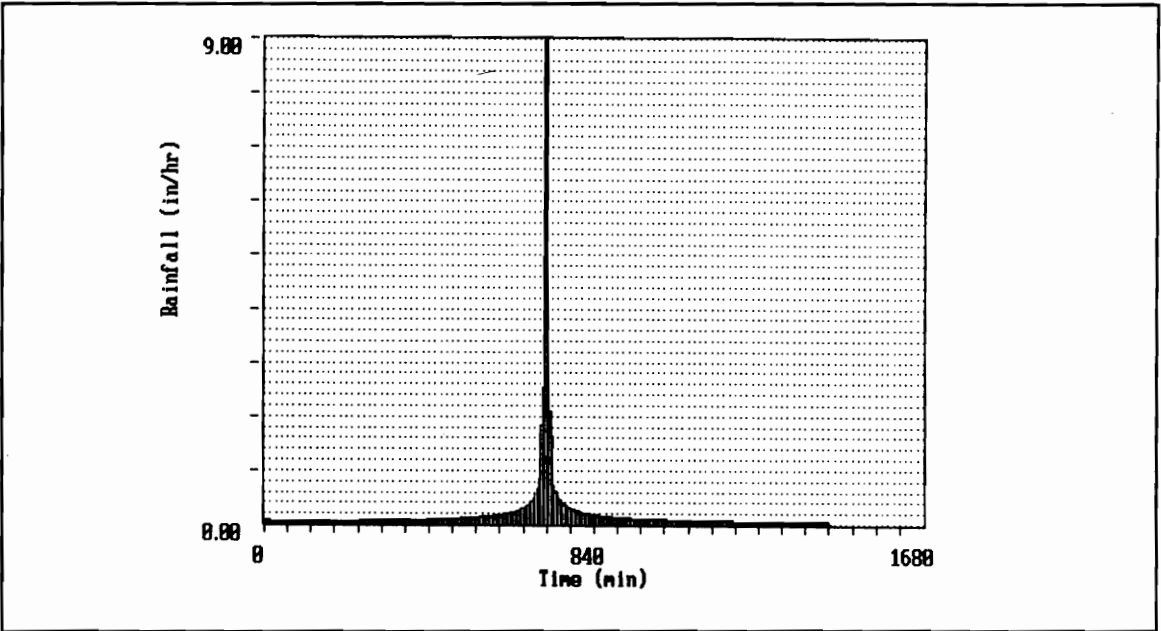


Figure A.59 - 5 year, 24 hour SCS Type II Rainfall

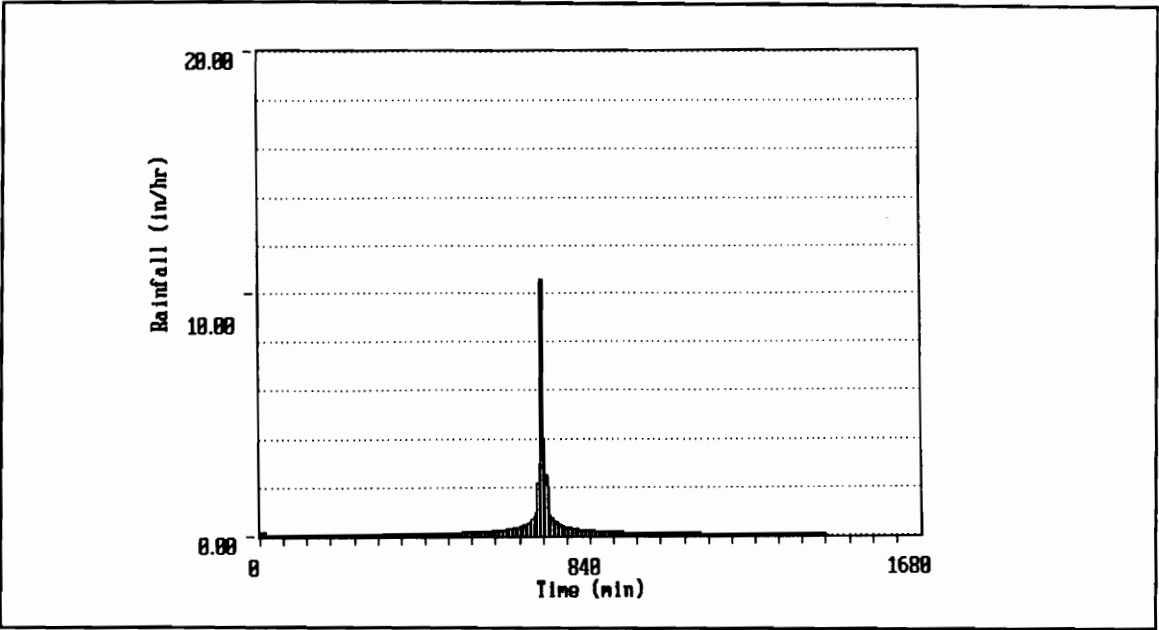


Figure A.60 - 10 year, 24 hour SCS Type II Rainfall

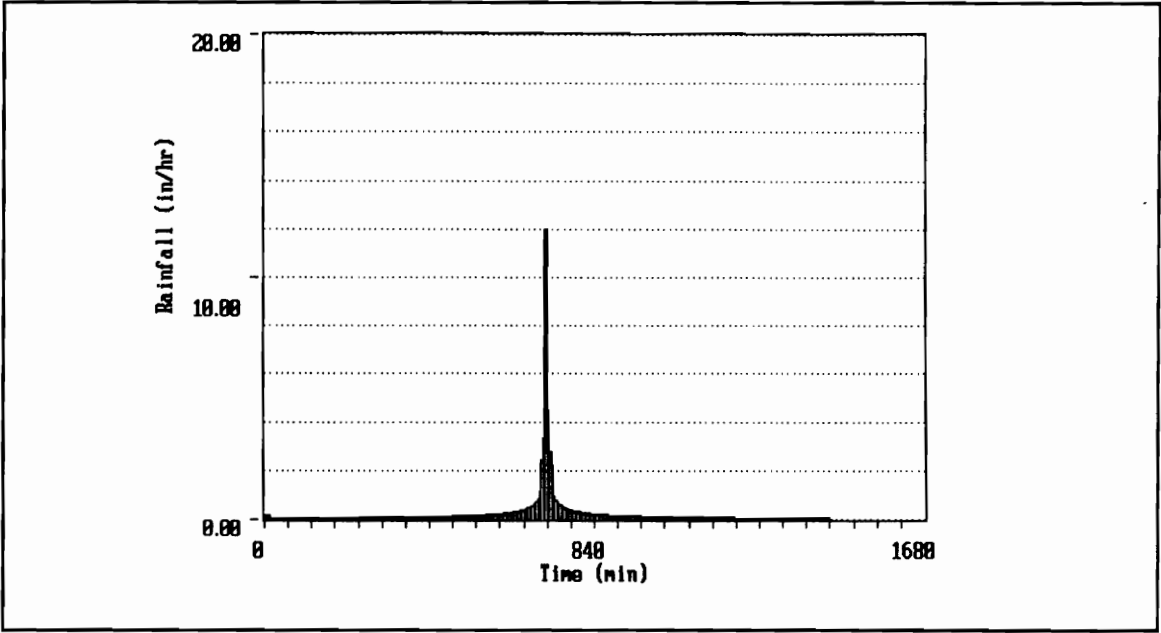


Figure A.61 - 25 year, 24 hour SCS Type II Rainfall

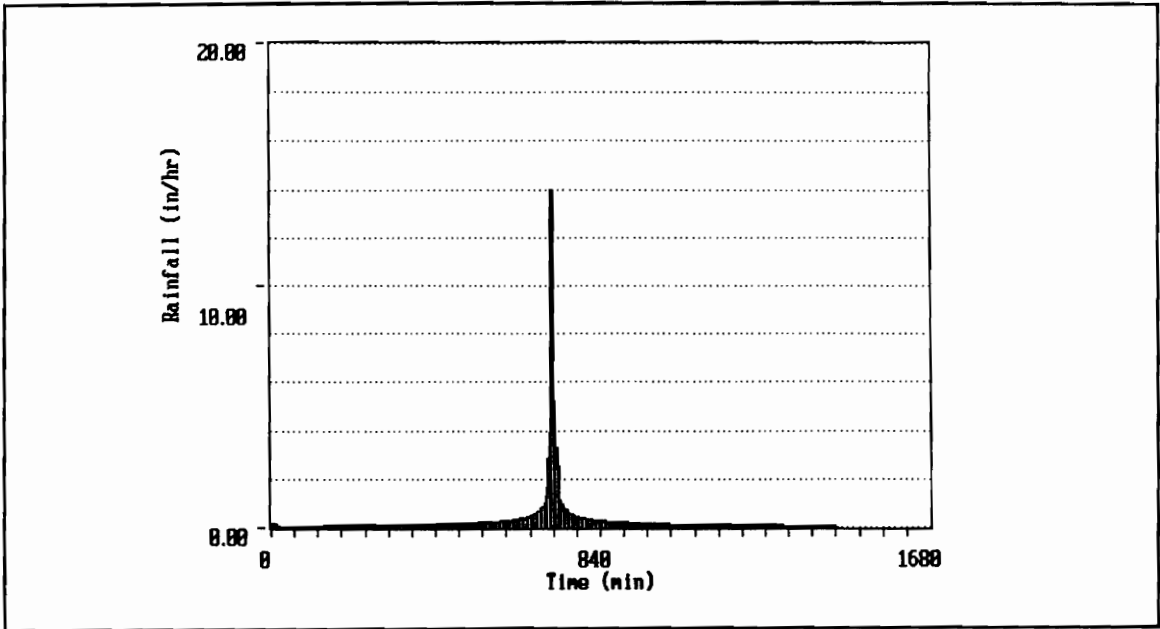


Figure A.62 - 50 year, 24 hour SCS Type II Rainfall

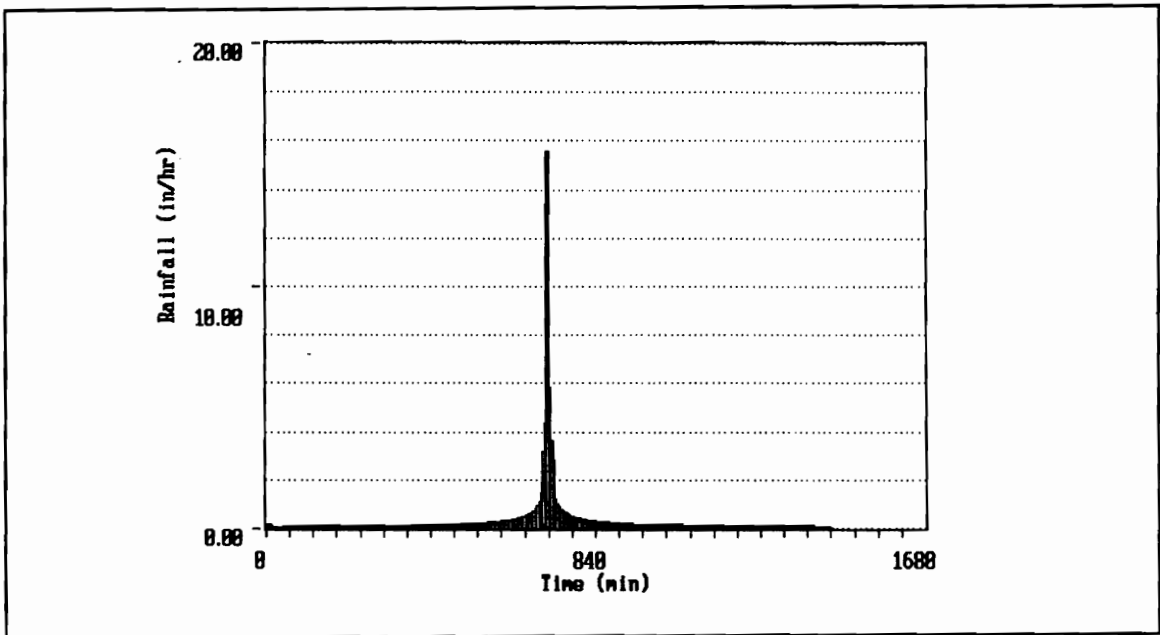


Figure A.63 - 100 year, 24 hour SCS Type II Rainfall

Appendix B

Tables of Evaluation Results

Table B.1 - Peak Flow Bias - Average

Average Peak Flow Bias	Snakelien Branch	Slave Run	Smilax Branch	SP Broad Run-ARC	Broad Run	Holmes Run 1	Holmes Run 2	Holmes Run 4	Gaged Flows	1-hr Yamell	2-hr Yamell	24-hr SCS	All Events
1 SWMM	0.310	0.789	1.596	-0.312	1.018	0.128	0.012	1.552	0.535	0.716	0.628	0.662	0.637
2 PSM-QUAL	0.247	-0.042	0.199	-0.464	0.396	0.712	1.768	1.430	0.402	0.403	0.499	0.840	0.538
3 TR-20	0.050	-0.217	0.980	-0.139	0.965	0.071	0.206	1.527	-0.090	0.175	0.330	1.309	0.439
4 HEC-1	0.718	-0.205	-0.158	0.901	1.136	2.262	7.662	3.841	1.574	2.555	2.441	1.600	2.050
5 SCS UH Whole	-0.511	-0.208	0.605	-0.315	0.042	-0.368	-0.009	0.411	-0.141	0.095	0.274	-0.395	-0.040
6 SCS UH Subareas	-0.018	-0.208	0.465	-0.174	0.718	0.304	0.889	1.053	-0.166	0.125	0.343	1.211	0.387
7 Snyder UH Whole	-0.514	-0.688	0.089	-0.596	0.253	-0.335	-0.036	0.369	-0.428	-0.354	-0.191	0.256	-0.175
8 Snyder UH Subareas	-0.085	-0.688	0.399	-0.327	0.418	0.261	0.770	0.864	-0.223	-0.015	0.183	1.144	0.331
9 Clark UH Whole	-0.464	-0.635	0.236	-0.569	0.415	-0.292	0.047	0.512	-0.384	-0.280	-0.090	0.391	-0.086
10 Clark UH Subareas	0.000	-0.635	0.447	-0.273	0.623	0.318	0.869	1.026	-0.170	0.073	0.284	1.304	0.433
11 TR-55	0.591	0.227	1.774	0.201	2.440	1.326	2.268	3.023	0.000	0.000	0.000	1.481	1.481
12 Rational Whole	0.000	0.030	1.502	-0.341	1.385	0.470	0.851	2.228	0.000	1.029	0.327	0.000	0.766
13 Rational Subareas	0.487	0.030	1.333	-0.031	1.724	1.046	1.877	2.670	0.000	1.249	0.964	0.000	1.142
14 Mod. Rational Whole	-0.117	-0.004	1.347	-0.598	1.274	-0.017	0.464	1.824	0.000	0.493	0.585	0.000	0.543
15 Mod. Rational Subareas	0.932	-0.004	2.259	0.231	1.870	3.533	4.592	4.606	0.000	2.246	2.305	0.000	2.278
16 Universal Rational	-0.205	-0.166	0.770	-0.341	0.842	0.439	0.790	1.479	0.000	0.686	0.000	0.216	0.451
17 USGS-3 Regression	-0.069	-0.171	1.140	-0.272	0.809	1.157	1.143	1.808	0.000	0.703	0.676	0.000	0.693
18 USGS-7 Regression	0.061	0.032	1.580	-0.182	0.813	1.015	1.234	2.081	0.000	0.913	0.689	0.000	0.829
19 Anderson	0.797	1.294	3.636	-0.307	0.920	2.273	2.918	4.605	0.000	2.290	1.628	0.000	2.017
20 All Models	0.041	-0.184	0.753	-0.219	0.769	0.523	1.353	1.588					
21 Sophisticated	0.331	0.082	0.654	-0.004	0.879	0.793	2.412	2.087					
22 Unit Hydrographs	-0.265	-0.510	0.373	-0.376	0.411	-0.018	0.421	0.706					
23 Design Rainfall	0.255	-0.003	1.485	-0.169	1.503	1.194	1.848	2.638					
24 Peak Only	0.263	0.385	2.118	-0.254	0.847	1.482	1.765	2.831					

Table B.2 - Peak Flow Bias - Standard Deviation

Standard Deviation Peak Flow Bias	Snakeden Branch	Slave Run	Smlax Branch	SF-Broad Run-ARC	Broad Run	Holmes Run 1	Holmes Run 2	Holmes Run 4	Gaged Flows	1-hr Yarnell	2-hr Yarnell	24-hr SCS	All Events
1 SWMM	0.299	0.556	0.885	0.266	1.022	0.391	0.579	2.533	2.158	0.872	0.791	0.741	1.256
2 PSRM-QUAL	0.229	0.436	0.398	0.212	0.952	0.561	0.698	1.810	1.751	0.634	0.658	0.886	1.075
3 TR-20	0.393	0.319	0.962	0.356	1.190	0.591	0.576	1.290	0.927	0.594	0.645	1.102	0.989
4 HEC-1	0.370	0.274	0.262	0.775	0.756	1.094	15.379	2.389	2.777	8.967	7.323	1.518	6.008
5 SCS UH W	0.352	0.365	0.861	0.259	0.961	0.571	0.878	1.063	0.881	0.572	0.647	0.927	0.805
6 SCS UH S	0.411	0.365	0.763	0.302	1.061	0.759	0.944	1.040	0.929	0.476	0.556	0.829	0.879
7 Snyder UH W	0.189	0.248	0.586	0.165	0.777	0.397	0.504	0.611	0.581	0.339	0.412	0.771	0.608
8 Snyder UH S	0.382	0.248	0.772	0.251	0.874	0.732	0.886	0.930	0.866	0.456	0.532	0.727	0.823
9 Clark UH W	0.208	0.293	0.654	0.178	0.876	0.425	0.549	0.675	0.625	0.386	0.471	0.866	0.679
10 Clark UH S	0.420	0.293	0.786	0.268	1.000	0.748	0.929	1.028	0.928	0.487	0.566	0.785	0.886
11 TR-55	0.227	0.132	0.613	0.109	0.478	0.260	0.371	0.526	0.000	0.000	0.000	1.072	1.072
12 Rational W	0.086	0.085	0.158	0.027	0.186	0.052	0.031	0.225	0.000	0.904	0.513	0.000	0.847
13 Rational S	0.090	0.085	0.152	0.057	0.173	0.055	0.083	0.130	0.000	0.953	0.806	0.000	0.903
14 Mod Rat W	0.070	0.082	0.206	0.098	0.181	0.263	0.406	0.160	0.000	0.914	0.773	0.000	0.836
15 Mod Rat S	0.129	0.082	0.289	0.299	0.202	0.548	0.334	0.266	0.000	1.744	1.801	0.000	1.766
16 Univ Rat S	0.125	0.082	0.286	0.176	0.256	0.330	0.329	0.456	0.000	0.712	0.000	0.508	0.659
17 USGS-3	0.322	0.350	0.782	0.180	0.665	0.479	0.488	0.814	0.000	0.954	0.789	0.000	0.887
18 USGS-7	0.326	0.372	0.841	0.197	0.671	0.453	0.476	0.830	0.000	1.024	0.741	0.000	0.926
19 Anderson	0.323	0.470	0.756	0.160	0.619	0.566	0.609	1.130	0.000	1.726	1.506	0.000	1.658
20 All	0.508	0.546	0.987	0.489	0.976	1.112	4.726	1.756					
21 Sophis	0.405	0.581	0.969	0.702	1.018	1.130	8.203	2.273					
22 UHs	0.408	0.369	0.748	0.284	0.940	0.689	0.896	0.938					
23 Des Hyt	0.472	0.141	0.593	0.365	0.552	1.360	1.599	1.209					
24 Peak Only	0.496	0.766	1.345	0.177	0.615	0.746	0.975	1.566					

Table B.3 - Peak Flow Standard Error - Average

Average Peak Flow Standard Error	Snakeden Branch	Stave Run	Smlax Branch	SF Broad Run-ARC	Broad Run	Holmes Run 1	Holmes Run 2	Holmes Run 4	Gaged Flows	1-hr Yamell	2-hr Yamell	24-hr SCS	All Events
1 SWMM	0.408	0.911	1.628	0.321	1.343	0.238	0.423	1.552	1.053	0.857	0.761	0.761	0.835
2 PFRM-QUAL	0.299	0.397	0.372	0.464	0.798	0.782	1.768	1.458	0.944	0.593	0.657	1.011	0.799
3 TR-20	0.325	0.307	1.068	0.317	1.253	0.462	0.488	1.599	0.659	0.455	0.508	1.310	0.734
4 HEC-1	0.742	0.249	0.212	0.913	1.292	2.298	7.662	3.841	1.920	2.622	2.498	1.657	2.179
5 SCS UH Whole	0.515	0.327	0.820	0.332	0.857	0.551	0.745	0.980	0.725	0.461	0.533	0.866	0.645
6 SCS UH Subareas	0.327	0.327	0.691	0.287	1.046	0.661	1.092	1.133	0.697	0.392	0.505	1.211	0.701
7 Snyder UH Whole	0.514	0.688	0.468	0.596	0.669	0.416	0.408	0.548	0.631	0.436	0.398	0.688	0.537
8 Snyder UH Subareas	0.314	0.688	0.663	0.340	0.794	0.626	0.981	0.957	0.686	0.393	0.471	1.159	0.670
9 Clark UH Whole	0.464	0.635	0.549	0.569	0.794	0.410	0.442	0.656	0.632	0.424	0.415	0.792	0.565
10 Clark UH Subareas	0.334	0.635	0.686	0.315	0.961	0.666	1.073	1.108	0.706	0.407	0.515	1.311	0.737
11 TR-55	0.591	0.227	1.774	0.201	2.440	1.326	2.268	3.023	0.000	0.000	0.000	1.481	1.481
12 Rational Whole	0.057	0.067	1.502	0.341	1.385	0.470	0.851	2.228	0.000	1.048	0.554	0.863	0.863
13 Rational Subareas	0.487	0.067	1.333	0.054	1.724	1.046	1.877	2.670	0.000	1.256	0.993	0.000	1.157
14 Mod. Rational Whole	0.118	0.064	1.347	0.598	1.274	0.247	0.468	1.824	0.000	0.755	0.749	0.000	0.752
15 Mod. Rational Subareas	0.932	0.064	2.259	0.279	1.870	3.533	4.592	4.606	0.000	2.258	2.318	0.000	2.290
16 Universal Rational	0.205	0.166	0.770	0.341	0.842	0.439	0.790	1.479	0.000	0.778	0.000	0.480	0.629
17 USGS-3 Regression	0.256	0.309	1.140	0.272	0.852	1.157	1.143	1.808	0.000	0.873	0.857	0.000	0.867
18 USGS-7 Regression	0.257	0.295	1.580	0.207	0.854	1.015	1.234	2.081	0.000	1.013	0.819	0.000	0.941
19 Anderson	0.797	1.294	3.636	0.307	0.920	2.273	2.918	4.605	0.000	2.250	1.833	0.000	2.094
20 All Models	0.421	0.450	0.930	0.416	1.065	0.845	1.580	1.684					
21 Sophisticated	0.443	0.466	0.820	0.504	1.172	0.945	2.585	2.112					
22 Unit Hydrographs	0.411	0.550	0.646	0.406	0.853	0.555	0.790	0.897					
23 Design Rainfall	0.405	0.105	1.485	0.335	1.503	1.242	1.848	2.638					
24 Peak Only	0.437	0.633	2.118	0.262	0.875	1.482	1.765	2.831					

Table B.4 - Peak Flow Standard Error - Standard Deviation

Standard Deviation Peak Flow Standard Error	Snakeeden Branch	Slave Run	Smilax Branch	SF Broad Run-ARC	Broad Run	Holmes Run 1	Holmes Run 2	Holmes Run 4	Gaged Flows	1-hr Yarnell	2-hr Yarnell	24-hr SCS	All Events
1 SWMM	0.126	0.303	0.821	0.255	0.493	0.333	0.385	2.535	1.954	0.790	0.682	0.637	1.119
2 PRM-QUAL	0.151	0.164	0.236	0.212	0.637	0.453	0.698	1.786	1.523	0.457	0.496	0.680	0.897
3 TR-20	0.216	0.229	0.859	0.205	0.864	0.363	0.357	1.196	0.652	0.416	0.513	1.100	0.794
4 HEC-1	0.316	0.232	0.219	0.760	0.420	1.013	15.379	2.389	2.544	8.947	7.304	1.454	5.963
5 SCS UH W	0.346	0.259	0.649	0.236	0.400	0.389	0.438	0.550	0.509	0.345	0.454	0.504	0.481
6 SCS UH S	0.240	0.259	0.556	0.193	0.722	0.465	0.686	0.948	0.627	0.293	0.412	0.829	0.655
7 Snyder UH W	0.189	0.248	0.351	0.165	0.452	0.307	0.286	0.450	0.344	0.220	0.212	0.421	0.333
8 Snyder UH S	0.226	0.248	0.551	0.232	0.538	0.446	0.632	0.831	0.565	0.226	0.301	0.702	0.580
9 Clark UH W	0.208	0.293	0.413	0.178	0.537	0.307	0.316	0.529	0.364	0.213	0.233	0.515	0.384
10 Clark UH S	0.245	0.293	0.580	0.215	0.665	0.450	0.670	0.934	0.618	0.270	0.364	0.772	0.653
11 TR-55	0.227	0.132	0.613	0.109	0.478	0.260	0.371	0.526	0.000	0.000	0.000	1.072	1.072
12 Rational W	0.060	0.055	0.158	0.027	0.186	0.052	0.031	0.225	0.000	0.882	0.226	0.000	0.746
13 Rational S	0.090	0.055	0.152	0.029	0.173	0.055	0.083	0.130	0.000	0.943	0.769	0.000	0.883
14 Mod Rat W	0.068	0.047	0.206	0.098	0.181	0.050	0.402	0.160	0.000	0.708	0.612	0.000	0.653
15 Mod Rat S	0.129	0.047	0.289	0.250	0.202	0.548	0.334	0.266	0.000	1.729	1.784	0.000	1.750
16 Univ Rat S	0.125	0.082	0.286	0.176	0.256	0.330	0.329	0.456	0.000	0.607	0.000	0.266	0.490
17 USGS-3	0.176	0.209	0.782	0.180	0.596	0.479	0.488	0.814	0.000	0.796	0.573	0.000	0.714
18 USGS-7	0.177	0.188	0.841	0.164	0.607	0.453	0.476	0.830	0.000	0.921	0.585	0.000	0.810
19 Anderson	0.323	0.470	0.756	0.160	0.619	0.566	0.609	1.130	0.000	1.726	1.731	0.000	1.538
20 All	0.286	0.358	0.822	0.336	0.639	0.892	4.656	1.664					
21 Sophus	0.277	0.352	0.832	0.486	0.655	1.005	8.150	2.250					
22 UHs	0.259	0.307	0.529	0.238	0.567	0.407	0.594	0.756					
23 Des Hrt	0.350	0.092	0.350	0.219	0.552	1.315	1.599	1.209					
24 Peak Only	0.343	0.566	1.345	0.164	0.572	0.746	0.975	1.566					

Table B.5 - Volume Bias - Average

Average Volume Bias	Snake den Branch	Slave Run	Smilax Branch	SF Broad Run-ABC	Broad Run	Holmes Run 1	Holmes Run 2	Holmes Run 4	Gaged Flows	1-hr Yarnell	2-hr Yarnell	24-hr SCS	All Events
1 SWMM	-0.152	-0.057	-0.232	-0.296	-0.436	1.293	-0.105	0.959	0.270	-0.140	-0.143	-0.145	-0.045
2 PSRM-QUAL	-0.307	-0.460	-0.659	-0.419	-0.535	-0.383	-0.198	-0.517	-0.328	-0.638	-0.537	-0.230	-0.435
3 TR-20	-0.451	-0.477	-0.517	-0.369	-0.535	-0.560	-0.455	-0.524	-0.615	-0.653	-0.571	-0.114	-0.486
4 HEC-1	-0.002	-0.033	-0.729	0.839	-0.363	0.435	0.850	0.185	0.848	-0.146	-0.118	0.062	0.151
5 SCS UH Whole	-0.657	-0.475	-0.522	-0.364	-0.758	-0.764	-0.691	-0.692	-0.594	-0.646	-0.563	-0.663	-0.617
6 SCS UH Subareas	-0.461	-0.475	-0.539	-0.335	-0.543	-0.557	-0.477	-0.534	-0.635	-0.678	-0.580	-0.078	-0.490
7 Snyder UH Whole	-0.468	-0.703	-0.541	-0.381	-0.546	-0.553	-0.429	-0.479	-0.605	-0.672	-0.572	-0.200	-0.511
8 Snyder UH Subareas	-0.464	-0.703	-0.541	-0.363	-0.545	-0.559	-0.480	-0.537	-0.636	-0.683	-0.583	-0.079	-0.499
9 Clark UH Whole	-0.467	-0.703	-0.540	-0.376	-0.546	-0.550	-0.426	-0.478	-0.605	-0.672	-0.572	-0.193	-0.509
10 Clark UH Subareas	-0.464	-0.703	-0.540	-0.346	-0.545	-0.558	-0.480	-0.537	-0.635	-0.683	-0.583	-0.070	-0.496
11 TR-55	-0.134	-0.228	-0.130	0.118	-0.067	-0.071	0.062	-0.012	0.000	0.000	0.000	-0.058	-0.058
12 Rational Whole	-0.991	-0.985	-0.986	-0.996	-0.992	-0.996	-0.995	-0.991	0.000	-0.989	-0.996	0.000	-0.992
13 Rational Subareas	-0.574	-0.985	-0.570	-0.546	-0.600	-0.636	-0.591	-0.532	0.000	-0.652	-0.591	0.000	-0.629
15 Mod. Rational Subareas	0.418	-0.986	0.466	-0.220	-0.144	0.323	0.521	0.325	0.000	-0.177	0.363	0.000	0.117
16 Universal Rational	-0.183	-0.244	-0.317	0.040	-0.389	-0.023	0.024	-0.154	0.000	0.111	0.000	-0.423	-0.156
17 USGS-3 Regression	-0.992	-0.988	-0.988	-0.996	-0.994	-0.994	-0.994	-0.992	0.000	-0.991	-0.995	0.000	-0.992
18 USGS-7 Regression	-0.991	-0.985	-0.986	-0.996	-0.994	-0.995	-0.994	-0.992	0.000	-0.989	-0.995	0.000	-0.991
19 Anderson	-0.984	-0.986	-0.975	-0.986	-0.993	-0.991	-0.989	-0.985	0.000	-0.981	-0.992	0.000	-0.985
20 All Models	-0.419	-0.554	-0.534	-0.313	-0.561	-0.429	-0.326	-0.360					
21 Sophisticated	-0.228	-0.257	-0.534	-0.061	-0.472	-0.133	0.023	0.026					
22 Unit Hydrographs	-0.497	-0.627	-0.537	-0.361	-0.581	-0.590	-0.497	-0.543					
23 Design Rainfall	-0.357	-0.727	-0.374	-0.408	-0.523	-0.337	-0.262	-0.353					

Table B.6 - Volume Bias - Standard Deviation

Standard Deviation Volume Bias	Snakeden Branch	Stave Run	Smlax Branch	SF Broad Run-ARC	Broad Run	Holmes Run 1	Holmes Run 2	Holmes Run 4	Gaged Flows	1-hr Yarnell	2-hr Yarnell	24-hr SCS	All Events
1 SWMM	0.092	0.644	0.171	0.226	0.231	6.543	0.258	2.812	2.225	0.205	0.201	0.201	1.105
2 PSRM-QUAL	0.201	0.553	0.137	0.325	0.348	0.343	0.345	0.224	0.499	0.146	0.137	0.331	0.350
3 TR-20	0.226	0.205	0.282	0.307	0.351	0.301	0.330	0.293	0.334	0.110	0.121	0.132	0.292
4 HEC-1	0.286	0.858	0.123	1.056	0.520	1.025	1.343	0.670	1.383	0.808	0.696	0.442	0.970
5 SCS UH W	0.269	0.208	0.286	0.309	0.292	0.218	0.286	0.258	0.351	0.108	0.119	0.452	0.297
6 SCS UH S	0.226	0.208	0.270	0.415	0.359	0.315	0.342	0.292	0.308	0.109	0.116	0.201	0.313
7 Snyder UH W	0.222	0.211	0.271	0.313	0.360	0.312	0.359	0.294	0.338	0.100	0.111	0.330	0.307
8 Snyder UH S	0.224	0.211	0.269	0.351	0.357	0.314	0.340	0.290	0.306	0.104	0.114	0.156	0.311
9 Clark UH W	0.223	0.211	0.272	0.321	0.361	0.316	0.364	0.295	0.338	0.100	0.111	0.334	0.309
10 Clark UH S	0.225	0.211	0.270	0.396	0.358	0.312	0.340	0.291	0.306	0.104	0.114	0.194	0.320
11 TR-55	0.100	0.090	0.148	0.062	0.072	0.109	0.133	0.104	0.000	0.000	0.000	0.144	0.144
12 Rational W	0.001	0.001	0.001	0.000	0.001	0.000	0.000	0.001	0.000	0.003	0.001	0.000	0.004
13 Rational S	0.022	0.001	0.018	0.027	0.023	0.011	0.014	0.020	0.000	0.172	0.042	0.000	0.140
15 Mod Rat S	0.353	0.002	0.350	0.237	0.240	0.339	0.432	0.372	0.000	0.374	0.608	0.000	0.579
16 Univ Rat S	0.356	0.345	0.296	0.558	0.204	0.372	0.359	0.309	0.000	0.292	0.000	0.132	0.350
17 USGS-3	0.003	0.005	0.004	0.001	0.002	0.001	0.001	0.002	0.000	0.004	0.001	0.000	0.004
18 USGS-7	0.003	0.005	0.004	0.001	0.002	0.001	0.001	0.002	0.000	0.005	0.001	0.000	0.005
19 Anderson	0.003	0.006	0.004	0.001	0.002	0.001	0.001	0.002	0.000	0.010	0.003	0.000	0.010
20 All	0.377	0.470	0.360	0.576	0.375	0.555	0.661	0.560	0.000	0.000	0.000	0.000	0.000
21 Sophis	0.269	0.638	0.267	0.778	0.378	0.696	0.869	1.560					
22 UHs	0.239	0.232	0.268	0.347	0.352	0.305	0.345	0.291					
23 Des Hrt	0.586	0.394	0.587	0.496	0.396	0.587	0.660	0.564					

Table B.7 - Volume Standard Error - Average

Average Volume Standard Error	Snakeden Branch	Slave Run	Smlax Branch	SF Broad Run-ARC	Broad Run	Holmes Run 1	Holmes Run 2	Holmes Run 4	Gaged Flows	1-hr Yarnell	2-hr Yarnell	24-hr SCS	All Events
1 SWMM	0.165	0.310	0.241	0.315	0.436	1.354	0.233	0.981	0.834	0.218	0.224	0.224	0.369
2 PSRM-QUAL	0.322	0.622	0.659	0.468	0.560	0.428	0.345	0.526	0.503	0.638	0.537	0.286	0.491
3 TR-20	0.451	0.477	0.517	0.418	0.566	0.560	0.470	0.524	0.632	0.653	0.571	0.146	0.498
4 HEC-1	0.200	0.377	0.729	0.839	0.537	0.556	0.887	0.340	1.177	0.413	0.351	0.345	0.562
5 SCS UH Whole	0.657	0.475	0.522	0.416	0.789	0.764	0.698	0.695	0.615	0.646	0.563	0.689	0.629
6 SCS UH Subareas	0.461	0.475	0.539	0.482	0.574	0.557	0.502	0.534	0.652	0.678	0.580	0.164	0.516
7 Snyder UH Whole	0.468	0.703	0.541	0.432	0.577	0.553	0.471	0.481	0.630	0.672	0.572	0.240	0.527
8 Snyder UH Subareas	0.464	0.703	0.541	0.456	0.576	0.559	0.503	0.537	0.652	0.683	0.583	0.146	0.520
9 Clark UH Whole	0.467	0.703	0.540	0.437	0.577	0.551	0.473	0.480	0.629	0.672	0.572	0.241	0.522
10 Clark UH Subareas	0.464	0.703	0.540	0.473	0.576	0.558	0.504	0.537	0.651	0.683	0.583	0.155	0.522
11 TR-55	0.134	0.228	0.139	0.118	0.067	0.088	0.121	0.074	0.000	0.000	0.000	0.121	0.121
12 Rational Whole	0.991	0.985	0.986	0.996	0.992	0.996	0.995	0.991	0.000	0.989	0.996	0.000	0.992
13 Rational Subareas	0.574	0.985	0.570	0.546	0.600	0.636	0.591	0.532	0.000	0.652	0.591	0.000	0.629
14 Mod. Rational Whole	0.993	0.986	0.988	0.998	0.992	0.997	0.996	0.993	0.000	0.992	0.993	0.000	0.993
15 Mod. Rational Subareas	0.418	0.986	0.466	0.247	0.227	0.335	0.521	0.356	0.000	0.274	0.615	0.000	0.460
16 Universal Rational	0.349	0.357	0.355	0.301	0.389	0.320	0.302	0.305	0.000	0.247	0.000	0.423	0.335
17 USGS-3 Regression	0.992	0.988	0.988	0.996	0.994	0.994	0.994	0.992	0.000	0.991	0.995	0.000	0.992
18 USGS-7 Regression	0.991	0.985	0.986	0.996	0.994	0.995	0.994	0.992	0.000	0.989	0.995	0.000	0.991
19 Anderson	0.984	0.966	0.975	0.996	0.993	0.991	0.989	0.985	0.000	0.981	0.992	0.000	0.985
20 All Models	0.476	0.617	0.572	0.512	0.596	0.564	0.552	0.585					
21 Sophisticated	0.284	0.446	0.537	0.510	0.530	0.446	0.484	0.593					
22 Unit Hydrographs	0.497	0.627	0.537	0.449	0.612	0.590	0.525	0.544					
23 Design Rainfall	0.580	0.753	0.590	0.521	0.541	0.559	0.596	0.545					
24 Peak Only	0.989	0.979	0.983	0.996	0.994	0.994	0.992	0.990					

Table B.8 - Volume Standard Error - Standard Deviation

Standard Deviation Volume Standard Error	Snakeden Branch	Stave Run	Smilax Branch	SF Broad Run-ARC	Broad Run	Holmes Run 1	Holmes Run 2	Holmes Run 4	Gaged Flows	1-hr Yarnell	2-hr Yarnell	24-hr SCS	All Events
1 SWMM	0.064	0.564	0.157	0.197	0.231	6.484	0.146	2.805	2.077	0.116	0.098	0.102	1.042
2 FSRM-QUAL	0.175	0.350	0.137	0.245	0.304	0.282	0.188	0.199	0.316	0.146	0.137	0.283	0.265
3 TR-20	0.226	0.205	0.282	0.233	0.296	0.301	0.308	0.293	0.300	0.110	0.121	0.094	0.271
4 HEC-1	0.200	0.767	0.123	1.056	0.327	0.962	1.318	0.604	1.110	0.707	0.610	0.279	0.803
5 SCS UH W	0.269	0.208	0.286	0.229	0.188	0.218	0.270	0.250	0.311	0.108	0.119	0.410	0.271
6 SCS UH S	0.226	0.208	0.270	0.217	0.304	0.315	0.302	0.292	0.271	0.109	0.116	0.139	0.268
7 Snyder UH W	0.222	0.211	0.271	0.234	0.306	0.312	0.298	0.291	0.288	0.100	0.111	0.301	0.278
8 Snyder UH S	0.224	0.211	0.269	0.209	0.303	0.314	0.303	0.290	0.269	0.104	0.114	0.095	0.275
9 Clark UH W	0.223	0.211	0.272	0.225	0.306	0.315	0.296	0.292	0.289	0.100	0.111	0.300	0.277
10 Clark UH S	0.225	0.211	0.270	0.222	0.303	0.312	0.303	0.291	0.269	0.104	0.114	0.134	0.275
11 TR-55	0.100	0.090	0.137	0.062	0.072	0.093	0.069	0.067	0.000	0.000	0.000	0.096	0.096
12 Rational W	0.001	0.001	0.001	0.000	0.001	0.000	0.000	0.001	0.000	0.000	0.000	0.000	0.004
13 Rational S	0.022	0.001	0.018	0.027	0.023	0.011	0.014	0.020	0.000	0.172	0.042	0.000	0.140
14 Mod Rat W	0.001	0.002	0.002	0.001	0.001	0.001	0.001	0.000	0.000	0.005	0.003	0.000	0.004
15 Mod Rat S	0.353	0.002	0.350	0.206	0.155	0.327	0.432	0.339	0.000	0.309	0.342	0.000	0.368
16 Univ Rat S	0.172	0.213	0.245	0.176	0.204	0.165	0.172	0.141	0.000	0.188	0.000	0.132	0.184
17 USGS-3	0.003	0.005	0.004	0.001	0.002	0.001	0.001	0.002	0.000	0.004	0.001	0.000	0.004
18 USGS-7	0.003	0.005	0.004	0.001	0.002	0.001	0.001	0.002	0.000	0.005	0.001	0.000	0.005
19 Anderson	0.003	0.006	0.004	0.001	0.002	0.001	0.001	0.003	0.000	0.010	0.003	0.000	0.010
20 All	0.302	0.384	0.296	0.409	0.316	0.417	0.488	0.842					
21 Sophis	0.208	0.522	0.262	0.589	0.290	0.548	0.720	1.442					
22 UHs	0.239	0.232	0.268	0.220	0.294	0.305	0.301	0.289					
23 Des Hvt	0.362	0.341	0.364	0.374	0.370	0.375	0.378	0.378					
24 Peak Only	0.004	0.011	0.007	0.001	0.002	0.002	0.003	0.004					

Table B.9 - Time to Peak Bias - Average

Average Peak Time Bias	Snakeden Branch	Slave Run	Simlax Branch	SF Broad Run-ARC	Broad Run	Holmes Run 1	Holmes Run 2	Holmes Run 4	Gaged Flows	1-hr Yarnell	2-hr Yarnell	24-hr SCS	All Events
1 SWMM	-0.025	0.037	-0.160	-0.145	-0.121	-0.215	-0.101	-0.113	0.115	-0.262	-0.223	-0.046	-0.107
2 PSM-QUAL	-0.105	-0.006	-0.137	-0.096	-0.144	-0.065	-0.191	-0.233	0.173	-0.302	-0.207	-0.138	-0.123
3 TR-20	0.010	-0.059	0.017	-0.153	-0.102	-0.417	-0.360	-0.203	-0.174	-0.212	-0.200	-0.056	-0.160
4 HEC-1	-0.101	0.411	-0.109	-0.242	-0.232	-0.179	0.146	-0.138	0.210	-0.197	-0.179	-0.058	-0.060
5 SCS UH Whole	-0.120	0.618	0.085	-0.168	-0.362	-0.513	-0.475	-0.245	0.213	-0.095	-0.083	-0.635	-0.156
6 SCS UH Subareas	-0.037	0.618	0.137	-0.119	0.011	-0.222	-0.302	-0.199	0.310	-0.177	-0.156	-0.038	-0.021
7 Snyder UH Whole	0.192	0.472	0.113	-0.063	-0.086	-0.153	-0.212	0.024	0.345	-0.028	-0.030	-0.145	0.031
8 Snyder UH Subareas	-0.033	0.472	0.098	-0.107	0.016	-0.219	-0.301	-0.199	0.360	-0.172	-0.158	-0.044	-0.107
9 Clark UH Whole	0.228	0.481	0.115	0.010	-0.073	-0.089	-0.159	0.073	0.352	0.043	0.027	-0.132	0.068
10 Clark UH Subareas	-0.017	0.481	0.103	-0.107	0.016	-0.248	-0.303	-0.202	0.359	-0.172	-0.158	-0.045	-0.109
11 TR-55	-0.021	0.008	-0.013	-0.045	0.001	-0.062	-0.068	-0.028	0.000	0.000	0.000	-0.029	-0.029
12 Rational Whole	-0.986	-0.982	-0.983	-0.995	-0.986	-0.995	-0.995	-0.987	0.000	-0.985	-0.995	0.000	-0.989
13 Rational Subareas	-0.580	-0.982	-0.703	-0.354	-0.305	-0.528	-0.621	-0.669	0.000	-0.648	-0.501	0.000	-0.593
14 Mod. Rational Whole	-0.988	-0.985	-0.986	-0.995	-0.988	-0.995	-0.994	-0.989	0.000	-0.988	-0.992	0.000	-0.990
15 Mod. Rational Subareas	-0.151	-0.985	-0.463	-0.321	-0.365	-0.357	-0.412	-0.313	0.000	-0.377	-0.470	0.000	-0.427
16 Universal Rational	0.611	0.017	0.044	0.535	0.193	0.442	0.295	0.484	0.000	1.344	0.000	-0.688	0.328
17 USGS-3 Regression	-0.986	-0.982	-0.983	-0.995	-0.986	-0.995	-0.995	-0.987	0.000	-0.985	-0.995	0.000	-0.989
18 USGS-7 Regression	-0.986	-0.982	-0.983	-0.995	-0.986	-0.995	-0.995	-0.987	0.000	-0.985	-0.995	0.000	-0.989
19 Anderson	-0.986	-0.982	-0.983	-0.995	-0.986	-0.995	-0.995	-0.987	0.000	-0.985	-0.995	0.000	-0.989
20 All Models	-0.112	0.092	-0.123	-0.203	-0.209	-0.299	-0.304	-0.231					
21 Sophisticated	-0.055	0.096	-0.097	-0.159	-0.150	-0.219	-0.127	-0.172					
22 Unit Hydrographs	0.036	0.523	0.108	-0.092	-0.080	-0.241	-0.292	-0.125					
23 Design Rainfall	-0.294	-0.639	-0.501	-0.317	-0.401	-0.367	-0.423	-0.369					
24 Peak Only	-0.986	-0.982	-0.983	-0.995	-0.986	-0.995	-0.995	-0.987					

Table B.10 - Time to Peak Bias - Standard Deviation

Standard Deviation Peak Time Bias	Snakeden Branch	Slave Run	Smlax Branch	SF Broad Run-ARC	Broad Run	Holmes Run 1	Holmes Run 2	Holmes Run 4	Gaged Flows	1-hr Yarnell	2-hr Yarnell	24-hr SCS	All Events
1 SWMM	0.051	1.119	0.139	0.190	0.165	0.738	0.239	0.177	0.897	0.237	0.178	0.048	0.483
2 PSRM-QUAL	0.096	2.217	0.313	0.157	0.204	0.311	0.122	0.246	1.509	0.112	0.096	0.325	0.772
3 TR-20	0.328	0.308	0.617	0.206	0.314	0.297	0.271	0.202	0.682	0.233	0.176	0.047	0.367
4 HEC-1	0.096	2.099	0.304	0.198	0.187	0.574	1.474	0.191	1.532	0.832	0.686	0.038	0.931
5 SCS UH W	0.624	2.559	0.609	0.206	0.439	0.397	0.390	0.470	1.923	0.182	0.141	0.476	1.015
6 SCS UH S	0.337	2.559	0.578	0.206	0.188	0.362	0.261	0.208	1.901	0.180	0.146	0.030	0.947
7 Snyder UH W	0.347	3.080	0.622	0.284	0.245	0.359	0.262	0.155	2.201	0.168	0.146	0.328	1.098
8 Snyder UH S	0.336	3.080	0.587	0.209	0.186	0.362	0.261	0.207	2.183	0.183	0.142	0.028	0.353
9 Clark UH W	0.356	3.078	0.625	0.265	0.248	0.358	0.268	0.173	2.201	0.150	0.125	0.332	1.096
10 Clark UH S	0.380	3.078	0.583	0.209	0.191	0.293	0.261	0.208	2.181	0.189	0.153	0.028	0.352
11 TR-55	0.000	0.000	0.004	0.000	0.003	0.000	0.000	0.005	0.000	0.000	0.000	0.027	0.027
12 Rational W	0.001	0.001	0.000	0.000	0.000	0.000	0.000	0.001	0.000	0.002	0.000	0.000	0.005
13 Rational S	0.021	0.001	0.000	0.000	0.000	0.000	0.000	0.019	0.000	0.222	0.114	0.000	0.200
14 Mod Rat W	0.002	0.003	0.003	0.000	0.003	0.000	0.001	0.002	0.000	0.005	0.003	0.000	0.004
15 Mod Rat S	0.167	0.003	0.112	0.031	0.133	0.010	0.025	0.097	0.000	0.249	0.234	0.000	0.244
16 Univ Rat S	1.401	0.915	0.929	1.034	1.036	0.990	0.924	1.269	0.000	0.356	0.000	0.146	1.056
17 USGS-3	0.001	0.001	0.000	0.000	0.000	0.000	0.000	0.001	0.000	0.002	0.000	0.000	0.005
18 USGS-7	0.001	0.001	0.000	0.000	0.000	0.000	0.000	0.001	0.000	0.002	0.000	0.000	0.005
19 Anderson	0.001	0.001	0.000	0.000	0.000	0.000	0.000	0.001	0.000	0.002	0.000	0.000	0.005
20 All	0.540	2.196	0.399	0.418	0.425	0.515	0.580	0.452	0.000	0.002	0.000	0.000	0.005
21 Sophis	0.183	1.615	0.384	0.193	0.227	0.522	0.771	0.208	0.000	0.000	0.000	0.000	0.005
22 UHs	0.422	2.861	0.590	0.234	0.292	0.375	0.299	0.284	0.000	0.000	0.000	0.000	0.005
23 Des Hyt	0.885	0.641	0.600	0.751	0.665	0.715	0.659	0.810	0.000	0.000	0.000	0.000	0.005
24 Peak Only	0.001	0.001	0.000	0.000	0.000	0.000	0.000	0.001	0.000	0.002	0.000	0.000	0.005

Table B.11 - Time to Peak Standard Error - Average

Average Peak Time Standard Error	Snakeeden Branch	Slave Run	Smilax Branch	SF Broad Run-ARC	Broad Run	Holmes Run 1	Holmes Run 2	Holmes Run 4	Gaged Flows	1-hr Yamell	2-hr Yamell	24-hr SCS	All Events
1 SWMM	0.041	0.421	0.160	0.186	0.144	0.516	0.181	0.159	0.334	0.293	0.231	0.048	0.225
2 PFRM-QUAL	0.107	0.900	0.228	0.125	0.174	0.191	0.193	0.273	0.436	0.302	0.207	0.138	0.268
3 TR-20	0.124	0.127	0.214	0.203	0.163	0.421	0.360	0.242	0.433	0.247	0.211	0.056	0.233
4 HEC-1	0.105	0.513	0.209	0.252	0.237	0.402	0.667	0.182	0.444	0.422	0.363	0.058	0.320
5 SCS UH Whole	0.403	0.630	0.179	0.212	0.382	0.522	0.477	0.328	0.654	0.157	0.127	0.635	0.389
6 SCS UH Subareas	0.166	0.630	0.149	0.184	0.107	0.310	0.302	0.239	0.640	0.208	0.168	0.038	0.258
7 Snyder UH Whole	0.193	1.017	0.202	0.205	0.119	0.254	0.221	0.093	0.735	0.143	0.126	0.148	0.281
8 Snyder UH Subareas	0.163	1.017	0.162	0.178	0.106	0.307	0.301	0.239	0.686	0.210	0.174	0.044	0.208
9 Clark UH Whole	0.228	1.026	0.202	0.141	0.124	0.192	0.172	0.133	0.733	0.130	0.105	0.139	0.270
10 Clark UH Subareas	0.210	1.026	0.161	0.178	0.115	0.288	0.303	0.242	0.691	0.217	0.187	0.045	0.214
11 TR-55	0.021	0.008	0.013	0.045	0.003	0.062	0.068	0.028	0.000	0.000	0.000	0.031	0.031
12 Rational Whole	0.986	0.982	0.983	0.995	0.986	0.995	0.995	0.987	0.000	0.985	0.995	0.000	0.989
13 Rational Subareas	0.580	0.982	0.703	0.354	0.305	0.528	0.621	0.669	0.000	0.648	0.501	0.000	0.593
14 Mod. Rational Whole	0.988	0.985	0.986	0.995	0.988	0.995	0.994	0.989	0.000	0.988	0.992	0.000	0.990
15 Mod. Rational Subareas	0.193	0.985	0.463	0.321	0.365	0.357	0.412	0.313	0.000	0.377	0.480	0.000	0.433
16 Universal Rational	1.338	0.875	0.889	0.990	0.991	0.948	0.885	1.211	0.000	1.344	0.000	0.688	1.016
17 USGS-3 Regression	0.986	0.982	0.983	0.995	0.986	0.995	0.995	0.987	0.000	0.985	0.995	0.000	0.989
18 USGS-7 Regression	0.986	0.982	0.983	0.995	0.986	0.995	0.995	0.987	0.000	0.985	0.995	0.000	0.989
19 Anderson	0.986	0.982	0.983	0.995	0.986	0.995	0.995	0.987	0.000	0.985	0.995	0.000	0.989
20 All Models	0.523	0.767	0.323	0.314	0.300	0.437	0.420	0.350	0.000	0.985	0.995	0.000	0.989
21 Sophisticated	0.094	0.490	0.203	0.192	0.179	0.383	0.350	0.214					
22 Unit Hydrographs	0.227	0.891	0.176	0.183	0.159	0.312	0.296	0.212					
23 Design Rainfall	0.736	0.846	0.708	0.668	0.665	0.688	0.696	0.746					
24 Peak Only	0.986	0.982	0.983	0.995	0.986	0.995	0.995	0.987					

Table B.12 - Time to Peak Standard Error - Standard Deviation

Standard Deviation Peak Time Standard Error	Snakehead Branch	Slave Run	Smilax Branch	SF Broad Run-ARC	Broad Run	Holmes Run 1	Holmes Run 2	Holmes Run 4	Gaged Flows	1-hr Yarnell	2-hr Yarnell	24-hr SCS	All Events
1 SWMM	0.039	1.033	0.139	0.148	0.145	0.561	0.184	0.136	0.839	0.196	0.168	0.046	0.440
2 PSRM-QUAL	0.092	2.016	0.251	0.135	0.178	0.251	0.119	0.198	1.453	0.112	0.096	0.325	0.734
3 TR-20	0.303	0.285	0.577	0.155	0.286	0.290	0.271	0.150	0.551	0.195	0.162	0.047	0.325
4 HEC-1	0.091	2.075	0.244	0.184	0.181	0.441	1.316	0.148	1.480	0.742	0.608	0.038	0.876
5 SCS UH W	0.484	2.556	0.587	0.157	0.421	0.384	0.387	0.414	1.819	0.131	0.102	0.476	0.950
6 SCS UH S	0.294	2.556	0.575	0.148	0.154	0.287	0.261	0.158	1.815	0.142	0.132	0.030	0.911
7 Snyder UH W	0.346	2.938	0.598	0.202	0.230	0.293	0.254	0.125	2.101	0.090	0.077	0.326	1.062
8 Snyder UH S	0.294	2.938	0.572	0.149	0.153	0.288	0.261	0.157	2.101	0.136	0.121	0.028	0.304
9 Clark UH W	0.356	2.935	0.601	0.223	0.226	0.313	0.259	0.130	2.103	0.084	0.070	0.329	1.064
10 Clark UH S	0.313	2.935	0.569	0.149	0.152	0.251	0.261	0.158	2.098	0.135	0.116	0.028	0.300
11 TR-55	0.000	0.000	0.004	0.000	0.001	0.000	0.000	0.005	0.000	0.000	0.000	0.024	0.000
12 Rational W	0.001	0.001	0.000	0.000	0.000	0.000	0.000	0.001	0.000	0.002	0.000	0.000	0.005
13 Rational S	0.021	0.001	0.000	0.000	0.000	0.000	0.000	0.019	0.000	0.222	0.114	0.000	0.200
14 Mod Rat W	0.002	0.003	0.003	0.003	0.003	0.000	0.001	0.002	0.000	0.005	0.003	0.000	0.004
15 Mod Rat S	0.110	0.003	0.112	0.031	0.133	0.010	0.025	0.097	0.000	0.249	0.212	0.000	0.234
16 Univ Rat S	0.646	0.042	0.046	0.559	0.201	0.462	0.308	0.516	0.000	0.356	0.000	0.146	0.426
17 USGS-3	0.001	0.001	0.001	0.000	0.000	0.000	0.000	0.001	0.000	0.002	0.000	0.000	0.005
18 USGS-7	0.001	0.001	0.000	0.000	0.000	0.000	0.000	0.001	0.000	0.002	0.000	0.000	0.005
19 Anderson	0.001	0.001	0.000	0.000	0.000	0.000	0.000	0.001	0.000	0.002	0.000	0.000	0.005
20 All	0.447	2.059	0.520	0.342	0.366	0.405	0.501	0.368	0.000	0.002	0.000	0.000	0.005
21 Sophis	0.166	1.541	0.340	0.161	0.204	0.416	0.698	0.164					
22 UHs	0.357	2.767	0.574	0.172	0.258	0.317	0.295	0.225					
23 Des Hgt	0.566	0.310	0.324	0.459	0.395	0.407	0.351	0.477					
24 Peak Only	0.001	0.001	0.000	0.000	0.000	0.000	0.000	0.001					

Table B.13 - Time Base Bias - Average

Average Time Base Bias	Soakden Branch	Stave Run	Smilax Branch	SF Broad Run-ARC	Broad Run	Holmes Run 1	Holmes Run 2	Holmes Run 4	Gaged Flows	1-hr Yamell	2-hr Yamell	24-hr SCS	All Events
1 SWMM	0.308	1.101	-0.692	-0.026	-0.554	16.959	0.120	-0.257	0.209	0.068	0.068	-0.151	0.020
2 PSRM-QUAL	-0.330	0.218	-0.677	-0.209	-0.636	-0.694	-0.619	-0.603	-0.227	-0.691	-0.663	-0.209	-0.451
3 TR-20	-0.428	0.145	-0.694	-0.190	-0.679	-0.323	-0.346	-0.501	-0.349	-0.532	-0.521	-0.122	-0.382
4 HEC-1	-0.430	0.702	-0.311	0.071	-0.622	-0.355	-0.369	-0.648	-0.402	-0.436	-0.470	-0.116	-0.254
5 SCS UH Whole	-0.699	0.030	-0.708	-0.196	-0.877	-0.814	-0.807	-0.829	-0.402	-0.721	-0.700	-0.642	-0.620
6 SCS UH Subareas	-0.446	0.030	-0.700	-0.039	-0.683	-0.637	-0.704	-0.679	-0.371	-0.731	-0.691	-0.152	-0.488
7 Snyder UH Whole	-0.321	-0.111	-0.682	0.406	-0.667	-0.438	-0.505	-0.594	-0.216	-0.448	-0.424	-0.366	-0.366
8 Snyder UH Subareas	-0.410	-0.111	-0.688	0.082	-0.657	-0.621	-0.690	-0.659	-0.298	-0.624	-0.589	-0.278	-0.520
9 Clark UH Whole	-0.362	-0.231	-0.700	0.265	-0.690	-0.477	-0.540	-0.621	-0.271	-0.536	-0.506	-0.362	-0.421
10 Clark UH Subareas	-0.440	-0.231	-0.704	0.038	-0.682	-0.681	-0.700	-0.673	-0.364	-0.684	-0.642	-0.253	-0.549
11 TR-55	-0.056	0.152	-0.472	-0.154	-0.393	-0.377	-0.400	-0.426	0.000	0.000	0.000	-0.266	-0.266
12 Rational Whole	-0.998	-0.992	-0.999	-0.997	-0.999	-0.999	-0.999	-0.999	0.000	-0.998	-0.998	0.000	-0.998
13 Rational Subareas	-0.901	-0.992	-0.956	-0.652	-0.956	-0.886	-0.906	-0.937	0.000	-0.949	-0.815	0.000	-0.898
14 Mod. Rational Whole	-0.998	-0.993	-0.999	-0.997	-0.999	-0.999	-0.999	-0.999	0.000	-0.998	-0.998	0.000	-0.998
15 Mod. Rational Subareas	-0.866	-0.993	-0.921	-0.649	-0.939	-0.859	-0.880	-0.914	0.000	-0.896	-0.859	0.000	-0.876
16 Universal Rational	0.063	0.645	-0.617	2.339	-0.562	0.508	0.176	-0.336	0.000	0.673	0.000	-0.119	0.277
17 USGS-3 Regression	-0.998	-0.992	-0.999	-0.997	-0.999	-0.999	-0.999	-0.999	0.000	-0.998	-0.998	0.000	-0.998
18 USGS-7 Regression	-0.998	-0.992	-0.999	-0.997	-0.999	-0.999	-0.999	-0.999	0.000	-0.998	-0.998	0.000	-0.998
19 Anderson	-0.998	-0.992	-0.999	-0.997	-0.999	-0.999	-0.999	-0.999	0.000	-0.998	-0.998	0.000	-0.998
20 All Models	-0.441	-0.032	-0.706	-0.045	-0.718	-0.516	-0.564	-0.654	0.000	-0.998	-0.998	0.000	-0.998
21 Sophisticated	-0.220	0.542	-0.593	-0.088	-0.623	-0.275	-0.311	-0.501					
22 Unit Hydrographs	-0.446	-0.105	-0.697	0.093	-0.710	-0.609	-0.658	-0.673					
23 Design Rainfall	-0.618	-0.483	-0.833	-0.016	-0.816	-0.536	-0.622	-0.762					
24 Peak Only	-0.998	-0.992	-0.999	-0.997	-0.999	-0.999	-0.999	-0.999					

Table B.14 - Time Base Bias - Standard Deviation

Standard Deviation Time Base Bias	Snakeden Branch	Stave Run	Smilax Branch	SF Broad Run-ARC	Broad Run	Holmes Run 1	Holmes Run 2	Holmes Run 4	Gaged Flows	1-hr Yarnell	2-hr Yarnell	24-hr SCS	All Events
1 SWMM	0.452	1.966	0.241	0.361	0.807	8.2054	0.346	0.275	1.603	0.732	0.851	0.400	0.938
2 PSRM-QUAL	0.571	1.479	0.277	0.181	0.308	0.212	0.302	0.376	1.080	0.420	0.375	0.299	0.654
3 TR-20	0.381	1.071	0.227	0.151	0.250	0.265	0.247	0.282	0.814	0.299	0.294	0.306	0.501
4 HEC-1	0.409	2.509	0.216	0.382	0.334	0.394	0.157	0.232	1.860	0.364	0.337	0.393	0.977
5 SCS UH W	0.327	1.043	0.251	0.141	0.163	0.158	0.181	0.188	0.768	0.219	0.220	0.525	0.497
6 SCS UH S	0.351	1.043	0.195	0.477	0.233	0.292	0.213	0.228	0.762	0.222	0.234	0.447	0.519
7 Snyder UH W	0.313	1.280	0.196	0.334	0.249	0.192	0.183	0.189	0.974	0.453	0.443	0.287	0.592
8 Snyder UH S	0.328	1.280	0.188	0.175	0.236	0.288	0.206	0.218	0.936	0.347	0.349	0.217	0.352
9 Clark UH W	0.330	1.185	0.203	0.246	0.244	0.195	0.193	0.201	0.895	0.387	0.383	0.291	0.542
10 Clark UH S	0.342	1.185	0.199	0.418	0.230	0.217	0.209	0.225	0.863	0.289	0.300	0.377	0.371
11 TR-55	0.018	0.042	0.011	0.012	0.009	0.003	0.009	0.012	0.000	0.000	0.000	0.211	0.211
12 Rational W	0.000	0.000	0.000	0.000	0.000	0.000	0.000	0.000	0.000	0.000	0.000	0.000	0.002
13 Rational S	0.000	0.000	0.000	0.005	0.000	0.001	0.002	0.001	0.000	0.030	0.119	0.000	0.100
14 Mod Rat W	0.000	0.001	0.000	0.000	0.000	0.000	0.000	0.000	0.000	0.002	0.002	0.000	0.002
15 Mod Rat S	0.023	0.001	0.018	0.049	0.013	0.018	0.017	0.016	0.000	0.084	0.109	0.000	0.100
16 Univ Rat S	0.135	0.938	0.092	1.609	0.021	0.283	0.214	0.099	0.000	1.396	0.000	0.458	1.107
17 USGS-3	0.000	0.000	0.000	0.000	0.000	0.000	0.000	0.000	0.000	0.003	0.001	0.000	0.002
18 USGS-7	0.000	0.000	0.000	0.000	0.000	0.000	0.000	0.000	0.000	0.003	0.001	0.000	0.002
19 Anderson	0.000	0.000	0.000	0.000	0.000	0.000	0.000	0.000	0.000	0.003	0.001	0.000	0.002
20 All	0.472	1.394	0.251	0.734	0.335	0.472	0.371	0.291	0.000	0.003	0.001	0.000	0.002
21 Sophis	0.547	1.846	0.289	0.307	0.474	0.550	0.363	0.327	0.000	0.000	0.000	0.000	0.000
22 UHs	0.348	1.150	0.203	0.373	0.236	0.259	0.220	0.216	0.000	0.000	0.000	0.000	0.000
23 Des Hgt	0.466	0.843	0.200	1.523	0.228	0.620	0.487	0.289	0.000	0.000	0.000	0.000	0.000
24 Peak Only	0.000	0.000	0.000	0.000	0.000	0.000	0.000	0.000	0.000	0.000	0.000	0.000	0.000

Table B.15 - Time Base Standard Error - Average

Average Time Base Standard Error	Snakeden Branch	Slave Run	Smlax Branch	SF Broad Run-ARC	Broad Run	Holmes Run 1	Holmes Run 2	Holmes Run 4	Gaged Flows	1-hr Yamell	2-hr Yamell	24-hr SCS	All Events
1 SWMM	0.386	1.160	0.692	0.262	0.813	17.080	0.273	0.327	0.707	0.608	0.603	0.318	0.531
2 PSRM-QUAL	0.577	0.668	0.677	0.234	0.636	0.694	0.619	0.616	0.568	0.765	0.716	0.305	0.589
3 TR-20	0.443	0.571	0.694	0.213	0.679	0.325	0.346	0.501	0.569	0.533	0.521	0.262	0.470
4 HEC-1	0.466	0.830	0.311	0.288	0.660	0.458	0.379	0.648	0.723	0.459	0.477	0.362	0.502
5 SCS UH Whole	0.704	0.616	0.708	0.222	0.877	0.814	0.807	0.829	0.601	0.721	0.700	0.760	0.697
6 SCS UH Subareas	0.456	0.616	0.700	0.286	0.683	0.641	0.704	0.679	0.575	0.731	0.691	0.380	0.594
7 Snyder UH Whole	0.362	0.597	0.682	0.431	0.667	0.438	0.505	0.594	0.622	0.589	0.564	0.366	0.534
8 Snyder UH Subareas	0.420	0.597	0.688	0.118	0.657	0.627	0.690	0.659	0.595	0.631	0.600	0.319	0.551
9 Clark UH Whole	0.393	0.670	0.700	0.287	0.690	0.477	0.540	0.621	0.607	0.623	0.594	0.362	0.546
10 Clark UH Subareas	0.444	0.670	0.704	0.202	0.682	0.681	0.700	0.673	0.609	0.684	0.642	0.360	0.584
11 TR-55	0.056	0.152	0.472	0.154	0.393	0.377	0.400	0.426	0.000	0.000	0.000	0.304	0.304
12 Rational Whole	0.998	0.992	0.999	0.997	0.999	0.999	0.999	0.999	0.000	0.998	0.998	0.000	0.998
13 Rational Subareas	0.901	0.992	0.956	0.652	0.956	0.886	0.906	0.937	0.000	0.949	0.815	0.000	0.898
14 Mod. Rational Whole	0.998	0.993	0.999	0.997	0.999	0.999	0.999	0.999	0.000	0.998	0.998	0.000	0.998
15 Mod. Rational Subareas	0.866	0.993	0.921	0.649	0.939	0.859	0.880	0.914	0.000	0.896	0.859	0.000	0.876
16 Universal Rational	0.121	0.892	0.617	2.339	0.562	0.508	0.193	0.336	0.000	1.011	0.000	0.381	0.696
17 USGS-3 Regression	0.998	0.992	0.999	0.997	0.999	0.999	0.999	0.999	0.000	0.998	0.998	0.000	0.998
18 USGS-7 Regression	0.998	0.992	0.999	0.997	0.999	0.999	0.999	0.999	0.000	0.998	0.998	0.000	0.998
19 Anderson	0.998	0.992	0.999	0.997	0.999	0.999	0.999	0.999	0.000	0.998	0.998	0.000	0.998
20 All Models	0.551	0.747	0.706	0.439	0.741	0.619	0.605	0.600					
21 Sophisticated	0.468	0.807	0.593	0.249	0.697	0.479	0.397	0.522					
22 Unit Hydrographs	0.463	0.626	0.697	0.258	0.710	0.610	0.658	0.673					
23 Design Rainfall	0.658	0.873	0.833	1.095	0.816	0.771	0.708	0.762					
24 Peak Only	0.998	0.992	0.999	0.997	0.999	0.999	0.999	0.999					

Table B.16 - Time Base Standard Error - Standard Deviation

Standard Deviation Time Base Standard Error	Snakeden Branch	Slave Run	Simlax Branch	SF Broad Run-ARC	Broad Run	Holmes Run 1	Holmes Run 2	Holmes Run 4	Gaged Flows	1-hr Yarnell	2-hr Yarnell	24-hr SCS	All Events
1 SWMM	0.385	1.931	0.241	0.244	0.530	82.028	0.240	0.181	1.450	0.403	0.598	0.283	0.773
2 PSRM-QUAL	0.302	1.330	0.277	0.146	0.308	0.212	0.302	0.354	0.943	0.257	0.255	0.199	0.532
3 TR-20	0.363	0.910	0.227	0.115	0.250	0.263	0.247	0.282	0.676	0.297	0.294	0.196	0.419
4 HEC-1	0.365	2.468	0.216	0.255	0.246	0.261	0.130	0.232	1.711	0.333	0.327	0.185	0.875
5 SCS UH W	0.317	0.831	0.251	0.093	0.163	0.158	0.181	0.188	0.621	0.219	0.220	0.328	0.380
6 SCS UH S	0.337	0.831	0.195	0.379	0.233	0.282	0.213	0.228	0.619	0.222	0.234	0.277	0.392
7 Snyder UH W	0.261	1.130	0.196	0.299	0.249	0.192	0.183	0.189	0.775	0.235	0.234	0.287	0.446
8 Snyder UH S	0.314	1.130	0.188	0.151	0.236	0.274	0.206	0.218	0.778	0.335	0.329	0.148	0.301
9 Clark UH W	0.290	0.995	0.203	0.218	0.244	0.195	0.193	0.201	0.706	0.215	0.216	0.290	0.416
10 Clark UH S	0.336	0.995	0.199	0.366	0.230	0.217	0.209	0.225	0.708	0.289	0.300	0.274	0.312
11 TR-55	0.018	0.042	0.011	0.012	0.009	0.003	0.009	0.012	0.000	0.000	0.000	0.150	0.150
12 Rational W	0.000	0.000	0.000	0.000	0.000	0.000	0.000	0.000	0.000	0.003	0.001	0.000	0.002
13 Rational S	0.000	0.000	0.000	0.005	0.000	0.001	0.002	0.001	0.000	0.030	0.119	0.000	0.100
14 Mod Rat W	0.000	0.001	0.000	0.000	0.000	0.000	0.000	0.000	0.000	0.002	0.002	0.000	0.002
15 Mod Rat S	0.023	0.001	0.018	0.049	0.013	0.018	0.017	0.016	0.000	0.084	0.109	0.000	0.100
16 Univ Rat S	0.081	0.681	0.092	1.609	0.021	0.283	0.197	0.099	0.000	1.169	0.000	0.274	0.902
17 USGS-3	0.000	0.000	0.000	0.000	0.000	0.000	0.000	0.000	0.000	0.003	0.001	0.000	0.002
18 USGS-7	0.000	0.000	0.000	0.000	0.000	0.000	0.000	0.000	0.000	0.003	0.001	0.000	0.002
19 Anderson	0.000	0.000	0.000	0.000	0.000	0.000	0.000	0.000	0.000	0.003	0.001	0.000	0.002
20 All	0.367	1.176	0.251	0.590	0.280	0.324	0.300	0.276	0.000	0.003	0.001	0.000	0.002
21 Sophis	0.356	1.746	0.289	0.198	0.354	0.382	0.266	0.293	0.000	0.000	0.000	0.000	0.000
22 UHs	0.325	0.969	0.203	0.285	0.236	0.255	0.220	0.216	0.000	0.000	0.000	0.000	0.000
23 Des Hrt	0.405	0.414	0.200	1.048	0.228	0.269	0.348	0.289	0.000	0.000	0.000	0.000	0.000
24 Peak Only	0.000	0.000	0.000	0.000	0.000	0.000	0.000	0.000	0.000	0.000	0.000	0.000	0.000

Table B.17 - Volume-Shape Error - Average

Average Volume-Shape Bias	Snakeiden Branch	Slave Run	Simlax Branch	SF Broad Run-ABC	Broad Run	Holmes Run 1	Holmes Run 2	Holmes Run 4	Gaged Flows	1-hr Yarnell	2-hr Yarnell	24-hr SCS	All Events
1 SWMM	0.428	0.880	0.927	0.505	0.852	1.416	0.447	1.445	1.278	0.640	0.593	0.534	0.752
2 PSM-QUAL	0.565	0.922	0.753	0.637	0.784	1.740	1.018	0.895	0.903	1.310	0.800	0.646	0.915
3 TR-20	0.569	0.601	0.816	0.650	0.864	0.758	0.751	0.893	0.851	0.759	0.724	0.633	0.740
4 HEC-1	0.671	0.693	0.795	1.284	0.979	1.495	1.965	1.242	1.637	1.048	1.045	0.891	1.148
5 SCS UH Whole	0.696	0.597	0.743	0.581	0.930	0.829	0.899	0.884	0.839	0.733	0.702	0.818	0.772
6 SCS UH Subareas	0.630	0.597	0.804	0.660	0.817	0.809	0.888	0.827	0.897	0.772	0.741	0.624	0.756
7 Snyder UH Whole	0.560	0.732	0.706	0.761	0.756	0.578	0.591	0.643	0.838	0.697	0.630	0.508	0.666
8 Snyder UH Subareas	0.612	0.732	0.791	0.627	0.775	0.784	0.856	0.789	0.893	0.758	0.715	0.577	0.749
9 Clark UH Whole	0.552	0.731	0.739	0.737	0.788	0.580	0.602	0.675	0.841	0.700	0.639	0.532	0.675
10 Clark UH Subareas	0.636	0.731	0.814	0.645	0.812	0.800	0.881	0.814	0.900	0.774	0.736	0.621	0.772
11 TR-55	0.329	0.395	0.574	0.445	0.716	0.717	0.821	0.779	0.000	0.000	0.000	0.597	0.597
12 Rational Whole	1.009	1.015	1.014	1.004	1.008	0.993	0.994	0.998	0.000	1.009	0.997	0.000	1.004
13 Rational Subareas	1.027	1.015	1.187	0.867	1.108	1.127	1.268	1.146	0.000	1.097	1.087	0.000	1.093
14 Mod. Rational Whole	1.007	1.014	1.012	1.002	1.008	0.991	0.992	0.997	0.000	1.003	1.003	0.000	1.003
15 Mod. Rational Subareas	1.349	1.014	1.796	0.785	1.345	1.802	2.106	1.853	0.000	1.334	1.688	0.000	1.527
16 Universal Rational	1.261	1.150	0.948	1.771	0.993	1.173	1.118	1.023	0.000	1.092	1.087	0.000	1.180
17 USGS-3 Regression	1.008	1.012	1.012	1.004	1.006	0.995	0.994	0.997	0.000	1.007	0.998	0.000	1.004
18 USGS-7 Regression	1.009	1.015	1.014	1.004	1.006	0.994	0.995	0.998	0.000	1.009	0.998	0.000	1.004
19 Anderson	1.016	1.034	1.025	1.004	1.007	0.998	0.999	1.004	0.000	1.017	1.000	0.000	1.011
20 All Models	0.702	0.786	0.863	0.784	0.884	0.948	0.961	0.962					
21 Sophisticated	0.558	0.775	0.823	0.769	0.870	1.132	1.045	1.116					
22 Unit Hydrographs	0.614	0.687	0.766	0.668	0.813	0.730	0.786	0.772					
23 Design Rainfall	1.067	0.974	1.143	1.055	1.058	1.195	1.277	1.186					
24 Peak Only	1.011	1.021	1.017	1.004	1.006	0.996	0.996	1.000					

Table B.18 - Volume-Shape Error - Standard Deviation

Standard Deviation Volume-Shape Bias	Snakeaden Branch	Slave Run	Smlax Branch	SF Broad Run-ARC	Broad Run	Holmes Run 1	Holmes Run 2	Holmes Run 4	Gaged Flows	1-hr Yarnell	2-hr Yarnell	24-hr SCS	All Events
1 SWMM	0.077	0.858	0.175	0.392	0.112	4.493	0.154	3.420	2.556	0.261	0.233	0.210	1.288
2 PSRM-QUAL	0.171	0.660	0.123	0.245	0.208	1.631	0.190	0.256	0.530	1.225	0.167	0.210	0.722
3 TR-20	0.126	0.183	0.107	0.255	0.173	0.148	0.131	0.105	0.266	0.138	0.154	0.128	0.193
4 HEC-1	0.164	1.122	0.090	0.951	0.247	0.731	1.446	0.510	1.250	0.862	0.758	0.258	0.890
5 SCS UH W	0.206	0.181	0.112	0.277	0.156	0.144	0.089	0.098	0.260	0.132	0.162	0.233	0.209
6 SCS UH S	0.203	0.181	0.369	0.265	0.199	0.131	0.125	0.121	0.343	0.144	0.173	0.140	0.233
7 Snyder UH W	0.201	0.240	0.305	0.182	0.219	0.259	0.191	0.135	0.289	0.091	0.100	0.246	0.231
8 Snyder UH S	0.205	0.240	0.403	0.233	0.206	0.135	0.127	0.130	0.356	0.126	0.153	0.102	0.236
9 Clark UH W	0.203	0.240	0.284	0.199	0.208	0.256	0.178	0.125	0.292	0.091	0.105	0.241	0.227
10 Clark UH S	0.210	0.240	0.411	0.254	0.200	0.124	0.126	0.126	0.368	0.134	0.165	0.126	0.240
11 TR-55	0.014	0.041	0.045	0.019	0.077	0.051	0.072	0.076	0.000	0.000	0.000	0.185	0.185
12 Rational W	0.001	0.001	0.001	0.000	0.001	0.001	0.001	0.000	0.000	0.006	0.005	0.000	0.008
13 Rational S	0.004	0.001	0.012	0.017	0.021	0.009	0.013	0.018	0.000	0.069	0.171	0.000	0.116
14 Mod Rat W	0.001	0.002	0.002	0.001	0.001	0.001	0.001	0.000	0.000	0.009	0.007	0.000	0.008
15 Mod Rat S	0.174	0.002	0.230	0.084	0.151	0.263	0.350	0.299	0.000	0.342	0.534	0.000	0.487
16 Univ Rat S	0.154	0.096	0.350	0.355	0.359	0.138	0.163	0.288	0.000	0.471	0.000	0.096	0.350
17 USGS-3	0.003	0.005	0.004	0.001	0.002	0.002	0.002	0.002	0.000	0.006	0.005	0.000	0.007
18 USGS-7	0.003	0.005	0.004	0.001	0.002	0.002	0.001	0.002	0.000	0.007	0.005	0.000	0.008
19 Anderson	0.003	0.006	0.004	0.001	0.002	0.002	0.002	0.003	0.000	0.007	0.003	0.000	0.013
20 All	0.291	0.483	0.326	0.447	0.226	0.642	0.595	0.989					
21 Sophis	0.163	0.787	0.141	0.615	0.201	1.027	0.923	1.722					
22 UHs	0.207	0.227	0.327	0.241	0.203	0.211	0.195	0.148					
23 Des Hyt	0.317	0.224	0.429	0.461	0.257	0.382	0.498	0.417					
24 Peak Only	0.004	0.011	0.007	0.001	0.002	0.002	0.003	0.004					

Table B.19 - Root-Mean-Square Error - Average

Average Root-Mean-Square Error	Snakeiden Branch	Slave Run	Smilax Branch	SF Broad Run-ARC	Broad Run	Holmes Run 1	Holmes Run 2	Holmes Run 4	Gaged Flows	1-hr Yamell	2-hr Yamell	24-hr SCS	All Events
1 SWMM	0.841	1.499	2.307	0.882	1.655	0.952	0.781	2.084	1.928	1.300	1.168	1.136	1.374
2 PSRM-QUAL	1.169	1.505	1.460	1.005	1.434	2.276	2.047	1.732	1.628	1.950	1.411	1.311	1.573
3 TR-20	1.112	0.995	1.793	1.145	1.689	1.390	1.390	1.742	1.498	1.355	1.314	1.472	1.408
4 HEC-1	1.486	0.926	1.597	2.001	1.864	3.087	5.718	3.177	2.947	2.545	2.495	2.056	2.504
5 SCS UH Whole	1.341	0.992	1.538	0.965	1.650	1.333	1.482	1.506	1.469	1.249	1.208	1.486	1.351
6 SCS UH Subareas	1.240	0.992	1.564	1.045	1.562	1.389	1.650	1.547	1.539	1.327	1.277	1.364	1.374
7 Snyder UH Whole	1.175	1.410	1.265	1.173	1.321	0.901	0.969	1.039	1.404	1.174	1.043	1.002	1.152
8 Snyder UH Subareas	1.196	1.410	1.501	0.999	1.390	1.335	1.564	1.426	1.529	1.294	1.214	1.297	1.341
9 Clark UH Whole	1.147	1.376	1.359	1.136	1.416	0.889	0.989	1.123	1.416	1.172	1.058	1.068	1.175
10 Clark UH Subareas	1.262	1.376	1.581	1.003	1.506	1.382	1.631	1.507	1.553	1.327	1.264	1.418	1.406
11 TR-55	0.815	0.571	1.783	0.863	1.845	1.581	2.145	2.059	0.000	0.000	0.000	1.458	1.458
12 Rational Whole	2.414	1.612	2.153	1.645	2.031	1.580	1.634	1.675	0.000	1.977	1.619	0.000	1.843
13 Rational Subareas	2.370	1.612	2.776	1.415	2.439	1.787	2.253	2.251	0.000	2.290	1.818	0.000	2.113
14 Mod. Rational Whole	2.386	1.621	2.133	1.623	2.024	1.571	1.626	1.666	0.000	1.832	1.831	0.000	1.831
15 Mod. Rational Subareas	3.345	1.621	4.891	1.265	3.266	3.893	5.181	4.817	0.000	3.141	3.964	0.000	3.590
16 Universal Rational	2.358	1.762	2.205	2.267	1.941	1.832	1.963	2.035	0.000	1.864	0.000	2.227	2.046
17 USGS-3 Regression	2.413	1.607	2.139	1.645	2.017	1.589	1.639	1.667	0.000	1.968	1.624	0.000	1.839
18 USGS-7 Regression	2.418	1.614	2.162	1.646	2.017	1.587	1.640	1.673	0.000	1.977	1.625	0.000	1.845
19 Anderson	2.456	1.689	2.316	1.645	2.019	1.611	1.681	1.759	0.000	2.048	1.646	0.000	1.897
20 All Models	1.489	1.323	1.839	1.241	1.707	1.609	1.944	1.821					
21 Sophisticated	1.152	1.232	1.789	1.258	1.660	1.921	2.484	2.160					
22 Unit Hydrographs	1.227	1.259	1.468	1.054	1.474	1.201	1.381	1.339					
23 Design Rainfall	2.420	1.531	2.797	1.589	2.309	2.166	2.608	2.538					
24 Peak Only	2.429	1.637	2.205	1.645	2.017	1.596	1.654	1.700					

Table B.20 - Root-Mean-Square Error - Standard Deviation

Standard Deviation Root-Mean-Square Error	Snakeden Branch	Slave Run	Smlax Branch	SF Broad Run-ARC	Broad Run	Holmes Run 1	Holmes Run 2	Holmes Run 4	Gaged Flows	1-hr Yarnell	2-hr Yarnell	24-hr SCS	All Events
1 SWMM	0.208	0.519	0.600	0.527	0.292	0.622	0.458	3.782	2.793	0.794	0.651	0.547	1.505
2 PSRM-QUAL	0.416	0.630	0.298	0.398	0.274	1.492	0.611	1.087	0.950	1.106	0.311	0.473	0.810
3 TR-20	0.263	0.794	0.363	0.439	0.333	0.228	0.229	0.446	0.647	0.309	0.343	0.572	0.489
4 HEC-1	0.366	0.812	0.304	1.147	0.462	1.497	7.374	1.908	2.406	4.428	3.566	0.783	3.113
5 SCS UH W	0.454	0.797	0.240	0.412	0.282	0.304	0.261	0.288	0.620	0.289	0.330	0.478	0.459
6 SCS UH S	0.254	0.797	0.342	0.374	0.272	0.225	0.294	0.372	0.620	0.278	0.315	0.467	0.445
7 Snyder UH W	0.442	0.815	0.314	0.296	0.286	0.446	0.287	0.200	0.604	0.263	0.249	0.459	0.441
8 Snyder UH S	0.282	0.815	0.385	0.367	0.259	0.226	0.258	0.333	0.630	0.225	0.254	0.372	0.337
9 Clark UH W	0.441	0.828	0.270	0.307	0.272	0.445	0.282	0.200	0.597	0.273	0.270	0.478	0.444
10 Clark UH S	0.258	0.828	0.393	0.371	0.270	0.206	0.280	0.363	0.635	0.255	0.298	0.397	0.353
11 TR-55	0.104	0.036	0.431	0.045	0.293	0.232	0.322	0.300	0.000	0.000	0.000	0.629	0.629
12 Rational W	0.005	0.006	0.008	0.006	0.006	0.004	0.015	0.011	0.000	0.305	0.031	0.000	0.297
13 Rational S	0.027	0.006	0.068	0.006	0.099	0.023	0.062	0.059	0.000	0.392	0.355	0.000	0.440
14 Mod Rat W	0.029	0.021	0.023	0.022	0.011	0.008	0.016	0.013	0.000	0.305	0.278	0.000	0.289
15 Mod Rat S	0.400	0.021	0.466	0.076	0.447	0.713	0.921	0.744	0.000	1.173	1.661	0.000	1.509
16 Univ Rat S	0.249	0.390	0.452	0.320	0.302	0.084	0.130	0.162	0.000	0.329	0.000	0.245	0.341
17 USGS-3	0.004	0.006	0.033	0.008	0.014	0.007	0.011	0.009	0.000	0.306	0.027	0.000	0.294
18 USGS-7	0.006	0.009	0.043	0.008	0.014	0.006	0.010	0.011	0.000	0.307	0.029	0.000	0.297
19 Anderson	0.013	0.030	0.062	0.008	0.014	0.014	0.017	0.036	0.000	0.307	0.032	0.000	0.312
20 All	0.690	0.718	0.783	0.589	0.488	0.984	2.447	1.434					
21 Sophis	0.393	0.740	0.517	0.815	0.375	1.368	4.129	2.213					
22 UHs	0.365	0.820	0.384	0.359	0.291	0.384	0.398	0.300					
23 Des Hgt	0.731	0.399	1.200	0.469	0.601	1.002	1.471	1.286					
24 Peak Only	0.021	0.042	0.093	0.008	0.013	0.015	0.024	0.048					

Table B.21 - Shape Bias - Average

Average Shape Bias	Snakeden Branch	Slave Run	Smlax Branch	SF Broad Run-ARC	Broad Run	Holmes Run 1	Holmes Run 2	Holmes Run 4	Gaged Flows	1-hr Yamell	2-hr Yamell	24-hr SCS	All Events
1 SWMM	-0.200	-0.190	-0.273	-0.724	-0.511	-0.075	-0.155	1.068	0.153	-0.272	-0.259	-0.130	-0.133
2 PSRM-QUAL	-0.536	-0.826	-0.971	-1.462	-0.638	1.786	-0.343	-0.656	-0.325	-0.147	-1.099	-0.226	-0.451
3 TR-20	-0.806	-1.045	-0.806	-1.301	-0.637	-0.740	-0.584	-0.649	-0.498	-1.449	-1.197	-0.116	-0.820
4 HEC-1	-0.093	-0.456	-1.069	1.059	-0.480	0.234	1.136	0.112	0.506	-0.222	-0.166	0.156	0.062
5 SCS UH Whole	-1.120	-1.041	-0.804	-1.289	-0.907	-0.981	-0.870	-0.856	-0.489	-1.431	-1.179	-0.804	-0.983
6 SCS UH Subareas	-0.776	-1.041	-0.749	-1.317	-0.630	-0.740	-0.622	-0.662	-0.449	-1.503	-1.214	-0.076	-0.816
7 Snyder UH Whole	-0.796	-1.298	-0.776	-0.848	-0.650	-0.732	-0.568	-0.615	-0.432	-1.369	-1.099	-0.202	-0.781
8 Snyder UH Subareas	-0.782	-1.298	-0.740	-1.274	-0.649	-0.742	-0.626	-0.662	-0.438	-1.510	-1.210	-0.084	-0.784
9 Clark UH Whole	-0.799	-1.301	-0.759	-0.974	-0.650	-0.729	-0.563	-0.615	-0.439	-1.405	-1.126	-0.185	-0.795
10 Clark UH Subareas	-0.779	-1.301	-0.743	-1.315	-0.649	-0.738	-0.626	-0.664	-0.440	-1.519	-1.222	-0.081	-0.789
11 TR-55	-0.195	-0.186	-0.135	0.184	-0.067	-0.054	0.102	-0.003	0.000	0.000	0.000	-0.044	-0.044
12 Rational Whole	-2.054	-3.332	-1.856	-4.235	-1.283	-1.772	-1.702	-1.589	0.000	-2.023	-2.570	0.000	-2.228
13 Rational Subareas	-1.189	-3.332	-1.072	-2.318	-0.776	-1.124	-1.002	-0.844	0.000	-1.443	-1.482	0.000	-1.457
14 Mod. Rational Whole	-2.012	-3.034	-1.830	-4.374	-1.271	-1.791	-1.716	-1.580	0.000	-2.269	-2.131	0.000	-2.194
15 Mod. Rational Subareas	0.831	-3.034	0.853	-0.991	-0.187	0.602	0.923	0.535	0.000	-0.628	0.530	0.000	0.004
16 Universal Rational	-0.270	-0.228	-0.363	0.038	-0.478	-0.015	0.046	-0.139	0.000	0.122	0.000	-0.474	-0.176
17 USGS-3 Regression	-2.055	-3.342	-1.860	-4.234	-1.285	-1.769	-1.700	-1.590	0.000	-2.027	-2.568	0.000	-2.230
18 USGS-7 Regression	-2.053	-3.332	-1.855	-4.232	-1.285	-1.770	-1.700	-1.589	0.000	-2.023	-2.567	0.000	-2.227
19 Anderson	-2.039	-3.269	-1.834	-4.234	-1.285	-1.764	-1.692	-1.578	0.000	-2.001	-2.563	0.000	-2.212
20 All Models	-0.757	-1.328	-0.809	-1.285	-0.682	-0.472	-0.469	-0.510					
21 Sophisticated	-0.409	-0.629	-0.780	-0.607	-0.566	0.293	0.012	-0.032					
22 Unit Hydrographs	-0.842	-1.213	-0.762	-1.170	-0.689	-0.780	-0.646	-0.684					
23 Design Rainfall	-0.704	-2.113	-0.638	-1.837	-0.666	-0.583	-0.443	-0.534					
24 Peak Only	-2.049	-3.314	-1.850	-4.233	-1.285	-1.768	-1.697	-1.586					

Table B.22 - Shape Bias - Standard Deviation

Standard Deviation Shape Bias	Snakeeden Branch	Slave Run	Smilax Branch	SF Broad Run-ARC	Broad Run	Holmes Run 1	Holmes Run 2	Holmes Run 4	Gaged Flows	1-hr Yarnell	2-hr Yarnell	24-hr SCS	All Events
1 SWMM	0.104	0.201	0.196	0.519	0.237	0.259	0.213	2.453	1.932	0.502	0.480	0.326	1.025
2 PSRM-QUAL	0.416	0.365	0.411	1.382	0.409	3.824	0.477	0.406	0.385	3.276	0.585	0.335	1.726
3 TR-20	0.482	0.756	0.513	1.260	0.404	0.468	0.477	0.459	0.310	0.596	0.496	0.162	0.684
4 HEC-1	0.420	0.432	0.418	0.627	0.443	0.638	2.257	0.524	0.964	1.520	1.267	0.550	1.164
5 SCS UH W	0.438	0.749	0.514	1.256	0.332	0.330	0.377	0.356	0.311	0.599	0.498	0.601	0.626
6 SCS UH S	0.589	0.749	0.712	1.333	0.438	0.495	0.511	0.471	0.466	0.609	0.492	0.190	0.739
7 Snyder UH W	0.537	0.563	0.645	0.837	0.415	0.482	0.502	0.447	0.404	0.385	0.300	0.327	0.594
8 Snyder UH S	0.582	0.563	0.736	1.291	0.412	0.495	0.510	0.474	0.475	0.596	0.465	0.191	0.720
9 Clark UH W	0.535	0.559	0.662	0.975	0.416	0.486	0.507	0.448	0.403	0.438	0.342	0.336	0.626
10 Clark UH S	0.593	0.559	0.740	1.342	0.413	0.497	0.510	0.472	0.486	0.618	0.493	0.204	0.738
11 TR-55	0.149	0.070	0.161	0.096	0.088	0.130	0.156	0.120	0.000	0.000	0.000	0.172	0.172
12 Rational W	0.008	0.041	0.010	0.063	0.003	0.009	0.030	0.028	0.000	0.717	1.213	0.000	0.959
13 Rational S	0.048	0.041	0.038	0.095	0.031	0.023	0.040	0.025	0.000	0.973	0.614	0.000	0.849
14 Mod Rat W	0.048	0.313	0.028	0.152	0.013	0.022	0.034	0.028	0.000	1.024	0.899	0.000	0.955
15 Mod Rat S	0.695	0.313	0.635	1.071	0.309	0.608	0.743	0.592	0.000	1.253	1.381	0.000	1.439
16 Univ Rat S	0.556	0.356	0.341	0.316	0.243	0.371	0.439	0.426	0.000	0.371	0.000	0.180	0.418
17 USGS-3	0.012	0.054	0.017	0.067	0.005	0.009	0.028	0.025	0.000	0.720	1.213	0.000	0.960
18 USGS-7	0.013	0.055	0.017	0.067	0.005	0.009	0.028	0.025	0.000	0.716	1.212	0.000	0.959
19 Anderson	0.012	0.058	0.016	0.066	0.005	0.010	0.029	0.024	0.000	0.695	1.217	0.000	0.953
20 All	0.770	1.072	0.759	1.614	0.438	1.418	1.024	1.015					
21 Sophus	0.473	0.579	0.502	1.421	0.382	2.141	1.343	1.456					
22 UHs	0.552	0.630	0.661	1.183	0.410	0.467	0.491	0.442					
23 Des Hrt	1.180	1.424	1.082	1.955	0.511	1.030	1.124	0.907					
24 Peak Only	0.014	0.062	0.019	0.063	0.004	0.009	0.027	0.024					

Table B.23 - Shape Standard Error - Average

Average Shape Standard Error	Snakeden Branch	Slave Run	Smilax Branch	SF Broad Run-ARC	Broad Run	Holmes Run 1	Holmes Run 2	Holmes Run 4	Gaged Flows	1-hr Yarnell	2-hr Yarnell	24-hr SCS	All Events
1 SWMM	1.307	2.184	3.359	2.064	1.978	0.969	0.827	2.001	1.506	2.461	2.116	1.319	1.860
2 PSM-QUAL	2.084	2.524	2.196	2.904	1.721	3.448	2.639	1.998	1.346	4.017	2.825	1.528	2.445
3 TR-20	1.963	1.811	2.538	3.083	2.037	1.892	1.847	2.101	1.323	2.875	2.630	1.786	2.166
4 HEC-1	2.653	1.440	2.353	4.246	2.232	3.833	8.218	3.804	2.222	4.982	4.728	2.481	3.625
5 SCS UH Whole	2.295	1.808	2.193	2.716	1.989	1.742	1.882	1.833	1.280	2.669	2.416	1.830	2.061
6 SCS UH Subareas	2.154	1.808	2.197	2.837	1.879	1.880	2.167	1.865	1.346	2.832	2.554	1.635	2.104
7 Snyder UH Whole	2.088	2.358	1.812	2.719	1.579	1.170	1.215	1.266	1.219	2.512	2.110	1.203	1.770
8 Snyder UH Subareas	2.082	2.358	2.105	2.733	1.665	1.198	2.046	1.714	1.326	2.799	2.452	1.600	2.023
9 Clark UH Whole	2.043	2.267	1.937	2.777	1.696	1.147	1.230	1.370	1.237	2.525	2.144	1.274	1.804
10 Clark UH Subareas	2.193	2.267	2.212	2.754	1.809	1.869	2.141	1.813	1.357	2.850	2.532	1.740	2.115
11 TR-55	1.238	0.503	1.907	1.360	2.253	1.920	2.539	2.372	0.000	0.000	0.000	1.761	1.761
12 Rational Whole	5.004	5.466	4.052	6.994	2.628	2.843	2.827	2.714	0.000	3.973	4.221	0.000	4.066
13 Rational Subareas	4.913	5.466	5.225	6.017	3.156	3.216	3.897	3.648	0.000	4.482	4.377	0.000	4.442
14 Mod. Rational Whole	4.838	4.993	3.954	7.116	2.594	2.853	2.835	2.679	0.000	4.097	3.867	0.000	3.971
15 Mod. Rational Subareas	6.765	4.993	9.055	5.543	4.181	7.061	9.022	7.740	0.000	6.252	7.404	0.000	6.880
16 Universal Rational	4.085	2.492	3.083	3.521	2.432	2.253	2.618	2.782	0.000	3.218	0.000	2.599	2.908
17 USGS-3 Regression	5.002	5.447	4.025	6.997	2.609	2.860	2.836	2.701	0.000	3.957	4.231	0.000	4.060
18 USGS-7 Regression	5.012	5.471	4.069	7.001	2.609	2.856	2.839	2.711	0.000	3.974	4.232	0.000	4.071
19 Anderson	5.091	5.726	4.359	6.986	2.612	2.899	2.910	2.851	0.000	4.128	4.268	0.000	4.180
20 All Models	2.734	2.639	2.849	3.502	2.089	2.298	2.749	2.365					
21 Sophisticated	2.002	1.990	2.657	3.074	1.992	2.543	3.385	2.489					
22 Unit Hydrographs	2.142	2.145	2.076	2.756	1.770	1.603	1.780	1.655					
23 Design Rainfall	4.726	3.986	4.819	5.145	2.939	3.568	4.218	3.904					
24 Peak Only	5.035	5.548	4.151	6.998	2.610	2.872	2.862	2.754					

Table B.24 - Shape Standard Error - Standard Deviation

Standard Deviation Shape Standard Error	Snakeden Branch	Slave Run	Smilax Branch	SF Broad Run-ARC	Broad Run	Holmes Run 1	Holmes Run 2	Holmes Run 4	Gaged Flows	1-hr Yarnell	2-hr Yarnell	24-hr SCS	All Events
1 SWMM	0.456	0.787	1.754	0.934	0.535	0.325	0.278	2.598	2.017	1.477	1.153	0.552	1.453
2 PSRM-QUAL	1.140	0.817	0.951	1.915	0.345	3.148	0.986	0.741	0.731	1.998	0.755	0.462	1.576
3 TR-20	0.753	1.076	0.677	1.599	0.445	0.717	0.775	0.657	0.729	0.832	0.745	0.688	0.972
4 HEC-1	1.024	0.770	0.858	1.660	0.557	1.186	13.476	1.528	1.563	7.836	6.149	0.999	5.216
5 SCS UH W	0.798	1.067	0.605	1.670	0.384	0.524	0.623	0.567	0.680	0.846	0.711	0.688	0.905
6 SCS UH S	0.712	1.067	0.564	1.684	0.352	0.688	0.848	0.564	0.683	0.847	0.686	0.577	0.933
7 Snyder UH W	1.068	0.807	0.643	1.361	0.310	0.605	0.482	0.418	0.697	0.933	0.797	0.502	0.937
8 Snyder UH S	0.748	0.807	0.564	1.678	0.296	0.654	0.787	0.505	0.691	0.871	0.673	0.364	0.901
9 Clark UH W	1.057	0.771	0.600	1.454	0.309	0.585	0.456	0.435	0.691	0.956	0.808	0.499	0.936
10 Clark UH S	0.719	0.771	0.564	1.696	0.331	0.675	0.834	0.540	0.696	0.844	0.668	0.397	0.905
11 TR-55	0.162	0.024	0.444	0.054	0.343	0.293	0.417	0.392	0.000	0.000	0.000	0.707	0.707
12 Rational W	0.026	0.069	0.020	0.078	0.005	0.007	0.025	0.035	0.000	1.177	2.018	0.000	1.531
13 Rational S	0.043	0.069	0.106	0.099	0.124	0.030	0.045	0.143	0.000	0.933	1.229	0.000	1.042
14 Mod Rat W	0.171	0.500	0.107	0.147	0.039	0.018	0.028	0.031	0.000	1.584	1.436	0.000	1.501
15 Mod Rat S	0.664	0.500	0.731	0.258	0.535	1.225	1.518	1.134	0.000	1.405	2.158	0.000	1.932
16 Univ Rat S	0.905	0.510	0.280	0.531	0.312	0.237	0.193	0.300	0.000	0.854	0.000	0.414	0.737
17 USGS-3	0.012	0.046	0.045	0.071	0.015	0.014	0.035	0.055	0.000	1.179	2.013	0.000	1.530
18 USGS-7	0.011	0.039	0.062	0.070	0.015	0.012	0.036	0.058	0.000	1.186	2.015	0.000	1.534
19 Anderson	0.015	0.051	0.097	0.072	0.015	0.021	0.047	0.105	0.000	1.244	1.985	0.000	1.545
20 All	1.567	1.507	1.654	2.039	0.655	1.650	4.315	1.588					
21 Sophis	0.993	0.948	1.237	1.731	0.505	2.056	7.256	1.743					
22 UHs	0.852	0.907	0.600	1.568	0.354	0.688	0.791	0.546					
23 Des Hvt	1.643	1.737	2.471	1.933	0.772	2.014	2.715	2.166					
24 Peak Only	0.043	0.137	0.167	0.067	0.014	0.025	0.051	0.100					

Table B.25 - Weighted Shape Standard Error - Average

Average Wtd. Shape Standard Error	Snakeden Branch	Slave Run	Smlax Branch	SF Broad Run-ARC	Broad Run	Holmes Run 1	Holmes Run 2	Holmes Run 4	Gaged Flows	1-hr Yarnell	2-hr Yarnell	24-hr SCS	All Events
1 SWMM	3.427	5.444	13.098	3.945	4.765	1.672	1.307	5.268	2.928	7.498	5.806	3.096	4.869
2 PSRM-QUAL	4.079	4.056	2.976	4.434	2.740	7.397	6.259	3.730	2.074	7.646	4.909	3.189	4.481
3 TR-20	3.302	2.532	5.533	4.850	4.143	2.337	2.412	4.301	1.642	4.108	4.095	4.809	3.696
4 HEC-1	8.304	2.468	2.748	12.413	5.224	11.186	71.932	13.623	5.143	28.323	23.384	7.145	16.171
5 SCS UH Whole	3.072	2.524	4.076	4.361	2.483	1.729	2.335	2.520	1.510	3.930	3.916	2.133	2.894
6 SCS UH Subareas	3.718	2.524	3.764	4.247	3.401	2.638	4.063	3.243	1.598	3.868	3.972	4.297	3.463
7 Snyder UH Whole	3.502	3.122	2.661	4.175	2.303	1.387	1.658	1.756	1.325	3.492	3.082	2.269	2.561
8 Snyder UH Subareas	3.597	3.122	3.518	4.303	2.612	2.471	3.679	2.772	1.540	3.896	3.793	4.067	3.282
9 Clark UH Whole	3.391	2.979	2.975	4.362	2.655	1.351	1.681	2.019	1.358	3.515	3.175	2.556	2.672
10 Clark UH Subareas	3.858	2.979	3.779	4.293	3.118	2.618	3.992	3.098	1.610	3.985	4.005	4.598	3.540
11 TR-55	3.196	0.759	6.366	3.024	7.504	4.664	7.442	7.551	0.000	0.000	0.000	5.063	5.063
12 Rational Whole	4.073	4.465	5.448	5.029	2.613	2.122	2.238	2.902	0.000	3.900	3.130	0.000	3.611
13 Rational Subareas	12.310	4.465	16.089	6.971	8.047	4.794	8.588	9.882	0.000	10.159	6.785	0.000	8.893
14 Mod. Rational Whole	3.746	3.984	4.830	5.054	2.465	2.059	2.151	2.560	0.000	3.556	3.185	0.000	3.353
15 Mod. Rational Subareas	26.736	3.984	42.352	9.812	13.722	26.629	39.741	33.528	0.000	21.527	28.039	0.000	25.079
16 Universal Rational	6.611	3.234	7.679	5.073	4.778	3.810	5.215	6.565	0.000	7.120	0.000	3.621	5.371
17 USGS-3 Regression	4.060	4.273	4.839	5.073	2.281	2.383	2.395	2.674	0.000	3.625	3.284	0.000	3.497
18 USGS-7 Regression	4.261	4.581	5.820	5.126	2.285	2.320	2.440	2.863	0.000	3.962	3.295	0.000	3.712
19 Anderson	6.088	8.517	12.114	5.054	2.335	3.081	3.752	5.436	0.000	6.898	3.962	0.000	5.797
20 All Models	5.215	3.402	6.356	5.289	3.861	4.265	9.933	5.523					
21 Sophisticated	4.778	3.625	6.089	6.410	4.218	5.656	20.481	6.772					
22 Unit Hydrographs	3.523	2.875	3.462	4.290	2.762	2.034	2.902	2.588					
23 Design Rainfall	10.418	3.536	15.292	6.115	6.677	8.449	12.379	11.738					
24 Peak Only	4.803	5.790	7.591	5.084	2.300	2.595	2.862	3.658					

Table B.26 - Weighted Shape Standard Error - Standard Deviation

Standard Deviation Wtd. Shape Standard Error	Snake Branch	Slave Run	Smilax Branch	SF Broad Run-ARC	Broad Run	Holmes Run 1	Holmes Run 2	Holmes Run 4	Gaged Flows	1-hr Yarnell	2-hr Yarnell	24-hr SCS	All Events
1 SWMM	1.821	2.589	9.196	2.129	2.713	0.698	0.657	9.219	7.007	7.260	4.937	2.017	5.952
2 PRRM-QUAL	2.265	2.386	1.306	2.924	1.669	8.061	2.616	2.018	2.391	5.440	1.852	1.807	3.825
3 TR-20	1.264	1.688	3.005	2.407	2.728	1.131	1.118	2.608	1.539	1.761	1.859	2.873	2.381
4 HEC-1	4.105	1.521	1.112	6.235	2.110	4.261	199.298	7.300	6.424	118.662	82.732	4.222	73.118
5 SCS UH W	1.554	1.667	1.995	2.671	1.537	0.792	1.399	1.752	1.253	1.669	1.680	1.717	1.911
6 SCS UH S	1.233	1.667	1.598	2.437	2.129	1.450	2.402	1.828	1.286	1.542	1.473	2.143	1.947
7 Snyder UH W	1.894	1.732	0.879	2.201	1.192	0.700	0.697	0.790	1.120	1.758	1.521	1.155	1.630
8 Snyder UH S	1.279	1.732	1.373	2.713	1.443	1.297	2.115	1.434	1.233	1.717	1.453	1.488	1.819
9 Clark UH W	1.863	1.664	1.035	2.421	1.511	0.677	0.731	1.013	1.150	1.821	1.580	1.431	1.714
10 Clark UH S	1.254	1.664	1.600	2.698	1.885	1.412	2.332	1.681	1.316	1.659	1.488	1.704	1.947
11 TR-55	0.917	0.129	2.393	0.379	1.544	1.080	1.731	1.727	0.000	0.000	0.000	2.753	2.753
12 Rational W	0.100	0.082	0.305	0.064	0.132	0.008	0.017	0.182	0.000	1.070	1.383	0.000	1.241
13 Rational S	0.676	0.082	0.948	0.464	0.806	0.185	0.363	0.692	0.000	4.038	1.634	0.000	3.709
14 Mod Rat W	0.156	0.507	0.686	0.093	0.184	0.018	0.094	0.100	0.000	1.320	1.002	0.000	1.166
15 Mod Rat S	3.098	0.507	3.242	3.995	2.355	6.681	8.392	5.308	0.000	12.512	14.959	0.000	14.202
16 Univ Rat S	2.904	1.247	3.235	1.786	0.710	1.274	1.540	2.398	0.000	2.235	0.000	0.844	2.432
17 USGS-3	0.413	0.366	1.461	0.038	0.362	0.209	0.238	0.535	0.000	1.218	1.313	0.000	1.252
18 USGS-7	0.513	0.560	1.878	0.067	0.365	0.177	0.247	0.607	0.000	1.562	1.344	0.000	1.505
19 Anderson	0.971	1.741	2.417	0.026	0.369	0.444	0.615	1.451	0.000	3.624	0.938	0.000	3.238
20 All	5.119	2.022	8.439	3.664	2.943	5.961	57.750	7.380					
21 Sophis	3.283	2.400	6.413	5.121	2.494	5.981	102.535	7.258					
22 UHs	1.531	1.675	1.518	2.487	1.660	1.222	2.023	1.542					
23 Des Hyt	9.402	1.284	15.127	3.039	4.448	10.386	15.423	12.297					
24 Peak Only	1.134	2.230	3.793	0.054	0.344	0.454	0.752	1.579					

Appendix C

Watershed Comparison Graphs

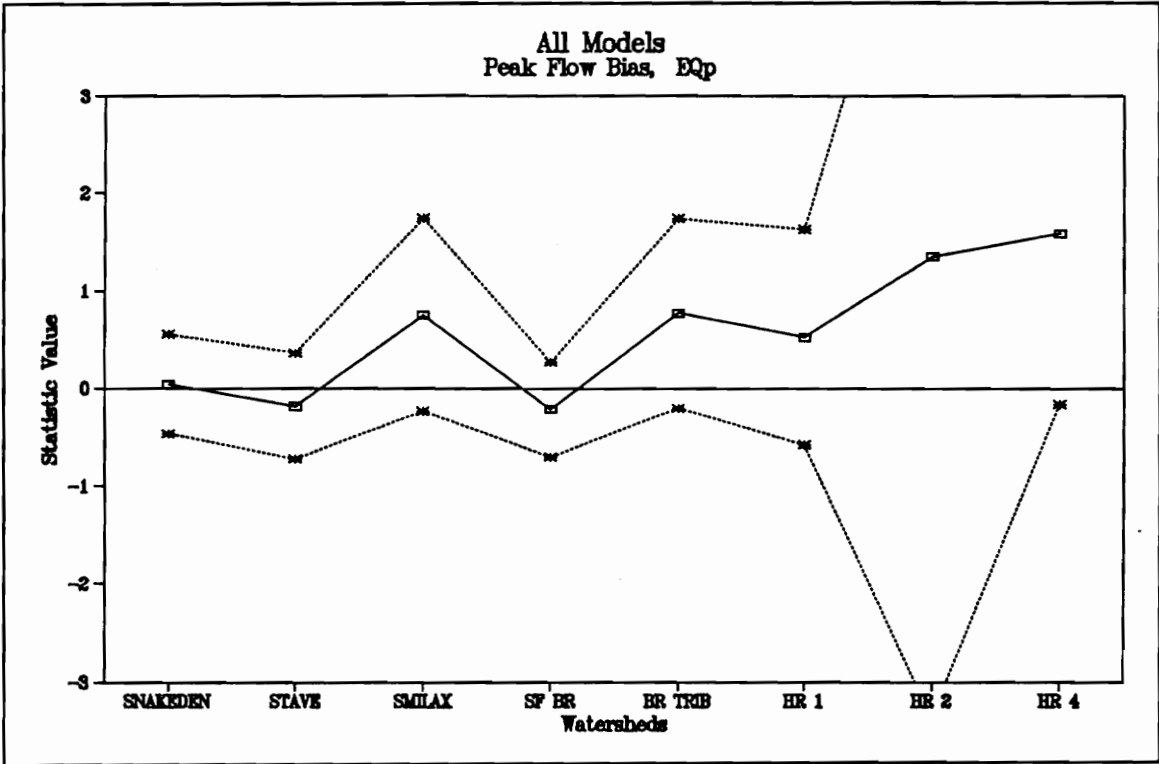


Figure C.1 - Peak Flow Bias for All Storms, All Models

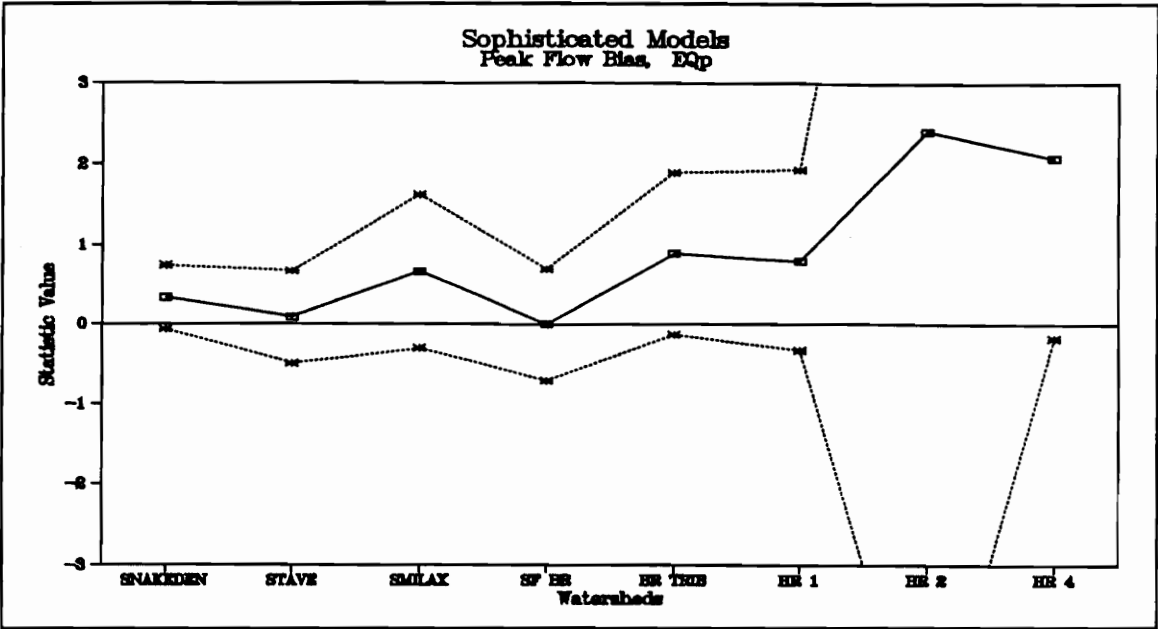


Figure C.2 - Peak Flow Bias for All Storms, Sophisticated Models

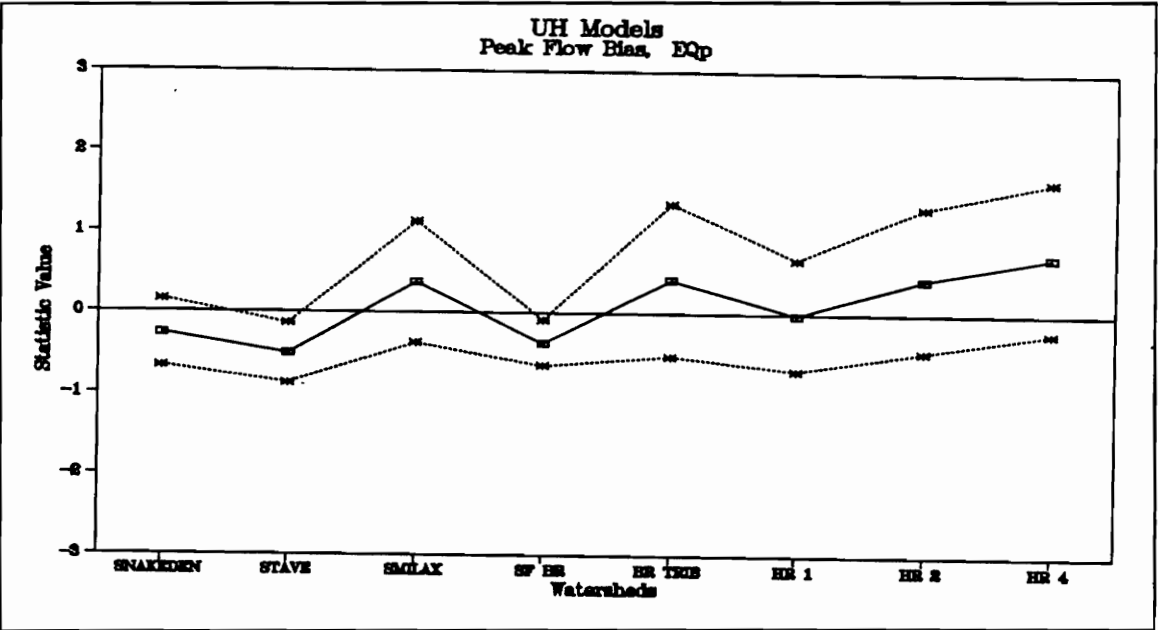


Figure C.3 - Peak Flow Bias for All Storms, Unit Hydrograph Models

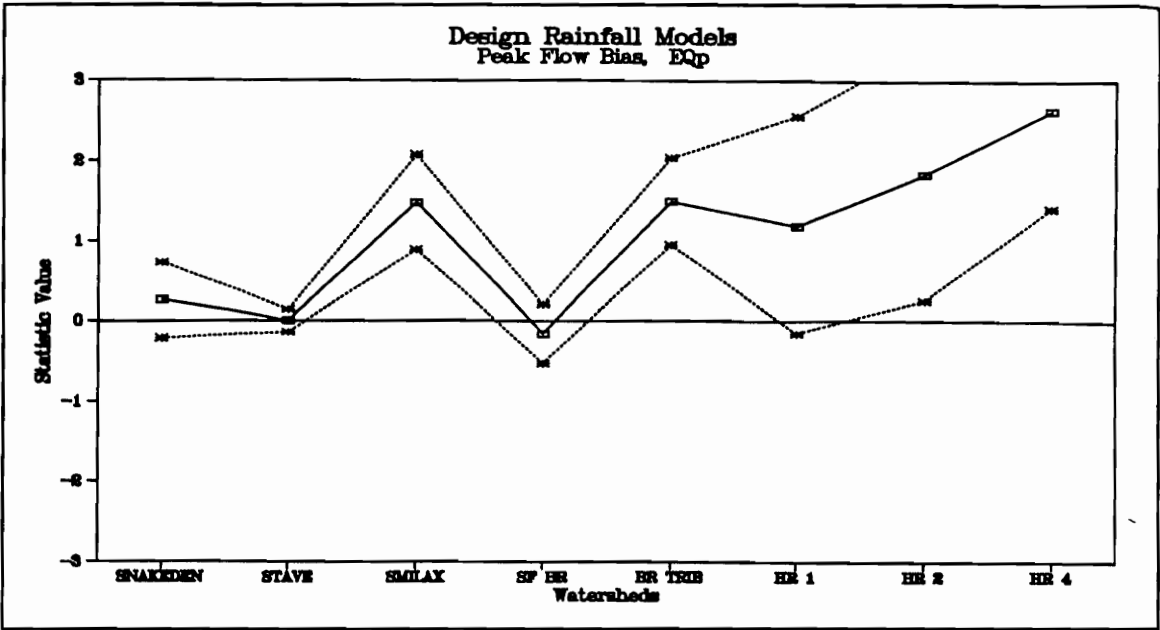


Figure C.4 - Peak Flow Bias for All Storms, Design Rainfall Models

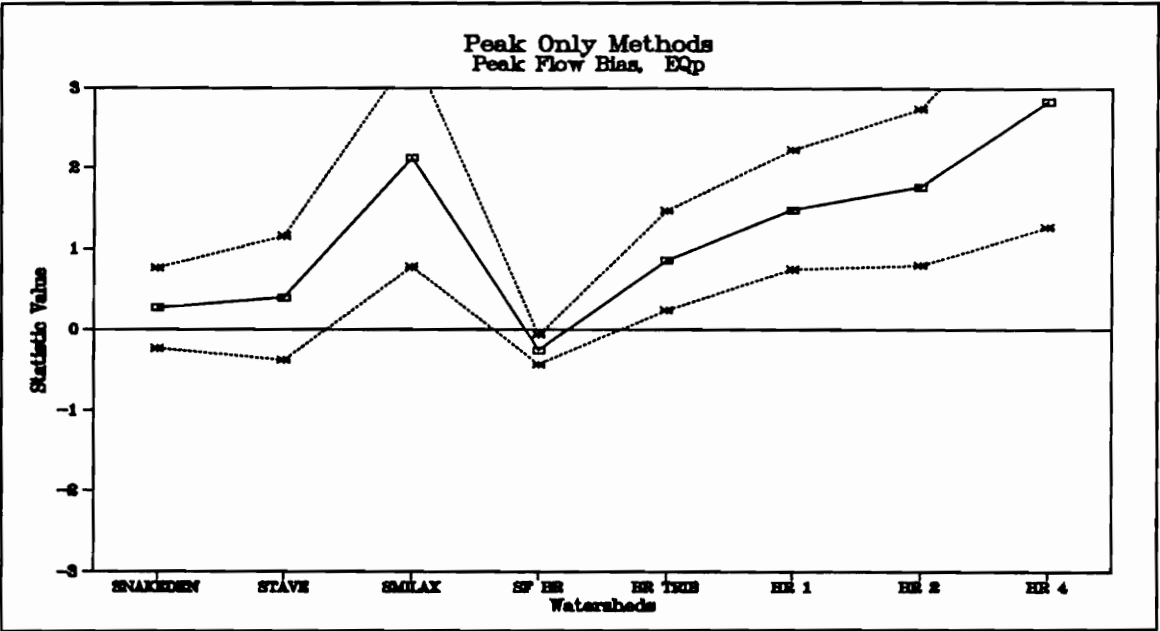


Figure C.5 - Peak Flow Bias for All Storms, Peak-Only Models

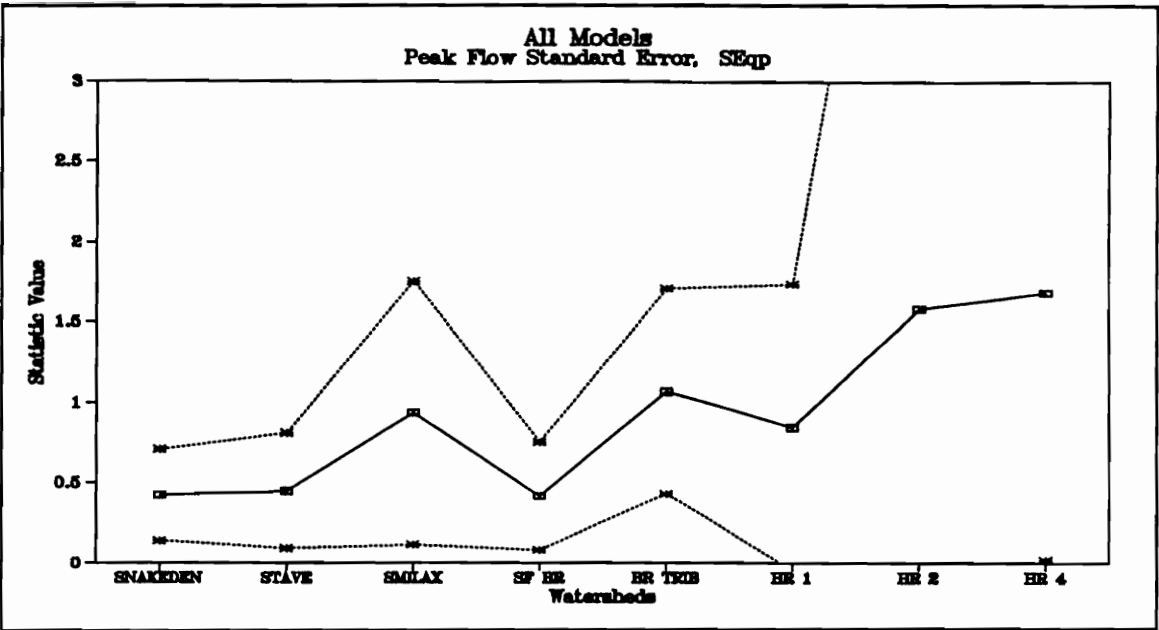


Figure C.6 - Peak Flow Standard Error for All Storms, All Models

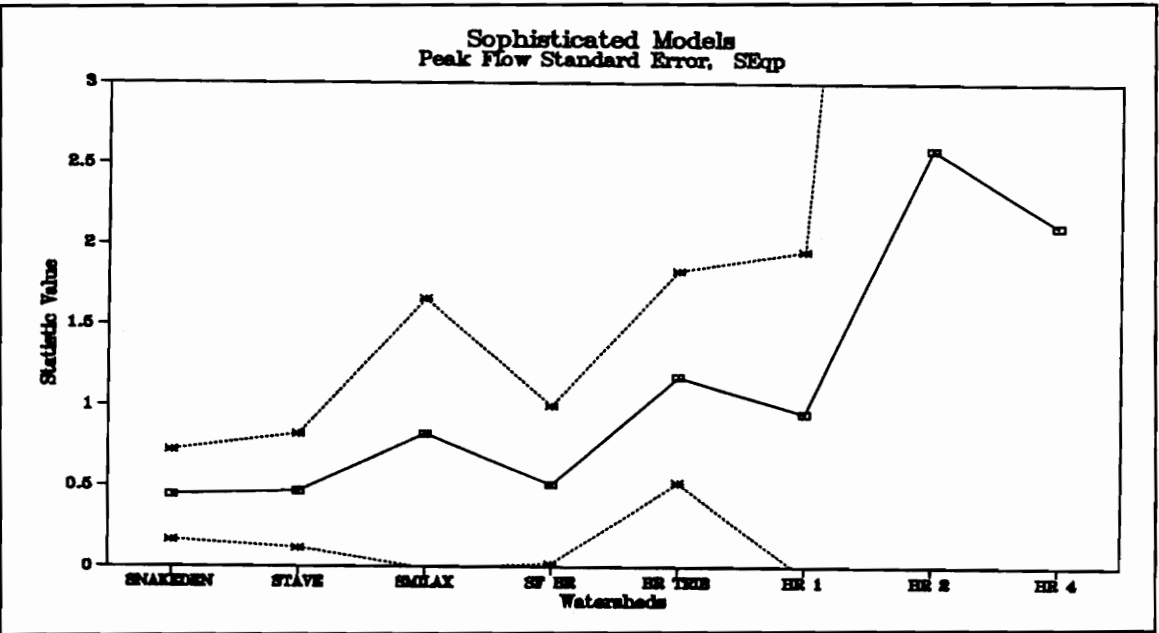


Figure C.7 - Peak Flow Standard Error for All Storms, Sophisticated Models

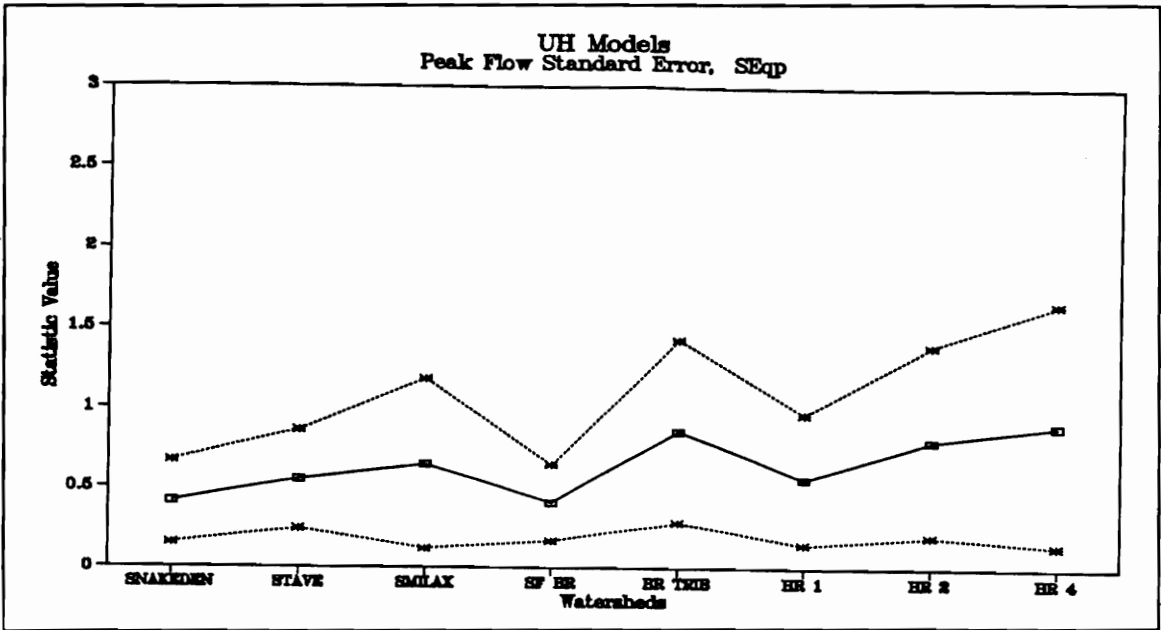


Figure C.8 - Peak Flow Standard Error for All Storms, Unit Hydrograph Models

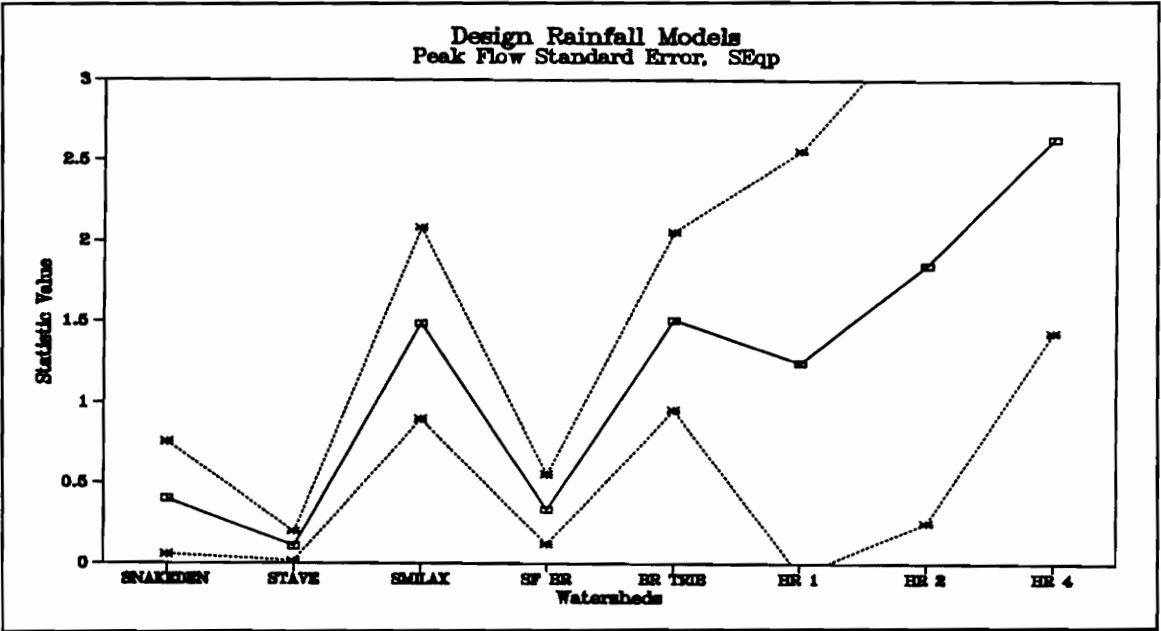


Figure C.9 - Peak Flow Standard Error for All Storms, Design Rainfall Models

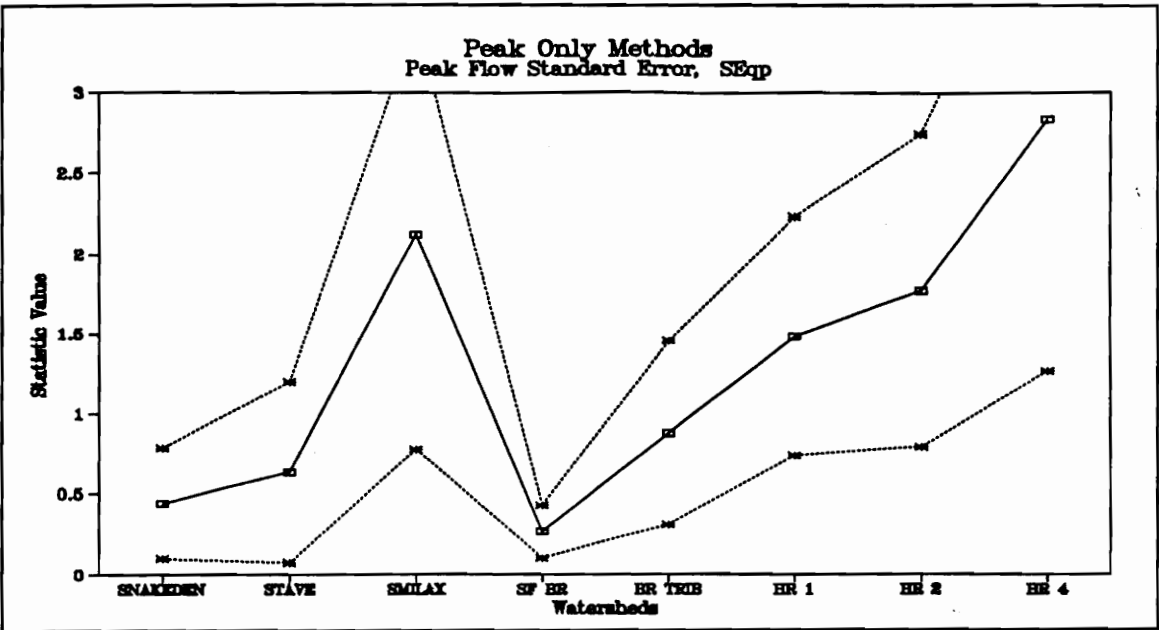


Figure C.10 - Peak Flow Standard Error for All Storms, Peak-Only Models

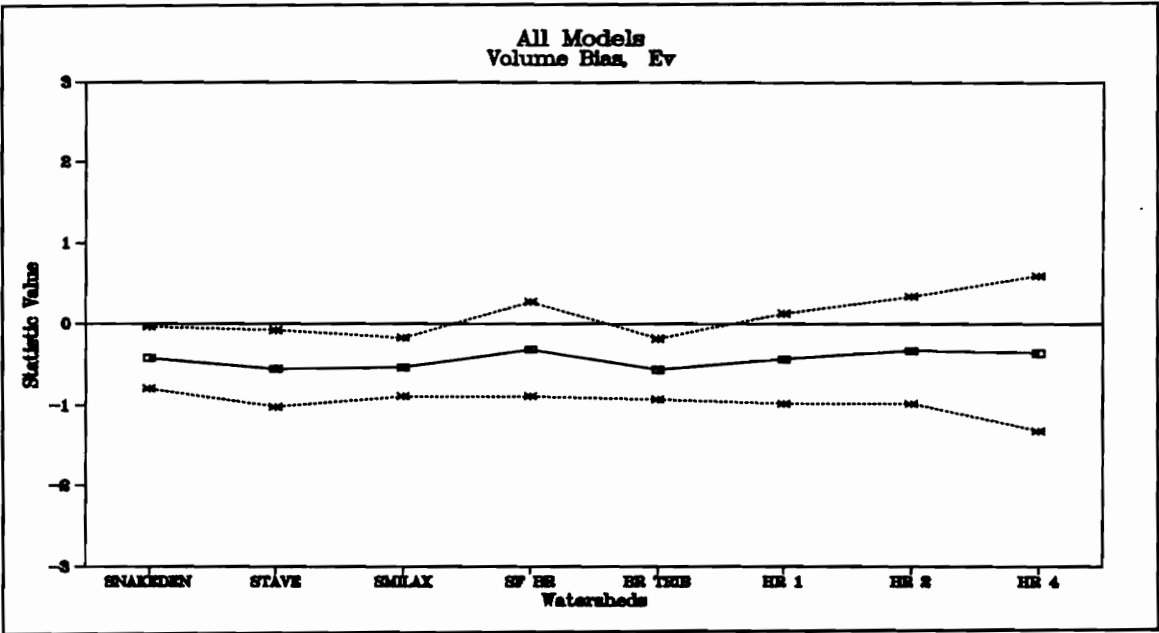


Figure C.11 - Volume Bias for All Storms, All Models

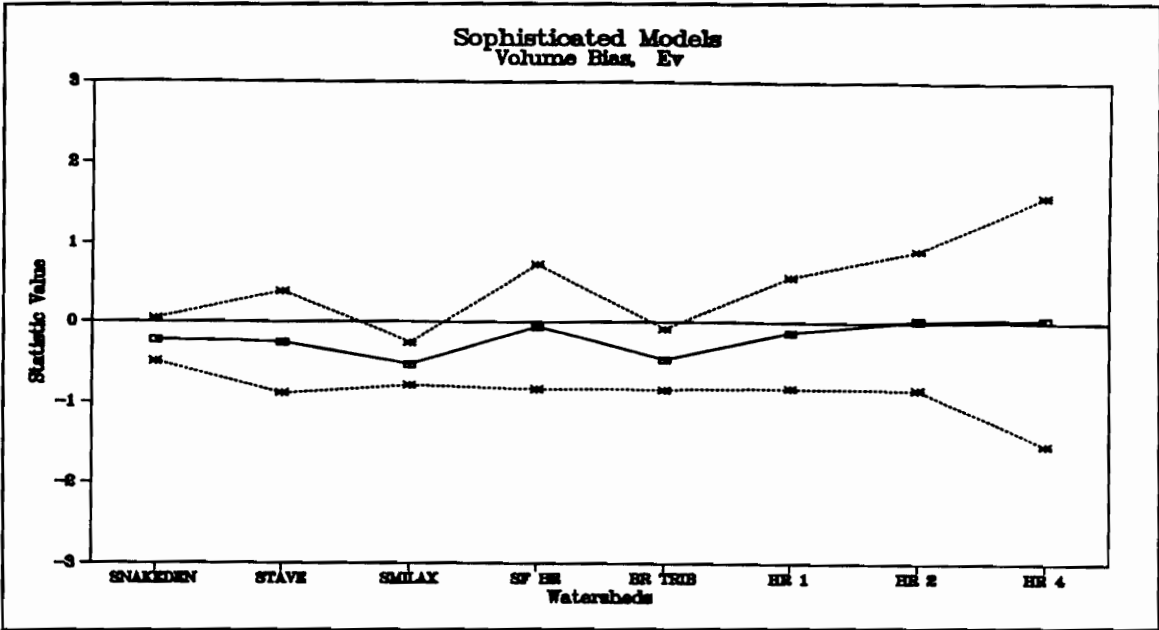


Figure C.12 - Volume Bias for All Storms, Sophisticated Models

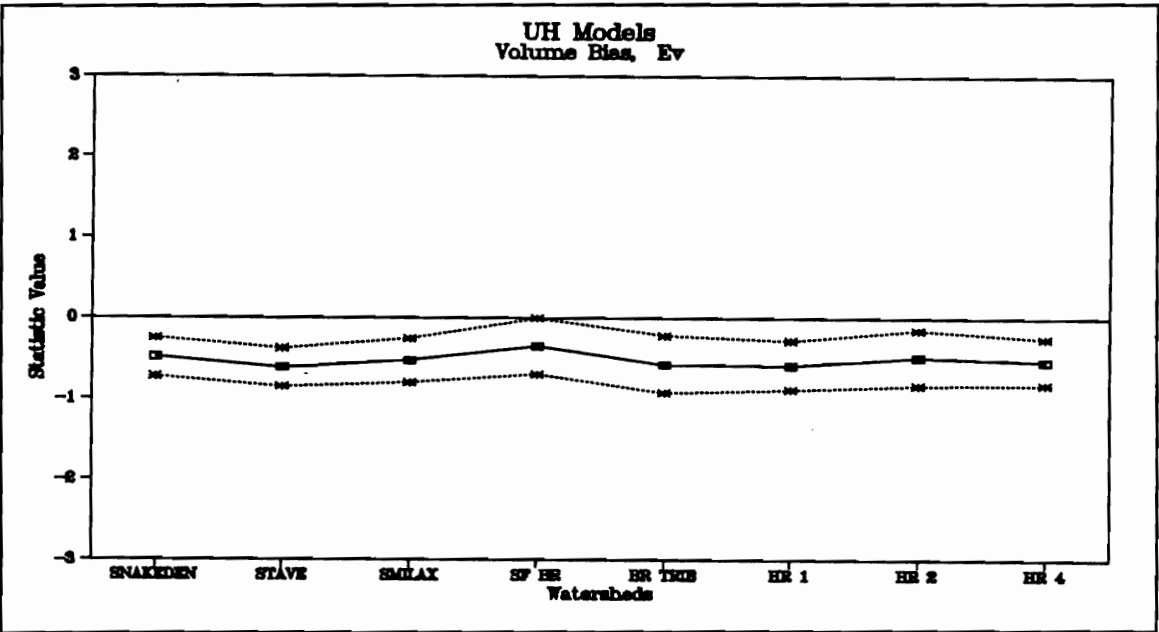


Figure C.13 - Volume Bias for All Storms, Unit Hydrograph Models

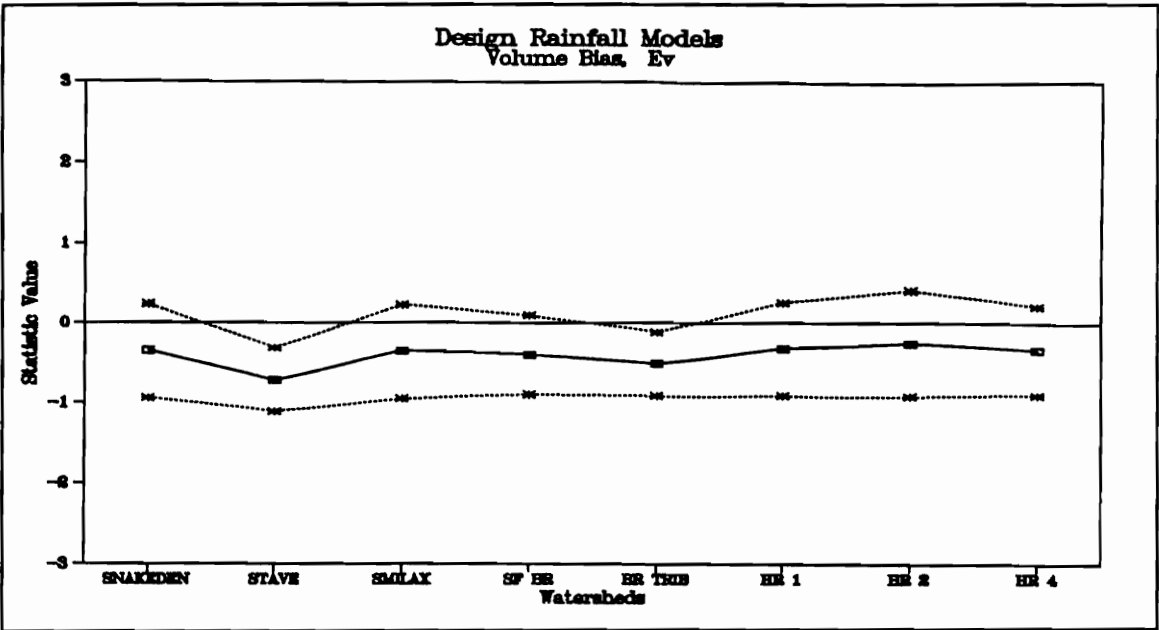


Figure C.14 - Volume Bias for All Storms, Design Rainfall Models

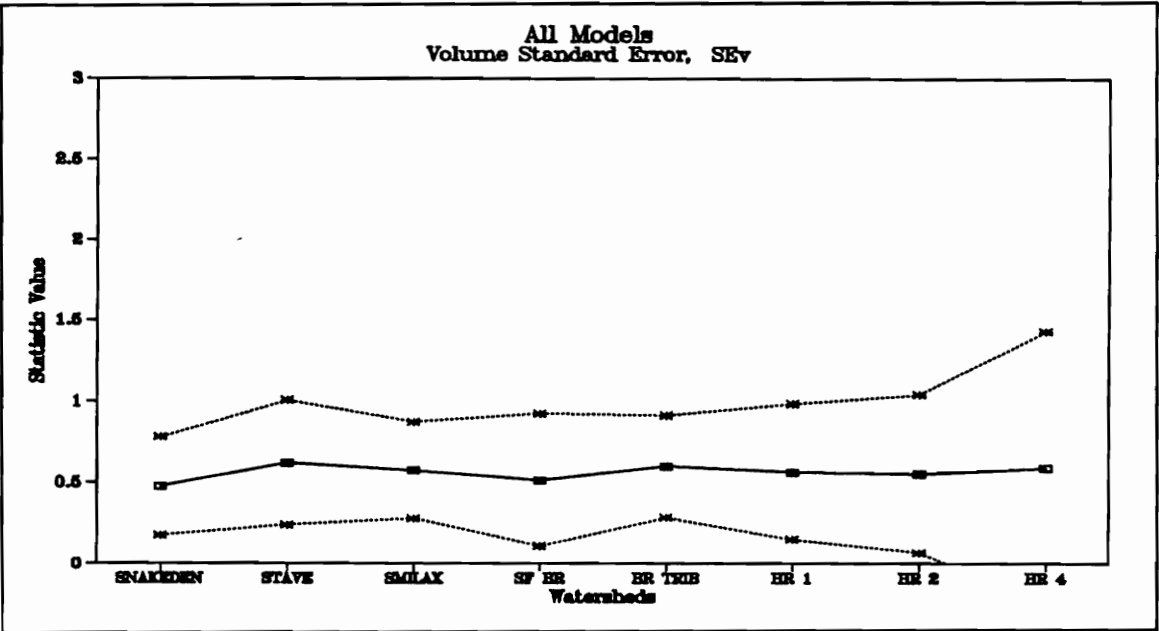


Figure C.15 - Volume Standard Error for All Storms, All Models

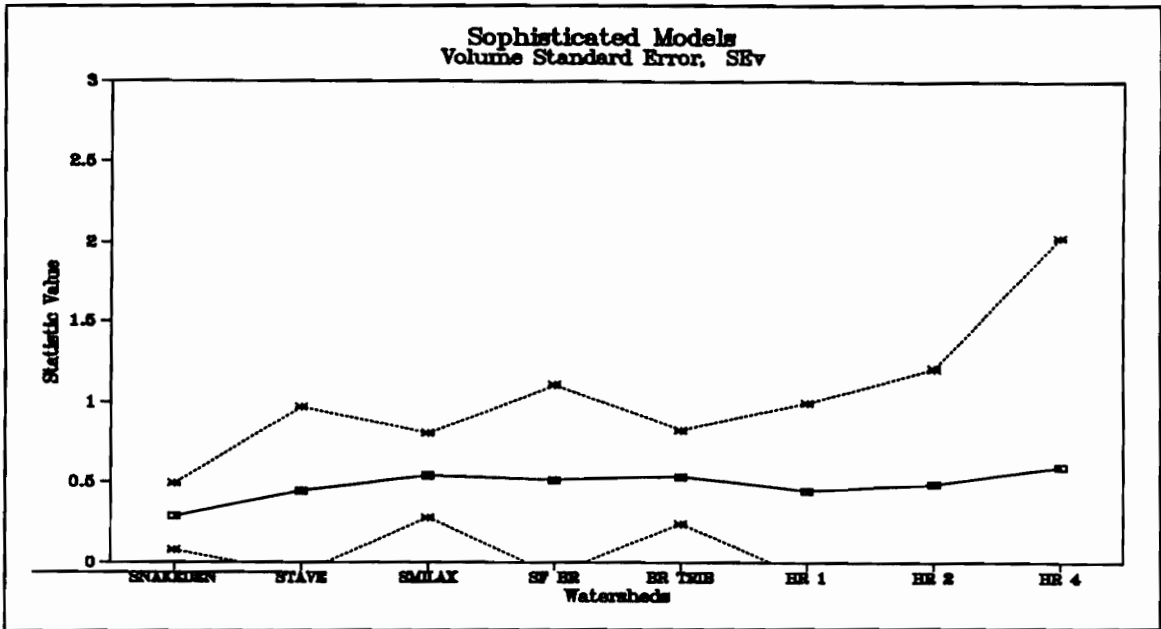


Figure C.16 - Volume Standard Error for All Storms, Sophisticated Models

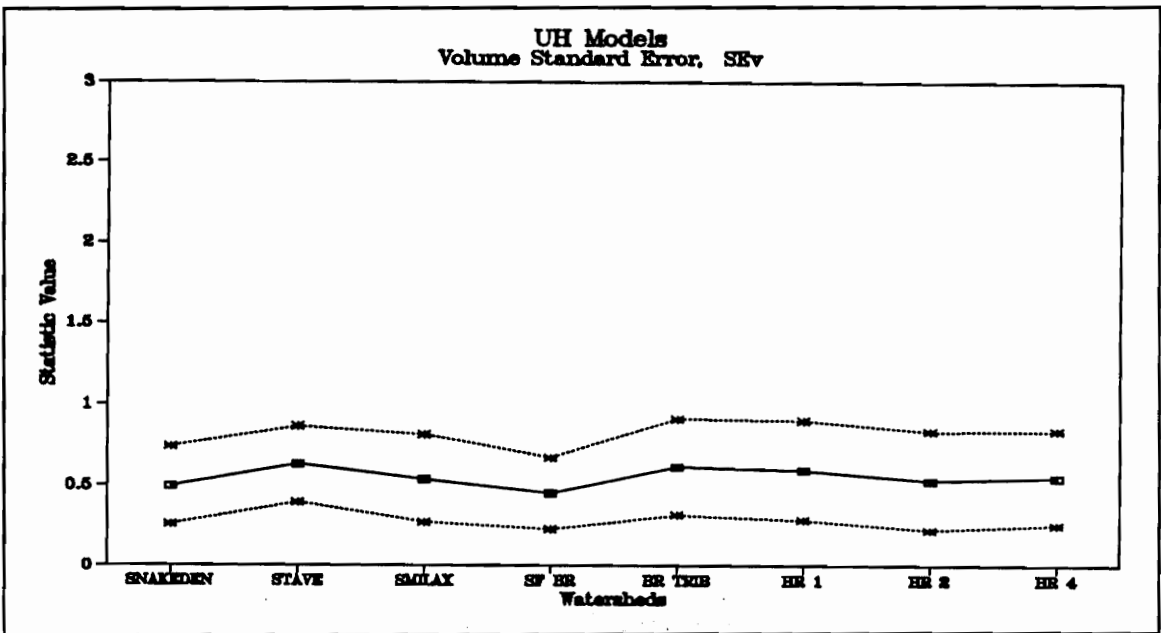


Figure C.17 - Volume Standard Error for All Storms, Unit Hydrograph Models

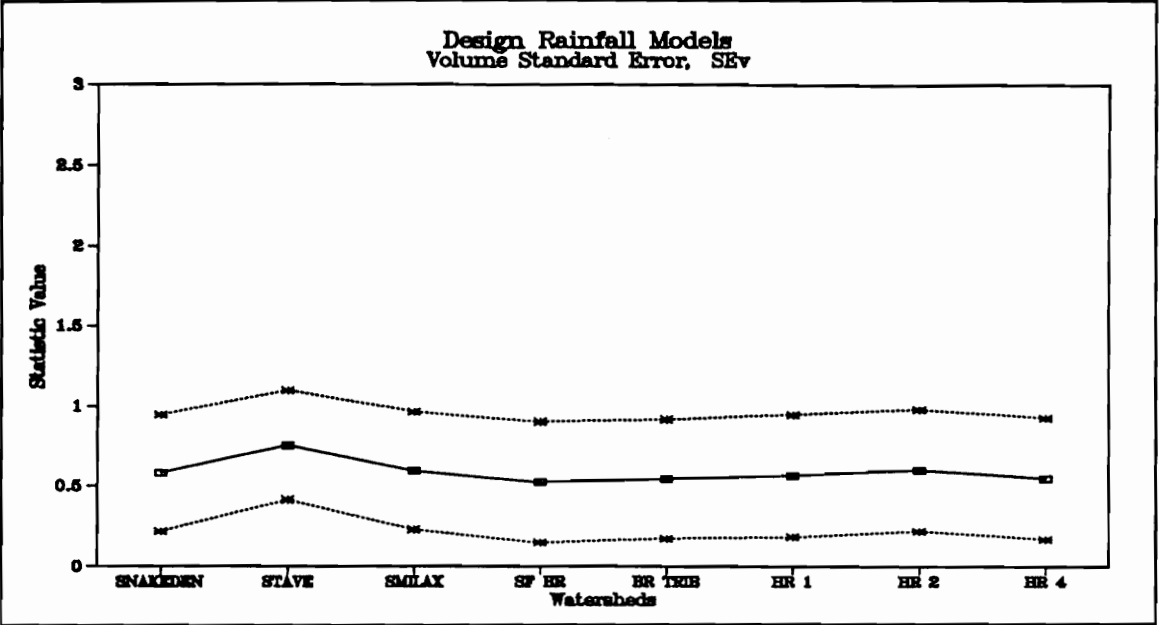


Figure C.18 - Volume Standard Error for All Storms, Design Rainfall Models

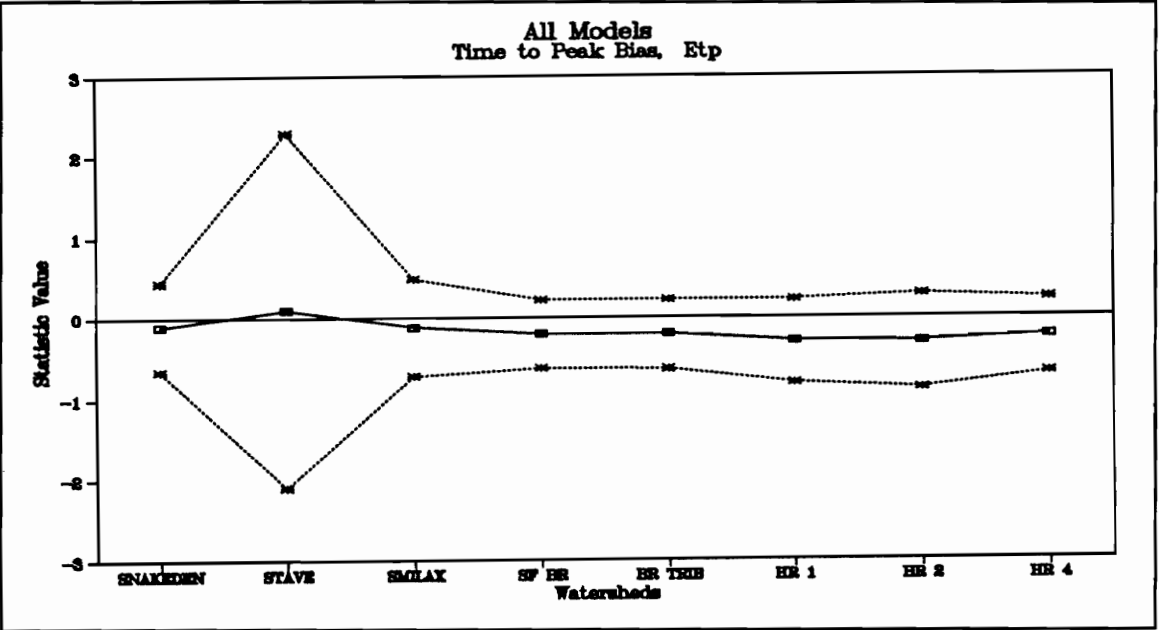


Figure C.19 - Time to Peak Bias for All Storms, All Models

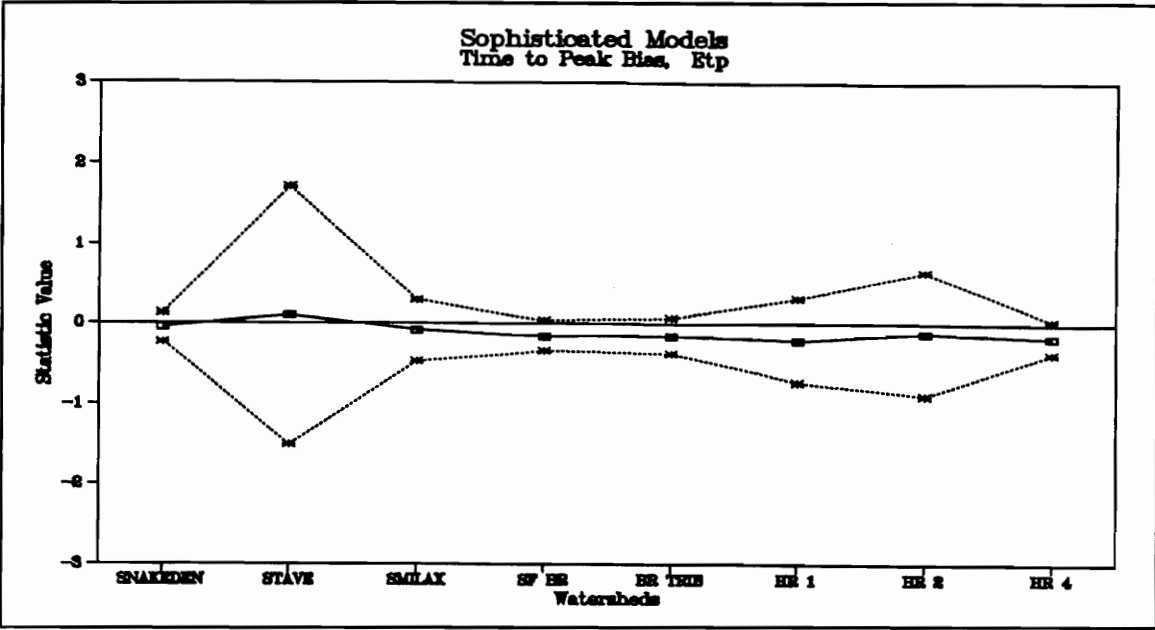


Figure C.20 - Time to Peak Bias for All Storms, Sophisticated Models

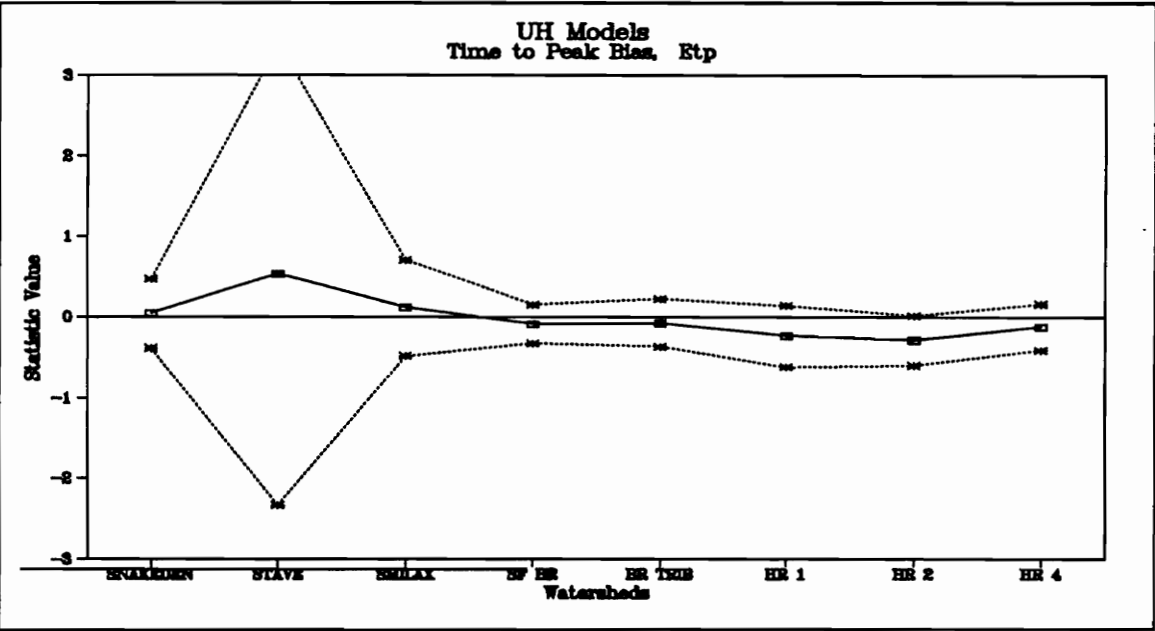


Figure C.21 - Time to Peak Bias for All Storms, Unit Hydrograph Models

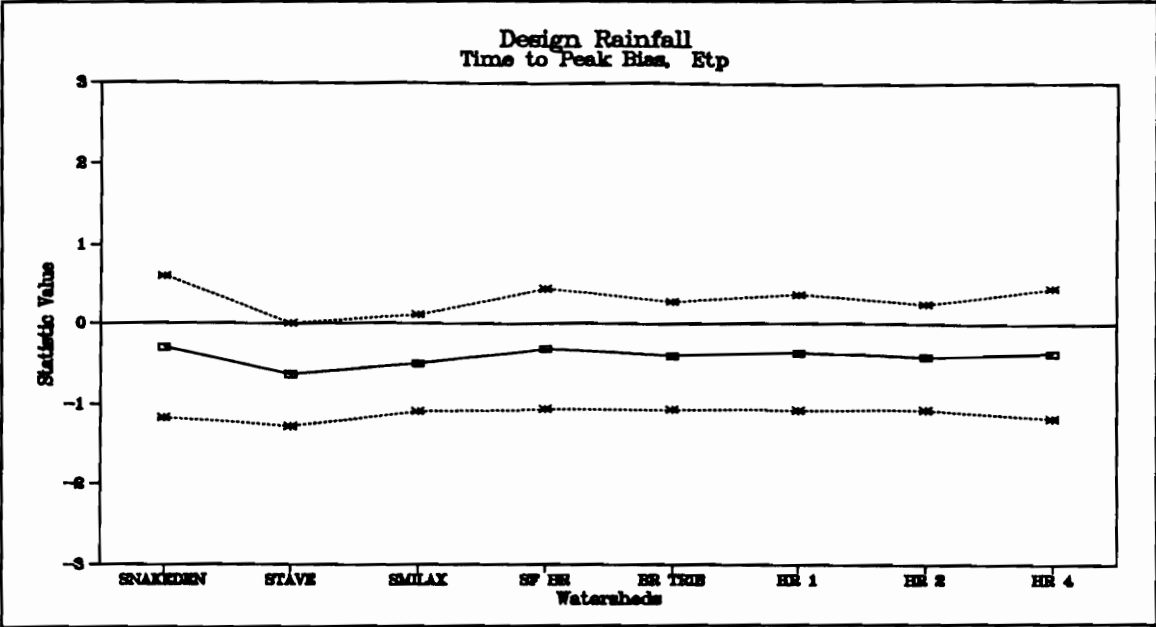


Figure C.22 - Time to Peak Bias for All Storms, Design Rainfall Models

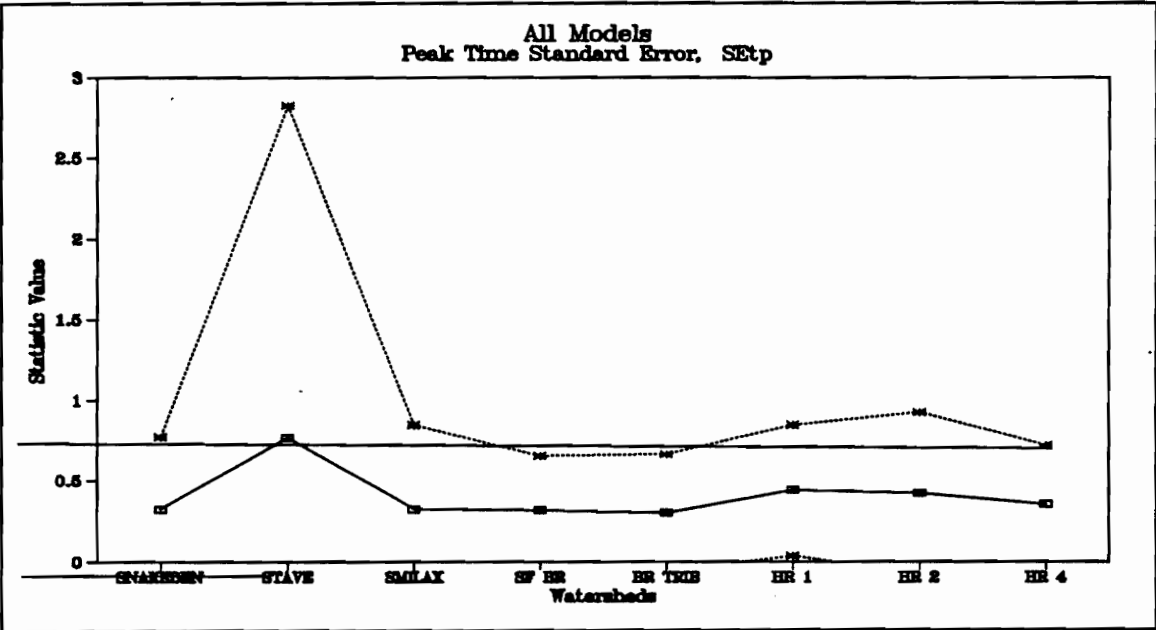


Figure C.23 - Time to Peak Standard Error for All Storms, All Models

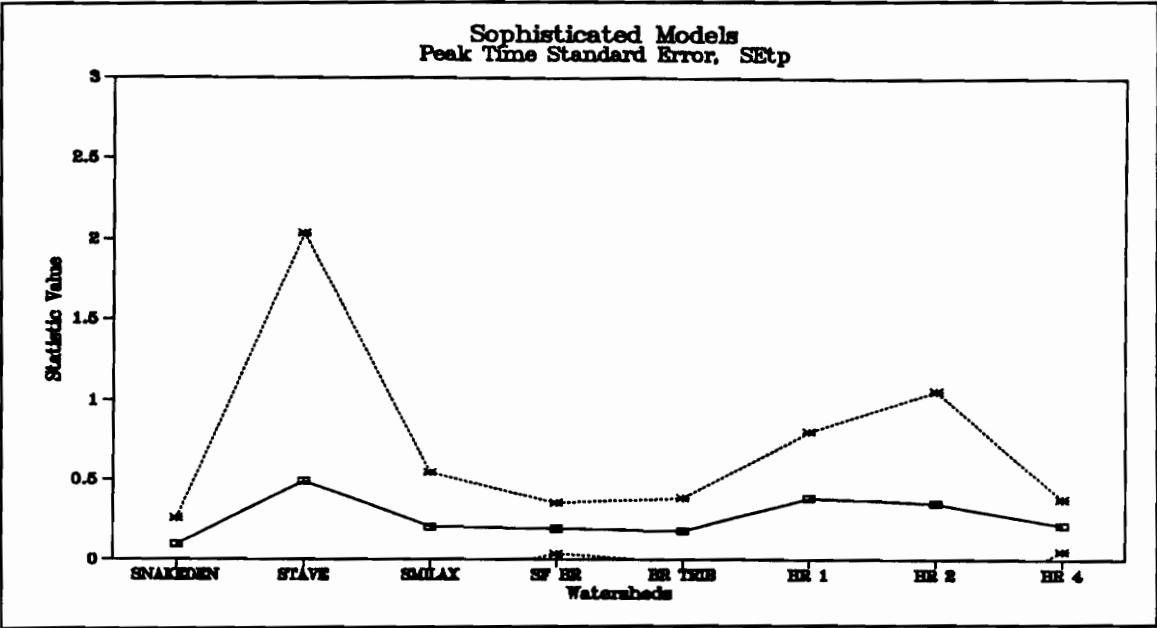


Figure C.24 - Time to Peak Standard Error for All Storms, Sophisticated Models

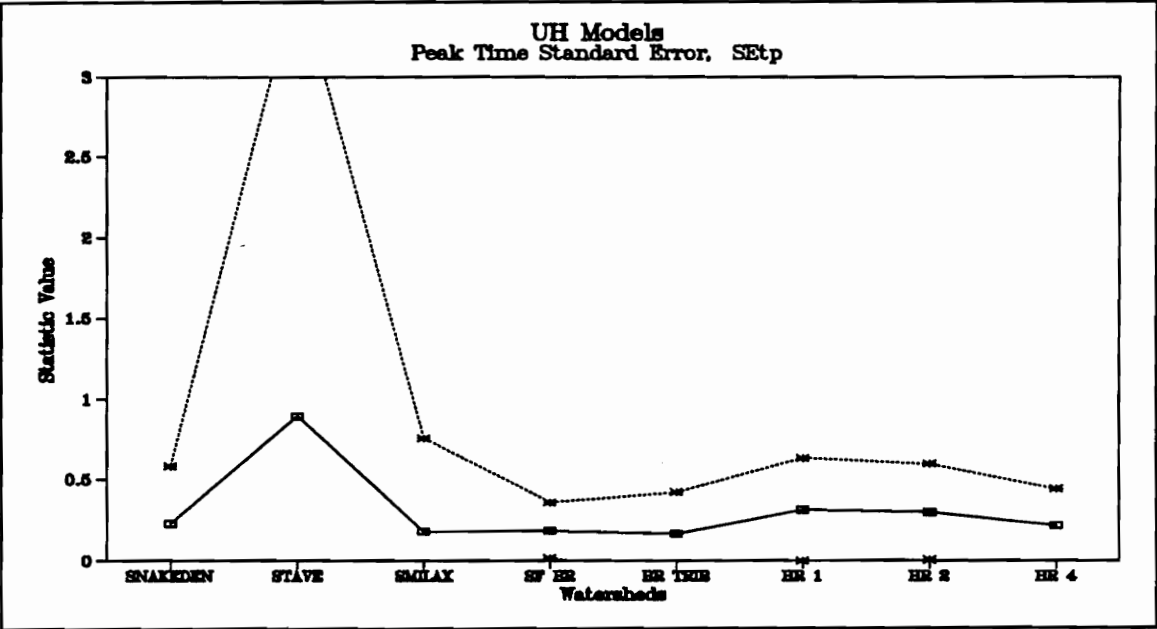


Figure C.25 - Time to Peak Standard Error for All Storms, Unit Hydrograph Models

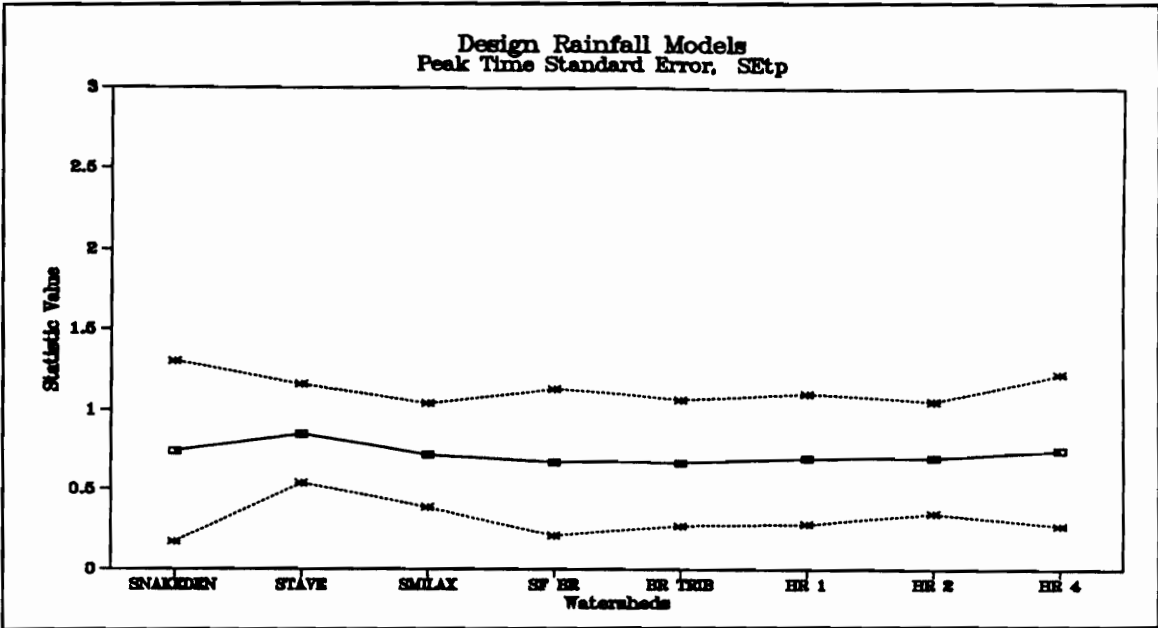


Figure C.26 - Time to Peak Standard Error for All Storms, Design Rainfall Models

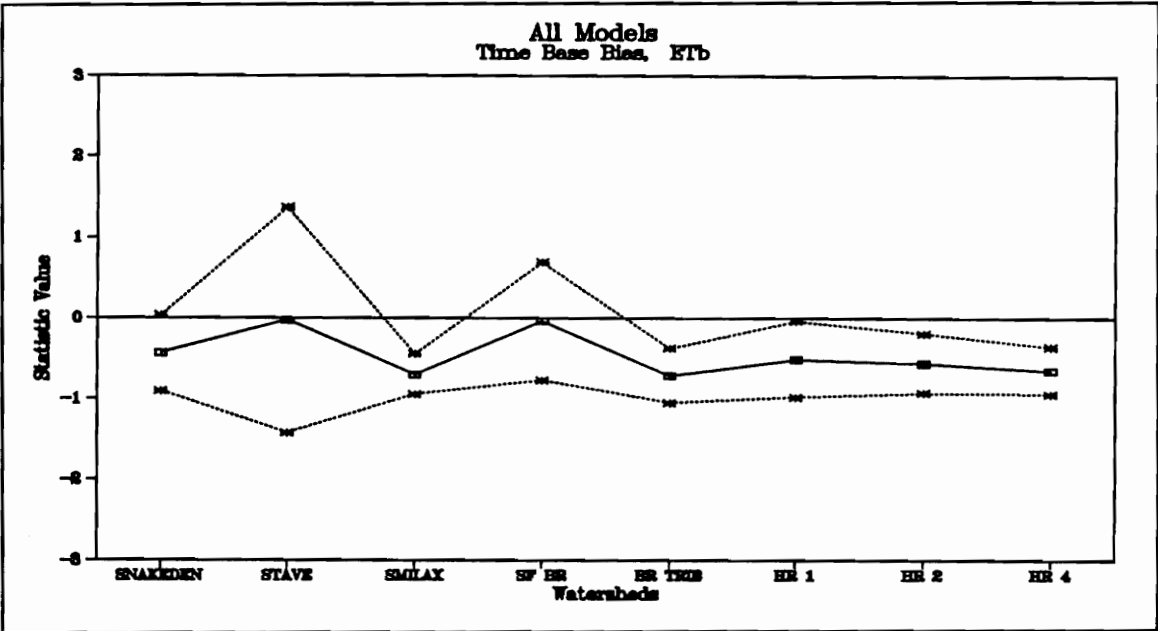


Figure C.27 - Time Base Bias for All Storms, All Models

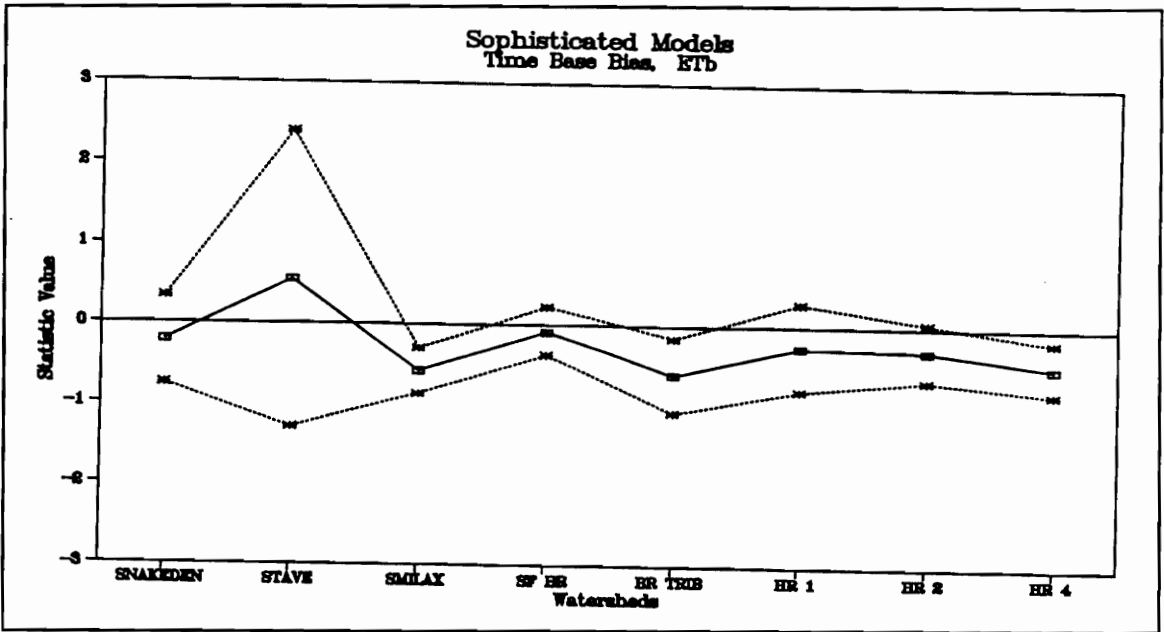


Figure C.28 - Time Base Bias for All Storms, Sophisticated Models

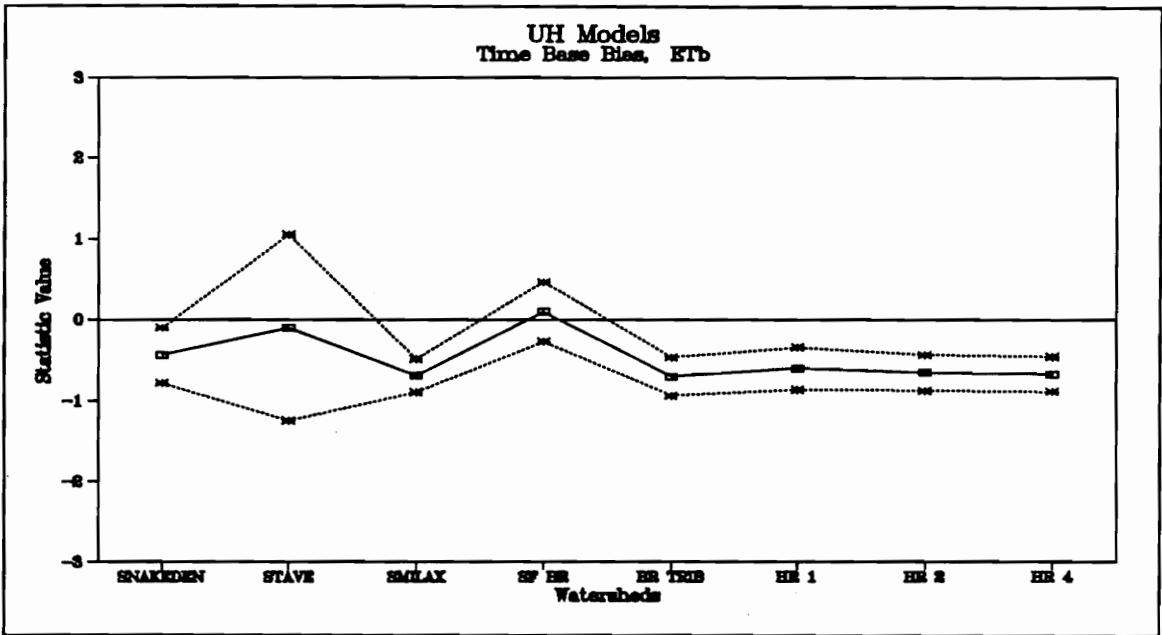


Figure C.29 - Time Base Bias for All Storms, Unit Hydrograph Models

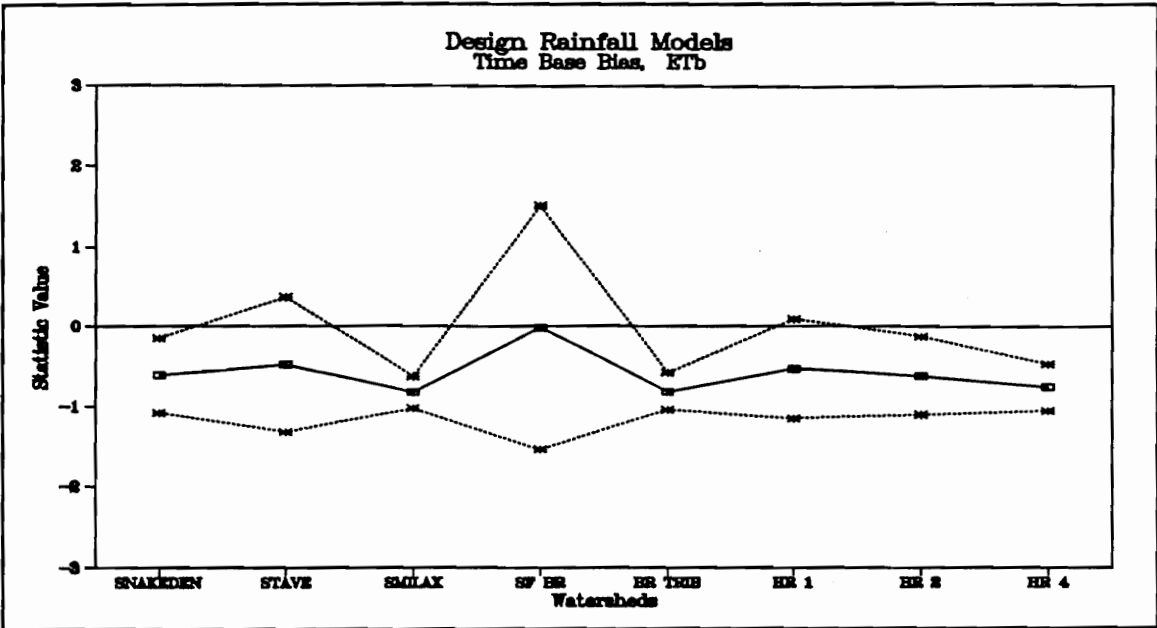


Figure C.30 - Time Base Bias for All Storms, Design Rainfall Models

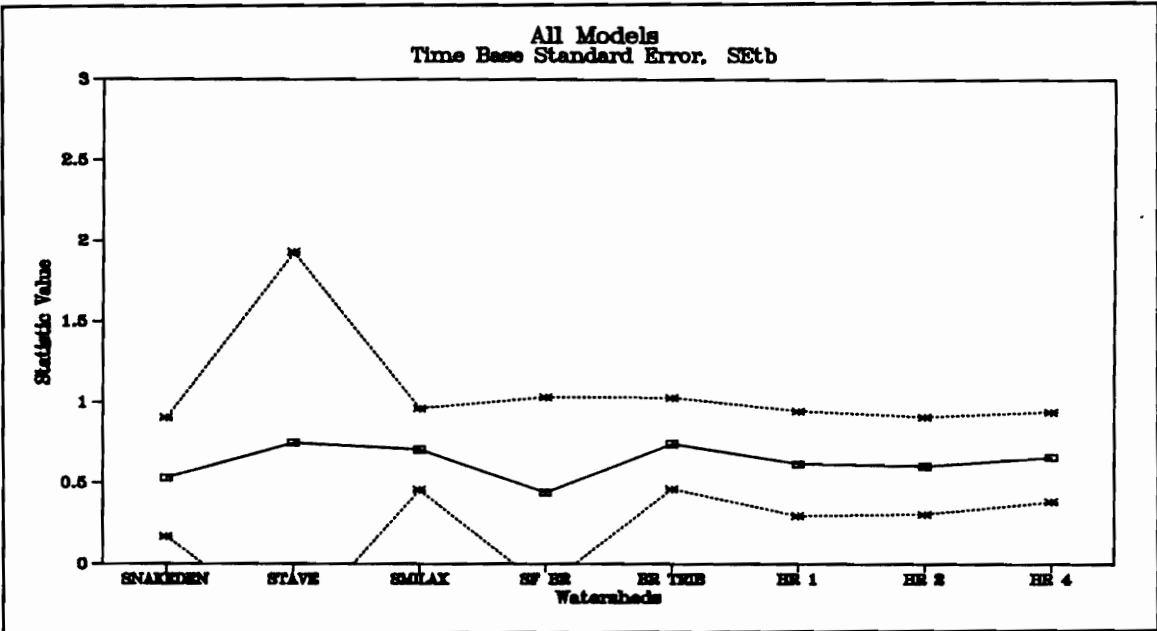


Figure C.31 - Time Base Standard Error for All Storms, All Models

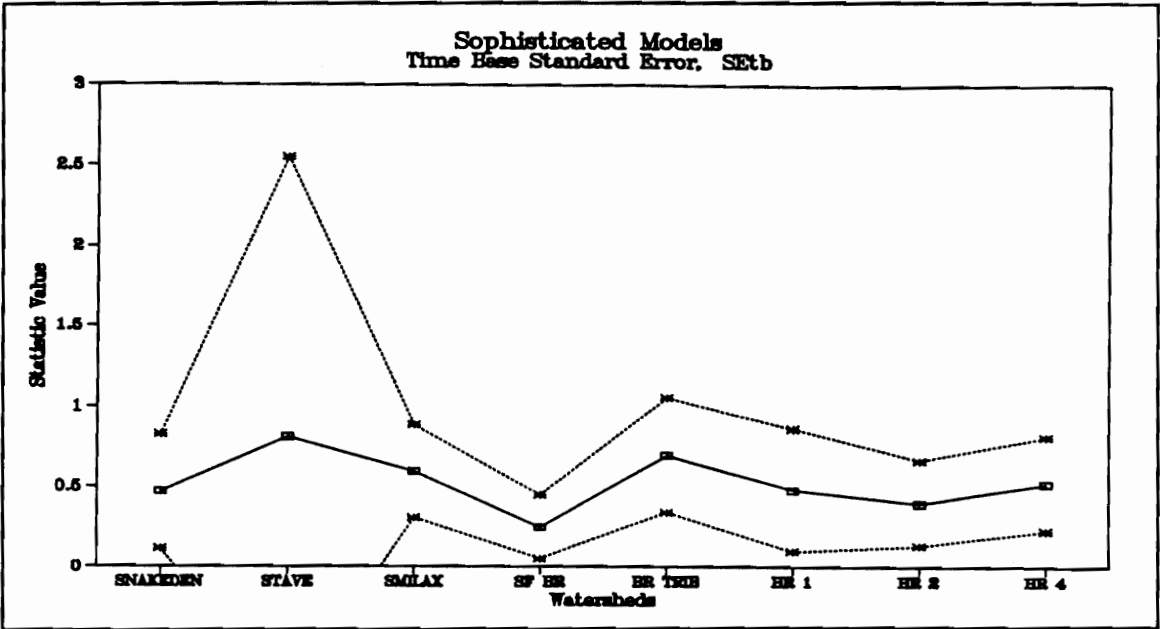


Figure C.32 - Time Base Standard Error for All Storms, Sophisticated Models

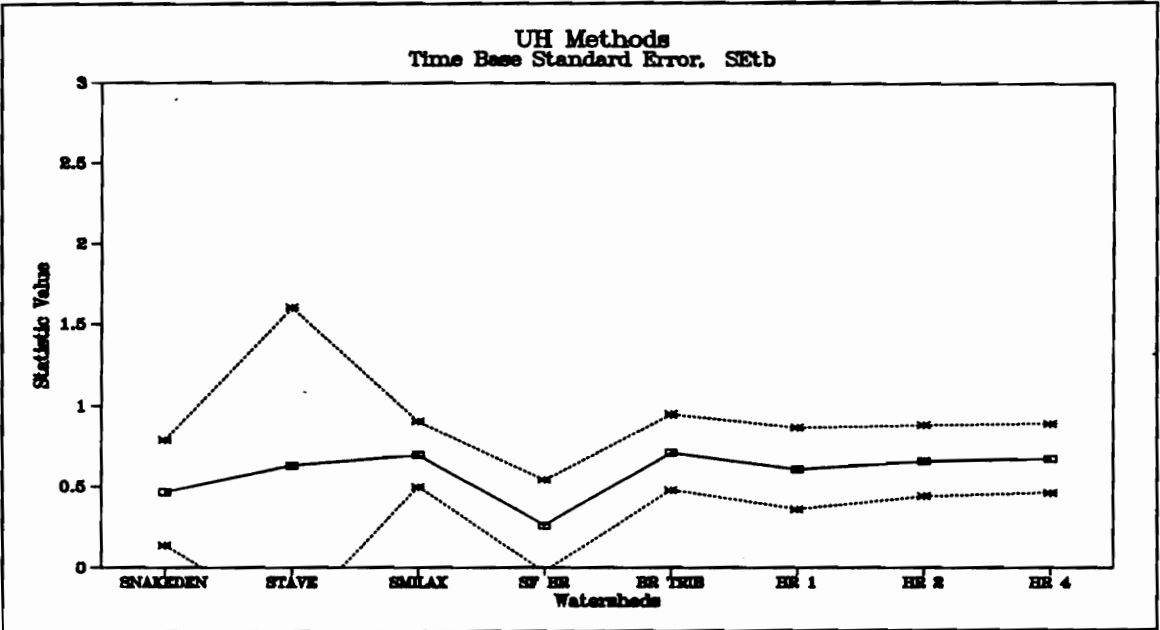


Figure C.33 - Time Base Standard Error for All Storms, Unit Hydrograph Models

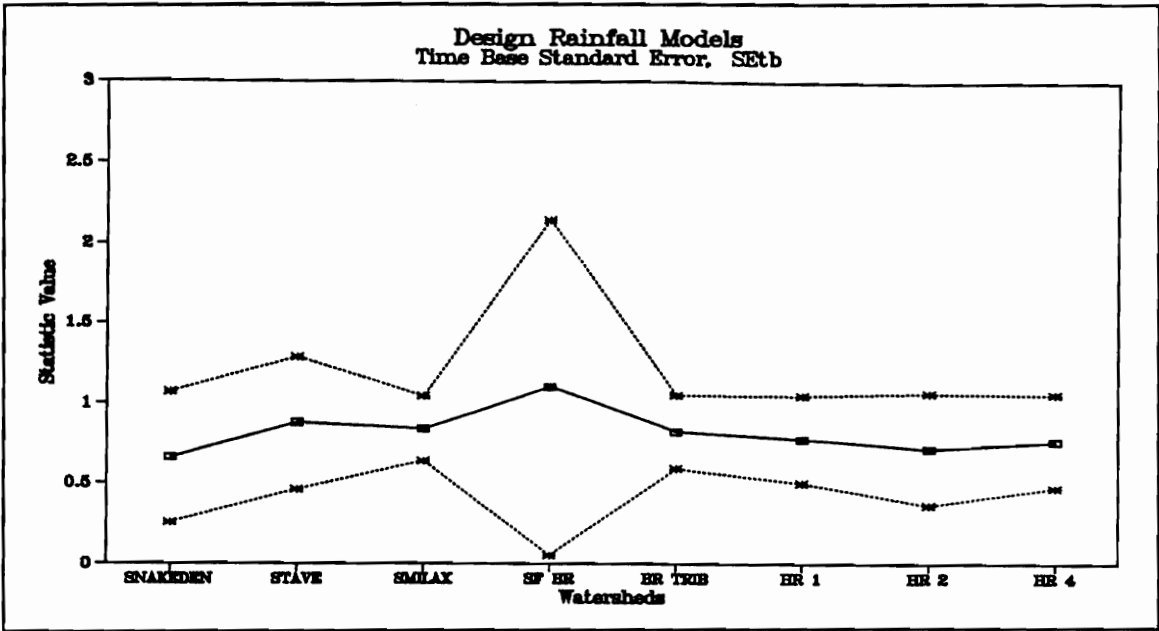


Figure C.34 - Time Base Standard Error for All Storms, Design Rainfall Models

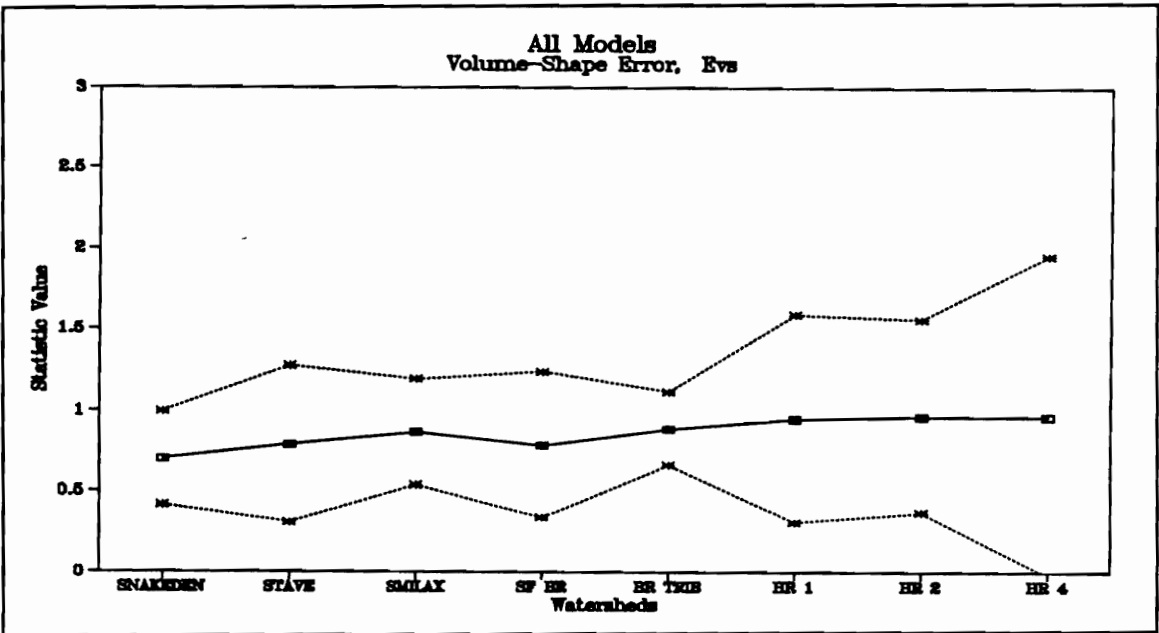


Figure C.35 - Volume-Shape Error for All Storms, All Models

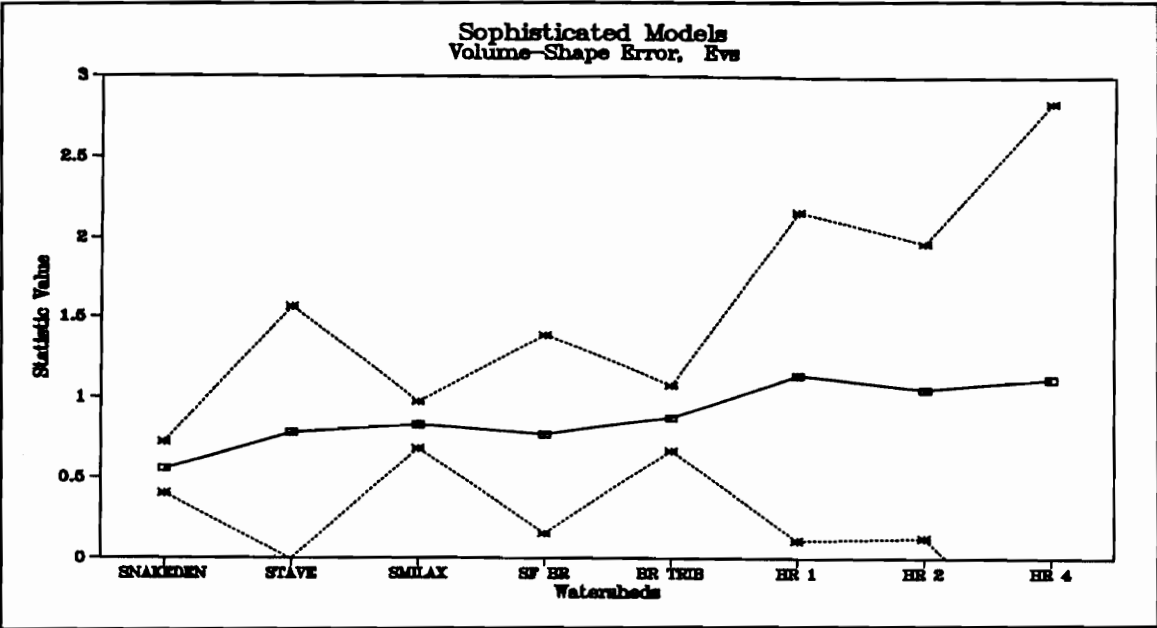


Figure C.36 - Volume-Shape Error for All Storms, Sophisticated Models

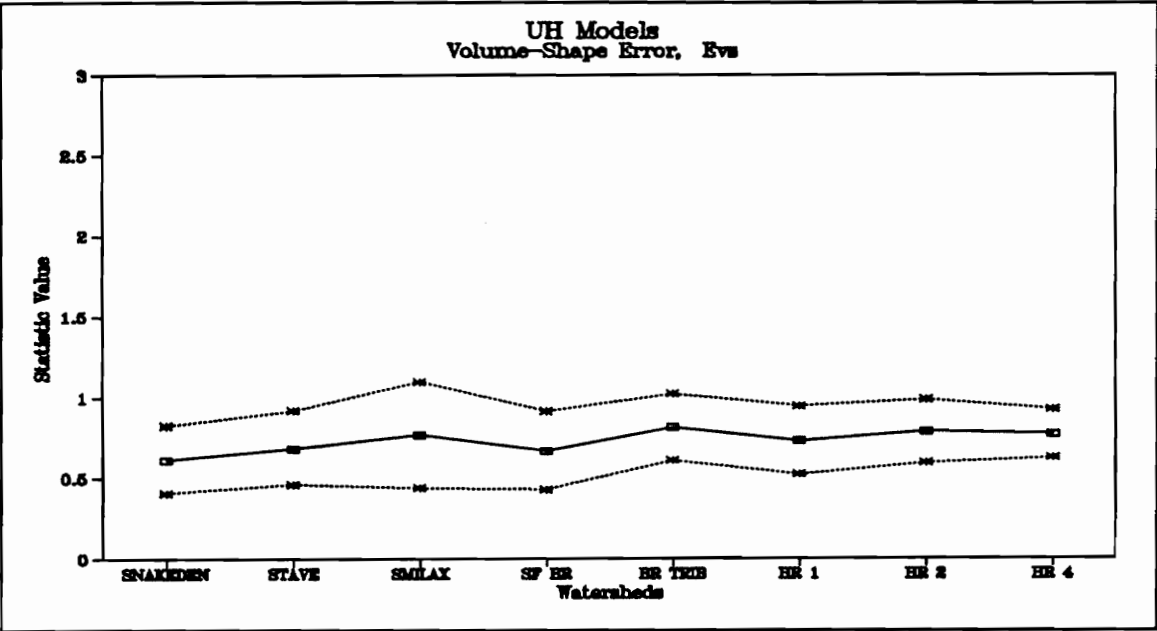


Figure C.37 - Volume-Shape Error for All Storms, Unit Hydrograph Models

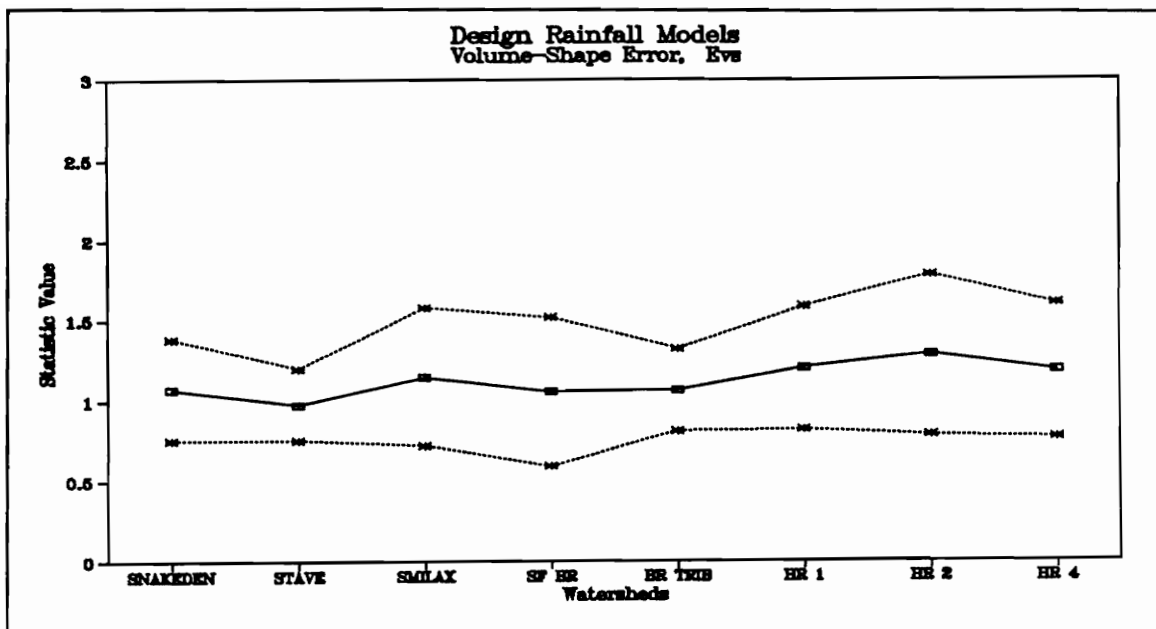


Figure C.38 - Volume-Shape Error for All Storms, Design Rainfall Models

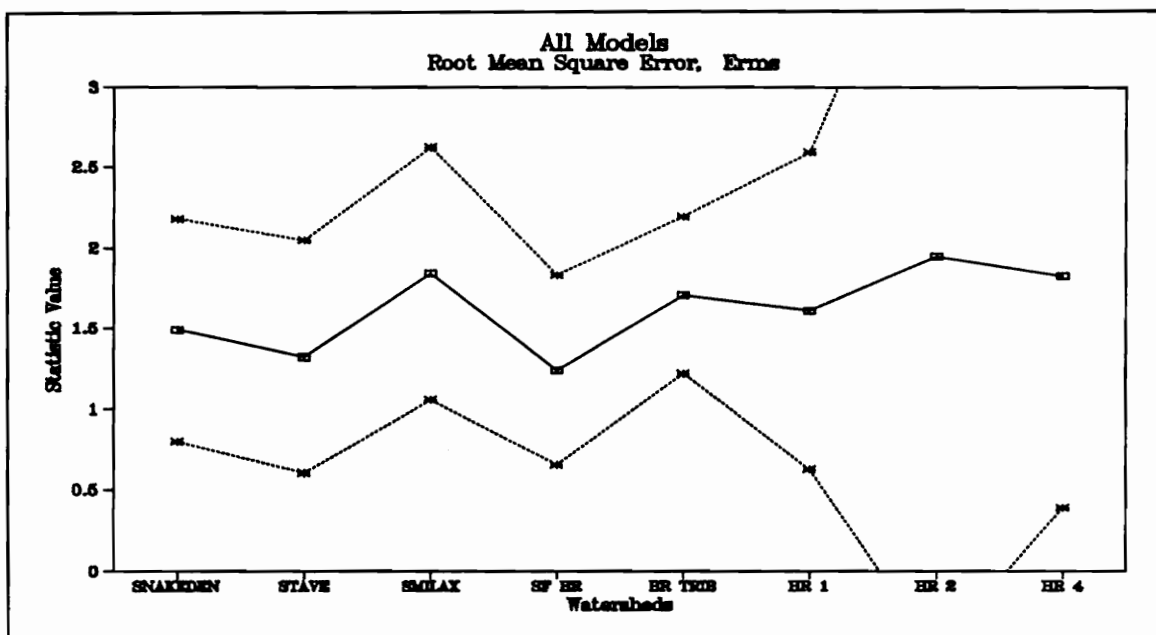


Figure C.39 - Root-Mean-Square Error for All Storms, All Models

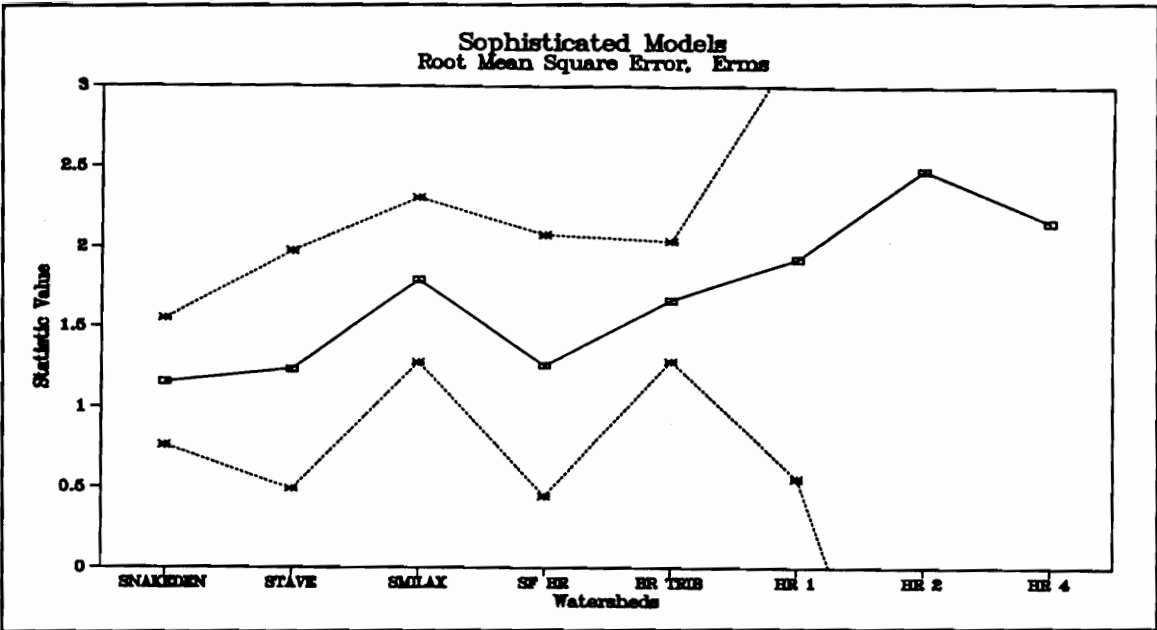


Figure C.40 - Root-Mean-Square Error for All Storms, Sophisticated Models

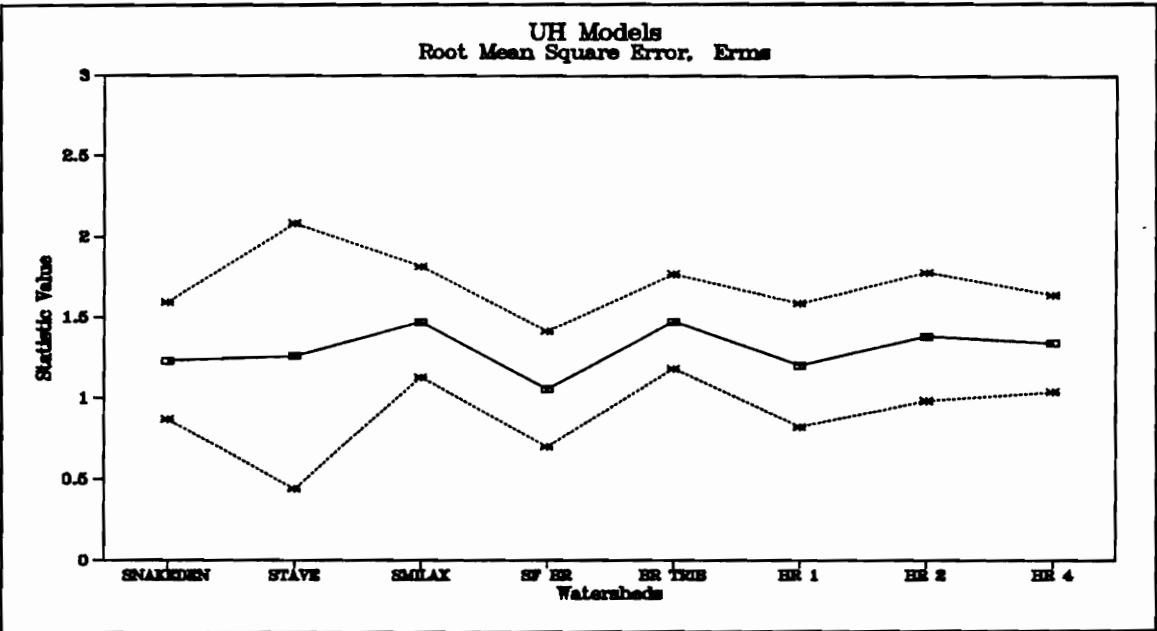


Figure C.41 - Root-Mean-Square Error for All Storms, Unit Hydrograph Models

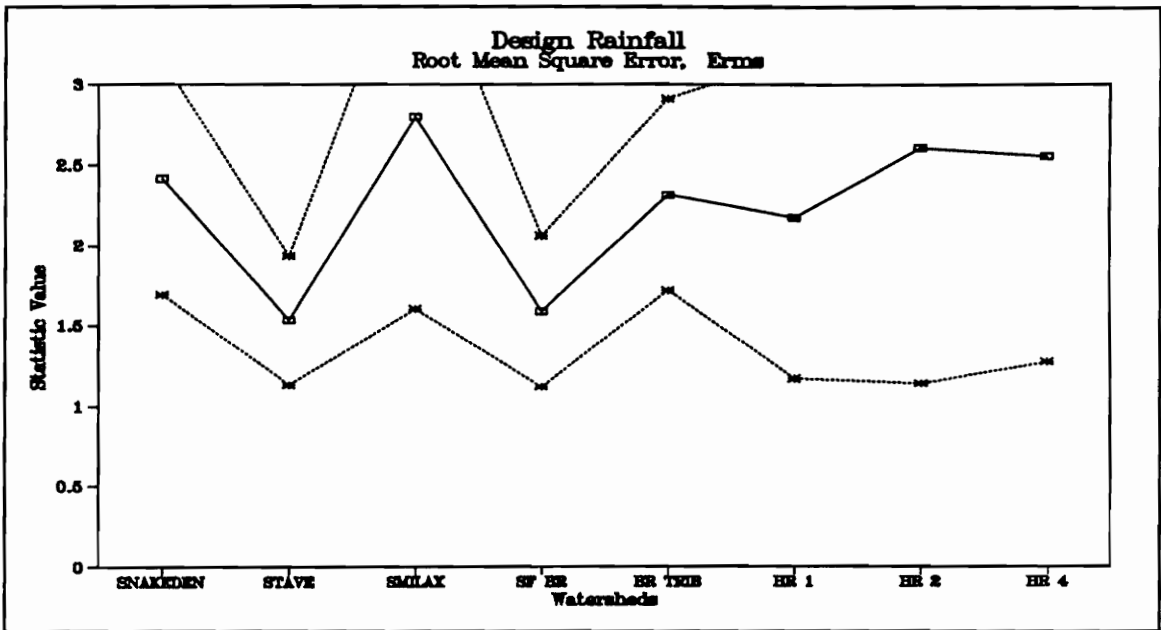


Figure C.42 - Root-Mean-Square Error for All Storms, Design Rainfall Models

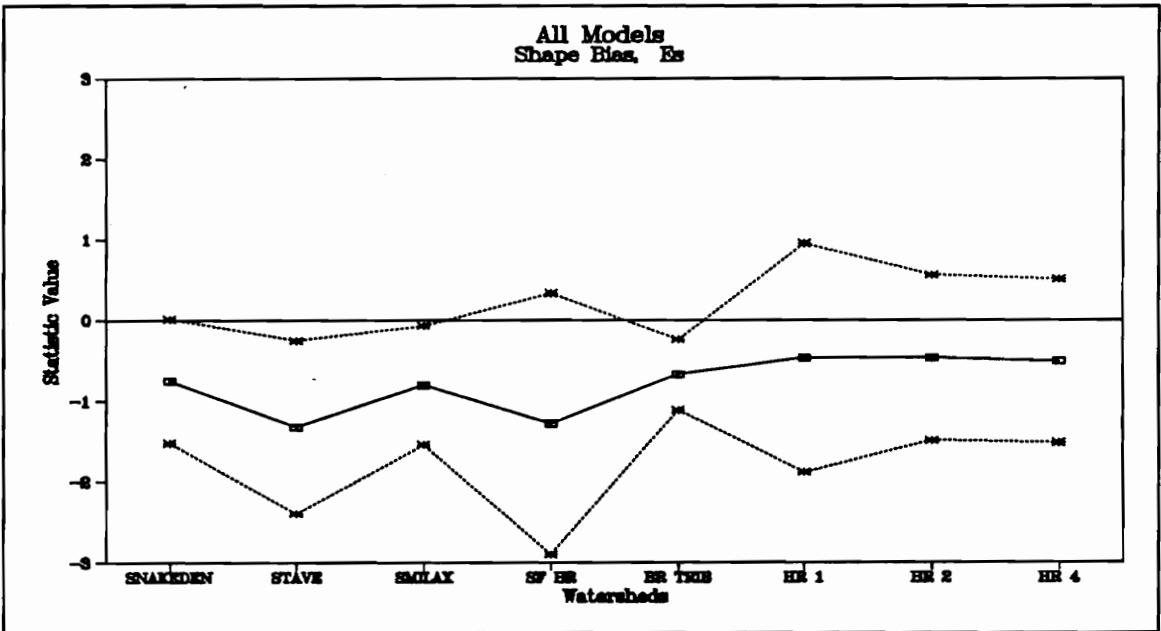


Figure C.43 - Shape Bias for All Storms, All Models

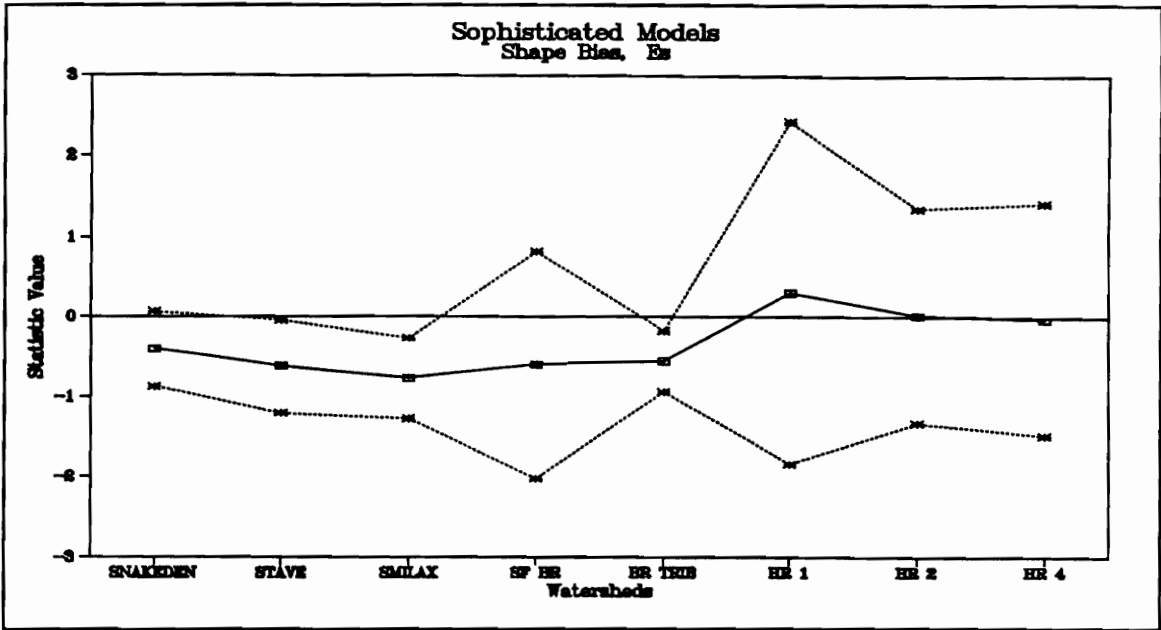


Figure C.44 - Shape Bias for All Storms, Sophisticated Models

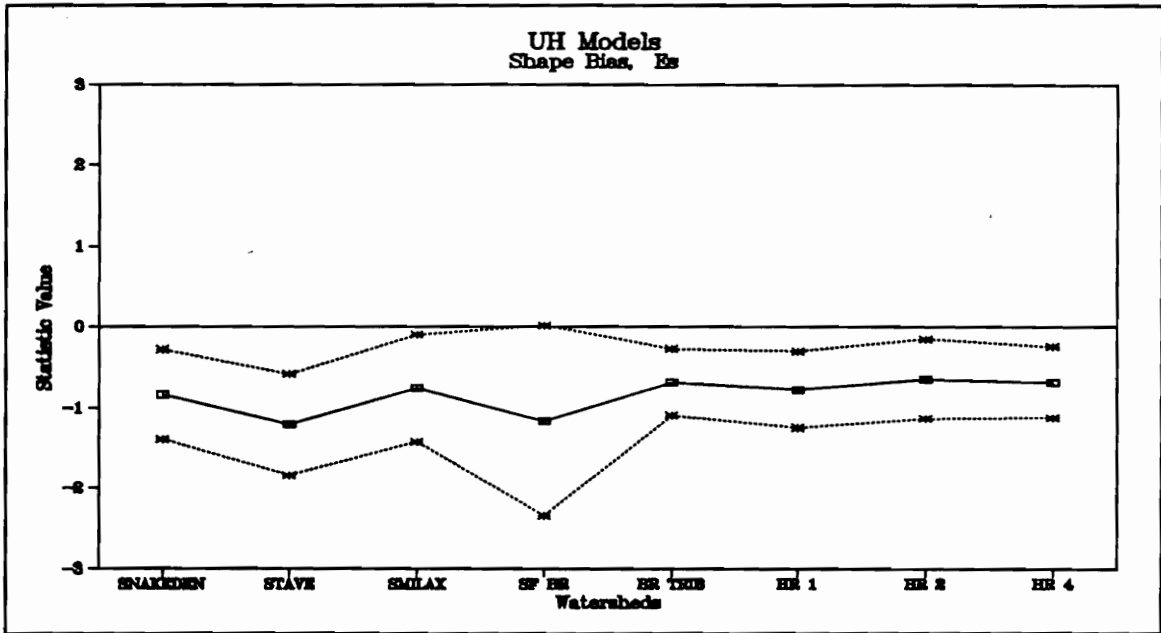


Figure C.45 - Shape Bias for All Storms, Unit Hydrograph Models

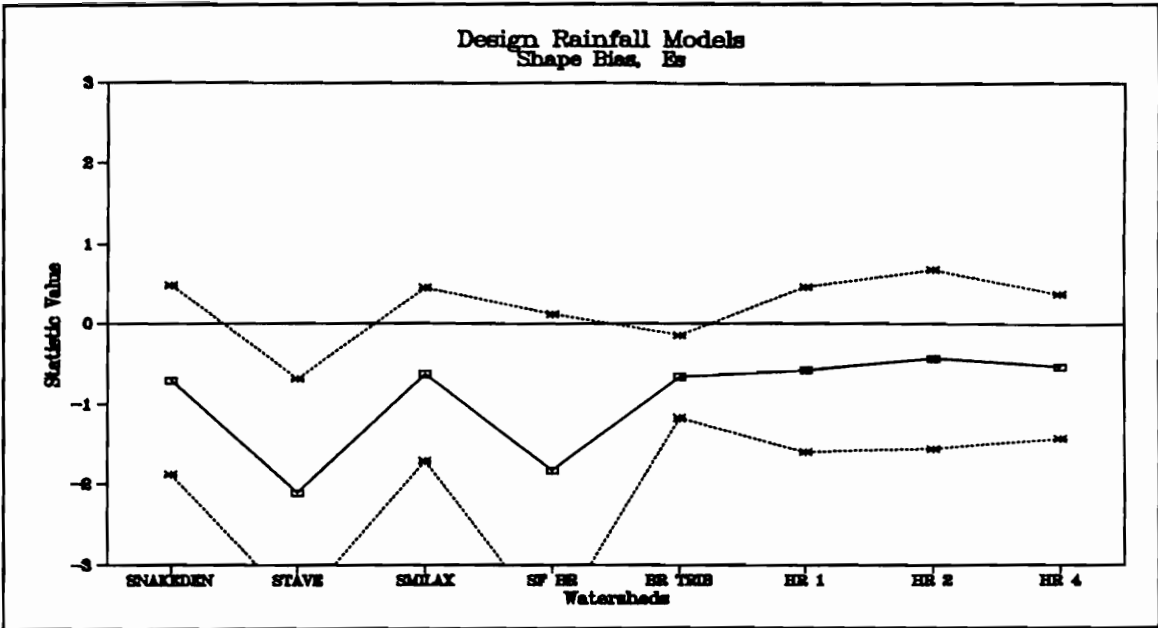


Figure C.46 - Shape Bias for All Storms, Design Rainfall Models

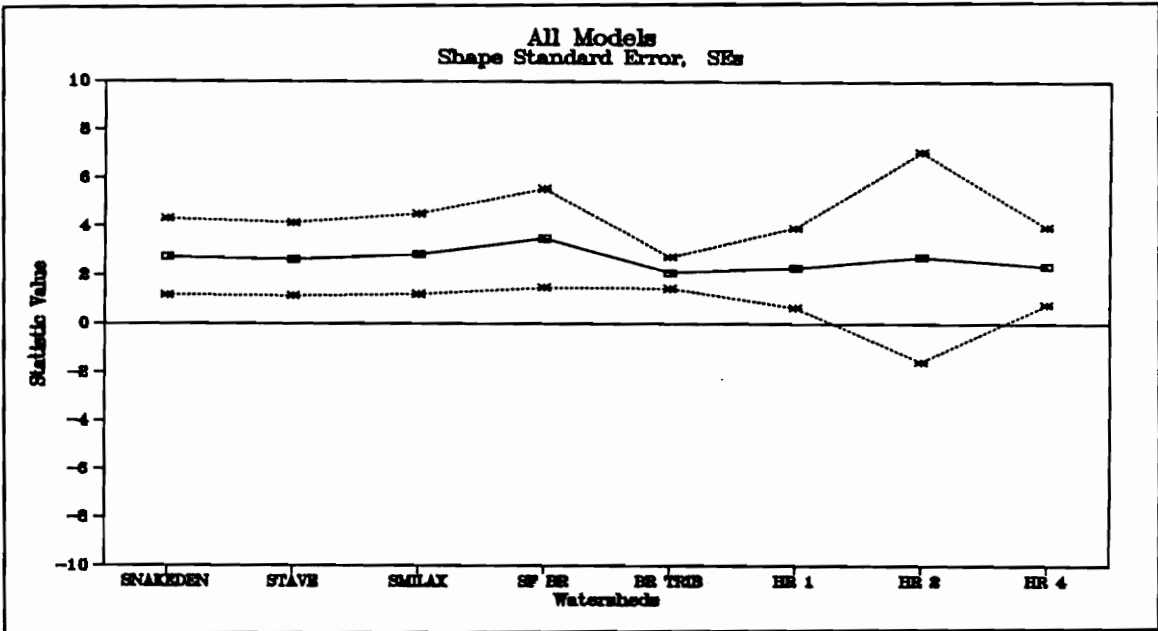


Figure C.47 - Shape Standard Error for All Storms, All Models

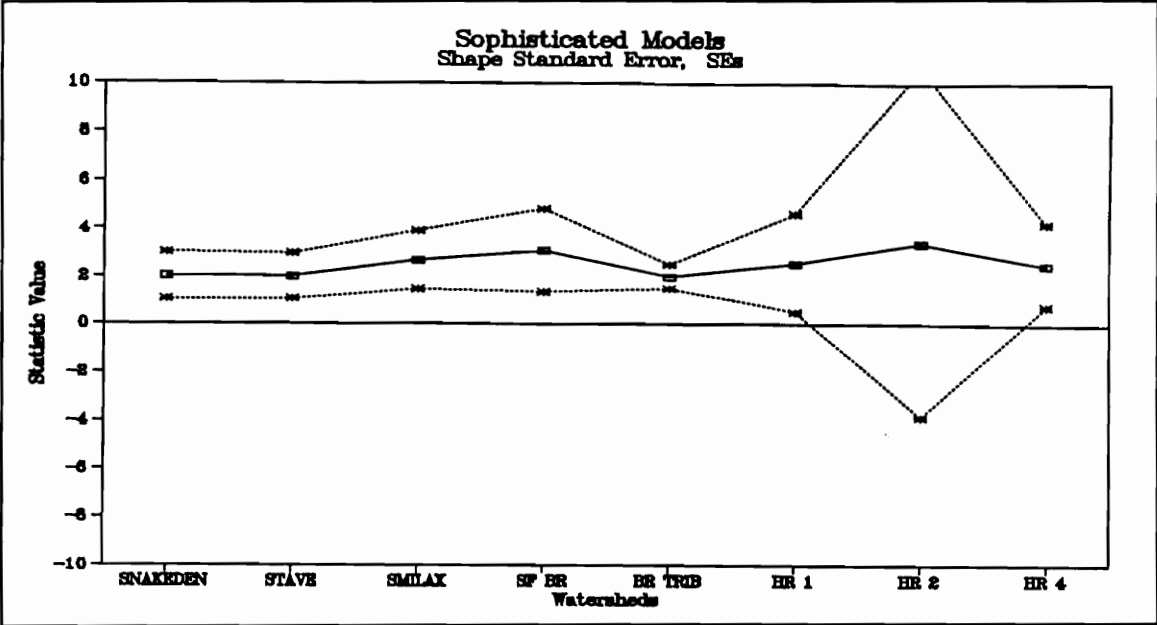


Figure C.48 - Shape Standard Error for All Storms, Sophisticated Models

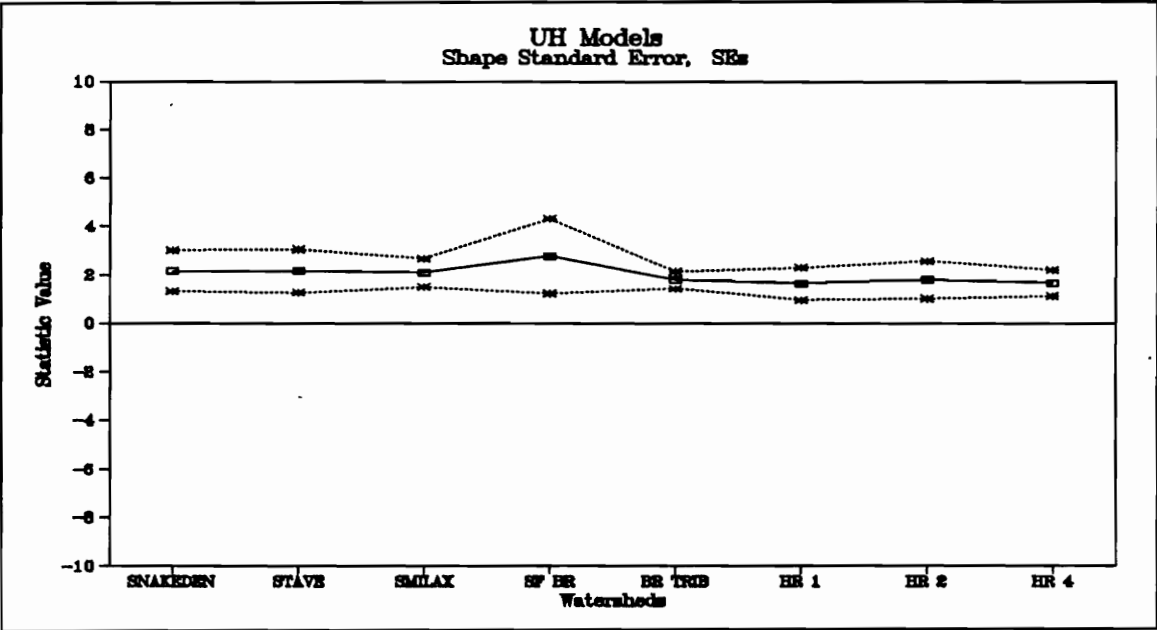


Figure C.49 - Shape Standard Error for All Storms, Unit Hydrograph Models

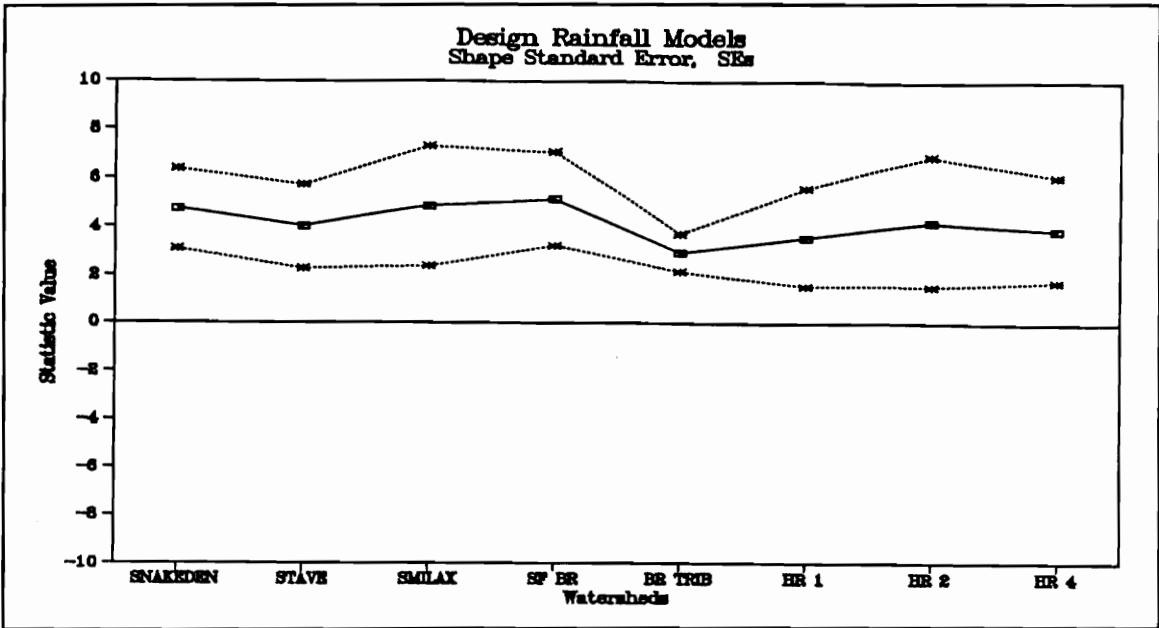


Figure C.50 - Shape Standard Error for All Storms, Design Rainfall Models

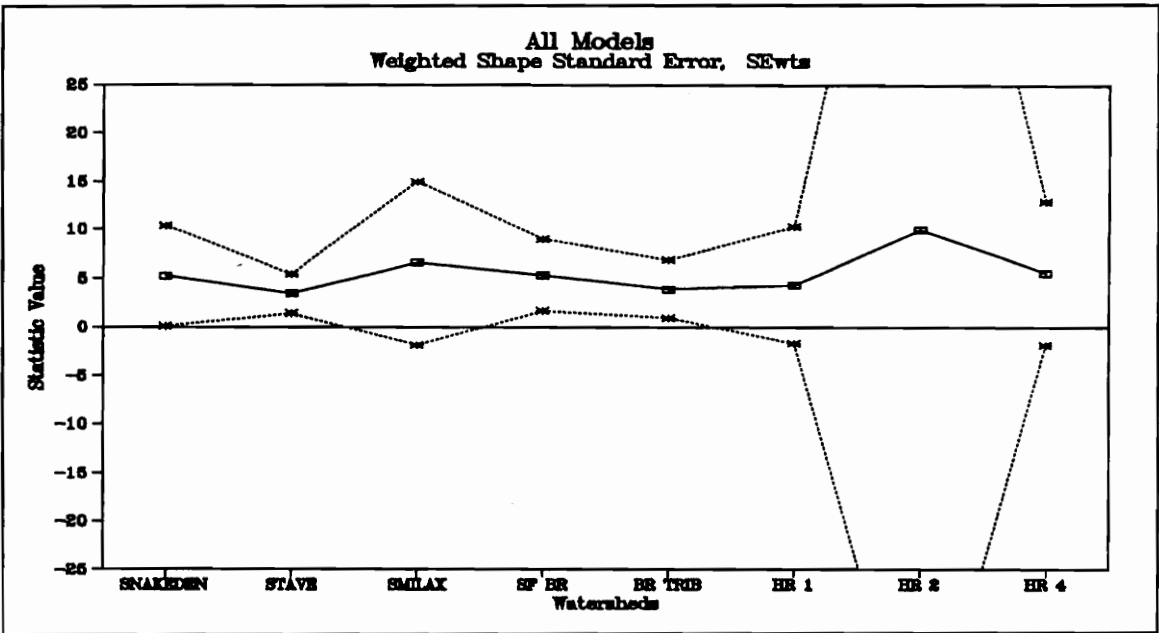


Figure C.51 - Weighted Shape Standard Error for All Storms, All Models

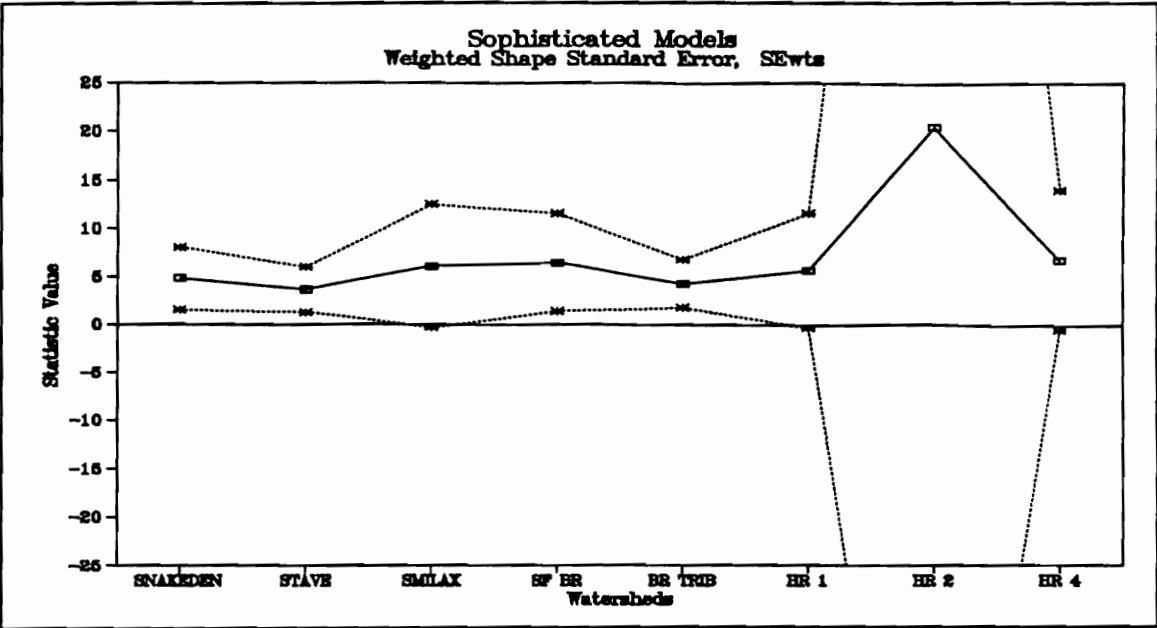


Figure C.52 - Weighted Shape Standard Error for All Storms, Sophisticated Models

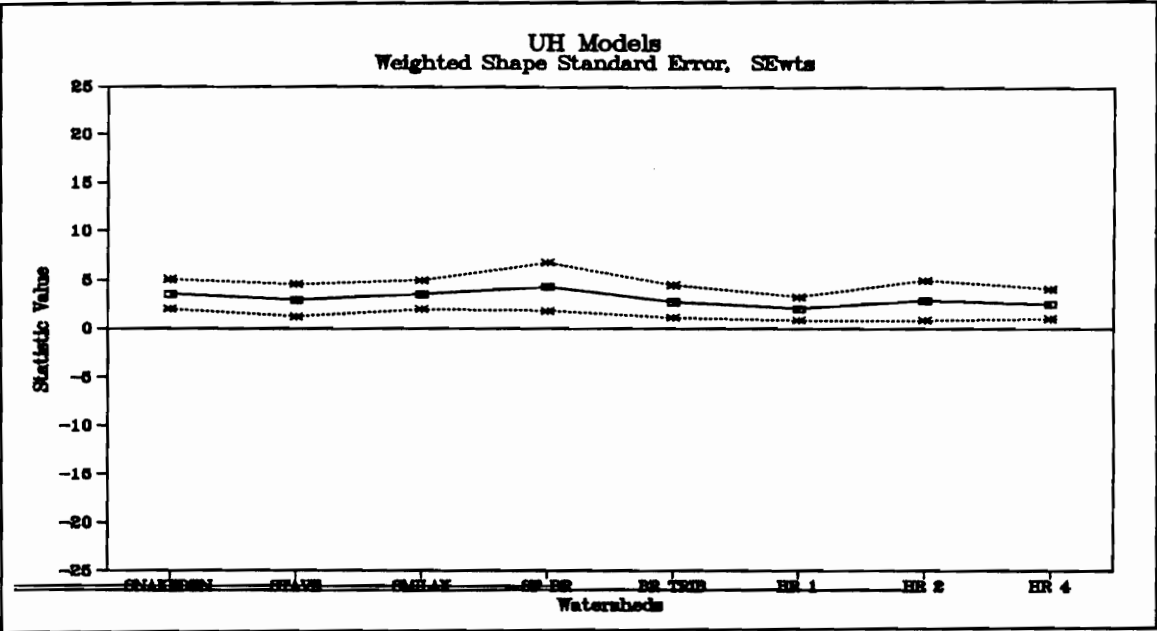


Figure C.53 - Weighted Shape Standard Error for All Storms, Unit Hydrograph Models

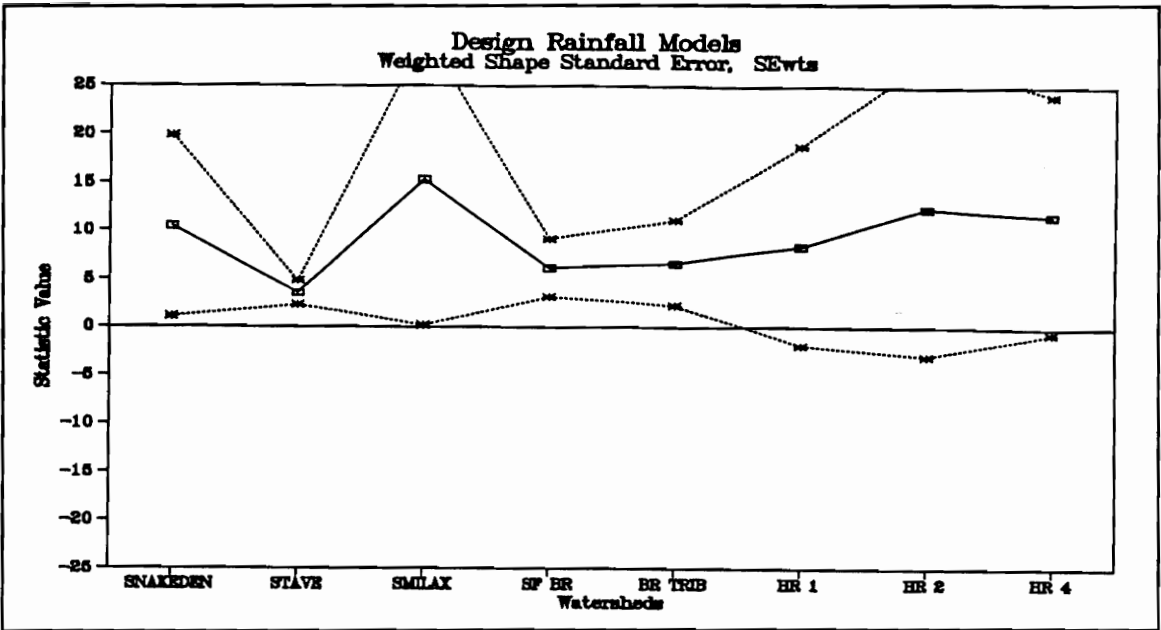


Figure C.54 - Weighted Shape Standard Error for All Storms, Design Rainfall Models

Appendix D

Model Comparison Graphs

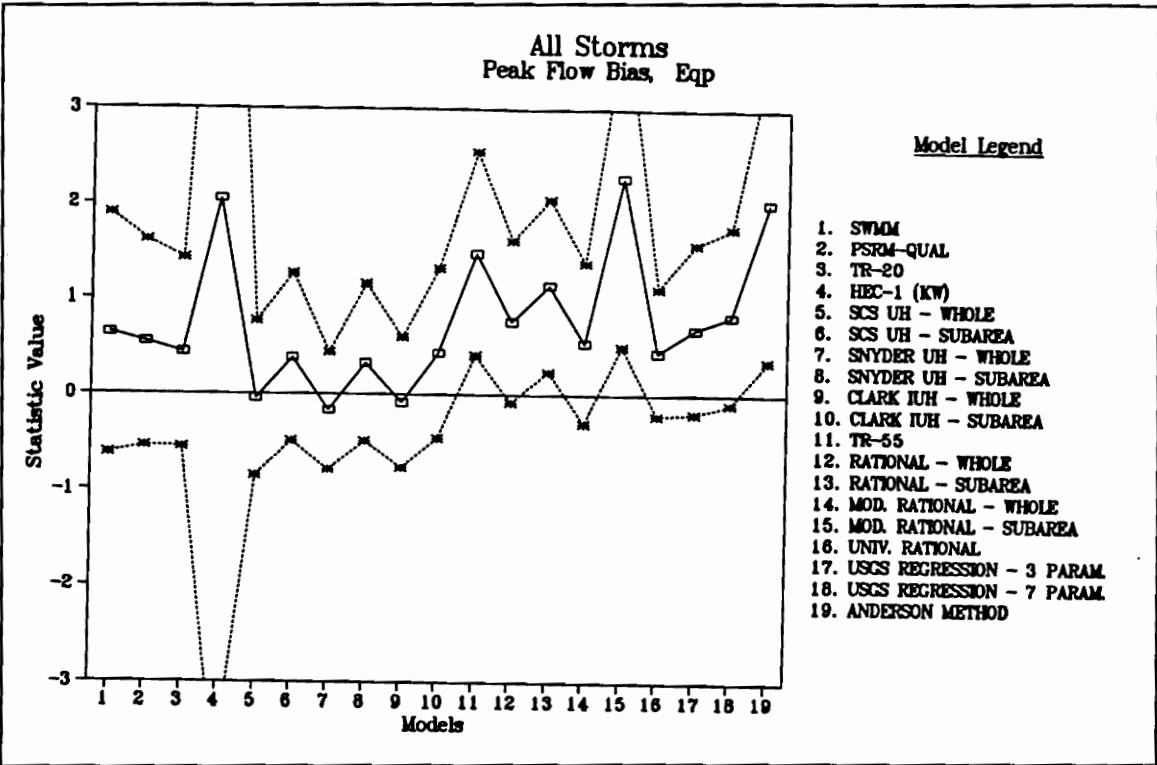


Figure D.1 - Peak Flow Bias for all models, all storms

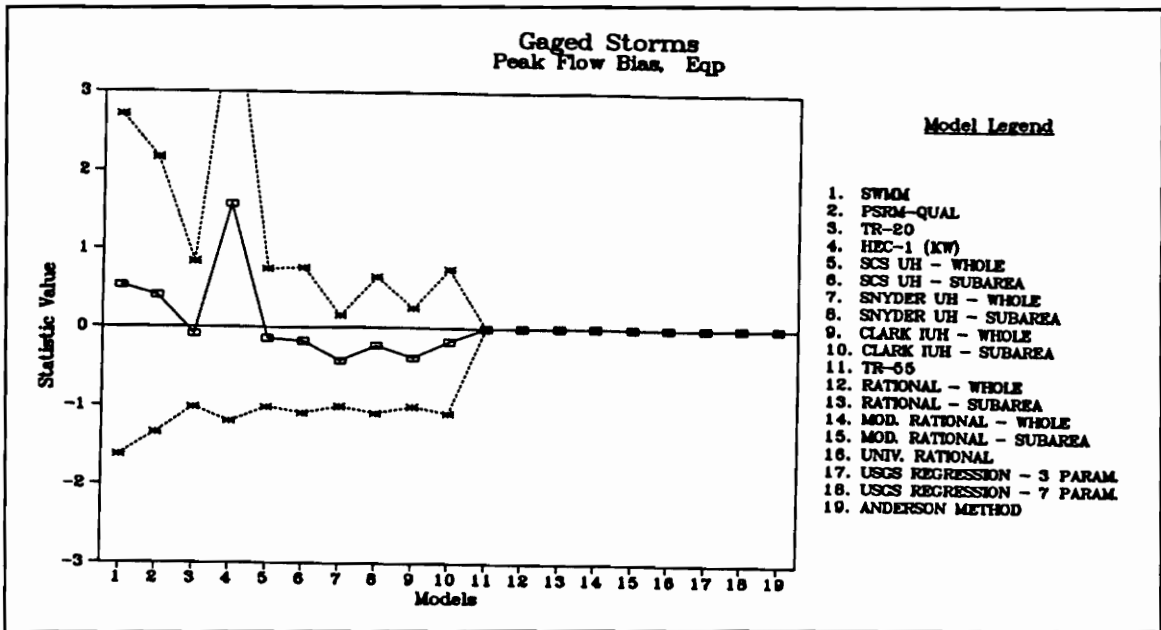


Figure D.2 - Peak Flow Bias for All Models, Gaged Storms

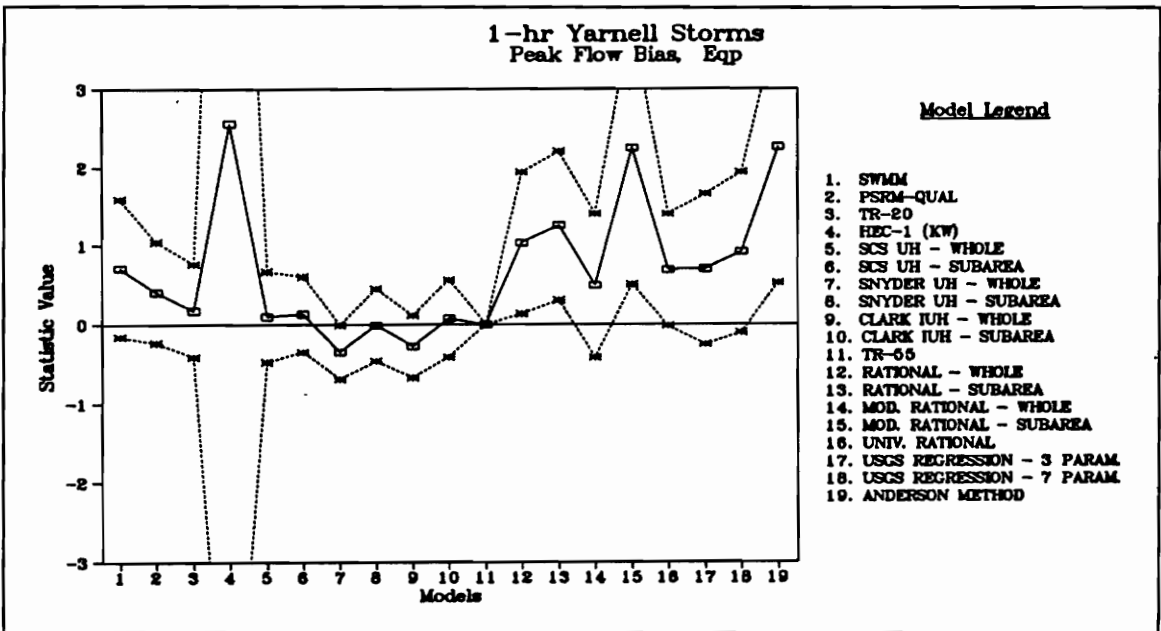


Figure D.3 - Peak Flow Bias for All Models, 1-hr Yarnell Storms

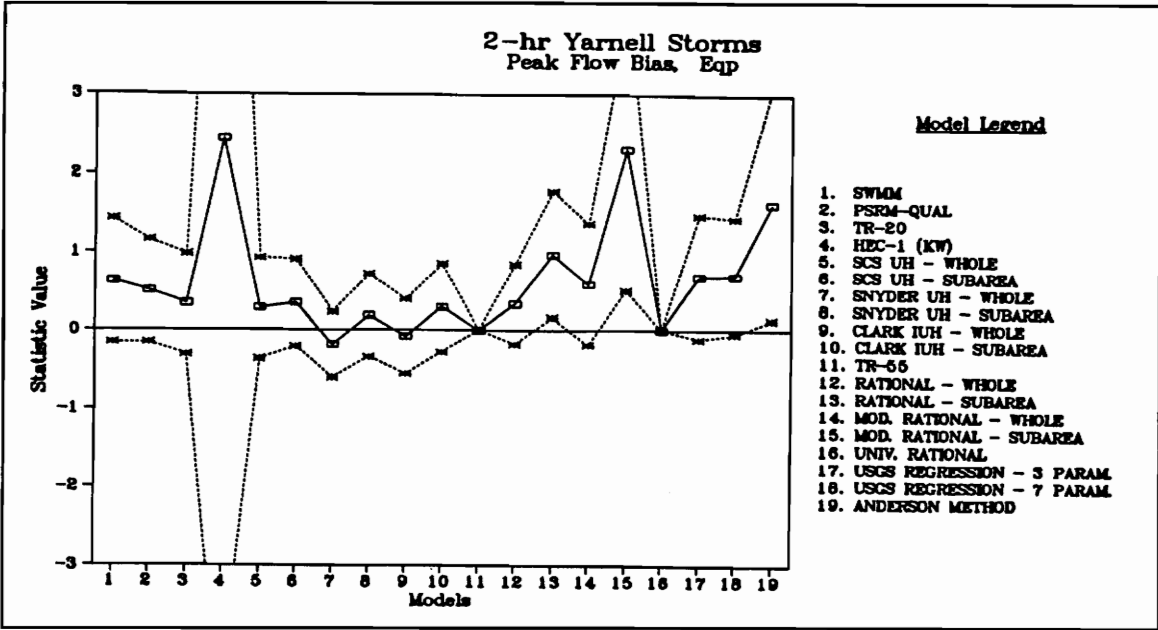


Figure D.4 - Peak Flow Bias for All Models, 2-hr Yarnell Storms

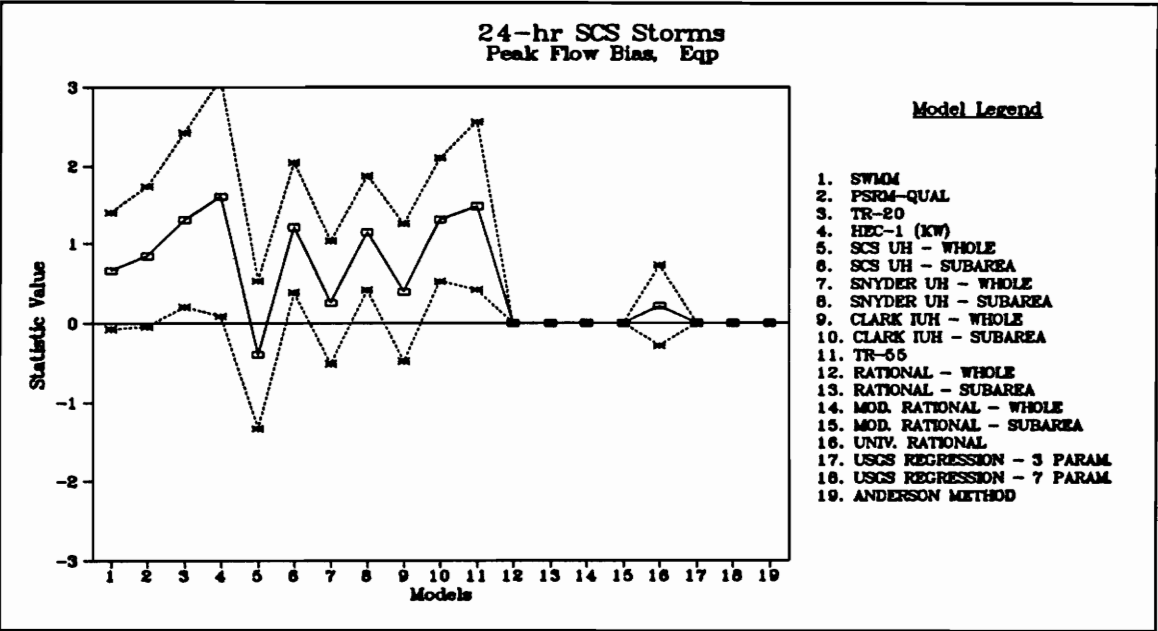


Figure D.5 - Peak Flow Bias for All Models, 24-hr SCS Storms

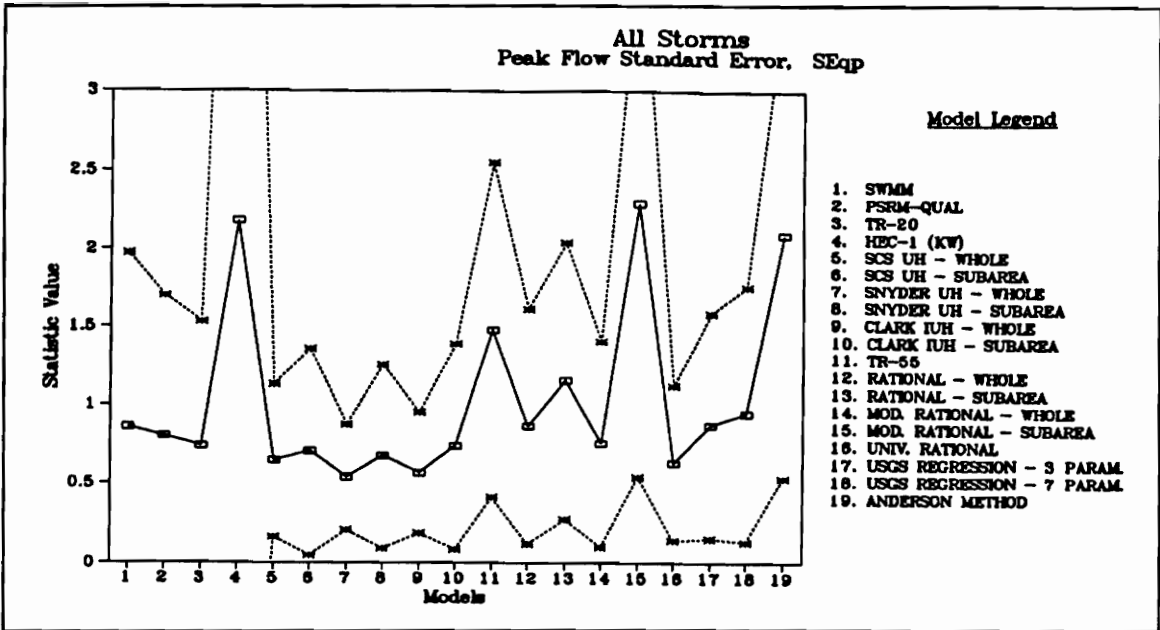


Figure D.6 - Peak Flow Standard Error for All Models, All Storms

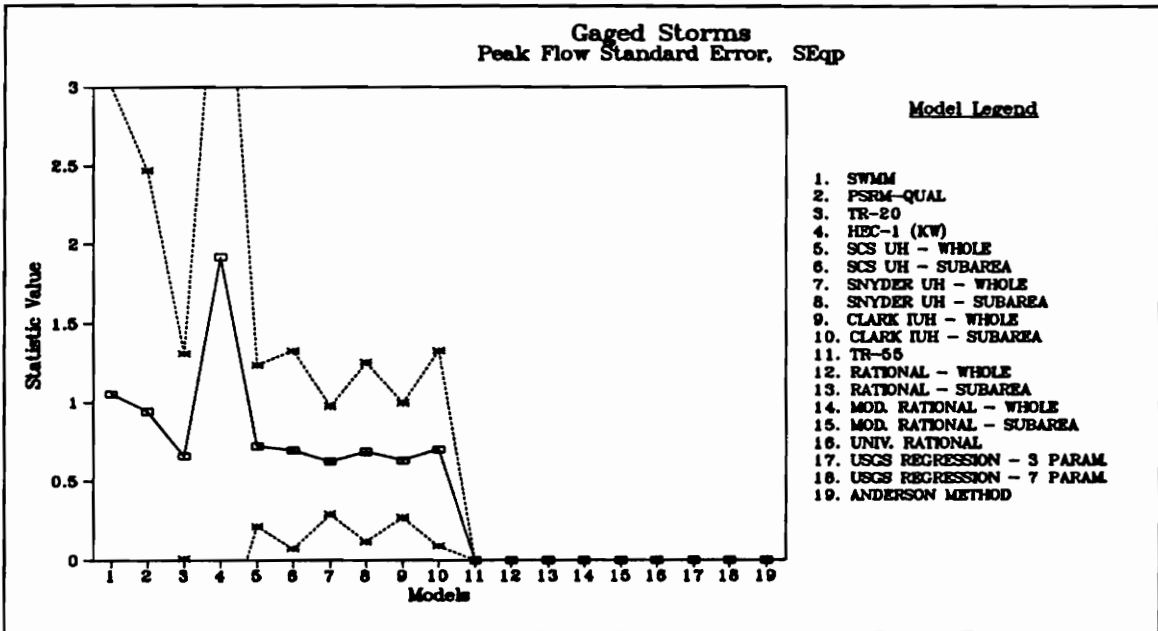


Figure D.7 - Peak Flow Standard Error for All Models, Gaged Storms

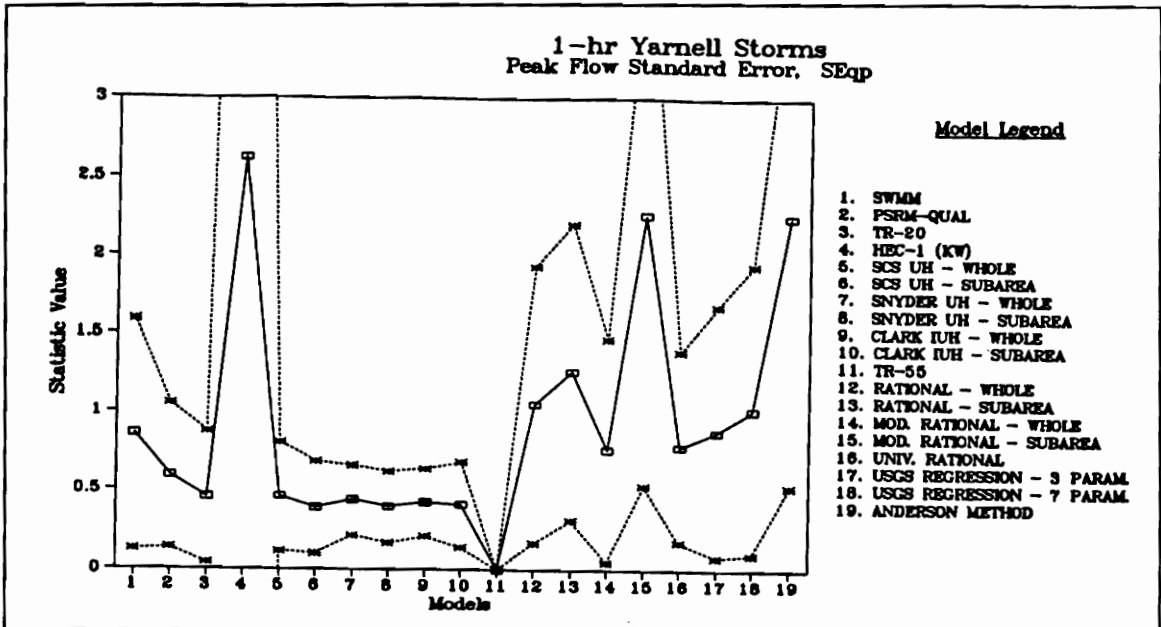


Figure D.8 - Peak Flow Standard Error for All Models, 1-hr Yarnell Storms

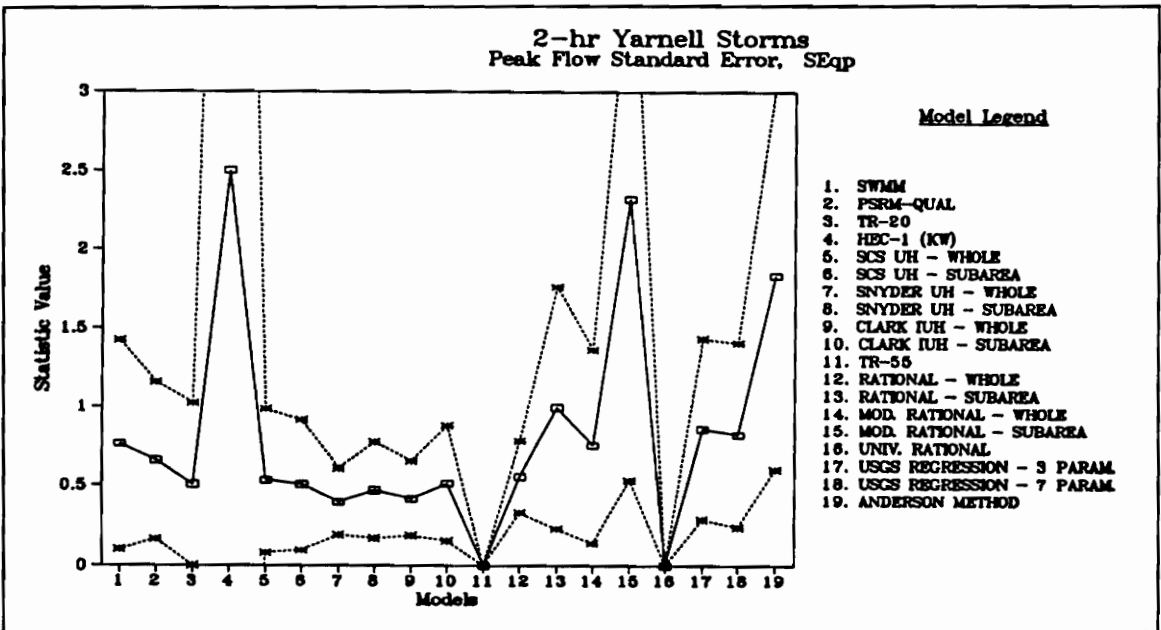


Figure D.9 - Peak Flow Standard Error for All Models, 2-hr Yarnell Storms

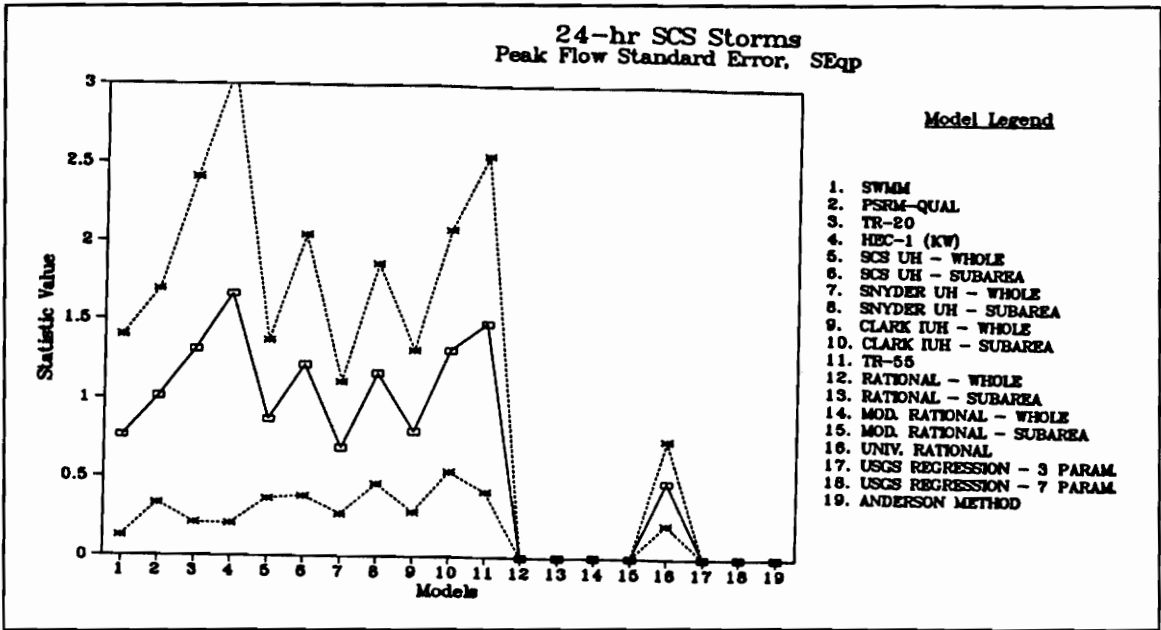


Figure D.10 - Peak Flow Standard Error for All Models, 24-hr SCS Storms

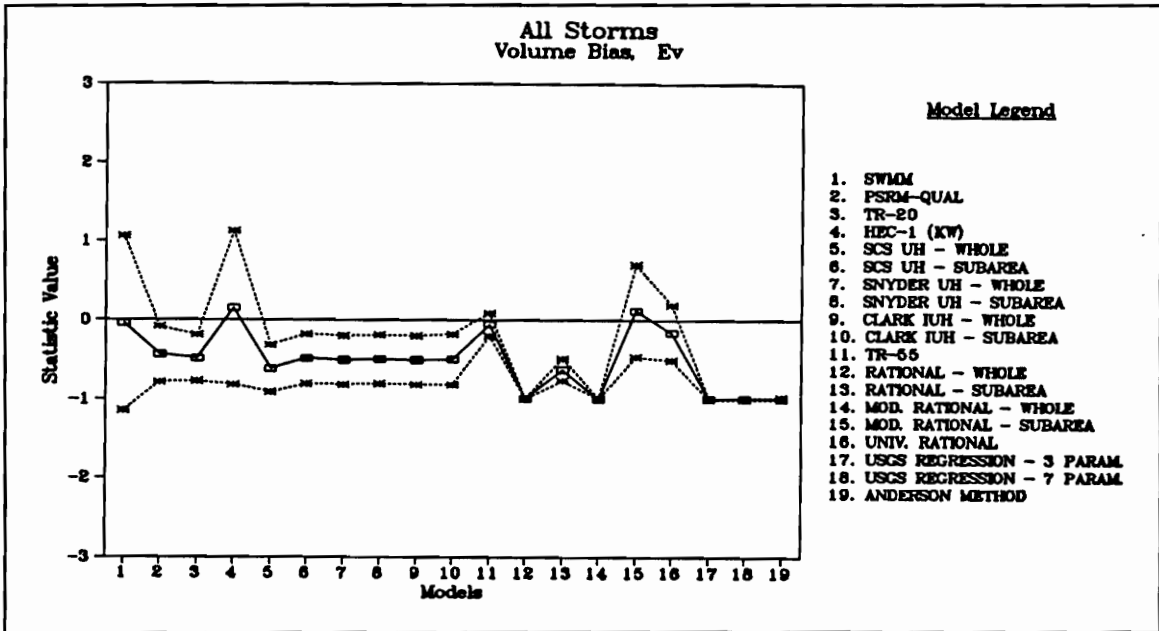


Figure D.11 - Volume Bias for All Models, All Storms

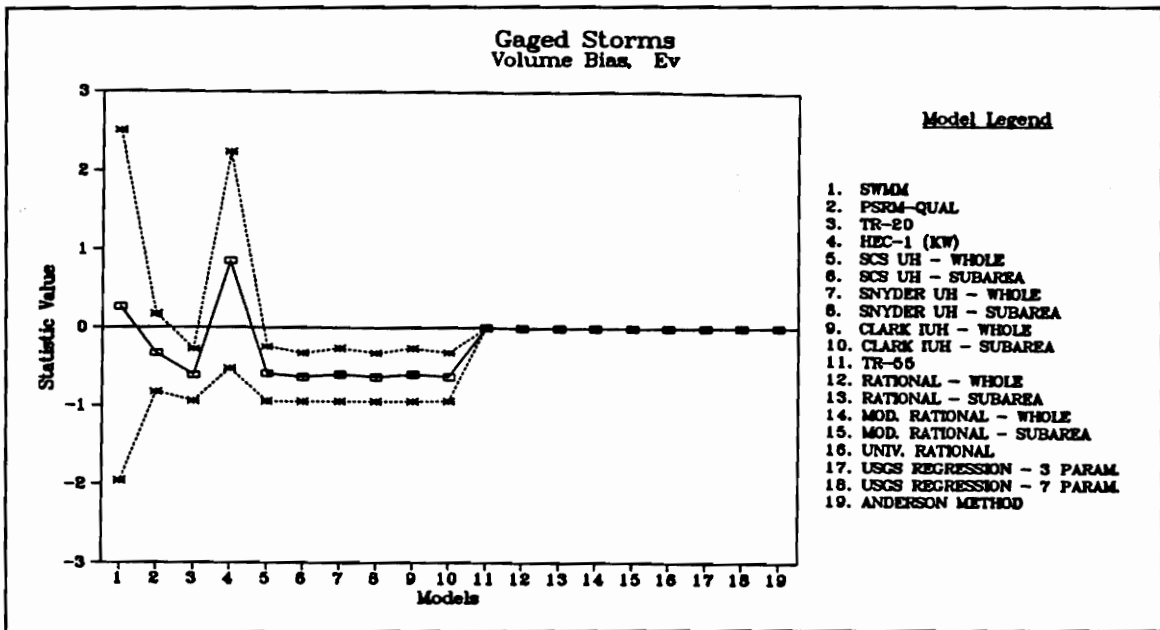


Figure D.12 - Volume Bias for All Models, Gaged Storms

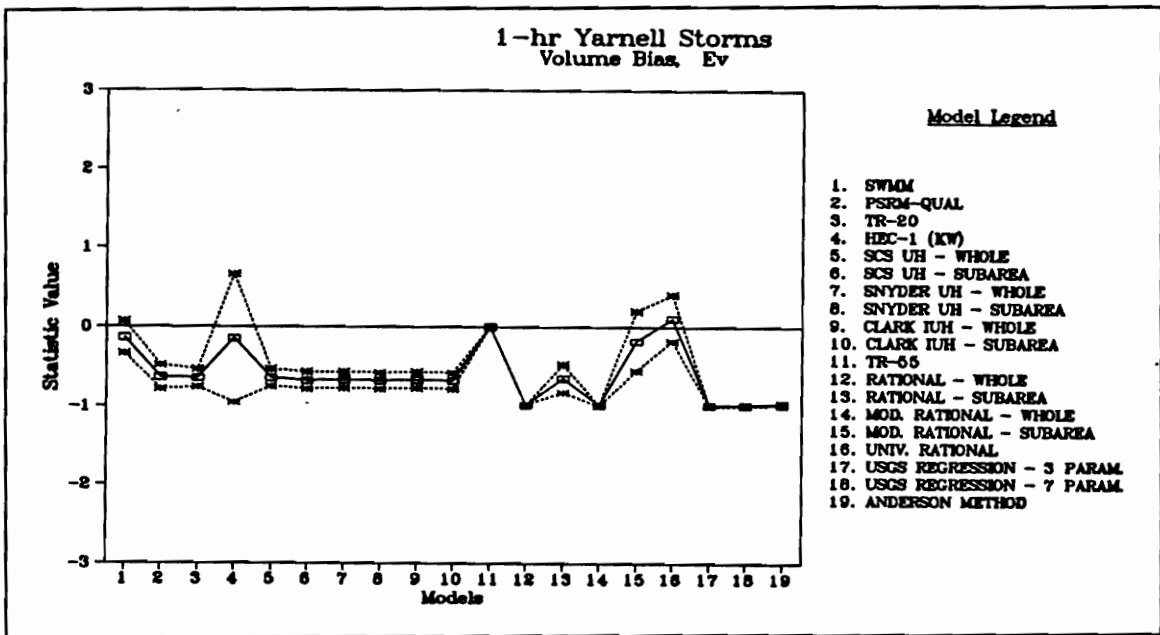


Figure D.13 - Volume Bias for All Models, 1-hr Yarnell Storms

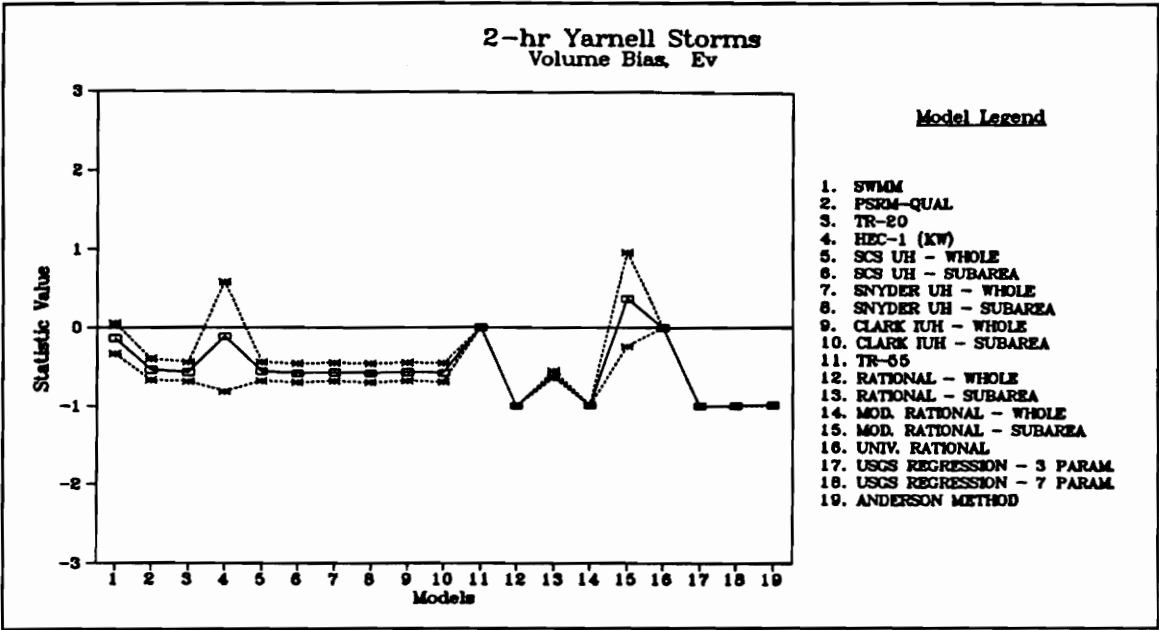


Figure D.14 - Volume Bias for All Models, 2-hr Yarnell Storms

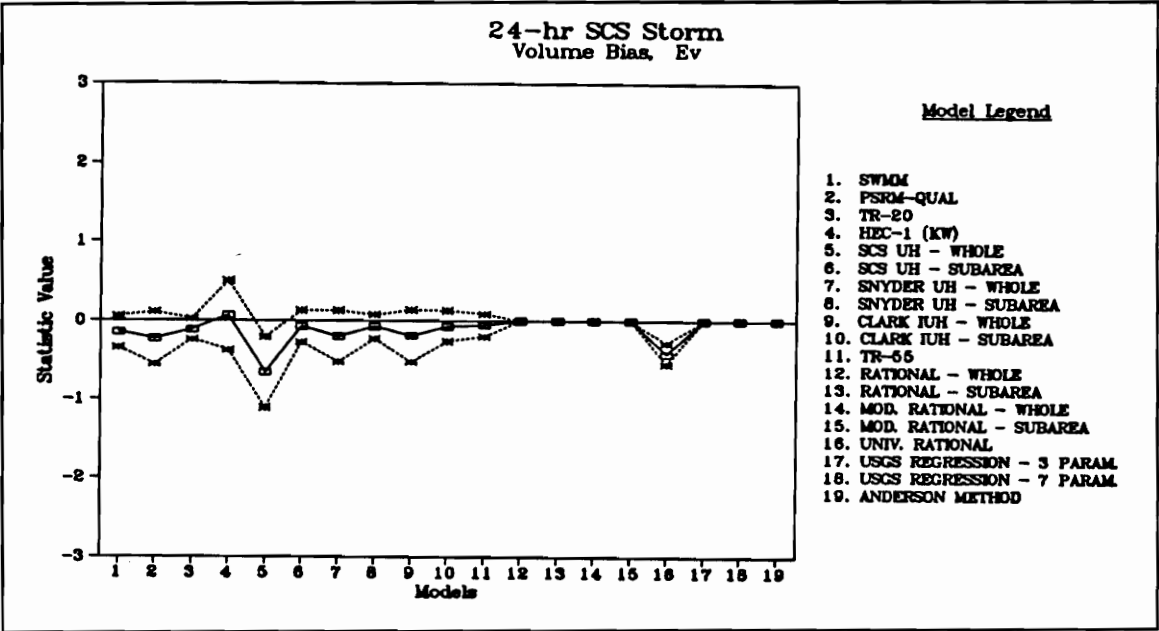


Figure D.15 - Volume Bias for All Models, 24-hr SCS Storms

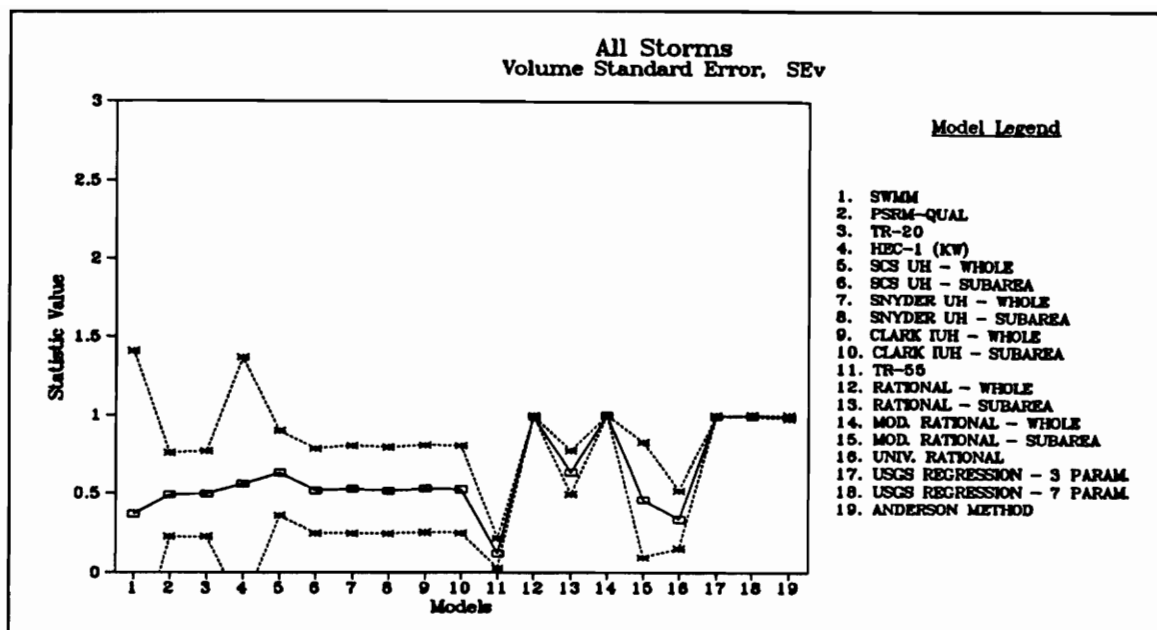


Figure D.16 - Volume Standard Error for All Models, All Storms

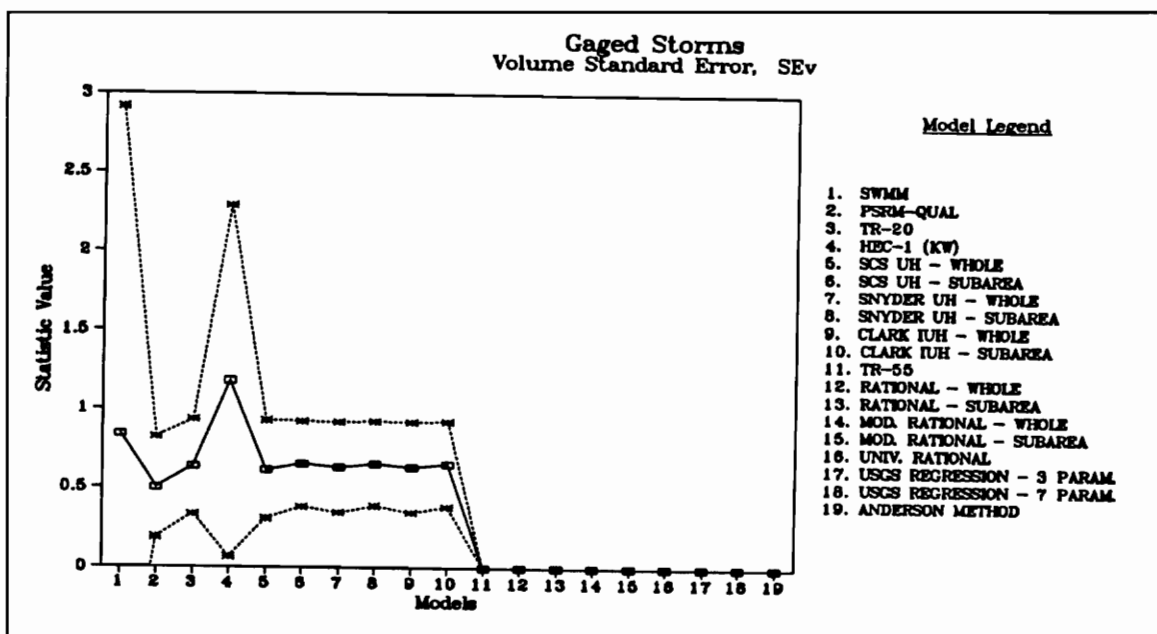


Figure D.17 - Volume Standard Error for All Models, Gaged Storms

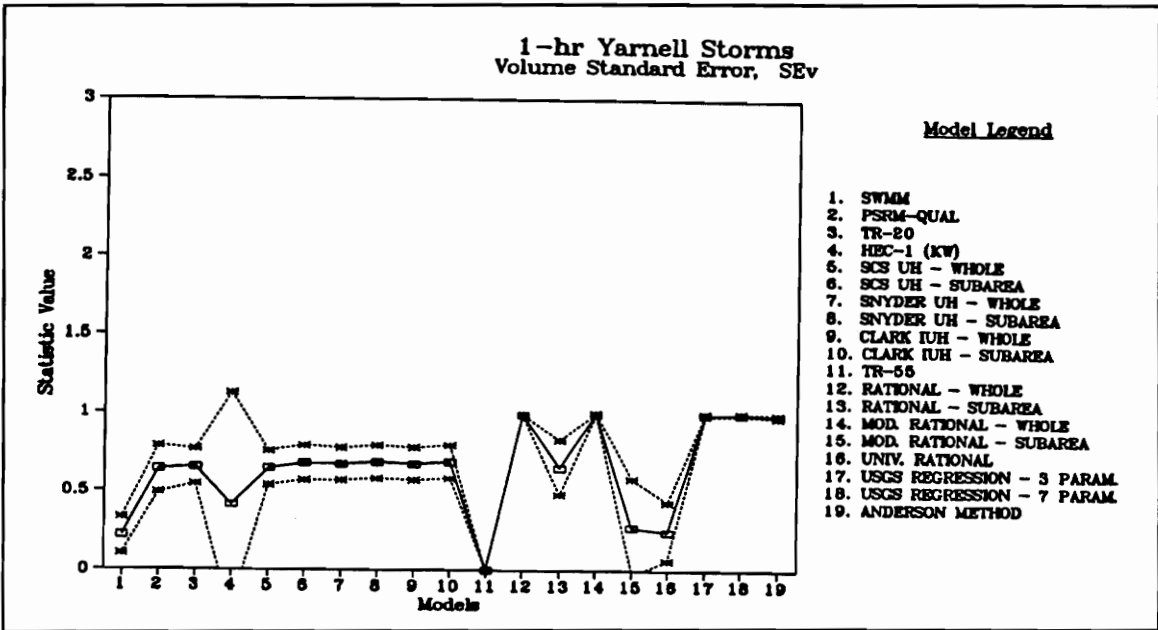


Figure D.18 - Volume Standard Error for All Models, 1-hr Yarnell Storms

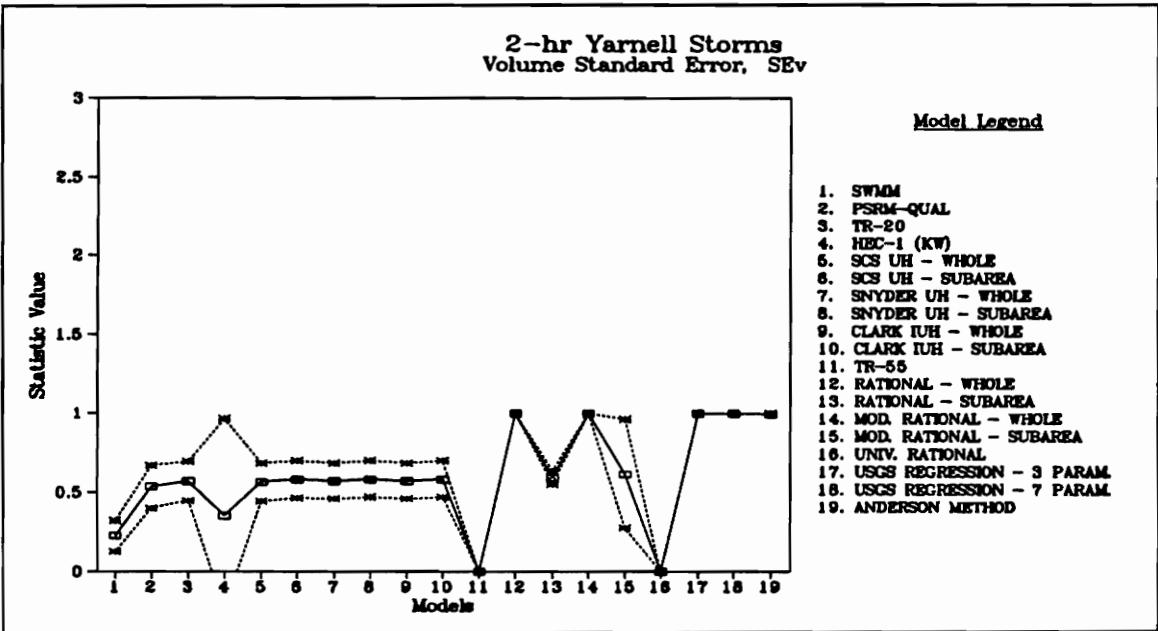


Figure D.19 - Volume Standard Error for All Models, 2-hr Yarnell Storms

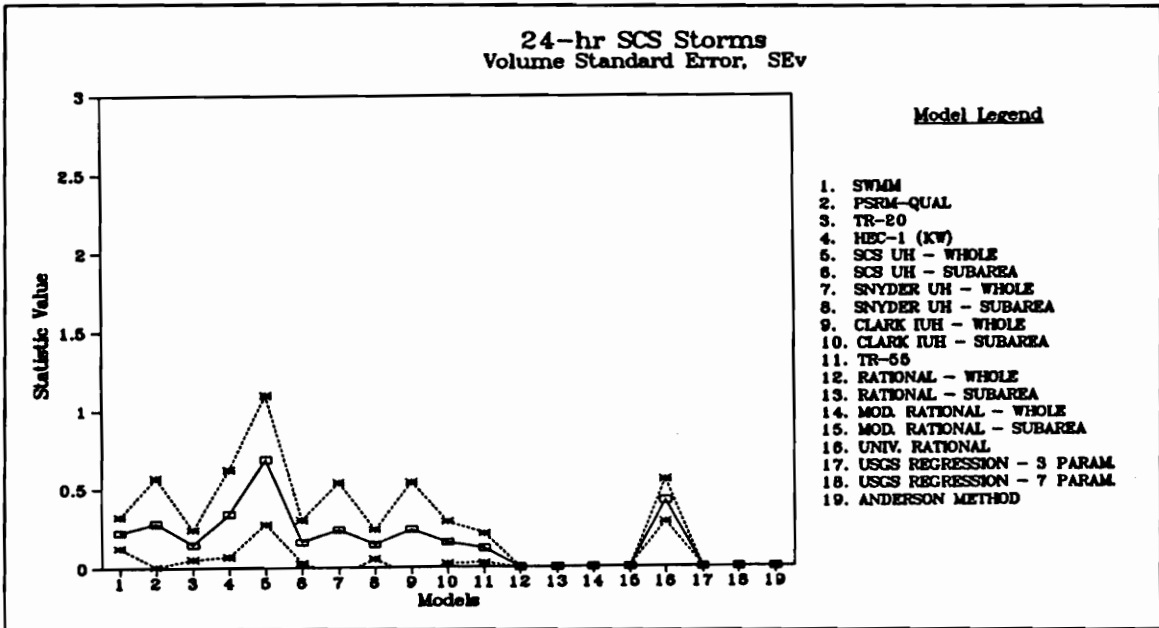


Figure D.20 - Volume Standard Error for All Models, 24-hr SCS Storms

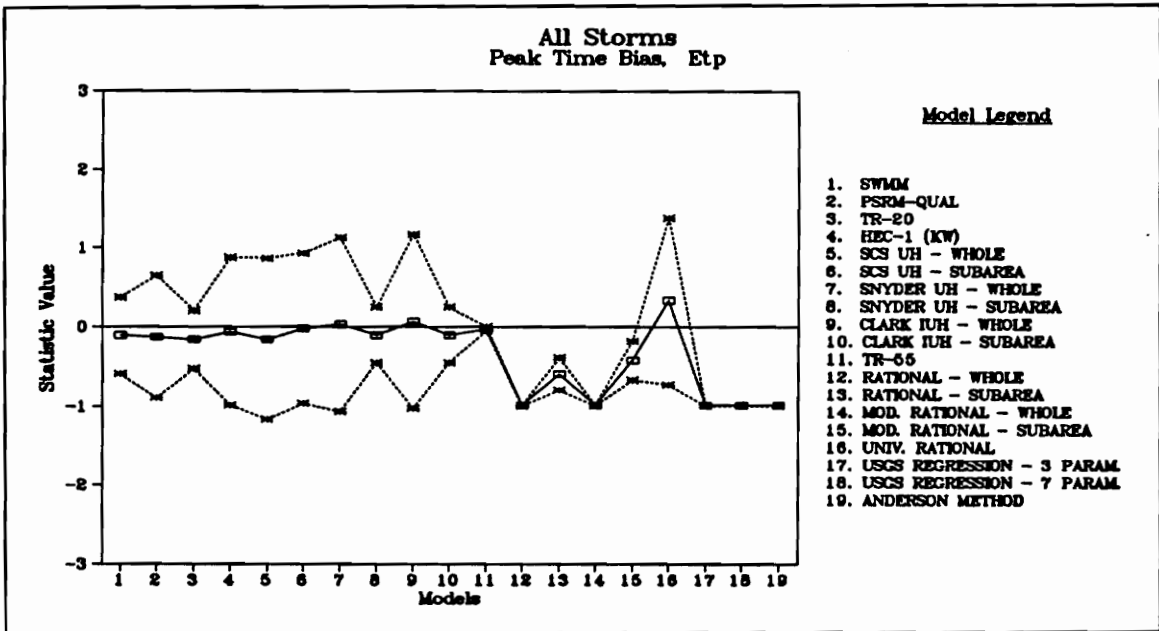


Figure D.21 - Time to Peak Bias for All Models, All Storms

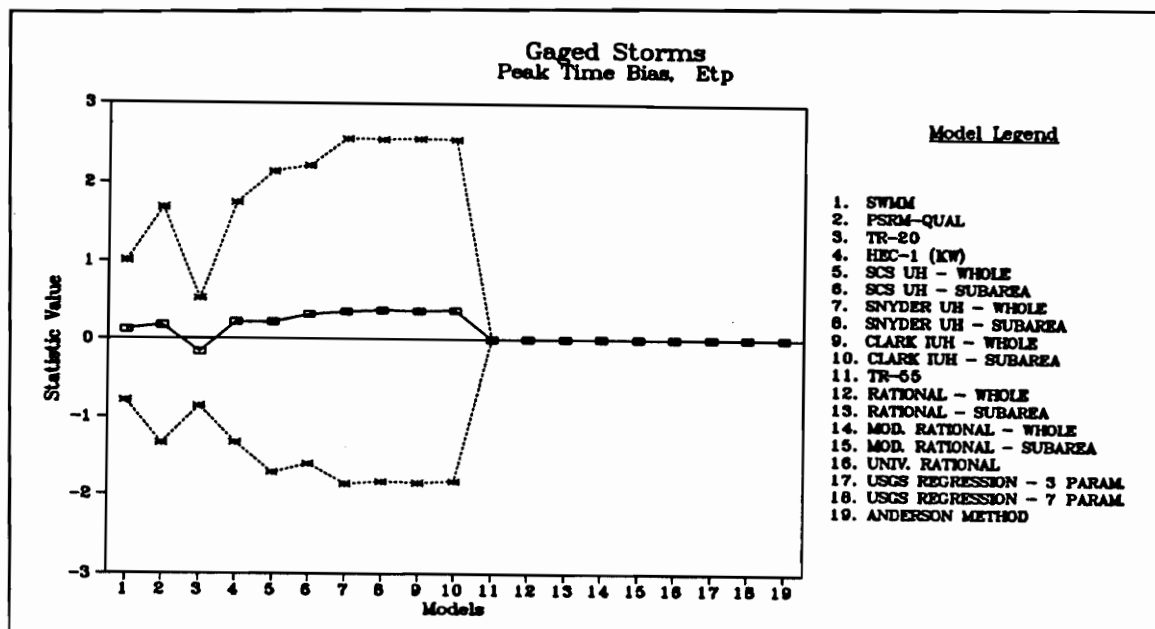


Figure D.22 - Time to Peak Bias for All Models, Gaged Storms

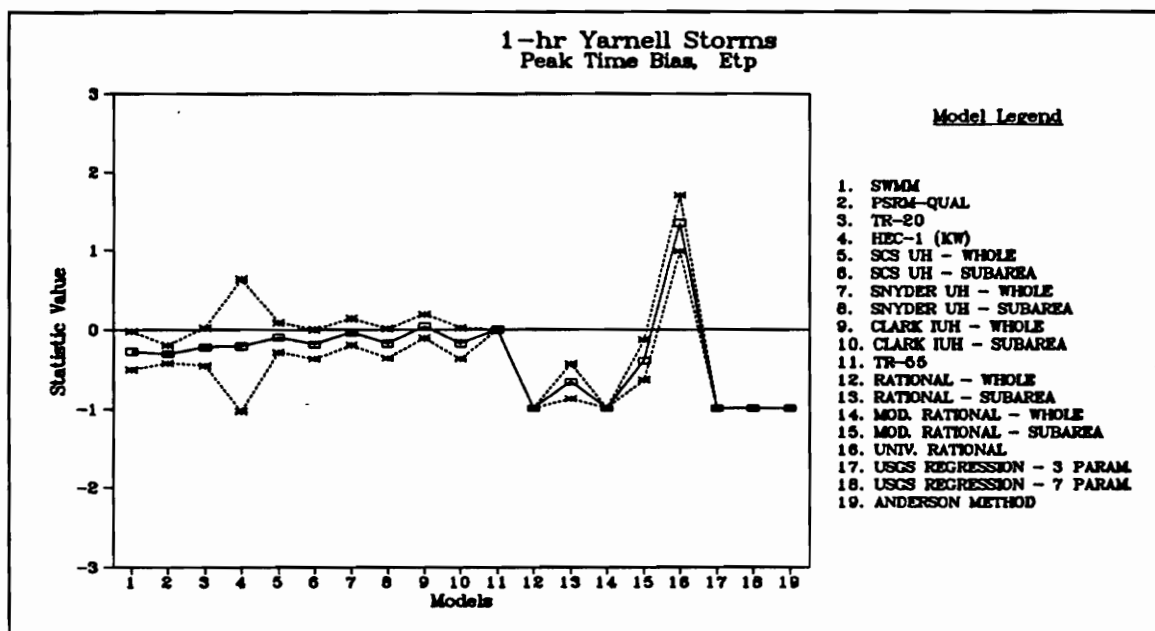


Figure D.23 - Time to Peak Bias for All Models, 1-hr Yarnell Storms

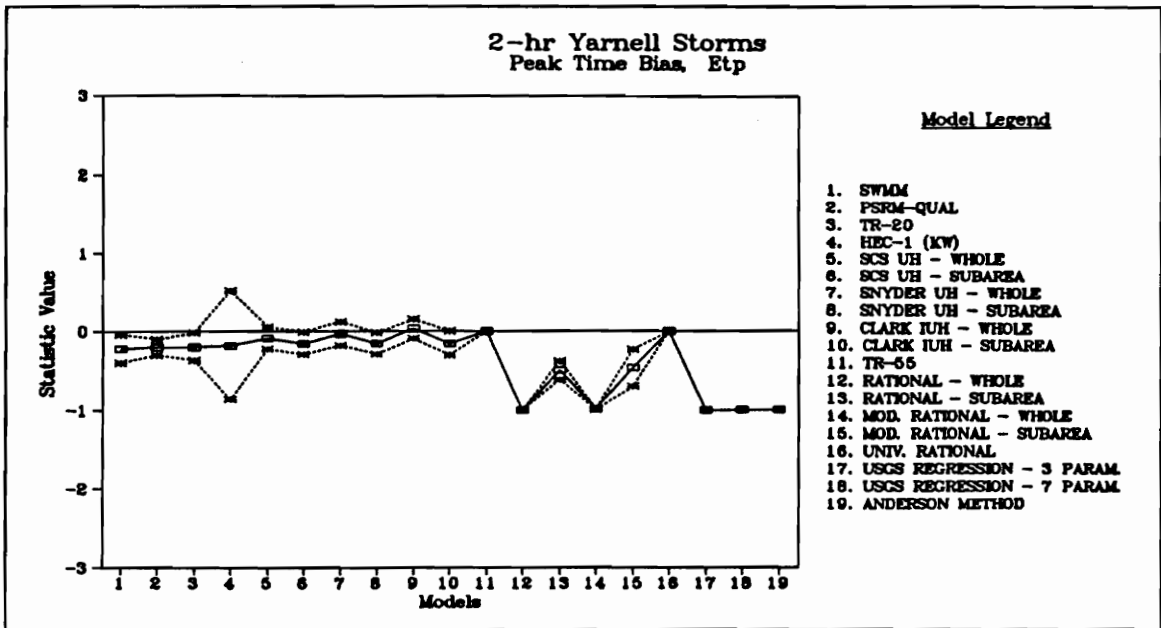


Figure D.24 - Time to Peak Bias for All Models, 2-hr Yarnell Storms

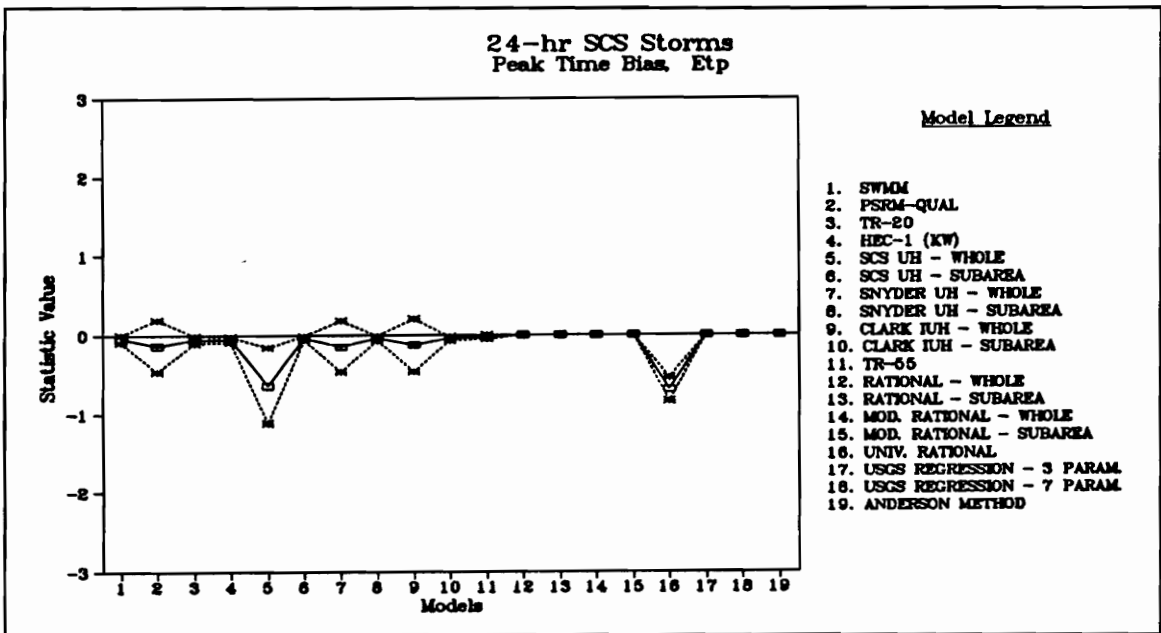


Figure D.25 - Time to Peak Bias for All Models, 24-hr SCS Storms

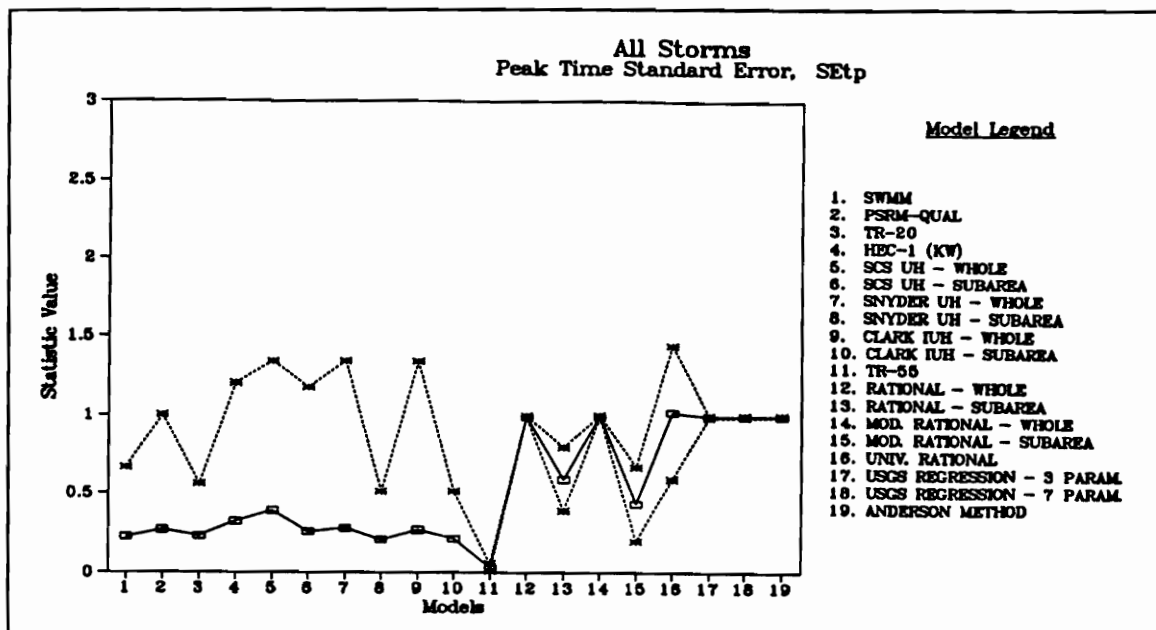


Figure D.26 - Time to Peak Standard Error for All Models, All Storms

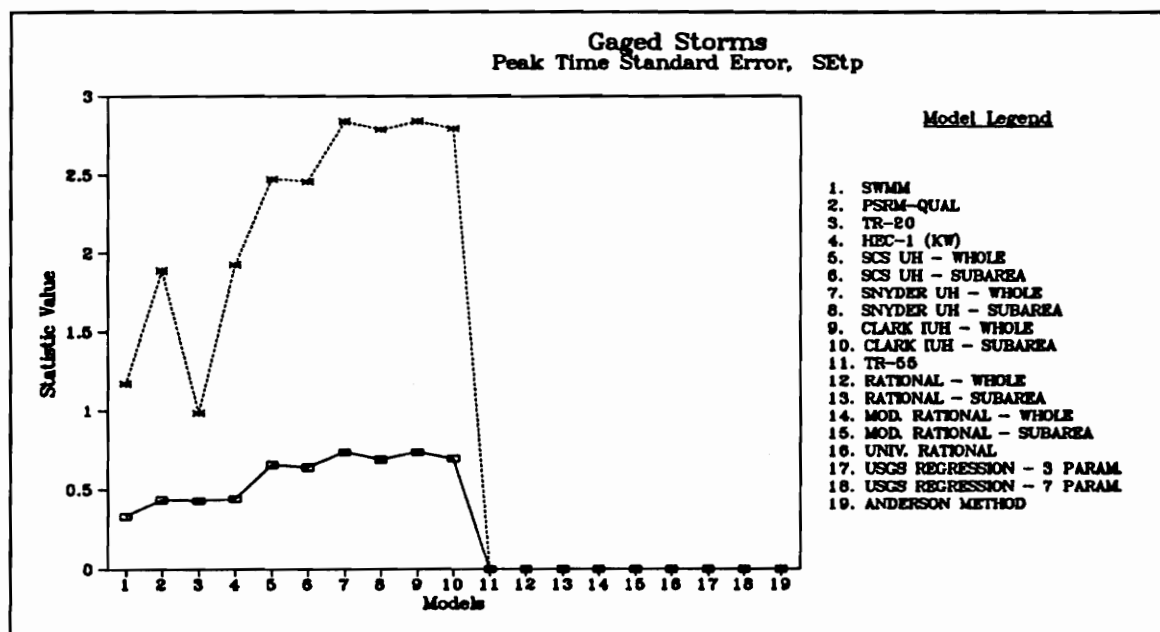


Figure D.27 - Time to Peak Standard Error for All Models, Gaged Storms

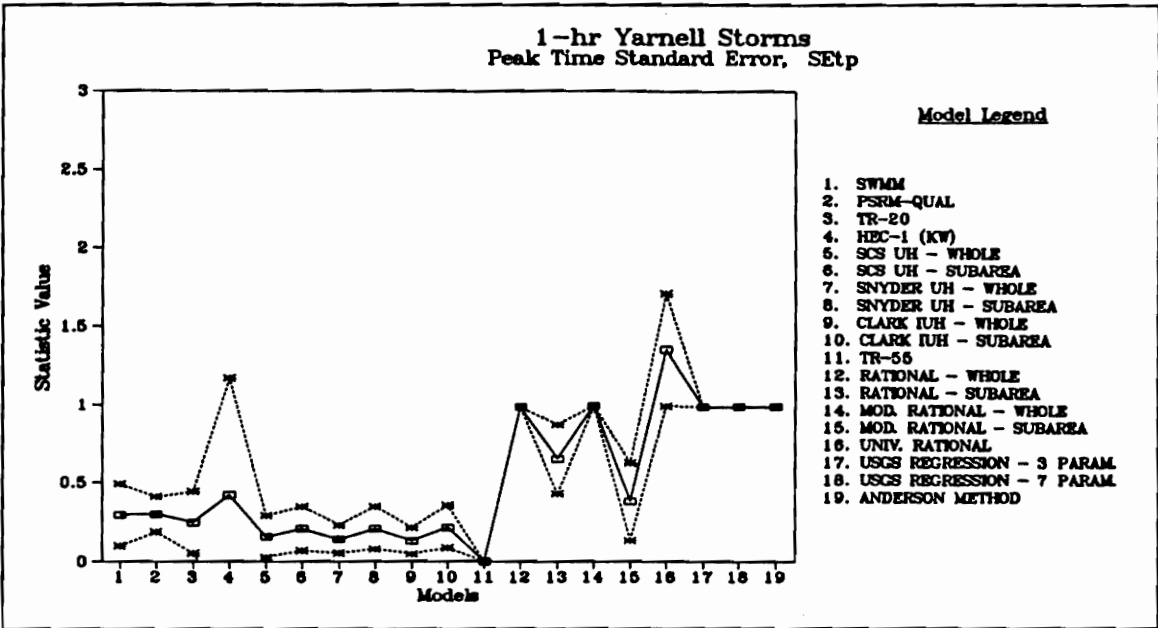


Figure D.28 - Time to Peak Standard Error for All Models, 1-hr Yarnell Storms

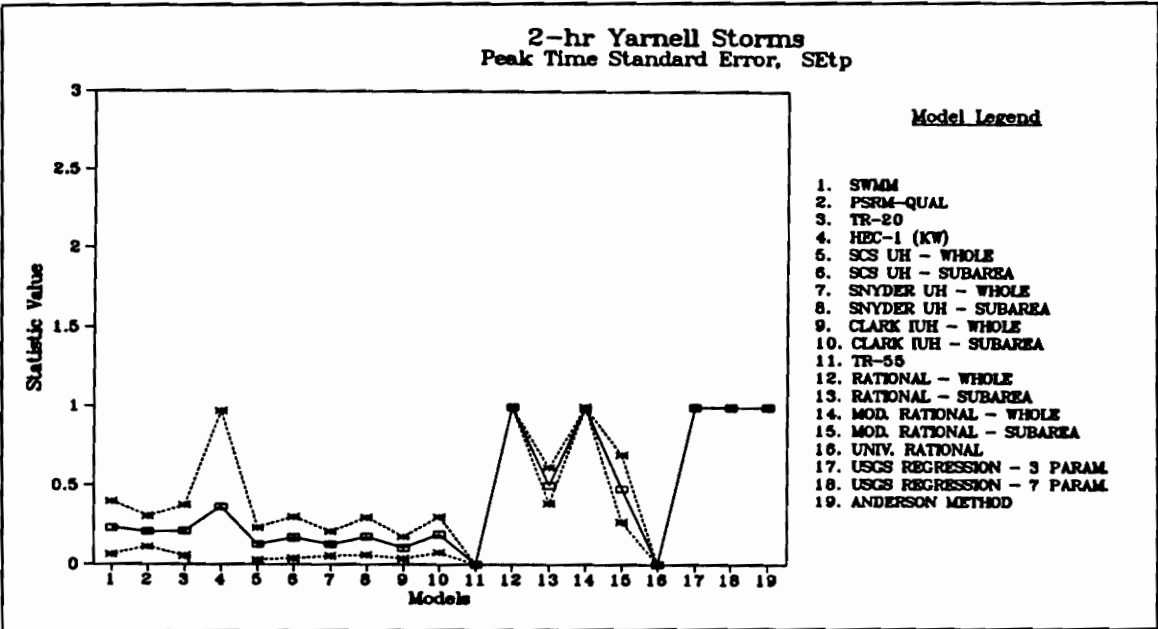


Figure D.29 - Time to Peak Standard Error for All Models, 2-hr Yarnell Storms

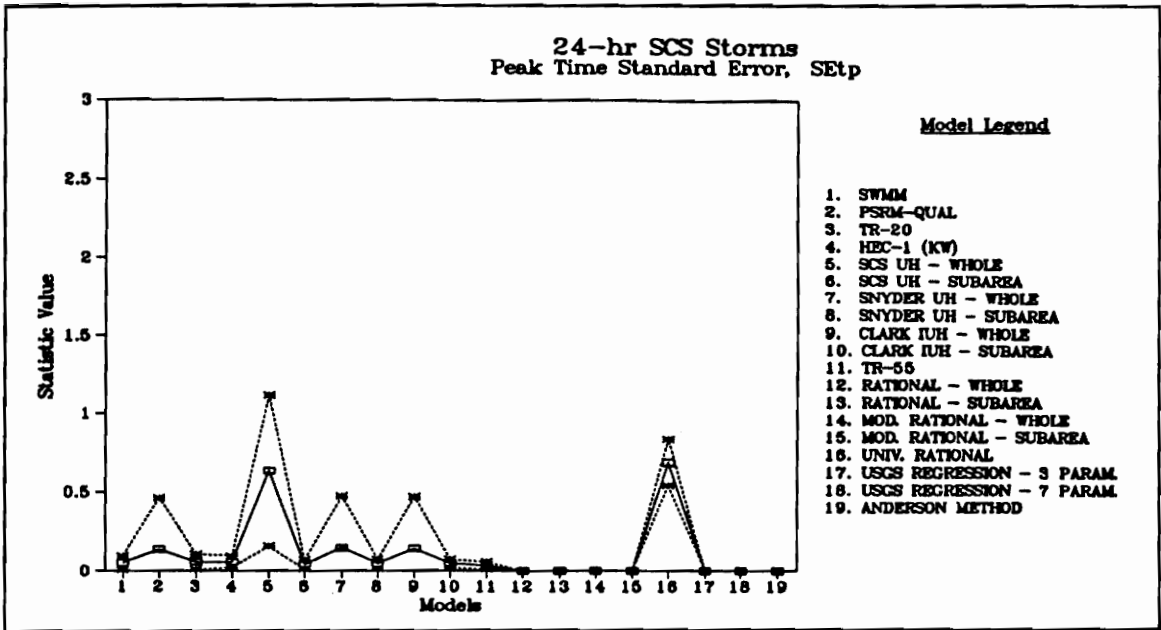


Figure D.30 - Time to Peak Standard Error for All Models, 24-hr SCS Storms

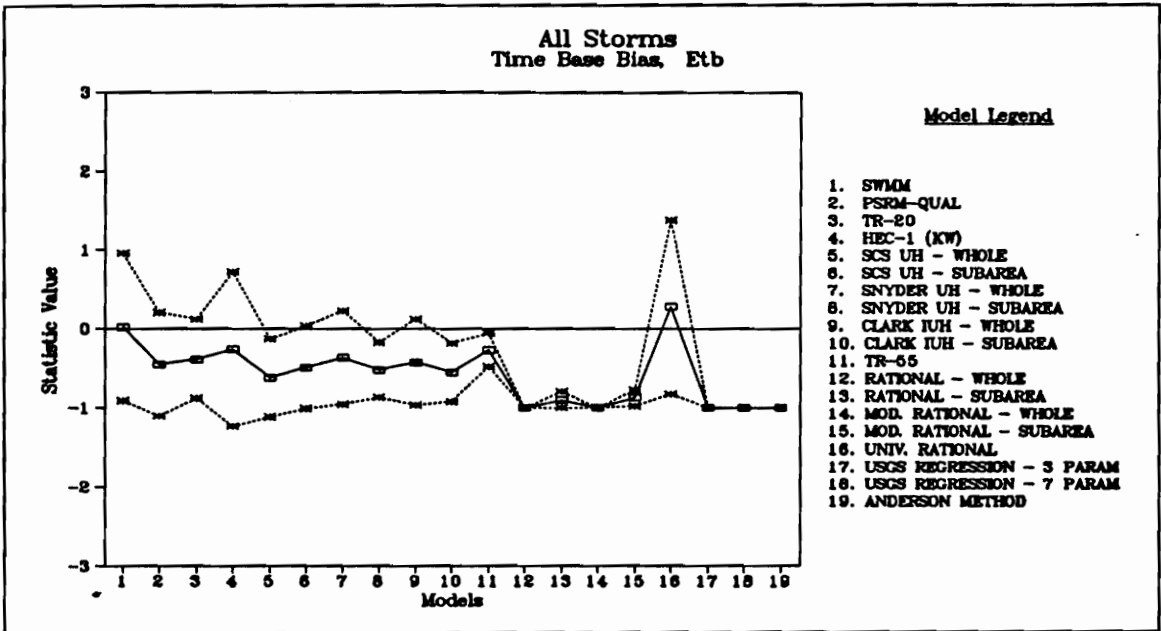


Figure D.31 - Time Base Bias for All Models, All Storms

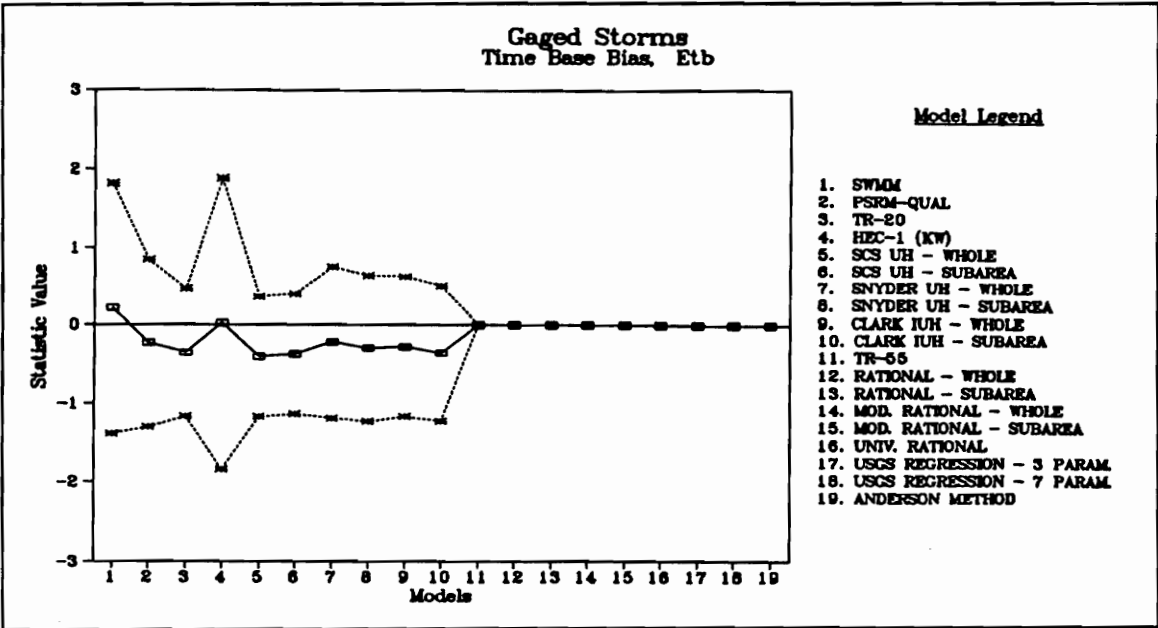


Figure D.32 - Time Base Bias for All Models, Gaged Storms

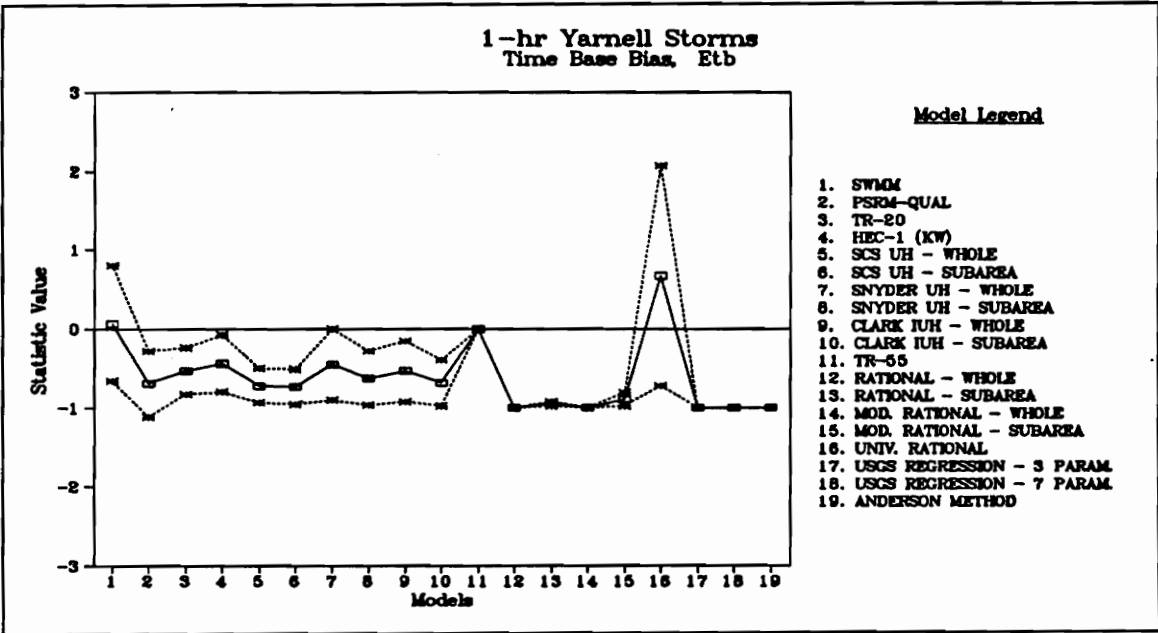


Figure D.33 - Time Base Bias for All Models, 1-hr Yarnell Storms

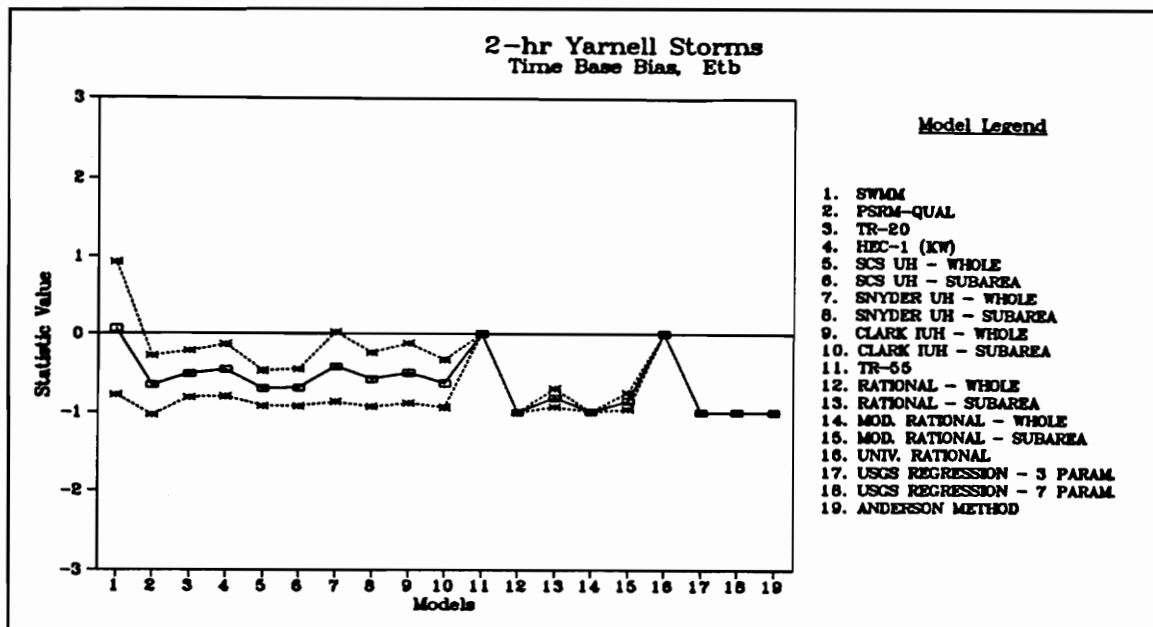


Figure D.34 - Time Base Bias for All Models, 2-hr Yarnell Storms

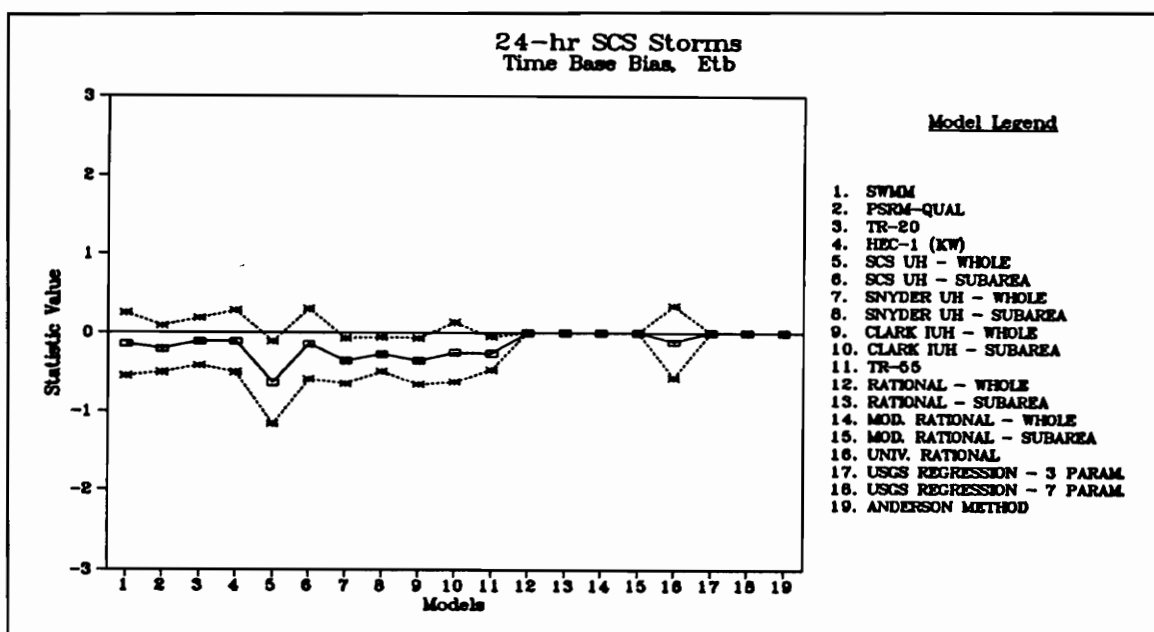


Figure D.35 - Time Base Bias for All Models, 24-hr SCS Storms

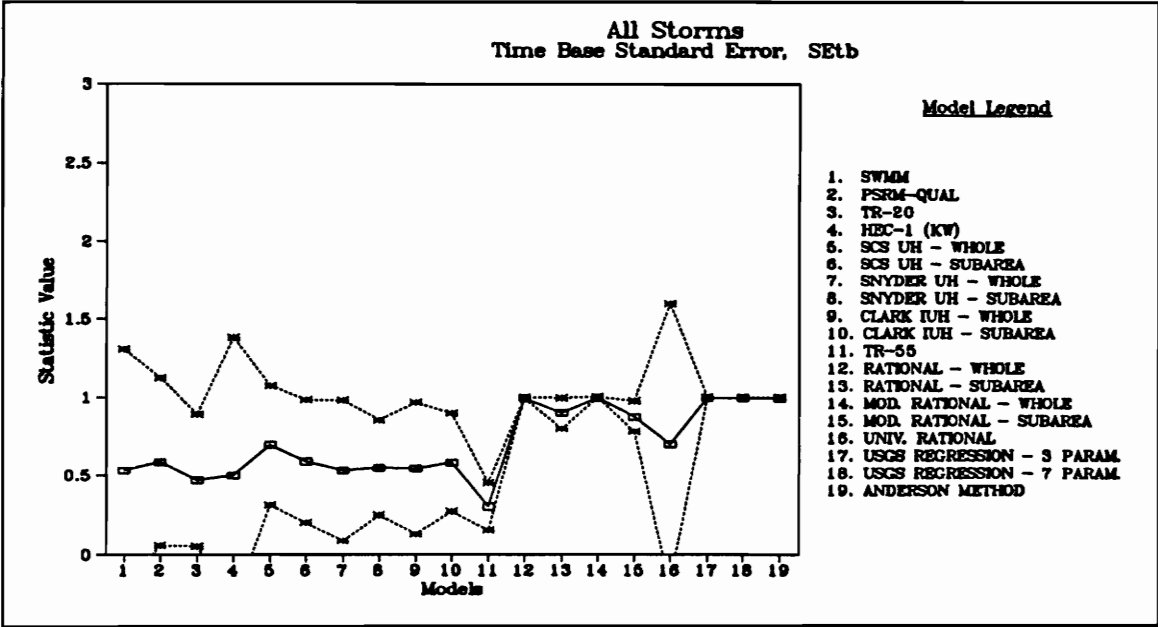


Figure D.36 - Time Base Standard Error for All Models, All Storms

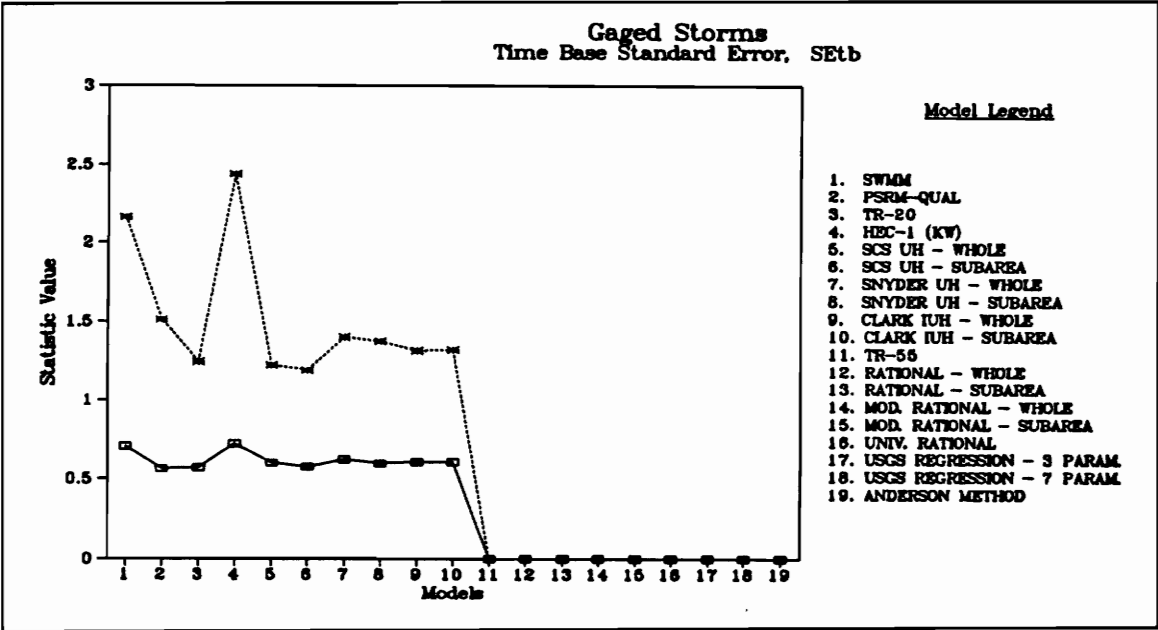


Figure D.37 - Time Base Standard Error for All Models, Gaged Storms

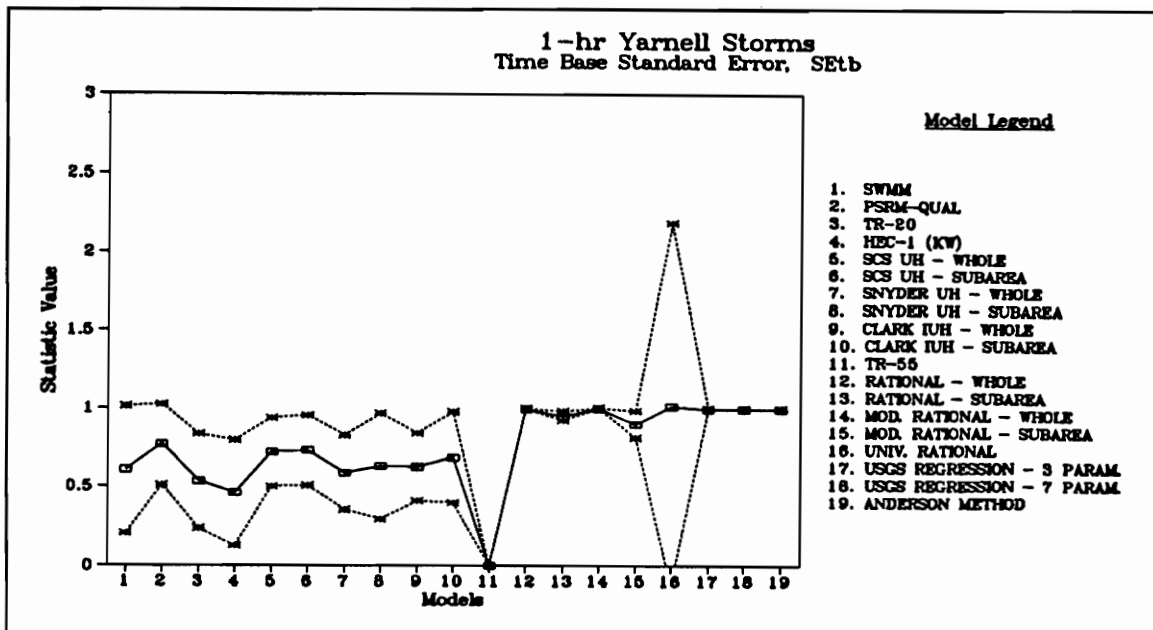


Figure D.38 - Time Base Standard Error for All Models, 1-hr Yarnell Storms

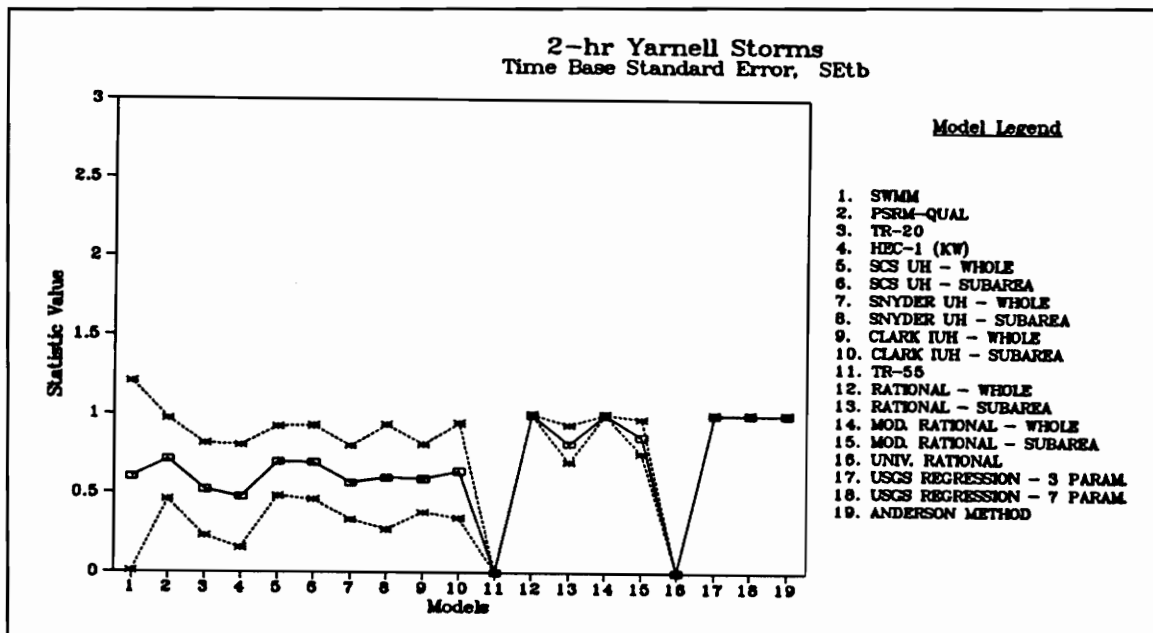


Figure D.39 - Time Base Standard Error for All Models, 2-hr Yarnell Storms

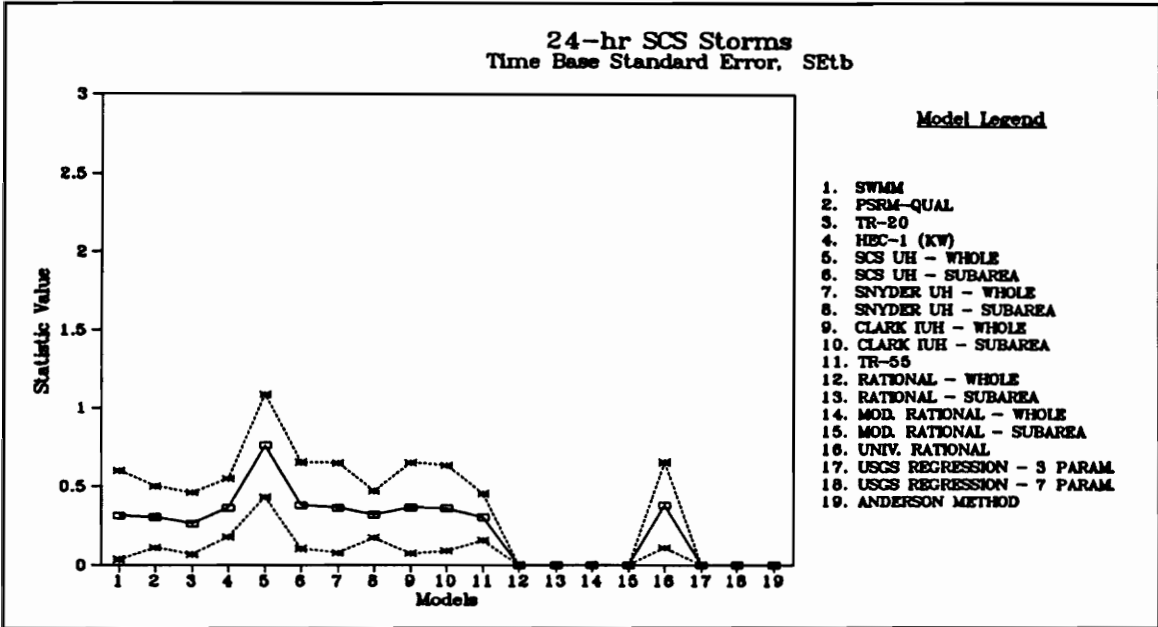


Figure D.40 - Time Base Standard Error for All Models, 24-hr SCS Storms

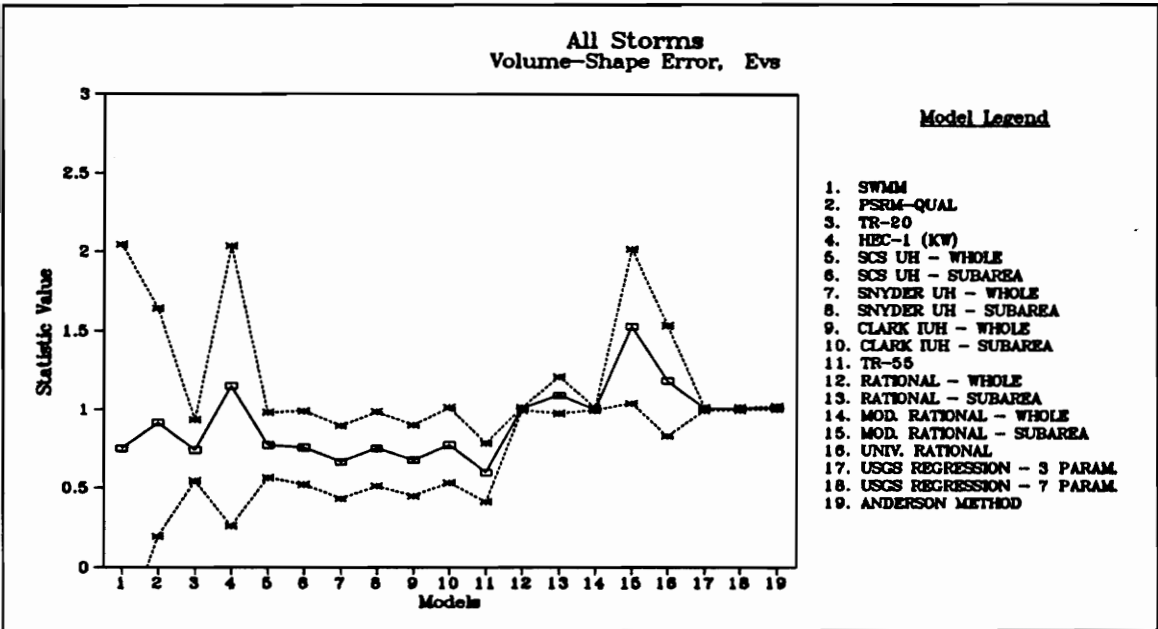


Figure D.41 - Volume-Shape Error for All Models, All Storms

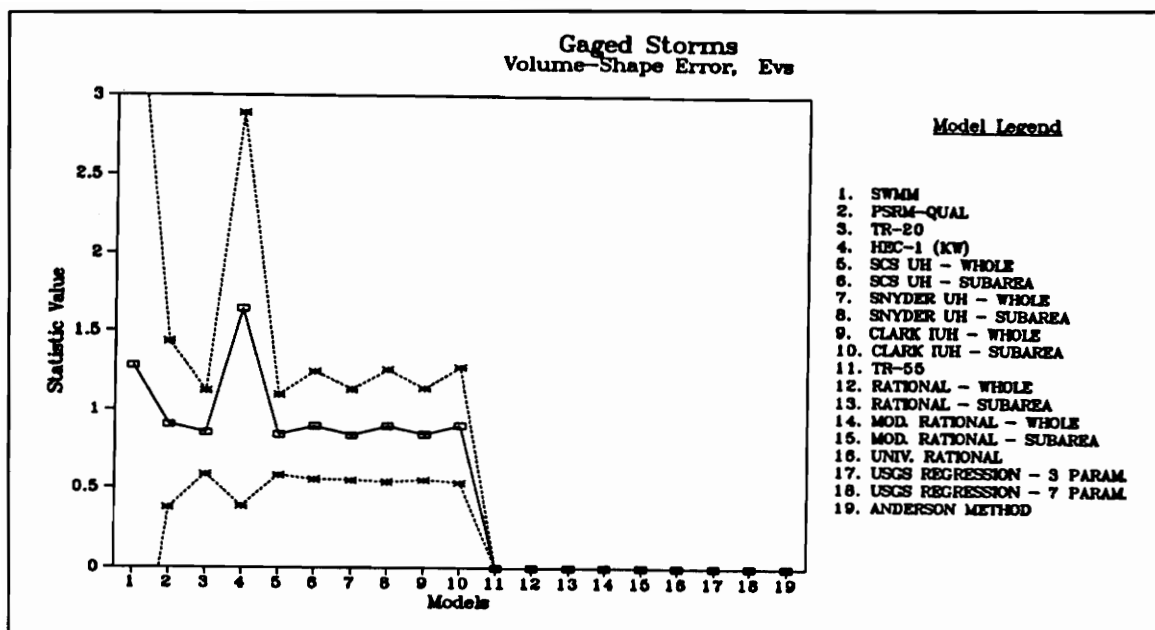


Figure D.42 - Volume-Shape Error for All Models, Gaged Storms

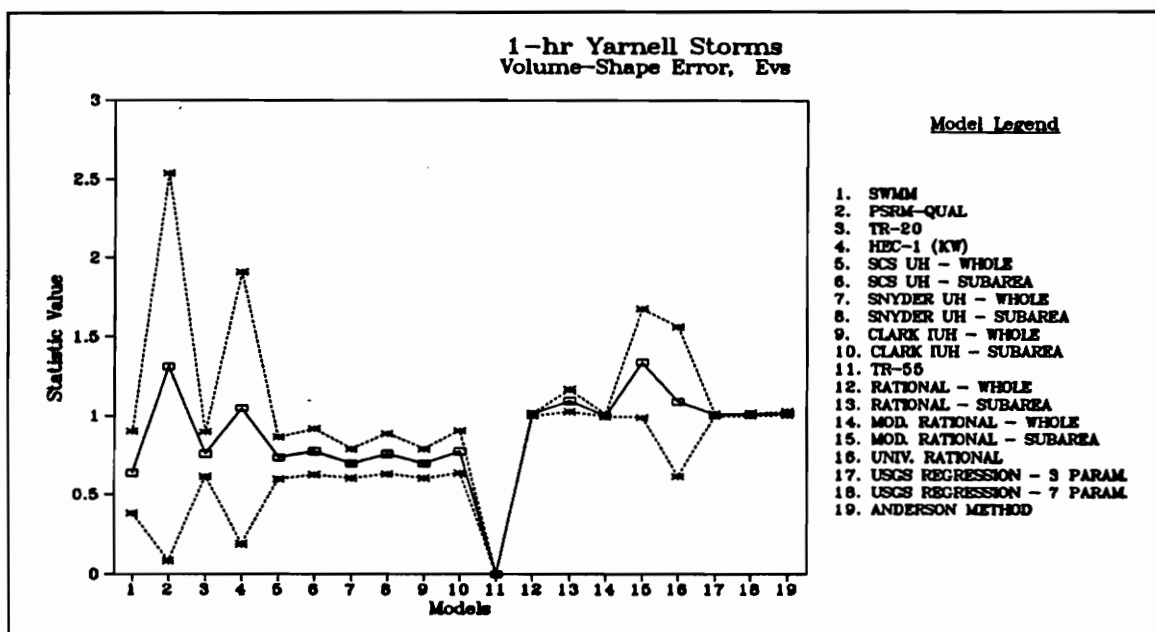


Figure D.43 - Volume-Shape Error for All Models, 1-hr Yarnell Storms

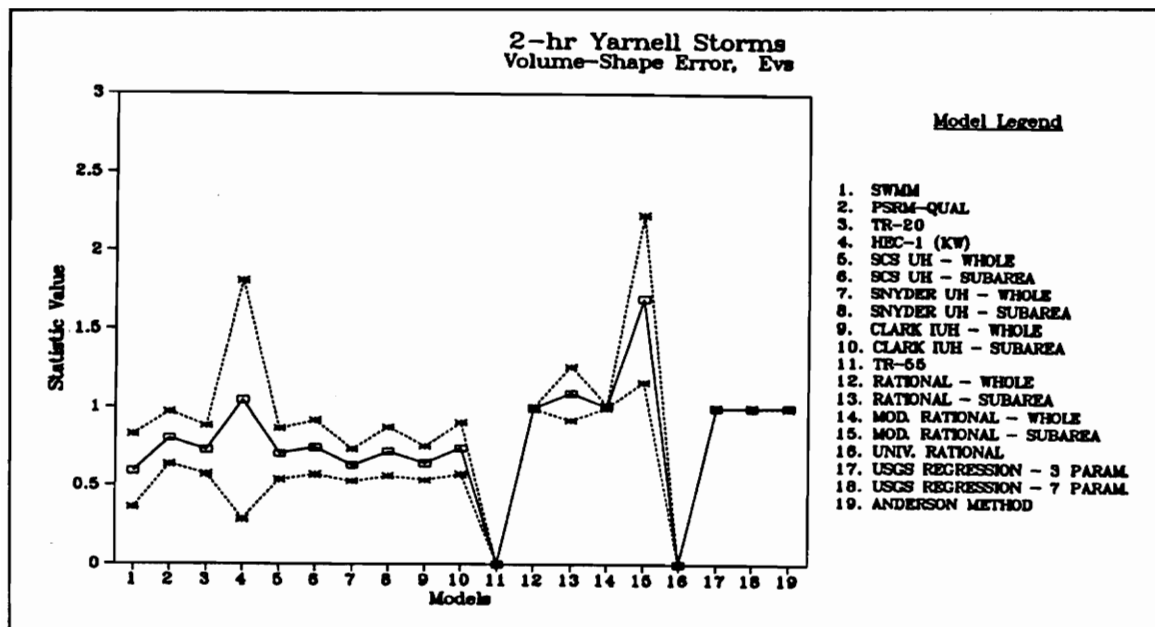


Figure D.44 - Volume-Shape Error for All Models, 2-hr Yarnell Storms

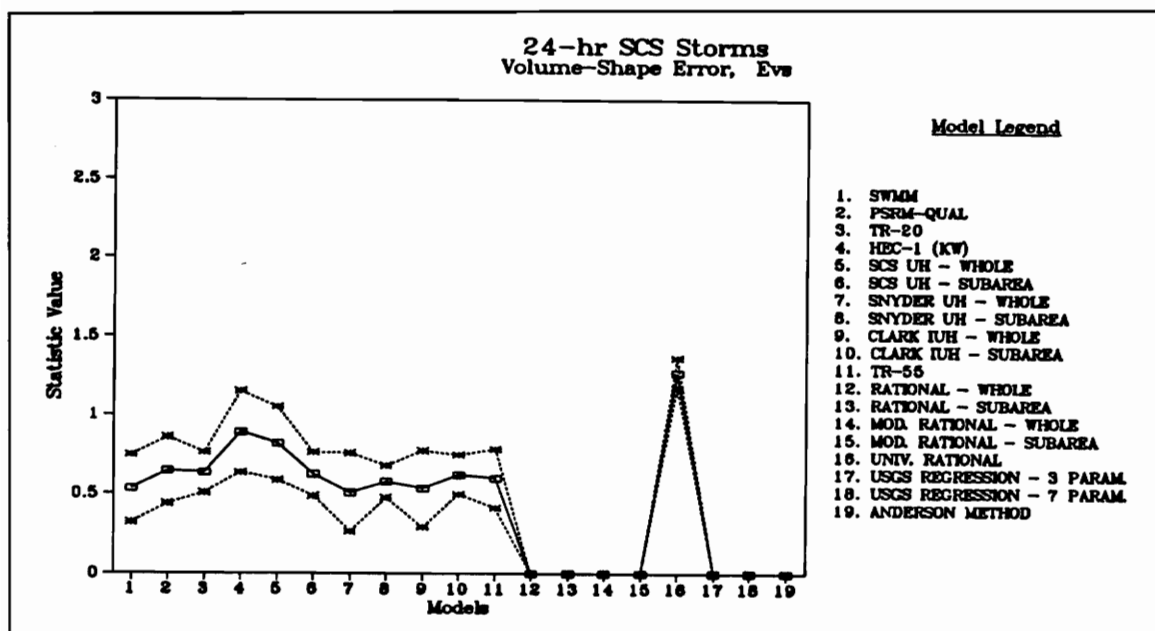


Figure D.45 - Volume-Shape Error for All Models, 24-hr SCS Storms

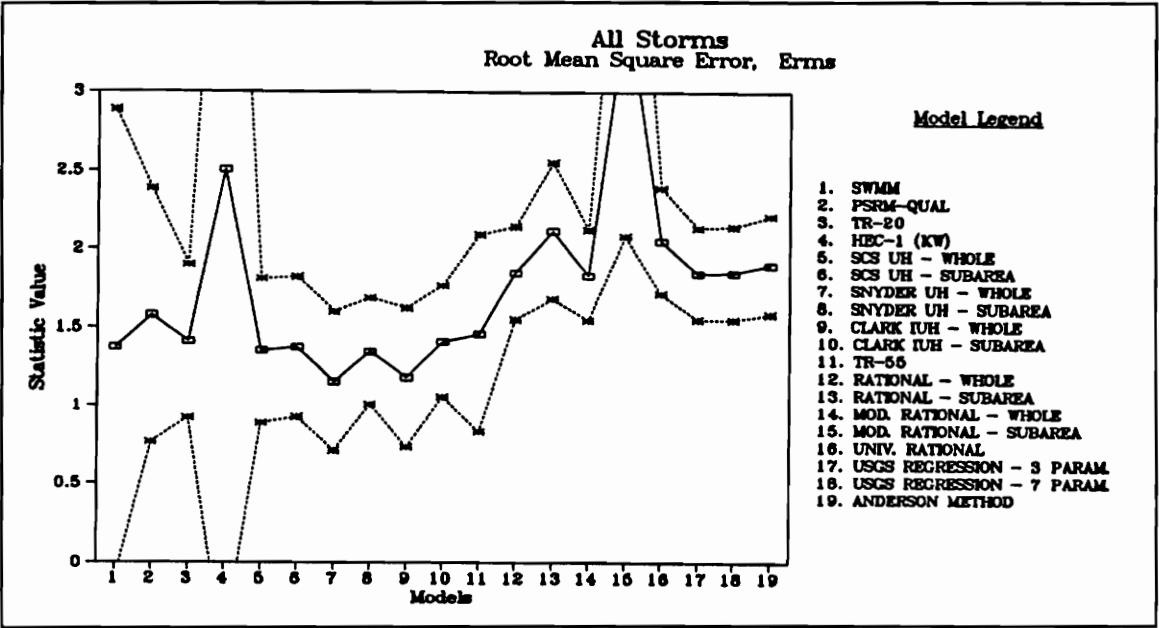


Figure D.46 - Root-Mean-Square Error for All Models, All Storms

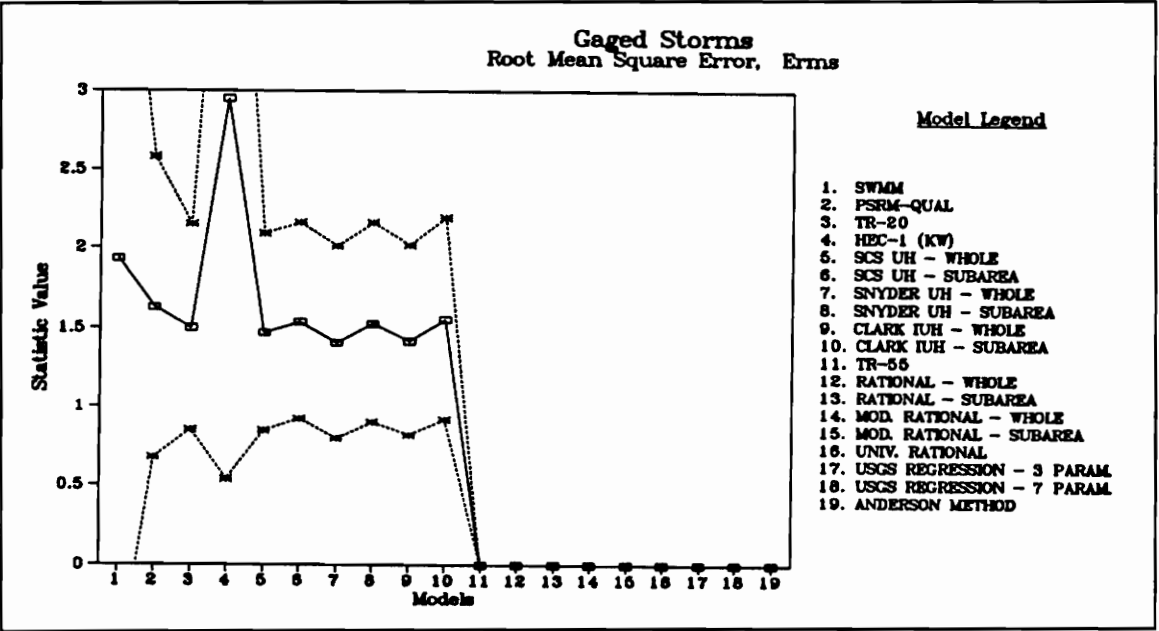


Figure D.47 - Root-Mean-Square Error for All Models, Gaged Storms

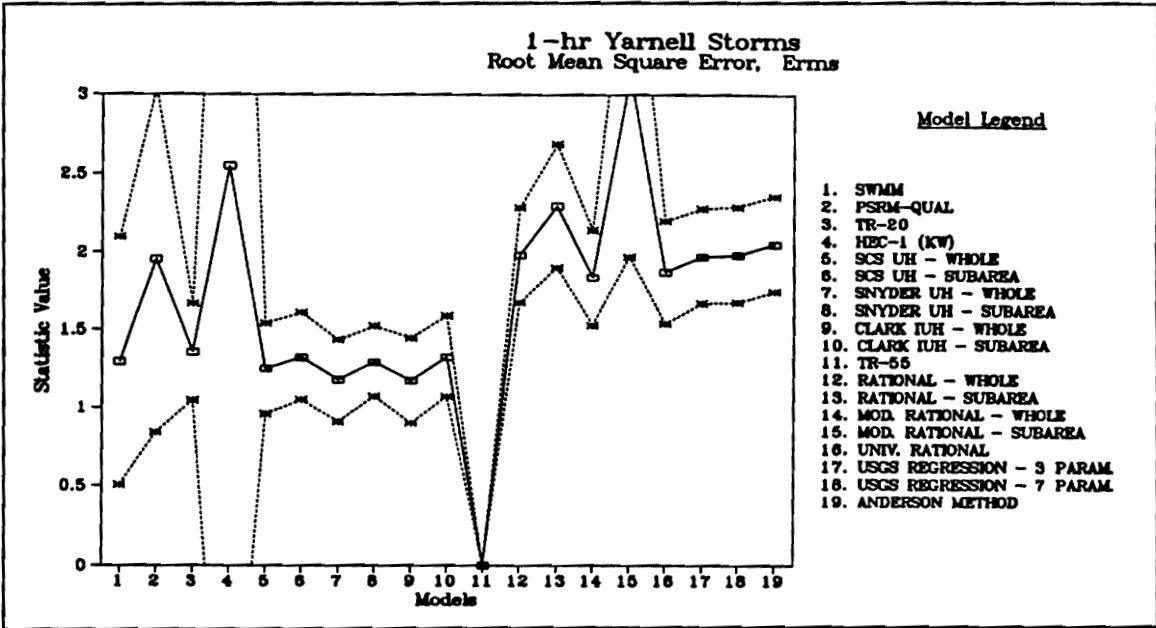


Figure D.48 - Root-Mean-Square Error for All Models, 1-hr Yarnell Storms

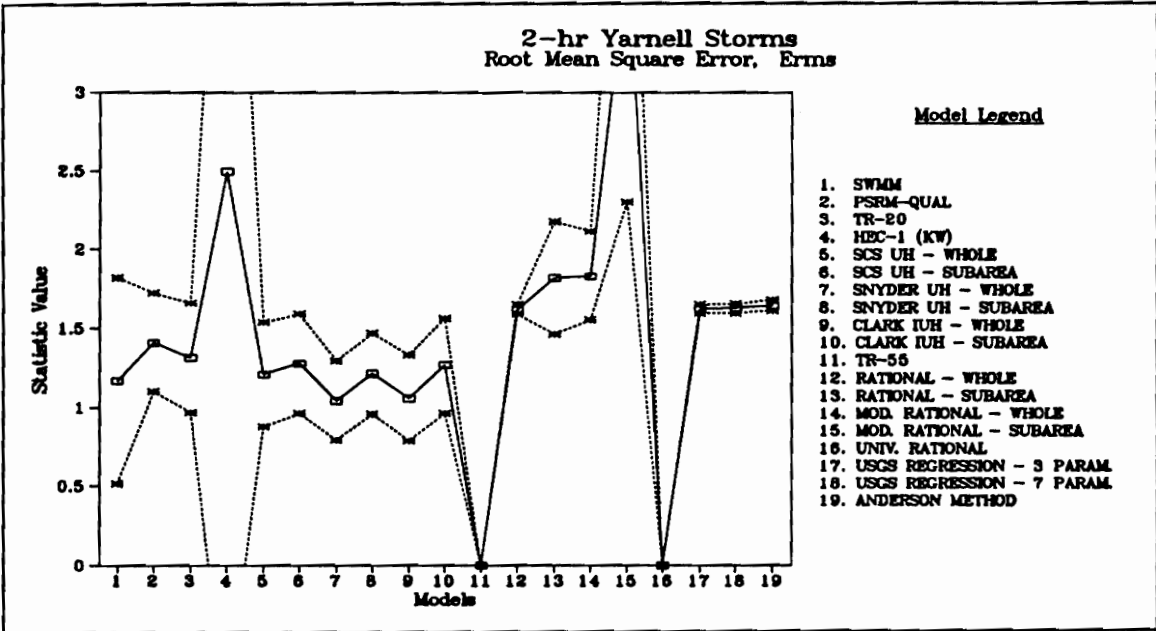


Figure D.49 - Root-Mean-Square Error for All Models, 2-hr Yarnell Storms

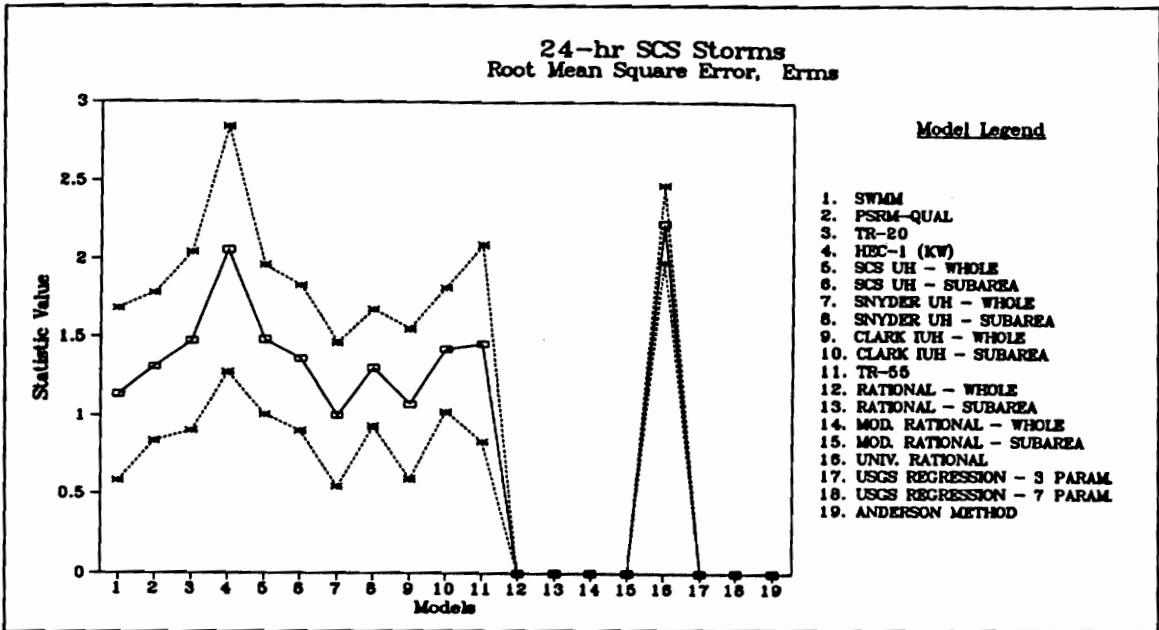


Figure D.50 - Root-Mean-Square Error for All Models, 24-hr SCS Storms

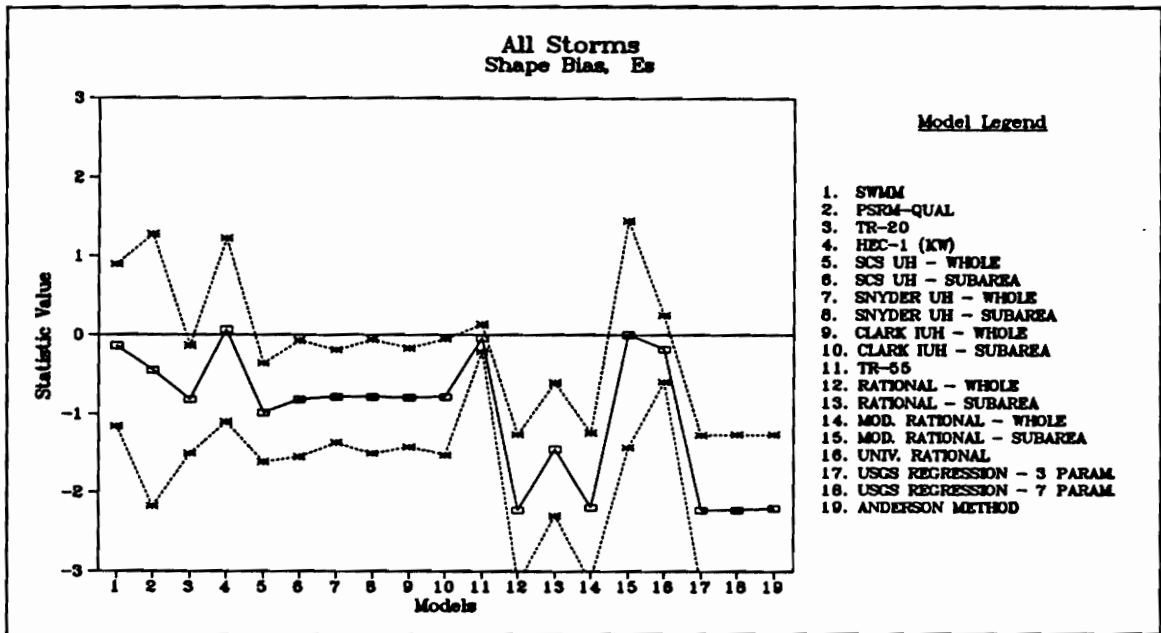


Figure D.51 - Shape Bias for All Models, All Storms

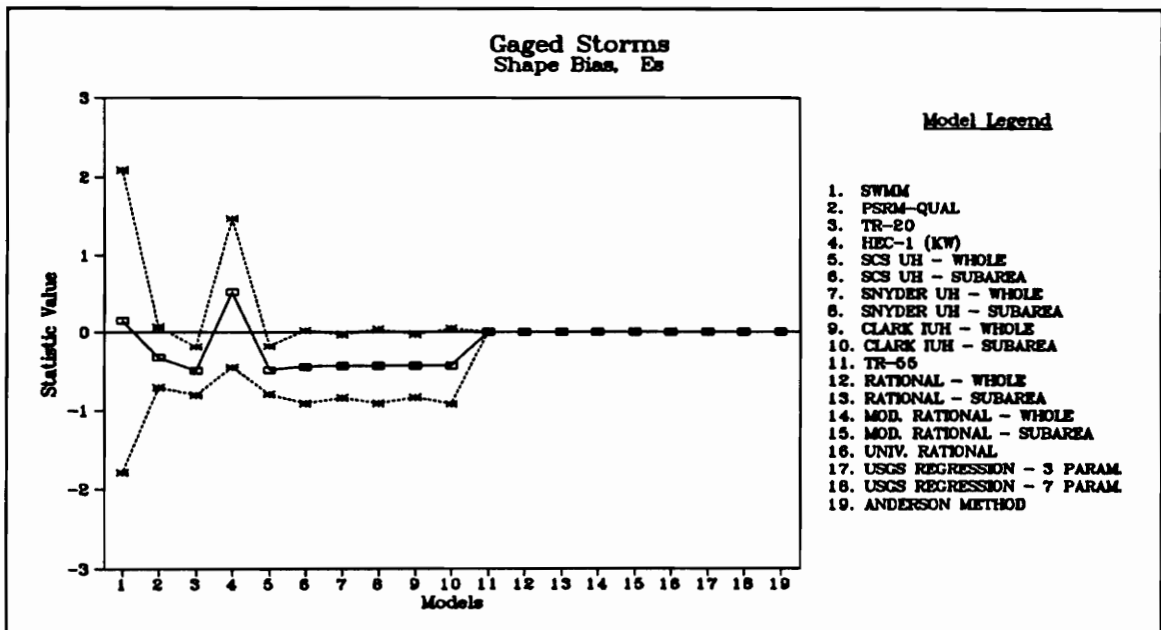


Figure D.52 - Shape Bias for All Models, Gaged Storms

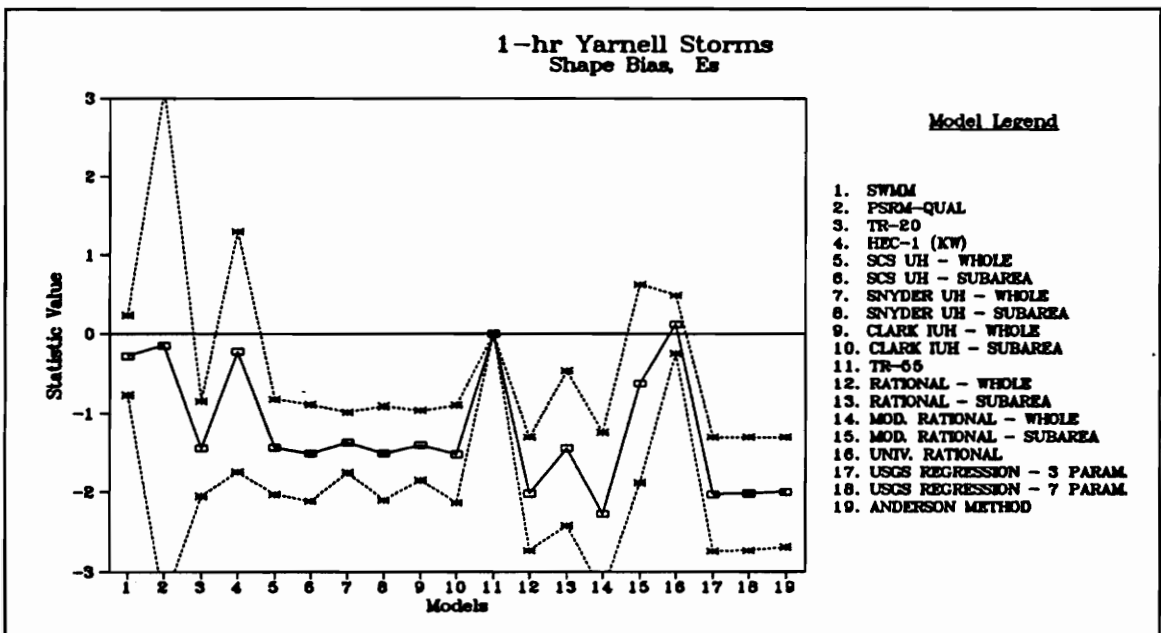


Figure D.53 - Shape Bias for All Models, 1-hr Yarnell Storms

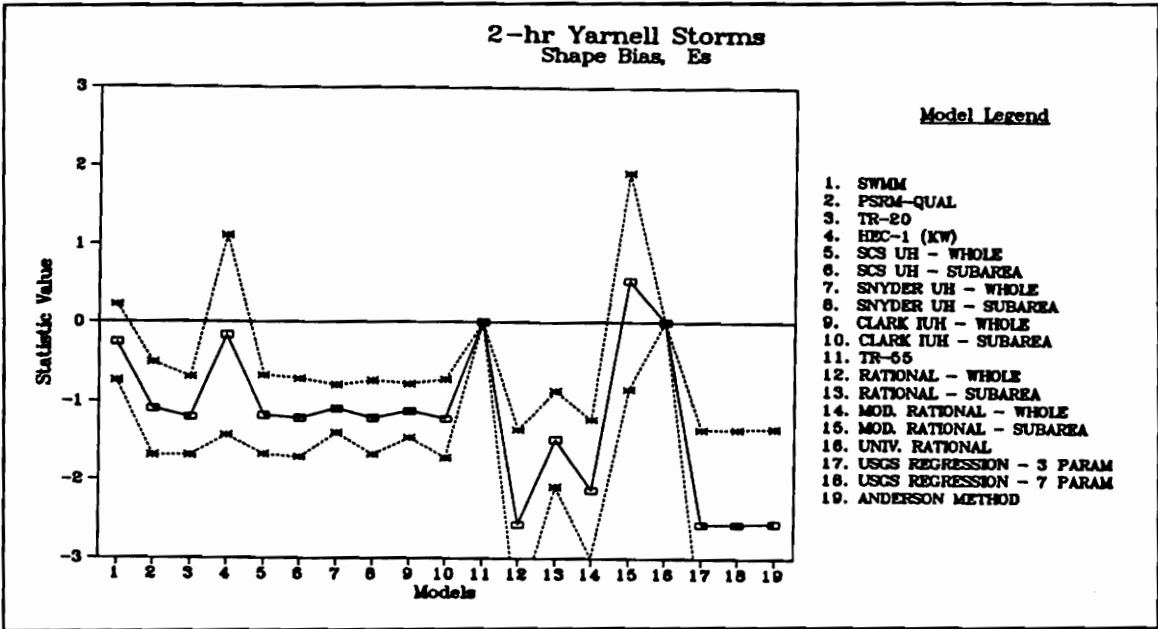


Figure D.54 - Shape Bias for All Models, 2-hr Yarnell Storms

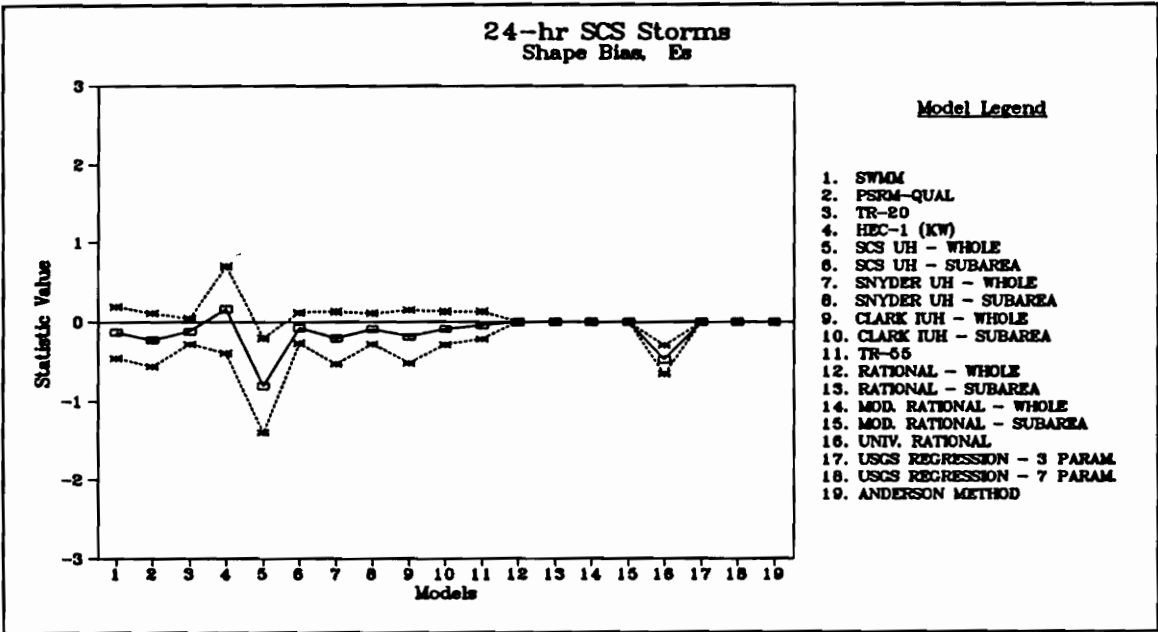


Figure D.55 - Shape Bias for All Models, 24-hr SCS Storms

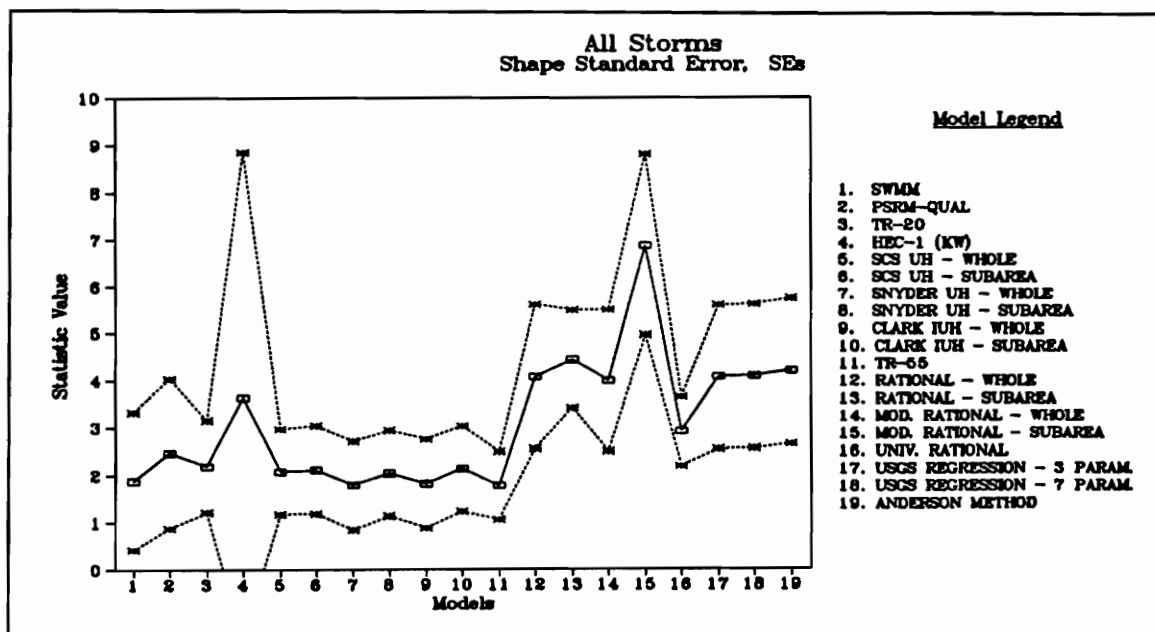


Figure D.56 - Shape Standard Error for All Models, All Storms

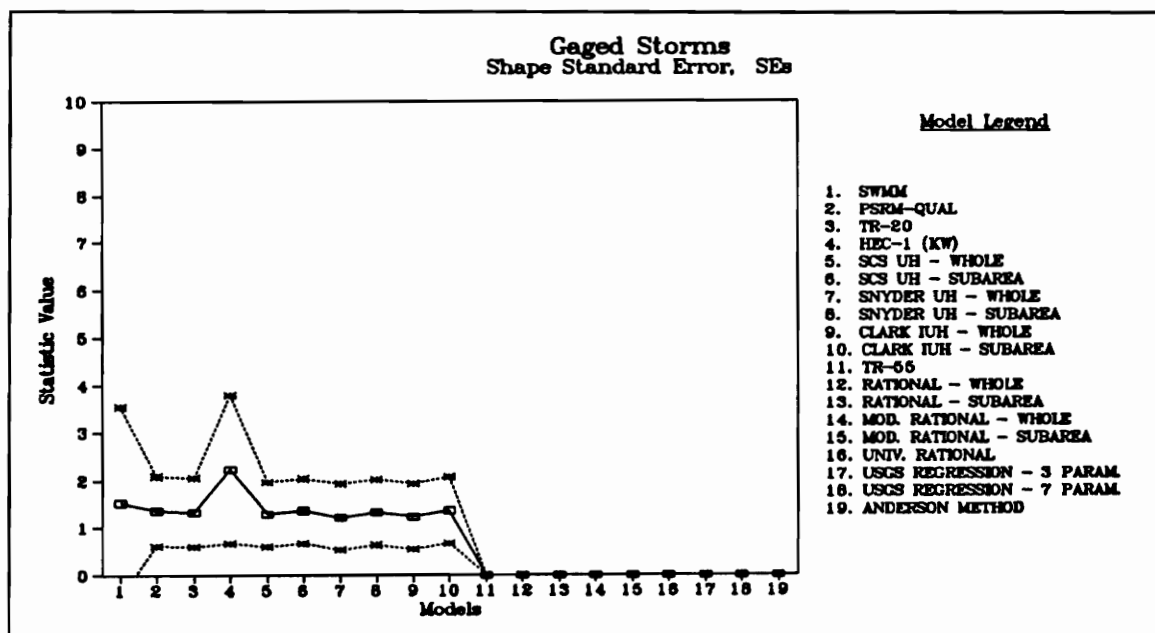


Figure D.57 - Shape Standard Error for All Models, Gaged Storms

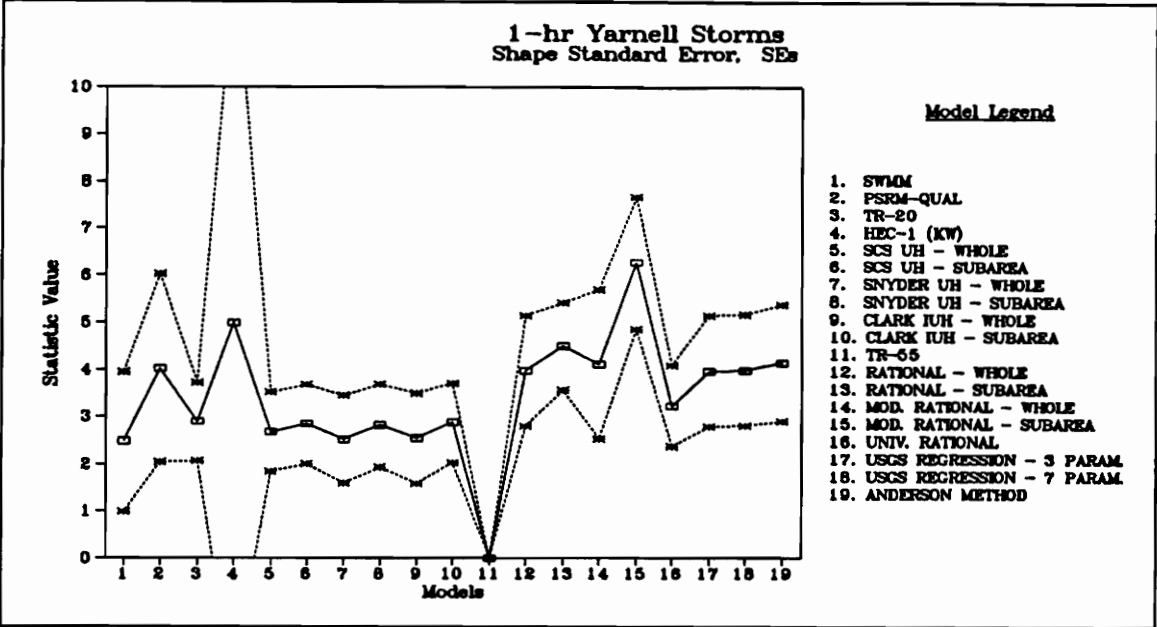


Figure D.58 - Shape Standard Error for All Models, 1-hr Yarnell Storms

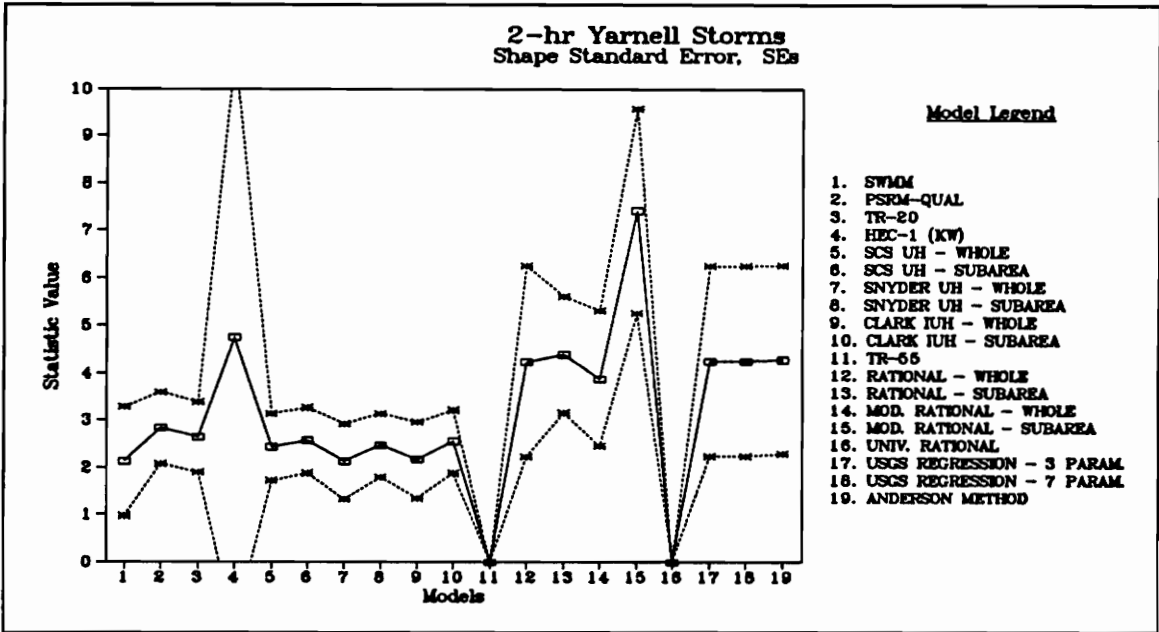


Figure D.59 - Shape Standard Error for All Models, 2-hr Yarnell Storms

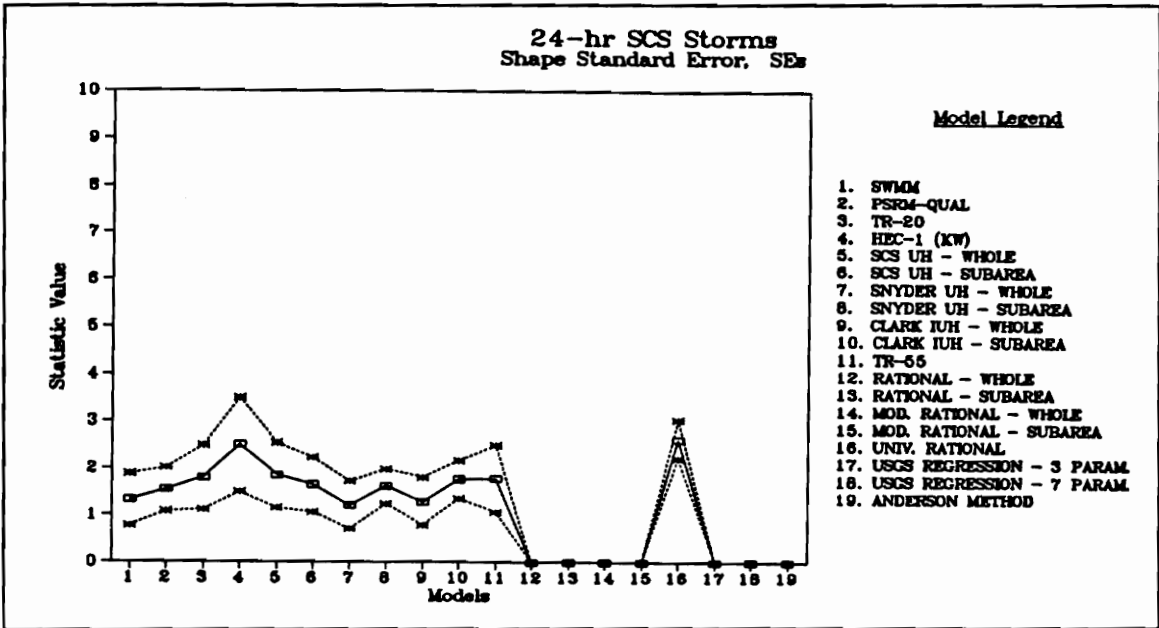


Figure D.60 - Shape Standard Error for All Models, 24-hr SCS Storms

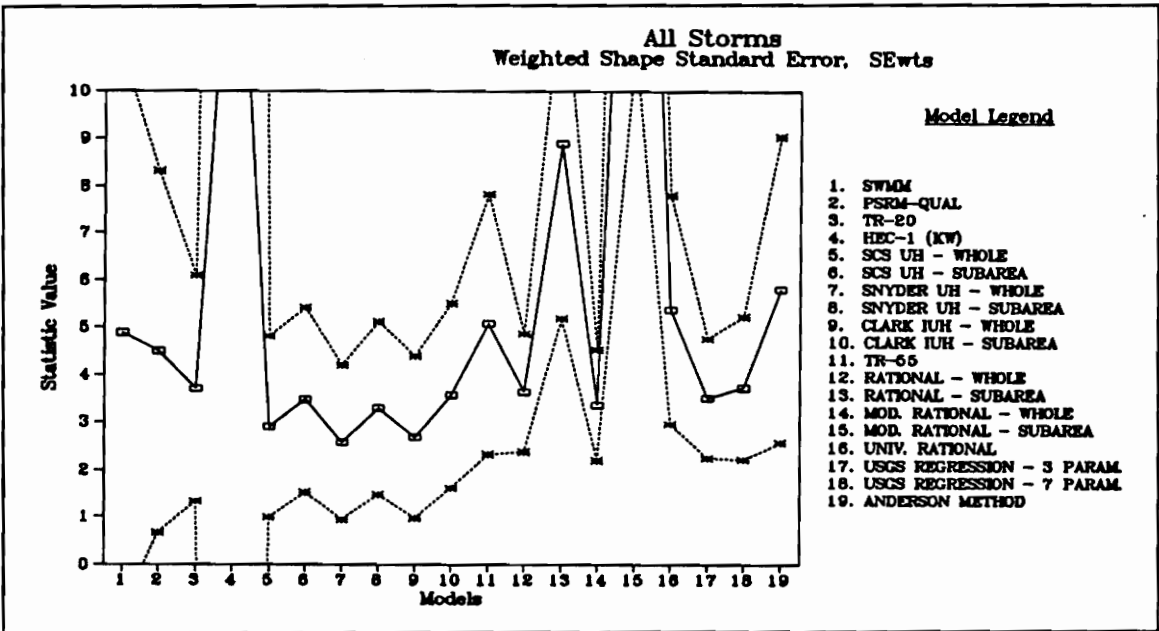


Figure D.61 - Weighted Shape Standard Error for All Models, All Storms

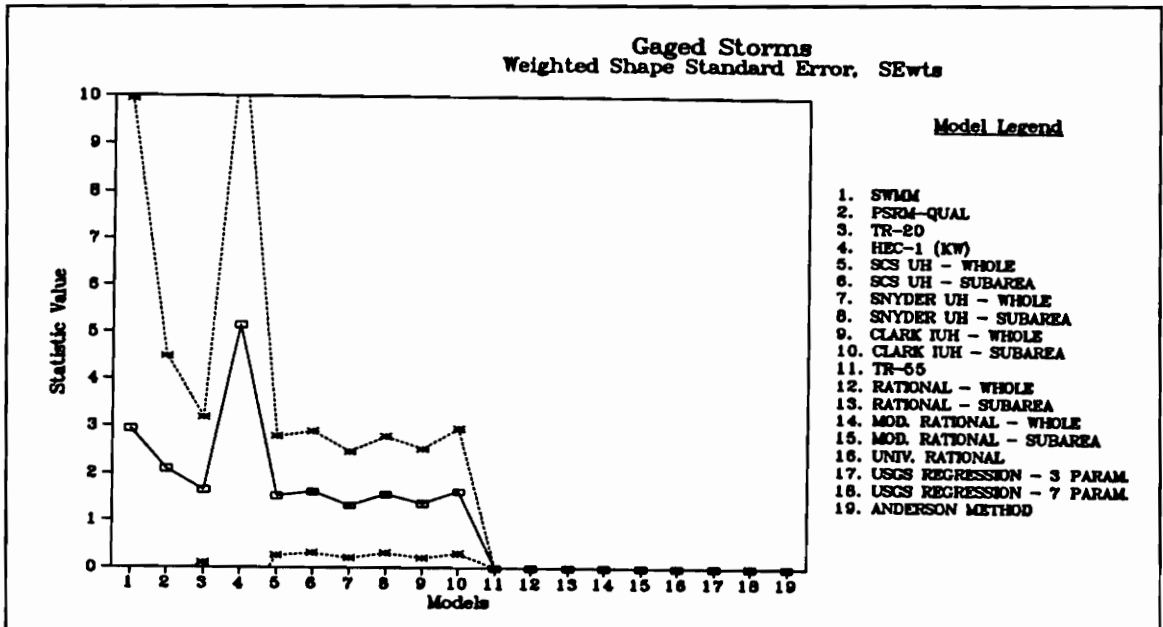


Figure D.62 - Weighted Shape Standard Error for All Models, Gaged Storms

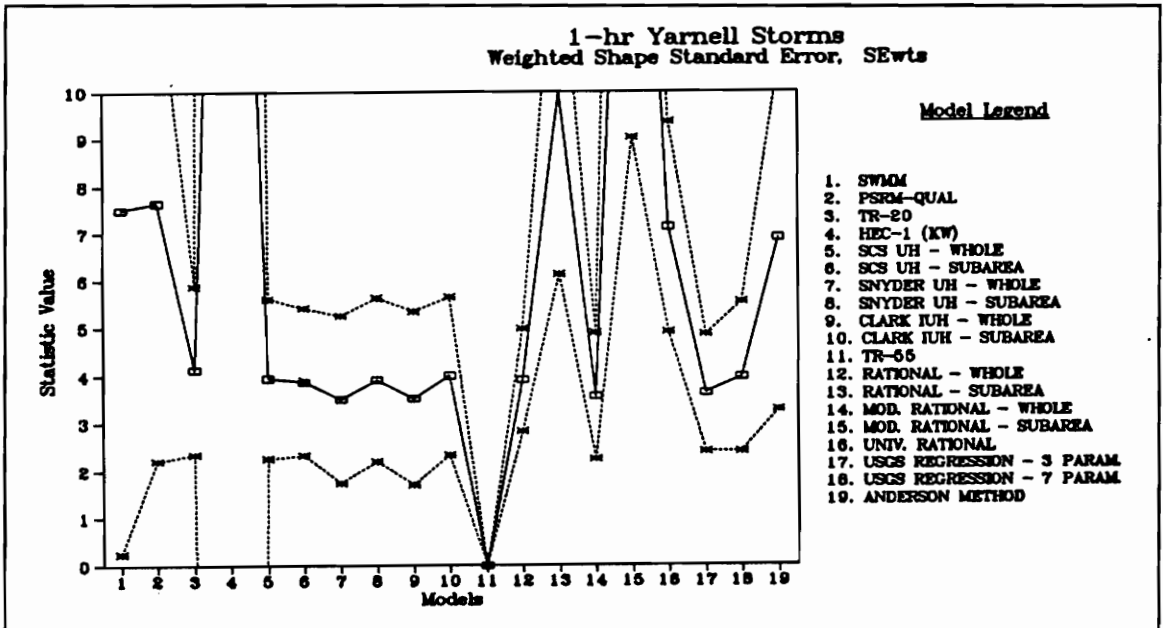


Figure D.63 - Weighted Shape Standard Error for All Models, 1-hr Yarnell Storms

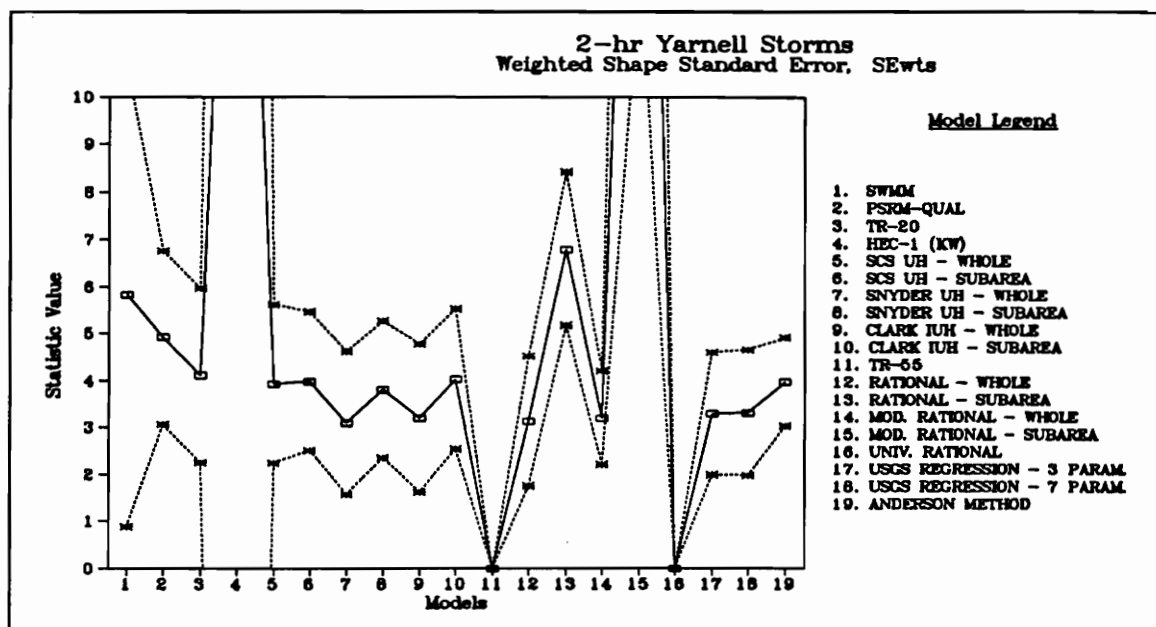


Figure D.64 - Weighted Shape Standard Error for All Models, 2-hr Yarnell Storms

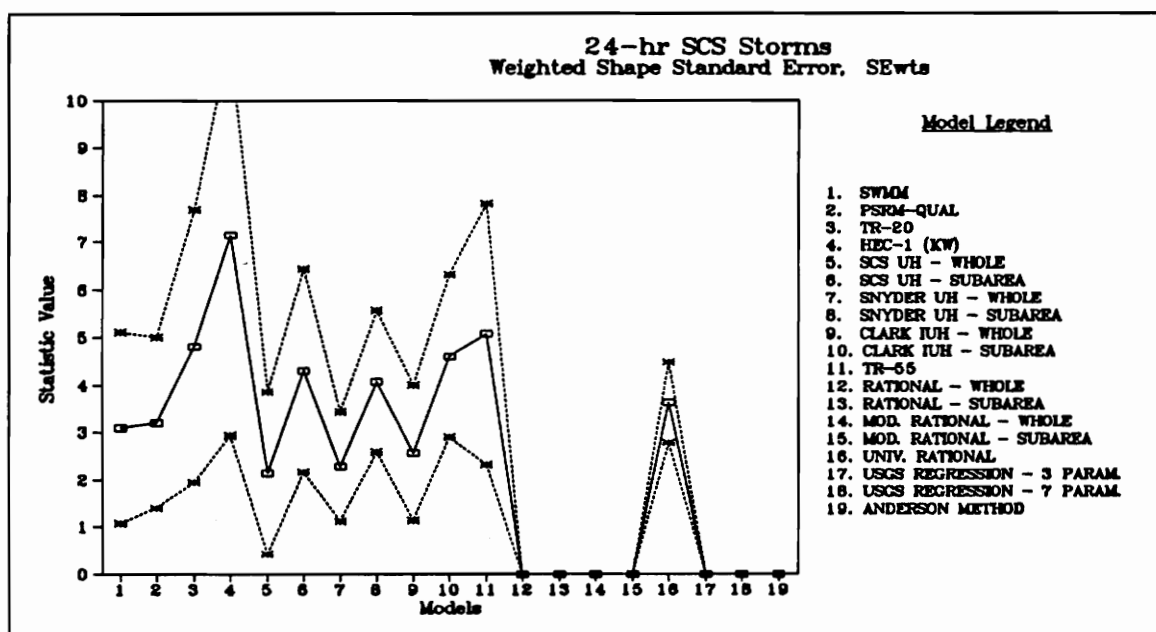


Figure D.65 - Weighted Shape Standard Error for All Models, 24-hr SCS Storms

Folio A

Watershed Maps

Vita

Aaron Brent Small was born in Williamsburg, Virginia on November 4, 1969. He graduated from Lafayette High School in May 1987. That same year he started undergraduate studies at Virginia Tech. He transferred into Civil Engineering in September 1988. He began simultaneous graduate studies and undergraduate studies in September 1991. Aaron received his Bachelor's degree in Civil Engineering in December 1991. Full time study towards the Master of Science in Civil Engineering degree followed undergraduate graduation.

A handwritten signature in black ink, appearing to read "Aaron B. Small". The signature is fluid and cursive, with the first name "Aaron" and last name "Small" clearly distinguishable, and a middle initial "B." in between.